



HAL
open science

Régulation de l'échangeur $\text{Na}^{+}/[\text{H}^{+}]$ 1 par les espèces réactives de l'oxygène

Denis Doyen

► **To cite this version:**

Denis Doyen. Régulation de l'échangeur $\text{Na}^{+}/[\text{H}^{+}]$ 1 par les espèces réactives de l'oxygène. Biologie moléculaire. Université Côte d'Azur, 2023. Français. NNT : 2023COAZ6007 . tel-04146530

HAL Id: tel-04146530

<https://theses.hal.science/tel-04146530v1>

Submitted on 30 Jun 2023

HAL is a multi-disciplinary open access archive for the deposit and dissemination of scientific research documents, whether they are published or not. The documents may come from teaching and research institutions in France or abroad, or from public or private research centers.

L'archive ouverte pluridisciplinaire **HAL**, est destinée au dépôt et à la diffusion de documents scientifiques de niveau recherche, publiés ou non, émanant des établissements d'enseignement et de recherche français ou étrangers, des laboratoires publics ou privés.

THÈSE DE DOCTORAT

Régulation de l'échangeur Na^[+]/[H⁺] 1 par les espèces réactives de l'oxygène

Denis DOYEN

Laboratoire de Physiomédecine Moléculaire LP2M - CNRS-UNS UMR 7370 - Nice

**Présentée en vue de l'obtention
du grade de docteur en** Sciences de
la vie et de la santé
d'Université Côte d'Azur

Dirigée par : Laurent Counillon

Soutenu le : 27 Mars 2023

Devant le jury, composé de :

Michel Lazdunski, Académicien des Sciences, IPMC, Valbonne

Laura Baciou, Directrice de Recherche, CNRS UMR 8000, Paris

Sébastien Roger, PU, EA4245, Tours

Dominique Lagadic-Gossmann, Directrice de Recherche, IRSET, Rennes

Jacques Levraut, PU-PH, Service des Urgences CHU de Nice, Nice

Régulation de l'échangeur Na⁺/H⁺ 1 par les espèces réactives de l'oxygène

Jury :

Président du jury

Michel Lazdunski, Professeur, Académicien des Sciences, IPMC, Valbonne

Rapporteurs

Laura Baciou, Directrice de Recherche, CNRS UMR 8000, Paris

Sébastien Roger, PU, EA4245, Tours

Examineurs

Dominique Lagadic-Gossmann, Directrice de Recherche, IRSET, Rennes

Jacques Levraut, PU-PH, Service des Urgences CHU de Nice, Nice

Titre: Régulation de l'échangeur Na⁺/H⁺1 par les espèces réactives de l'oxygène

Résumé

L'échangeur NHE1 Na⁺/H⁺ joue un rôle clef dans la régulation du pH et du volume intracellulaire. Son rôle est paradoxal au cours des phénomènes d'ischémie-reperfusion où son activation provoque une surcharge en sodium et indirectement en calcium ce qui peut provoquer des troubles lors de la reperfusion notamment dans les tissus excitables comme le coeur. Cet échangeur est régulé par le pH intracellulaire, le volume cellulaire et par une multitude de voies de signalisation. Plusieurs études et résultats préliminaires ont indiqué une possible régulation par les espèces réactives de l'oxygène qui sont produites lors de l'ischémie-reperfusion. L'objectif de cette étude est d'analyser par quels mécanismes ces espèces réactives de l'oxygène et en particulier l'anion superoxyde O₂⁻ régulent l'activité de NHE1 et de comprendre quelles régions et quels acides-aminés de NHE1 sont importants pour cette régulation.

L'activité de NHE1 wild type a été mesurée en présence de donneurs d'O₂⁻ (Ménadione) ou en inhibition de production d'O₂⁻ (Diphényliodonium (DPI) inhibiteur de la NaDPH oxydase). L'activité NHE1 a été quantifiée par flux de lithium en fonction du pH intracellulaire. La Ménadione a ainsi entraîné une activation de NHE1 tandis que le DPI a diminué l'activité de NHE1, démontrant que NHE1 est donc régulé par l'O₂⁻. Cette activation par Ménadione et inhibition par DPI sont perdues chez le mutant Cysless de NHE1 dépourvu de toutes ses cystéines. Les cystéines jouent donc un rôle clef dans la régulation de NHE1 par O₂⁻. Nous avons ensuite testé l'inhibition par le DPI sur des mutants de NHE1 sur chacune de ses cystéines. Cela a permis d'identifier plus précisément 3 cystéines clefs dans ce mécanisme.

Afin d'approfondir les groupements structuraux des cystéines potentiellement impliqués dans cette régulation, une analyse des modifications covalentes possibles a été menée incluant la recherche de nitrosylation par biotin switch, la recherche de ponts disulfures par exposition à l'iodoacétamide, et la glutathionylation. Cela a permis de montrer la présence de nitrosylation des cystéines, mais pas de ponts disulfures.

Parallèlement, nous avons constaté un profil d'adhésion et de migration très différent des cellules selon le type de mutant cystéine de NHE1 exprimé. Nous avons donc analysé l'expression de protéines d'adhésion et la liaison de NHE1 au cytosquelette. Par coimmunoprécipitation de NHE1 avec le complexe ERM (Ezrine/Radixine/Moesine) nous avons pu montrer que les cystéines de ce transporteur sont cruciales pour sa liaison avec le complexe ERM et donc à l'actine corticale.

Cette thèse a donc permis de montrer que l'activité de NHE1 est régulée par l'anion superoxyde O₂⁻ et que cette régulation met en jeu certaines cystéines de NHE1 que nous avons identifiées. Nous avons aussi pu montrer que certaines des cystéines de NHE1 sont cruciales pour l'interaction avec le cytosquelette d'actine et jouent un rôle clef dans l'adhésion et la migration cellulaire. L'ensemble de ce travail identifie une connexion clef entre production d'espèces réactives de l'oxygène, la régulation du pH intracellulaire et la motilité et l'adhésion.

Mots-clefs: NHE1 – Régulation – Espèces réactives de l'oxygène – Cystéines

Title: The Na⁺/H⁺ exchanger 1 activity is regulated by reactive oxygen species

Abstract

The NHE1 Na⁺/H⁺ exchanger plays a key role in regulating pH and intracellular volume. Its role is paradoxical during ischemia-reperfusion where its activation causes an overload in sodium and indirectly in calcium which can cause disorders during reperfusion, particularly in excitable tissues such as the heart. This exchanger is regulated by intracellular pH, cell volume and by a multitude of signaling pathways. Several studies and preliminary results have indicated a possible regulation by reactive oxygen species that are produced during ischemia-reperfusion. The objective of this study is to analyze by which mechanisms these reactive oxygen species and in particular the superoxide anion O₂⁻ regulate the activity of NHE1 and to understand which regions and which amino acids of NHE1 are important for this regulation.

The activity of NHE1 wild type was measured in the presence of O₂⁻ donors (Menadione) or in inhibition of O₂⁻ production (Diphenyliodonium (DPI) NaDPH oxidase inhibitor). NHE1 activity was quantified by lithium flux as a function of intracellular pH. Menadione caused an activation of NHE1 while DPI decreased the activity of NHE1, demonstrating that NHE1 is therefore regulated by O₂⁻. This activation by Menadione and inhibition by DPI are lost in the Cysless mutant of NHE1 deprived of all its cysteines. Cysteines therefore play a key role in the regulation of NHE1 by O₂⁻. We then tested the inhibition by DPI on mutants of NHE1 on each of its cysteines, which made it possible to identify more precisely 3 key cysteines in this mechanism.

In order to deepen the structural groups of cysteines potentially involved in this regulation, an analysis of possible covalent modifications was carried out including the search for nitrosylation by biotin switch, the search for disulfide bridges by exposure to iodoacetamide, and glutathionylation. This showed the presence of nitrosylation of the cysteines, but no disulphide bridges.

At the same time, we observed a very different adhesion and migration profile of cells depending on the type of NHE1 cysteine mutant expressed. We therefore analyzed the expression of adhesion proteins and the binding of NHE1 to the cytoskeleton. By coimmunoprecipitation of NHE1 with the ERM complex (Ezrin/Radixin/Moesin) we showed that the cysteines of this transporter are crucial for its binding to the ERM complex and therefore to cortical actin.

My thesis work has therefore made it possible to show that the activity of NHE1 is regulated by the superoxide anion O₂⁻ and that this regulation involves certain cysteines of NHE1 that we have identified. We also showed that some of the cysteines of NHE1 are crucial for the interaction with the actin cytoskeleton and play a key role in cell adhesion and migration. Taken together our study identifies a key connection between the production of reactive oxygen species, the regulation of intracellular pH and cell motility and adhesion.

Keywords: NHE1 – Regulation – Reactive oxygen species – Cysteines

Remerciements

Au **Professeur Michel LAZDUNSKI** : Votre présence dans mon jury est un grand honneur, tant sur le plan scientifique que personnel. Votre expertise et vos remarques seront d'un grand conseil pour améliorer les résultats de mes expérimentations. Votre rigueur et votre humanité font de vous un modèle pour la recherche azuréenne. Je garde un excellent souvenir de vos cours à la faculté de médecine, un des plus faciles à suivre malgré la complexité des sujets. Vos présentations scientifiques très pédagogiques et dynamiques sont toujours agréables à suivre. J'espère que j'aurai l'occasion d'en suivre d'autres.

Au **Docteur Laura BACIOU** : Je vous remercie encore d'avoir accepté et passé autant de temps à relire mon manuscrit de thèse. Vos conseils très pertinents m'ont permis d'améliorer mon travail. J'ai beaucoup apprécié votre accueil à l'occasion du GDR de détection des ROS à Aussois. Le bref séjour ainsi que les présentations y étaient très agréables. J'espère pouvoir y participer de nouveau et que nous pourrions collaborer dans le futur.

Au **Professeur Sébastien ROGER** : Merci infiniment d'avoir pris tout ce temps pour corriger mon travail de thèse, ainsi que pour votre disponibilité et gentillesse tout au long de nos échanges. Vos remarques très judicieuses m'ont permis d'améliorer mon travail. Nous n'avons pas encore eu l'occasion de nous rencontrer mais je suis convaincu que nous pourrions avoir des échanges très constructifs.

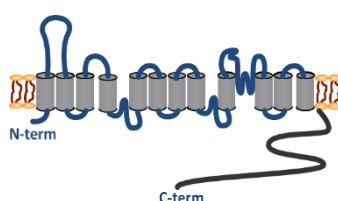
Au **Docteur Dominique LAGADIC-GOSSMANN** : Un grand merci de m'avoir accompagné au long de toutes ces années pour cette thèse qui se termine enfin ! Vos conseils et remarques très pertinents à chaque comité nous ont permis de réorienter nos expérimentations et d'obtenir des résultats intéressants. Je suis content d'enfin pouvoir vous rencontrer. Je ne doute pas que nous pourrions continuer à échanger pour envisager de futurs projets.

Au **Professeur Jacques LEVRAUT** : Je suis très heureux et honoré que vous ayez accepté de lire et juger mon travail malgré toutes les responsabilités que vous avez. Je serai très intéressé par votre expertise scientifique sur le pH cellulaire en rapport avec ma thèse et le lien potentiel clinique qui pourrait en être fait. Nous sommes très satisfaits que vous puissiez mener les différents projets du CHU de Nice à la tête de la CME. Votre calme et perspicacité sont un exemple pour notre institution. J'espère que vous trouverez du temps pour collaborer d'une manière ou d'une autre à nos recherches.

Au **Professeur Laurent COUNILLON** : Merci beaucoup Laurent de m'avoir accepté et dirigé en tant qu'étudiant de thèse depuis maintenant longtemps ! et ce malgré toutes les responsabilités que tu dois supporter. Ta vision et tes connaissances scientifiques que tu transmets que ce soit dans le laboratoire ou en cours sont impressionnantes, et me font toujours rappeler que la science reste un domaine beaucoup plus difficile à appréhender que la médecine. Je pense pouvoir dire que nous nous sommes tout de suite naturellement bien entendus et partageons le même humour ! Je suis très content d'avoir creusé mon trou dans le laboratoire et de pouvoir poursuivre des projets à cheval entre mon exercice médical et le laboratoire dans le futur avec l'équipe. Merci pour tout.

Table des Matières

Résumé – Mots clefs.....	p.3
Abstract – Keywords.....	p.4
Remerciements.....	p.5
Liste des abréviations.....	p.7
I. Généralités.....	p.10
<i>A. Historique et classification des transporteurs NHE.....</i>	<i>p.10</i>
<i>B. Structure de l'échangeur NHE1.....</i>	<i>p.11</i>
<i>C. Expression de l'échangeur NHE1.....</i>	<i>p.26</i>
<i>D. Fonctionnement des transporteurs NHE.....</i>	<i>p.28</i>
<i>E. Rôles de l'échangeur NHE1.....</i>	<i>p.43</i>
<i>F. Régulation de l'échangeur NHE1.....</i>	<i>p.46</i>
<i>G. Interaction de NHE1 avec les espèces réactives de l'oxygène.....</i>	<i>p.49</i>
<i>H. Implication de NHE1 durant l'ischémie-reperfusion.....</i>	<i>p.51</i>
II. Régulation de NHE1 par les espèces réactives de l'oxygène.....	p.92
A. Résumé.....	p.92
B. Matériel et Méthodes.....	p.94
C. Présentation de l'article complet.....	p.103
III. Conclusions - Perspectives.....	p.134
IV. Bibliographie.....	p.141



Liste des abréviations

ADN = Acide désoxyribonucléique

Arg = Arginine

Asp = Acide aspartique

ATP = Adenosine triphosphate

BCECF-AM = 2',7'-Bis-(2-Carboxyethyl)-5-(and-6)

BSA = Bovine serum albumin

CAII = Carbonic anhydrase II

CAM = Calmoduline

CHP1 = Calcineurine β -homologous protein 1

CPA = Cation-proton antiporter

Cys = Cysteine

DHPS = Deoxyhypusine synthase

DOHH = Deoxyhypusine hydroxylase

DMEM = Dulbecco's Modified Eagles

DUOX = dual oxidase

EE = Early endosome

eIF5A = Eukaryotic initiation factor 5A

EL1 = Extra-cellular loop 1

ER = Endoplasmic reticulum

ERK = Extracellular signal-regulated kinase

ERM = Ezrine, radixine, moesine

FCS = Foetal calf serum

GC7 = N1-guanyl-1,7-diaminoheptane

Glu = Glutamine

Gly = Glycine

GPx = glutathione peroxidase

GR = glutathione reductase

GST = glutathione S-transferase

H₂O₂ = Peroxyde d'hydrogène

HEPES = Acide 4-(2-hydroxyéthyl)-1-pipérazine éthane sulfonique

HIF = hypoxia inducible factor

His = Histidine

HO = heme oxygenase

HSP = Heat shock protein

kDa = Kilodalton

KEAP1 = Kelchlike ECH-associated protein 1

LE = Late endosome

Leu = Leucine

LPS = Lipopolysaccharide

LY = Lysosome

MAPK = Mitogen-activated protein kinase

MES = Acide 2-(N-morpholino)éthanosulfonique

Met = Methionine

N = Nucleus

NADPH = Nicotinamide adenine dinucleotide phosphate hydrogen

NaTDC = Na⁺-transporting carboxylic acid decarboxylase

NHE = Na⁺/[H⁺] exchanger

NIK = NF-kappa-β-inducing kinase

NO = Monoxyde d'azote

NOS = Nitric oxide synthase

NOX = NADPH oxidase

NRF2 = Nuclear factor erythroid-2-related factor 2

O_2^- = Anion superoxyde

$\cdot OH$ = Radical hydroxyle

PBS = Phosphate Buffer Saline

Ph = Phenylalanine

PHD = Prolyl-hydroxylase

PI3KAkt/PKG = PI3 kinase/Akt/Protein kinase G

PIP2 = Phosphatidylinositol-4,5-bisphosphate

PKC = Protein kinase C

RE = Recycling endosome

RNS = Espèces réactives de l'azote

ROCK = Rho-associated protein kinase

ROS = Espèces réactives de l'oxygène

RSK = p90 ribosomal S kinase

SDS = Dodécylsulfate de sodium

Ser = Serine

SGLT2 = Sodium/glucose cotransporteur 2

SHP-2 = Src homology-2 domain-containing protein tyrosine phosphatase-2

SLC9 = Solute carrier 9 A-C

SOD = Superoxide dismutase

TGN = Trans-Golgi network

Thr = Threonine

TM = Segment transmembranaire

tMCAo = Transient middle cerebral artery occlusion

Tyr = Tyrosine

XDH = Xanthine dehydrogenase

XOR = Xanthine oxido-reductase

I. Généralités

Le transporteur NHE1 est ubiquitaire se situant à la membrane plasmique de tous les types cellulaires des mammifères. Il est responsable d'un échange électroneutre en permettant la sortie d'un ion H^+ pour la rentrée d'un ion Na^+ .¹

Il est ainsi indispensable à la régulation acido-basique et hydro-électrolytique de la cellule. Il fait partie de la famille des solute carrier 9 A-C (SLC9) qui jouent un rôle capital dans le fonctionnement des cellules. La famille SLC9 se compose de 3 sous-familles: SLC9A, -B et -C. Les transporteurs de ces membres sont tous électroneutres sauf le NHE10 exprimé dans les spermatozoïdes.² La similitude d'acide aminés entre ces différentes branches est de 12 à 71%. Chaque branche a une expression, une régulation et un rôle physiologique particulier.³

A. Historique et classification des transporteurs NHE

Les échangeurs NHE sont apparus probablement très tôt dans l'évolution. En effet, archées, bactéries et eucaryotes sont tous dotés de ces transporteurs et dérivent du même ancêtre commun, ce qui signifie que cet ancêtre commun à tous les êtres vivants était également doté d'un échange Na^+/H^+ .⁴ Mitchell démontrait pour la première fois en 1966 l'existence d'un transport électroneutre à travers la membrane mitochondriale.⁵ La mise en évidence précise directe d'une activité NHE était obtenue chez la bactérie puis chez les mammifères.^{6,7} L'hypothèse a été faite que très tôt dans l'évolution l'apparition précoce du couplage du transport d'un ion Na^+ à celui des ions H^+ dans le même transporteur a pu permettre un gain énergétique pour la cellule en contribuant aux phénomènes de phosphorylation oxydative.⁸

Il existe 3 familles de transporteurs NHE : les familles cation-proton antiporter (CPA) CPA1 et CPA2 qui comportent des antiports de cation monovalent, et 1 famille NaTDC.⁹

Au cours de l'évolution, chez les procaryotes les NHE sont majoritairement

électrogéniques et possèdent une coopérativité négative pour les ions H⁺ dont le gradient de H⁺ favorise l'extrusion de Na⁺. Chez les eucaryotes, les échanges sont électroneutres et possèdent une coopérativité positive pour les H⁺ les rendant efficaces plutôt pour réguler le pH intracellulaire. Chez les vertébrés, les isoformes NHE sont très conservées mais cette conservation a tendance à diminuer quelque peu en alignant les séquences, par exemple celle de NHE1 avec les NHE des invertébrés.¹

Les NHE comportent plusieurs sous-groupes : un sous-groupe comprenant NHE1 à NHE5, un sous-groupe comprenant NHE6, 7 et 9 et NHE8 qui est classé dans une autre branche. L'évolution montre que les NHE ont probablement d'abord été des formes insérées dans les membranes des compartiments intra-cellulaires puis à la membrane plasmique.¹⁰ Actuellement, NHE1, 2 et 4 sont localisés à la membrane plasmique. NHE3, 5 et 8 transitent également dans les compartiments intracellulaires mais sont fonctionnels essentiellement à la membrane plasmique. Les NHE6, 7 et 9 se situent eux dans les compartiments intracellulaires.

B. Structure de l'échangeur NHE1

La structure de NHE1 a récemment enfin pu être très précisément décrite par Dong *et al.* en cryo-microscopie électronique.¹¹ NHE1 s'assemble en homodimère symétrique associé à son partenaire CHP1 qui permet l'expression de NHE1 à la membrane plasmique.¹¹ NHE1 contient 2 grandes parties: une partie transmembranaire avec environ 500 acides aminés avec 13 segments transmembranaires hélicaux nécessaires et suffisants pour assurer la fonction transport, et une queue intracellulaire de plus de 300 acides aminés importante pour la régulation du transporteur. La présence d'un peptide signal clivable à la partie N-terminale de NHE1 est controversée. La première boucle intracellulaire présente des parties très glycosylées ce qui donne à la protéine un poids moléculaire apparent de 110 kD. Les NHE1 non matures se situant dans le réticulum endoplasmique possèdent encore une partie N-terminale glycosylée (high mannose) qui

correspond à la bande caractéristique d'environ 85 kDa en Western Blot.¹² Le segment TM8 est important pour l'expression membranaire de NHE1: une mutation dans le segment TM8 est associée à une expression diminuée de NHE1 à la membrane. Il existe également des régions importantes pour le ciblage au niveau de la partie C-terminale de NHE1 et des mutations à ce niveau entraînent une perte de la coopérativité et une diminution de l'activité de NHE1.¹³

Pour chaque protomère, la partie transmembranaire nécessaire et suffisante pour le transport s'organise en une partie impliquée dans la dimérisation (et donc la coopérativité dans la réponse aux H⁺ intracellulaires) et une partie impliquée dans le transport, qui subirait une modification conformationnelle semblable à celle d'un ascenseur durant le transport des cations.¹¹

Dans la revue invitée suivante récemment publiée par notre équipe, « ***How Does Our Knowledge on the Na⁺/H⁺ Exchanger NHE1 Obtained by Biochemical and Molecular Analyses Keep up With Its Recent Structure Determination ?*** », ¹⁴ à partir de la récente description de NHE1 en cryo-microscopie électronique¹¹ nous avons analysé de façon restrospective comment les travaux d'études structure-fonction réalisés pendant les trois précédentes décennies étaient en adéquation ou en inadéquation avec les données structurales obtenues, notamment pour le transport des cations, la stabilisation du dimère, la transition allostérique, la régulation par les voies de signalisation intracellulaire, et les interactions pharmacologiques.¹⁴

Dans cette revue, l'analyse de la structure montre une conservation de la séquence entre les espèces concernant les acides aminés dans les segments transmembranaires qui sont responsables de la structure et du transport. Cette conservation est moins importante concernant les acides aminés retrouvés dans les boucles. Une différence de longueur des segments transmembranaires entre les prévisions par profils d'hydrophathie et les études topologiques est observée, expliquant au niveau des segments les plus longs une partie plus épaisse sur les côtés, et au niveau des segments les plus courts

une partie plus fine au milieu du dimère favorisant le couplage entre les protomères potentiellement importants pour les signaux mécaniques. Au niveau de l'interface du dimère est notée également une flexibilité dans les liaisons hydrogènes au niveau des hélices transmembranaires. Une partie importante pour la stabilité du dimère et la réaction allostérique est retrouvée entre Cys 561 et Ala 575 dans la région cytoplasmique, et forme avec une hélice amphipathique démarrant à la Pro 571 un complexe pouvant interagir avec son partenaire. A noter la présence d'hélices alpha interrompues notamment au niveau des segments transmembranaires (TM) 5, 12 et 13 qui exposent des groupements carbonyle ou amine hydrogène libres pour de potentielles interactions. Les interactions hélices-hélices hydrophobes de 2 segments TM11 face à face près de Ser 375, ainsi qu'au niveau de TM8 et TM1 dans la partie transmembranaire permettent de maintenir le dimère.

La modélisation 3D de la structure de NHE1 a permis aussi d'identifier des acides aminés clefs dont la conformation pourrait permettre de faciliter une interaction directe avec les inhibiteurs, ce qui confirme les études de mutagenèse : Leu 163 et Phe 162 de TM3¹⁵, Glu 346 du segment TM8, Leu 468 du segment TM11. D'autres acides aminés pourraient permettre de manière indirecte une interaction avec un inhibiteur (TM11 His 473, Met 476, TM2/EL2 Gly 148, Phe 155, His 349).

L'analyse permet de bien situer les acides aminés des régions impliqués dans le passage d'une conformation de basse à haute affinité pour les H⁺ et conférant ainsi à NHE1 cette fonction de senseur de protons. Cette fonction est liée notamment à des acides aminés non déprotonables qui se situent à des interfaces clefs de NHE1: dimère, partie C-terminale et zones charnières de NHE1. Ser 375 et Tyr 381 aussi ne sont pas déprotonables mais jouent un rôle important plutôt dans la conformation du dimère de NHE1.

A l'interface des 2 protomères se situe un acide aminé important Arg 327, identifié par le laboratoire en 2004, qui se situe aussi à proximité de Ser 375 et Tyr 381 précédemment cités, à distance idéale pour la réalisation de ponts d'hydrogène entre ces régions.

L'ensemble des données structurales et de mutagenèse montre une excellente adéquation avec le modèle de fonctionnement coopératif de NHE1 publié par l'équipe en 2004.¹⁶

Enfin, l'analyse de la structure permet aussi de mieux visualiser la réversibilité dans le transport, en mettant en évidence une symétrie dans la structure des acides aminés protonables (Glu 131, Asp 172, Asp 238 et Asp 267). La fixation de Na⁺ ou H⁺ entraîne un changement conformationnel réversible et la fixation du Na⁺ empêcherait la fixation de H⁺ et inversement.



How Does Our Knowledge on the Na⁺/H⁺ Exchanger NHE1 Obtained by Biochemical and Molecular Analyses Keep up With Its Recent Structure Determination?

Mallorie Poet^{1,2}, Denis Doyen^{1,2,3}, Emmanuel Van Obberghen^{1,2,3}, Gisèle Jarretou^{1,2}, Yann Bouret⁴ and Laurent Counillon^{1,2*}

¹Université Côte d'Azur, CNRS, Laboratoire de Physiologie Moléculaire (LP2M), Nice, France, ²Laboratories of Excellence Ion Channel Science and Therapeutics, Nice, France, ³Centre Hospitalier Universitaire de Nice, Nice, France, ⁴Université Côte d'Azur, CNRS, Institut de Physique de Nice (INPHYNI), Valbonne, France

OPEN ACCESS

Edited by:

Francesca Di Sole,
Des Moines University, United States

Reviewed by:

John Orłowski,
McGill University, Canada
Christian Martin Stock,
Hannover Medical School, Germany

*Correspondence:

Laurent Counillon
Laurent.Counillon@unice.fr

Specialty section:

This article was submitted to
Membrane Physiology and Membrane
Biophysics,
a section of the journal
Frontiers in Physiology

Received: 29 March 2022

Accepted: 06 June 2022

Published: 15 July 2022

Citation:

Poet M, Doyen D, Van Obberghen E, Jarretou G, Bouret Y and Counillon L (2022) How Does Our Knowledge on the Na⁺/H⁺ Exchanger NHE1 Obtained by Biochemical and Molecular Analyses Keep up With Its Recent Structure Determination? *Front. Physiol.* 13:907587. doi: 10.3389/fphys.2022.907587

Na⁺/H⁺ exchangers are membrane transporters conserved in all living systems and therefore are assumed to be amongst the most ancestral molecular devices that equipped the first protocells. Following the cloning and sequencing of its gene, the mammalian NHE1, that regulates pH and volume in all cells, has been thoroughly scrutinized by molecular and biochemical analyses. Those gave a series of crucial clues concerning its topology, dimeric organization, pharmacological profile, regulation, and the role of key amino acids. Recently thanks to cryogenic Electron Microscopy (Cryo-EM) the long-awaited molecular structures have been revealed. With this information in mind we will challenge the robustness of the earlier conclusions and highlight how the new information enriches our understanding of this key cellular player. At the mechanistic level, we will pinpoint how the NHE1 3D structures reveal that the previously identified amino acids and regions are organized to coordinate transported cations, and shape the allosteric transition that makes NHE1 able to sense intracellular pH and be regulated by signaling pathways.

Keywords: Na⁺/H⁺ exchanger 1, structure function studies, allosteric regulation, kinetics, protein 3D structure

INTRODUCTION

The Na⁺/H⁺ exchangers of the SLC9A gene family (NHEs) are expressed in all mammalian cells and tissues where they exert multiple physiological roles and share functional redundancy with other membrane transport proteins (Doyen et al., 2022). While NHE1 mostly regulates pH and cell volume, the epithelial NHE2, 3, 4 are important for mediating salt and bicarbonate balance across epithelia such as kidney and intestine while NHE8 is crucial for intestine goblet cells mucus secretion (for review see Aronson et al., 1982; Pedersen and Counillon 2019). The vesicular NHEs (6, 7, and 9) regulate pH in intracellular compartments. Several NHEs have been implicated in disease situations, that can be linked to NHE mutations, su1993bch as for example, the Christianson's syndrome for NHE6 (Gilfillan et al., 2008) that includes both neurodevelopmental and neurodegenerative defects, the autism spectrum disorders for NHE7 and NHE9 (Morrow et al., 2008), or chronic diarrhea (Schultheis et al., 1998). NHEs are also involved in acquired pathologies such as heart ischemia-reperfusion for NHE1 (Lazdunski et al., 1985, for review see for example; Pedersen and Counillon 2019).

Briefly, the mammalian Na^+/H^+ exchange activity was measured for the first time by Heini Murer and collaborators (Murer et al., 1976) and the first Na^+/H^+ exchanger cDNA encoding NHE1 was cloned a decade later by the Pouyssegur's group (Sardet et al., 1989). This was followed by the cloning of the other NHE2-9 isoforms expressed notably in epithelia or intracellular compartments (Tse et al., 1992; Tse et al., 1993; Orłowski et al., 1992; Attaphitaya et al., 1999; Numata and Orłowski 2001). The sequences of these exchangers led to the production of hydropathy plots that gave the first insight into the NHEs as membrane proteins, as well as sequence comparison that enabled to identify highly conserved amino acids possibly involved in transport or regulatory functions and hence pointing to conceivable pharmacological interventions. Thanks to these cDNAs and the selection of NHE-deficient cell lines, PS120 cells (Pouyssegur et al., 1984), and AP Cells (Rotin and Grinstein 1989), this also allowed the application of somatic cell genetics and site directed mutagenesis to study the relations between NHE's sequence, topology and function. This generated a whole set of key observations but an unified transport mechanism could not be presented in the absence of any structural data, because of the risk of missing or misinterpreting important information and of reliably connecting them. We will see in this review that kinetic schemes are also required to ensure a suitable treatment of mutagenesis data. In this context a long-awaited breakthrough in the field has been the nearly concomitant resolution of the structure of NHE1 and NHE9 by Cryo-EM (Dong et al., 2021) and (Winkleman et al., 2020). Both articles and their supplementary information highlight for these transporters their chief structural information, functional sites and mechanisms of regulation.

Hence, the purpose of our review, within this dedicated special issue on the Forever Young Na^+/H^+ exchanger, is not to recapitulate the information given in these articles but rather to revisit the main questions and findings that had intrigued the scientific community in the last 3 decades. In particular, we will evaluate to which extent the earlier findings stood the test of time or were forced to be re-conceptualized now that they can be refigured in the recently obtained structures. We will also highlight how biochemical, molecular and structural analysis have mutually enriched the efforts to decipher the particularly important physiological mechanism of proton sensing by NHEs.

For the sake of space and clarity, this review article will mostly focus on the ubiquitous NHE1 that has been subjected to most of the structure-function work. For this transporter, the paper by Dong et al. reports three Cryo-EM structures, 1) one NHE1 CHP1 complex obtained at pH6.5, 2) one generated at pH7.5 that is not noticeably different from the previous one but contains less information on the CHP1 interaction, and 3) one cariporide bound CHP1 complex that is slightly more open and probably stabilized as an outward-facing high affinity for H^+ form. Considering the three models we will mostly compare the pH6.5 and cariporide structures. Of note, the CHP1-NHE1 Cryo-EM structures are in good accordance with the previous structure of CHP1-with a part of NHE1 intracellular loop

obtained by Wakabayashi and colleagues (Ammar et al., 2006; Mishima et al., 2007).

TOPOLOGY AND STRUCTURAL ORGANIZATION OF NHE1

The first cDNA encoding a mammalian Na^+/H^+ exchanger was cloned using genetic complementation and revealed from the start the arrangement characteristic of a transmembrane protein, with 10–12 hydrophobic stretches identified by hydropathy plots as putative transmembrane segments (Sardet et al., 1989).

This topological model predicted a protein with both a N and C terminal inside with a protein globally divided into two large regions: a ~500 amino acids long transmembrane part that was subsequently shown to be necessary and sufficient for transport (Wakabayashi et al., 1992) and a large intracellular tail with multiple sites for regulatory proteins as well as intrinsically disordered regions (Hendus-Altenburger et al., 2017).

The global NHE1 transmembrane organization was subsequently confirmed by the following three observations: 1) the antibody accessibility against the intracellular loop requiring cell membrane permeabilization (Sardet Science 1990), 2) the identification of glycosylation sites on the extracellular loop 1 (Counillon et al., 1994; Tse et al., 1994), and 3) the analysis of protease accessibility assays (Shrode et al., 1998).

Subsequently, Shigeo Wakabayashi's group used the substituted cysteine accessibility method (Karlin and Akabas, 1998) to dissect the positioning of the different amino acids and loops (Wakabayashi et al., 2000). This yielded the first experimentally refined topological model of NHE1 that served as widely accepted reference for exploring the NHEs structure for the next 20 years, until the Cryo-EM structures of NHE1 and NHE9 were finally published. Strikingly this topology was also in good accordance with sequence alignment of NHEs across multiple species. See for example the multiple alignments of Na^+/H^+ exchangers sequences (Pfam0099) in the Pfam database of protein families (<https://pfam.xfam.org>).

This is likely explained by the fact that most of the amino acids in the transmembrane segments of a protein are much more conserved than in loops because they can be involved either in the protein structure, or in the transport mechanism, or in both. In contrast, loops are much more flexible allowing for more sequence variation, with of course some very conserved positions for important amino acids (Pedersen and Counillon 2019).

When unfolded in transmembrane segments, the overall structure for NHE1 reveals a generally satisfactory accordance with the previous topology models together with some interesting discrepancies relating to structurally and functionally important features (**Figure 1**). When excluding the first very short putative TM that was very early on supposed to be a cleaved signal peptide and does not appear on the Cryo-EM structures, all the TMs are in excellent accordance with the actual TM 1 to TM8, where a first topological inversion occurs (**Figure 1B**). This persists until the actual TM10 that was considered as a reentering loop in the previous topological models, while some hydropathy plots had

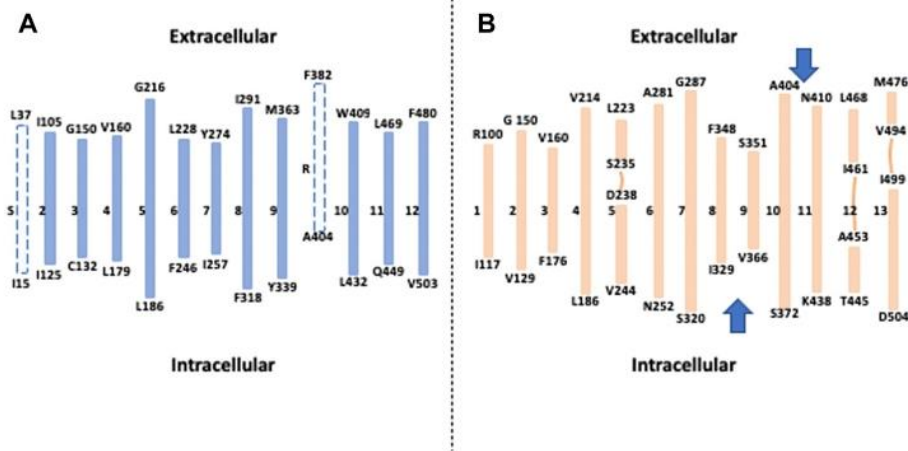


FIGURE 1 | How the Cryo-EM structure changed our view of NHE1 topology: **(A)** Topological model deduced from hydropathy plots, sequence conservation and cysteine accessibility assays. Dotted lines represent respectively a putative signal peptide (S) and a potential transmembrane segment that was subsequently described as a re-entering loop (R). **(B)** The different transmembrane segments obtained from the NHE1 structure at pH 6.5. The lines represent interrupted helices, and the two arrows show topological inversions compared to the model in A.

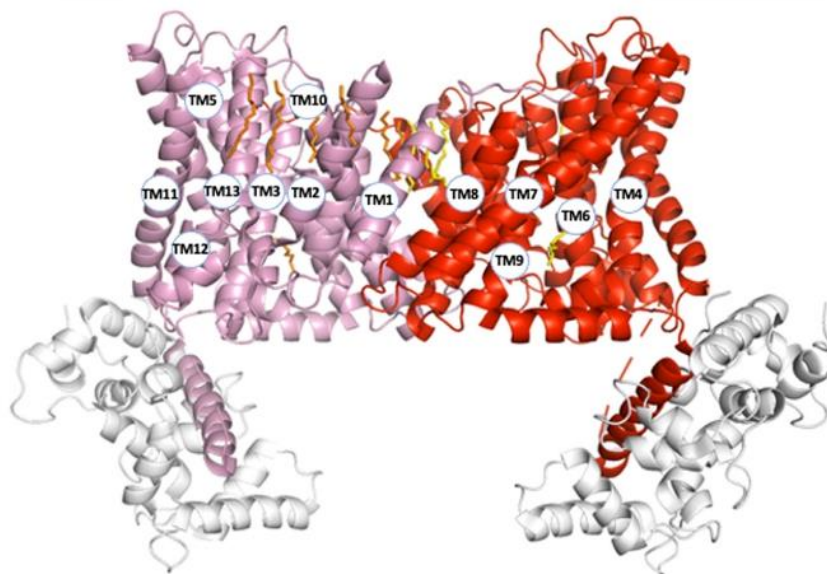


FIGURE 2 | NHE1 structural organization (pH 6.5). To visualize the organization of all transmembrane segments, the two protomers (respectively in pink and red) are represented within the symmetrical dimer. Numbers correspond to the transmembrane segments in **Figure 1B**. The CHP protein bound to NHE1 C-terminal region is represented in light grey.

envisioned it as a putative transmembrane segment (**Figure 1A**) (Wakabayashi et al., 2000). This results in a second topological inversion that enables to have the two last transmembrane segments in the same orientation as in the Wakabayashi's model, with finally the C terminal regulatory region in the cytosol as expected. When zooming on the transmembrane segments themselves, one notable difference is the actual boundaries of the helices between the models and the

structures. While transmembrane segments have been mostly predicted to start at hydrophobic residues to match the bilayer hydrophobicity, a significant part of the transmembrane segment's boundaries contain polar or charged amino acids. This is potentially interesting in terms of future functional characterization as many polar or charged residues that were left unnoticed because in formerly predicted flexible loops are now localized at the edge of more rigid helices where they could

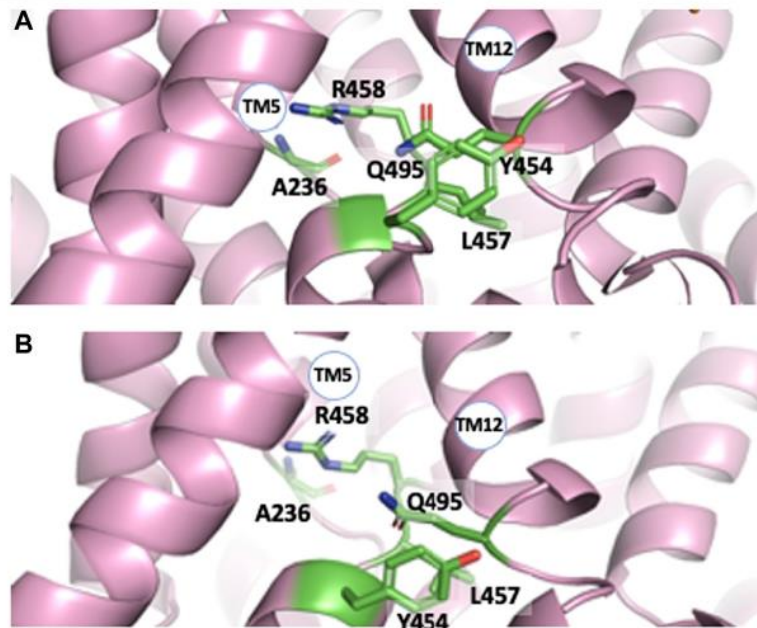


FIGURE 3 | The interrupted transmembrane alpha helical segments 5, 11, and 12, in the pH 6.5 (A) and Amiloride-Bound structure (B) respectively. Note the close vicinity of these regions and the rotation of the Tyr 453-Leu 457 plane with respect to Gln495 between both structures.

intervene in ion coordination or in lipid polar headgroups interaction for example. Furthermore, when comparing the alpha helices between the pH6.5 and cariporide-bound conformations, we could observe that in addition to substantial movements, the transmembrane helices' boundaries can be slightly different, suggesting some flexibility in hydrogen bonding at their edges. As we will see later, this is of particular importance for the allosteric transition that takes place at the dimer interface.

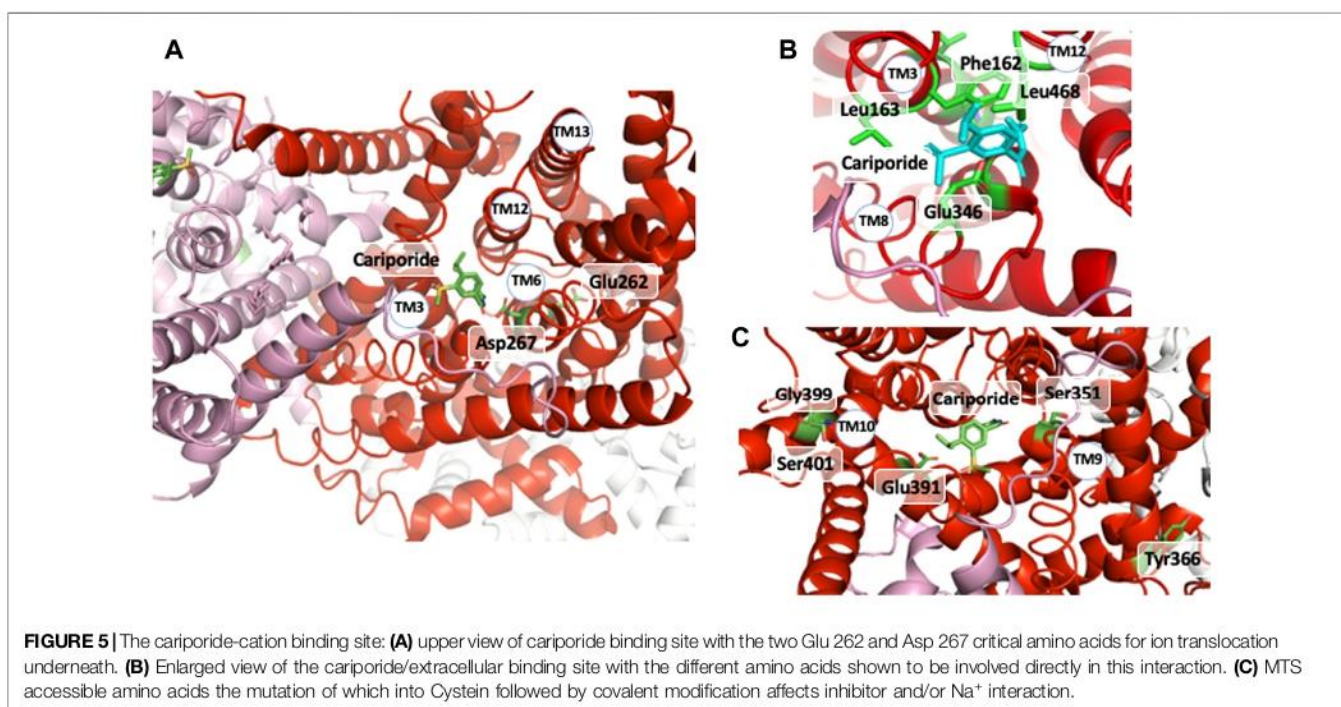
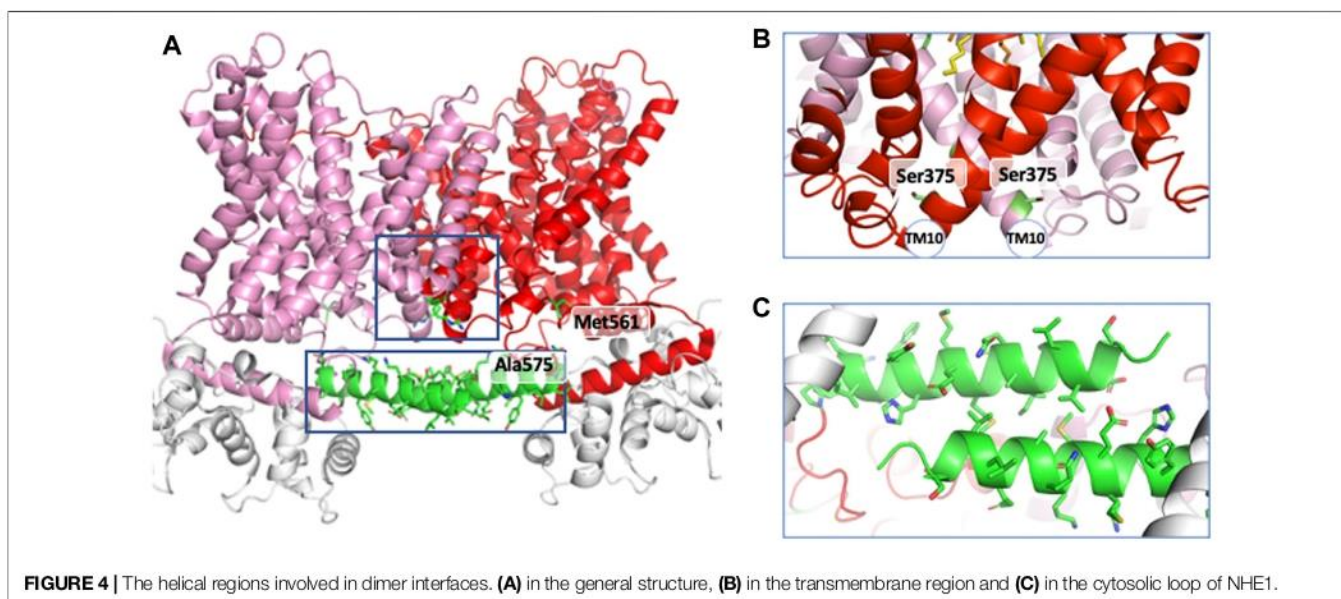
Taken together, the NHE model that has been used for more than 20 years has been accurately predicting 10 transmembrane segments out of 13, which is an impressive achievement. The main differences come from boundaries and stretches of sequences that were impossible to resolve given the information and experimental tools available.

Another remarkable feature is the high level of complexity of NHE1 structure, similar to those of many other transmembrane transporters. First the length of the transmembrane helices can vary considerably from simple to double for example, 17 amino acids for TM1 compared to 32 for TM10. These large differences fashion the overall shape of the NHE1 structure that is much thinner in the middle of the dimer, where it spans about 30 Å across the membrane plane, than on its side where it spans more than 50 Å, a geometry rendered possible by the large tilts of the longest helices (e.g., TM4, TM7, TM11) situated on the most external part of the structure (Figure 2). Such a geometry with tilted helices at the exterior and a comparatively smaller dimer interface could favor the mechanical coupling between the two protomers, because it would minimize the torque at the dimer interface. This could be important in the context of the NHE1 response to mechanical signals (Lacroix et al., 2008).

All structures also reveal interrupted alpha helices, principally in transmembrane segments 5, 12, and 13 with some amino acids in these regions showing important degrees of conservation (Pedersen and Counillon 2019). Such flexible stretches, that leave also free carbonyls and amine hydrogens for possible interactions, are clustered in very close vicinity to each other in all Cryo-EM structures (Figure 3). Several amino acids could be involved in their interlocking, such as for example Arg 458 (TM12) and Ala 236 backbone carbonyl (TM5). Gln 495 (TM12) is crammed between Leu 457 and Y 454 of TM11 in the pH 6.5 structure (Figure 3A) and is slightly upwards from the plane of these two residues in the cariporide bound sequence (Figure 3B). Noticeably also, the large TM12 flexible loop crosses the protein middle section making this segment starting on the external surface of NHE1 and connecting to the last helix in the core of the transport region. This latter helix is immediately followed by the C terminal regulatory region, with its lipid and CHP binding sites. Taken together, the location of these internal flexible loops makes their roles worth investigating in future studies.

THE DIMER INTERFACES

Following the production of the first anti NHE1 antibodies that enabled to visualize the protein in western blots (Sardet et al., 1990), it immediately became apparent that the transporter existed as a homodimer (Fafournoux et al., 1994). Its structure was disulfide bond independent, stable in the plasma membrane and to a certain extent SDS-resistant, the later point suggesting that hydrophobic helix-helix interactions in the transmembrane



part maintained the dimer (Lemmon et al., 1992). In parallel we found that the dimeric structure of NHE1 was crucial for its regulation by intracellular pH, (Lacroix et al., 2004) a feature the importance of which will be discussed in a later chapter. The oligomeric nature of NHEs led to the identification by the Wakabayashi's group of regions involved in this dimeric interaction (Hisamitsu et al., 2004; Hisamitsu et al., 2006). They used for a large part mutagenesis into cysteines followed by crosslinking, with an uncleavable bifunctional sulfhydryl reagent to map positions that would be in close vicinity within

the dimer. Briefly, this allowed to identify positions 375 and 381 in NHE1 transmembrane domain. This was completed by the discovery that the deletion of a short stretch of sequence between Cys561 and Ala575 in the soluble cytosolic region had a negative effect on the dimer stability and allosteric coupling of NHE1. In contrast, mutating the upstream position 538 had no impact (Hisamitsu et al., 2004; Hisamitsu et al., 2006). The possibility that lipids, in particular PIP₂, could be involved in the dimer stabilization cannot be excluded, as it has been found in the horse NHE9 dimer (Winklemann et al., 2020).

Examination of the NHE1 structure at the dimer interface within the transmembrane segment is in very good accordance with the previous findings. Indeed, it reveals a large plane of contact with strong helix-helix interactions, in particular between the 2TMs 11 that face each other close to Ser375, as well as TM8 and TM1 (Figures 4A,B). In the cariporide bound structure the Cys561-Ala575 stretch of sequence in the C terminal soluble tail is situated just before an amphipathic helix that starts at Pro571 and forms a beautiful antiparallel helix-helix interaction with its exact counterpart parallel to the membrane plane (Figures 4A,C). Hence the structure clearly shows how the 561–575 deletion will destroy this interaction.

TRANSPORTERS ARE NOT RECEPTORS: KINETICS AND STRUCTURE ARE INDISPENSABLE TO INTERPRET MUTAGENESIS

Schematically any analysis of the relationship between the structure and function of NHE1 has to address the following key questions: 1) how and where do the extracellular Na^+ and/or competitive inhibitors bind? 2) is it possible to identify key kinetic steps, regions and conformations that provide clues to the translocation mechanism, and 3) how does a proton bind and regulate the rate of exchange, thereby enabling cells to control their intracellular pH? Concerning the above-mentioned questions, we would like to stress that data obtained from studies using mutated transporters should be analyzed with caution in order to avoid erroneous conclusions. Therefore, in this review, we will draw attention to a series of key principles for the biochemical analysis of affinities and kinetics, which should help to correctly interpret the consequences of the mutations on the structure.

NHEs achieve both a kinetic and thermodynamic tour de force by 1) first allowing ions to cross the energy barrier provided by the hydrophobic membrane, and 2) secondly performing a coupled reaction that uses the energy stored in the Na^+ transmembrane gradient to transport H^+ ion against their electroosmotic gradient. In this context they can be considered as genuine enzymes that catalyze coupled reactions. Hence, it is important to realize that the mechanisms of transport can be formalized usefully using the conceptual and mathematical tools provided by enzyme kinetics as explained in the next section. Keeping this aspect in mind it helps to avoid mistakes that relate to fuzzy concepts called “affinity” for substrates or inhibitors, or “setpoints” or “sensing” for allosteric regulators.

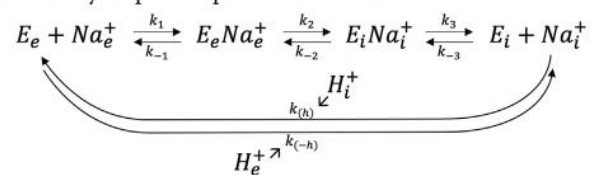
Na^+ and Inhibitor Interaction Are Interlocked: The Michaelis-Menten Equation is Great But Does Not Make It all

Like we previously mentioned, NHEs enable extracellular Na^+ to cross an energy activation barrier constituted by the hydrophobic bulk of membrane lipids and to flow according to its thermodynamic gradient between the outside and inside of cells. At steady-state, the shape of Na^+ dose response curves

for most of the NHEs can be approximated as a hyperbolic saturation function (Pedersen and Counillon 2019). Classically the Michaelis-Menten equation for a saturation curve with extracellular sodium can be written as

$$V = V_{max} \frac{[\text{Na}_e^+]}{K_m + [\text{Na}_e^+]} \quad (1)$$

Where K_m is classically referred from undergraduate textbook biology as the “affinity” for Na^+ . Because there is a transport mechanism, external Na^+ must bind, be translocated and then released upon proton exchange in the other direction. As NHE1 function is dictated by the thermodynamic gradients, the direction of transport is also fully reversible upon the respective Na^+ gradients on each side of the membrane. Consequently, we can write the following kinetic scheme in which every step can operate in each direction.



where the symbol (e) represents extracellular and (i) intracellular. For the sake of simplicity, $k_{(h)}$ and $k_{(-h)}$ represent apparent transport rates for H^+ that are too complex to be developed here mathematically as they contain the cooperative binding and transport mechanism for proton (Lacroix et al., 2004).

Such a simplified mechanism was symbolically encoded in the Maxima computer algebra system (<https://maxima.sourceforge.io>), thus allowing to express each intermediate as a function of $[E_o]$ (the total quantity of exchanger), $[\text{Na}_i^+]$ and $[\text{Na}_e^+]$, and finally express and simplify the net rate of $[\text{Na}_i^+]$ evolution that corresponds here to the transporters steady state velocity ($V = d[\text{Na}_i^+]/dt$). A tight monitoring of the symbolic results let us group the constants in a meaningful way, giving.

$$V = [E_o] \frac{\Lambda_{in} [\text{Na}_e^+] - \Lambda_{out} [\text{Na}_i^+]}{\alpha + \beta [\text{Na}_i^+] + \gamma [\text{Na}_e^+] + \delta [\text{Na}_i^+] [\text{Na}_e^+]} \quad (2)$$

with

$$\Lambda_{in} = k_1 k_2 k_3 k_{(h)}$$

$$\Lambda_{out} = k_{-1} k_{-2} k_{-3} k_{(-h)}$$

and

$$\alpha = [(k_2 + k_{-1})k_3 + k_{-1}k_{-2}] (k_{(-h)} + k_{(h)})$$

$$\beta = k_{-3} [(k_{-2} + k_2 + k_{-1})k_{(-h)} + k_{-1}k_{-2}]$$

$$\gamma = k_1 [(k_3 + k_{-2} + k_2)k_{(h)} + k_2 k_3]$$

$$\delta = (k_{-2} + k_2) k_1 k_{-3}$$

Eq. 2 may look rather complex at first but has several interesting built-in features. The numerator is nicely symmetrical with respect to the kinetic constants, to external Na_e^+ and internal Na_i^+ . The minus sign shows that the transport direction depends on the respective Na^+ concentrations. It also

shows how a rise in intracellular Na^+ concentration will slow down the inward Na^+/H^+ exchange.

Eq. 2 shape is also very close to the Michaelis-Menten Eq. 1 as it can be rearranged into Eq. 3 below.

$$V = [E_o] \frac{\left(\frac{\Delta_{in}}{\gamma + \delta [Na_e^+]}\right) [Na_e^+] - \left(\frac{\Delta_{out}}{\gamma + \delta [Na_e^+]}\right) [Na_i^+]}{\frac{\alpha + \beta [Na_e^+]}{\gamma + \delta [Na_e^+]} + [Na_e^+]} \quad (3)$$

If we consider that the intracellular Na_i^+ concentration is small enough compared to the extracellular Na_e^+ , we could then simplify Eq. 3 by neglecting Na_i^+ into Eq. 4 below.

$$V = \frac{\left(\frac{\Delta_{in}}{\gamma}\right) [E_o] [Na_e^+]}{\frac{\alpha}{\gamma} + [Na_e^+]} \quad (4)$$

Which is the Michaelis-Menten Eq. 1 for Na_e^+ where $V_{max} = \frac{\Delta_{in}}{\gamma} [E_o]$ and $K_m = \frac{\alpha}{\gamma}$.

This implies that when a mutation causes a change in K_m , it is risky to assign this to a change in extracellular Na^+ binding, because its effect could also originate from a change in the off constant (k_3) for intracellular sodium or more subtly by a change in the k_2 and or k_{-2} kinetic constants of the ion translocation itself. Such intricate effects are in principle impossible to tease out from steady state measurements because as it can be seen in such equations, the apparent constants have a complex shape and there are more unknown constants than measurable values.

Another important point which deserves attention concerns the inhibitory constants of the NHE acylguanidine inhibitors such as amiloride or cariporide, because they compete with extracellular sodium. Reciprocally Na^+ also makes competition with the inhibitors and as a consequence, the Michaelis Menten rate equation for transport turns into:

$$V = V_{max} \frac{[Na_e^+]}{K_m \left(1 + \frac{[I]}{K_i}\right) + [Na_e^+]}$$

Here $[I]$ is the inhibitor concentration, K_i the inhibitor dissociation constant (a true K_d on this occasion) and where V_{max} and K_m can have the previous complex expressions. The following facts have to be stressed: 1) a measured $K_{0.5}$ value cannot be assigned to a K_i value because of the presence of Na_e^+ , 2) published work reports different $K_{0.5}$ for the same inhibitor depending on the extracellular cation concentrations used for the measurements, and 3) in case a mutation changes the dose response curve of an inhibitor, the K_m for Na^+ has to be always measured and a data analysis has to be performed to calculate the actual K_i value if K_m is found changed. Taken together, these considerations show that transport data can yield the K_i values for inhibitors when properly treated. However, the situation is problematic if not unusable for Na^+ binding and transport as it is impossible to predict whether a particular position in an NHE is involved in the direct coordination or in the transport of Na^+ or both. In this respect, it is amazing that most of the residues and positions identified by structure-function studies fall in places that belong to these categories in

NHE1 3D structure as the structural complexity and organization now offers insight that could not be revealed by placing the identified crucial amino acids within the previous topological models. Indeed, a constellation of side chains atoms is remarkably in the right place to directly interact with the cariporide structure. As this inhibitor contains a guanidine moiety with a structure similar to a partly hydrated Na^+ , the NHE1 structure also reveals how this cation could sit in its external binding pocket (Figure 5). Those correspond to 1) Leu 163 and Phe162 in the remarkable VFFLFLPPII TM3 sequence (Counillon et al., 1993) (Counillon et al., 1997) (Touret et al., 2001) that makes a very beautiful π -stack with the inhibitors' aromatic ring (2.6 Å distance), 2) TM8 Glu346 that is at less than 2.8 Å from the guanidine group (Khadilkar et al., 2001; Noël et al., 2003). Of note a recent article by Fliegel's group highlighted Leu468 of TM11 that is also in a very close position to the hydrophobic 5-substituents of cariporide, thereby providing a molecular basis on the mechanism by which an increased hydrophobicity of these inhibitors' groups can decrease their K_i values by two orders of magnitude (Li et al., 2021). Finally, the absence of side chain of Gly352 that lies underneath the inhibitor appears to be a steric effect as an amino acid with a large side-chain would collide with the inhibitor (Khadilkar et al., 2001).

In a recent work, Jinadasa et al. (2015) used cysteine substitution and MTS accessibility to map amino acids involved in the interaction with ethylisopropylamiloride, a molecule close to cariporide. This revealed interesting candidates as shown in Figure 5C, clearly accessible to externally-applied MTS, but more likely to exert some distance effect on inhibitor or Na^+ interaction.

Apart from these residues that are obviously in direct interaction with the competitive inhibitor and very likely with the partially hydrated transported Na^+ , mutations at some other positions appear to have indirect distant effects. As explained above in the kinetic analysis of NHE1 transport, mutations that modify K_m or K_i values can have conformational effects that impact kinetic steps instead of binding. When far away but in the same plane as cariporide they likely exert such conformational domino effects on the structure, such as TM11 His 473, Met 476 (Li et al., 2021) or TM2/EL2 Gly 148; and Phe155, or His 349 (Orlowski and Kandasamy, 1996; Khadilkar et al., 2001). Similarly, we described mutations of amino acids in the TM3 sequence, that affected the K_m and apparent inhibition constants of competitors by such distance conformational effects. Those were in particular Gly 174 (Counillon et al., 1997), Ile 169 and 170, the mutation of which were able to revert the Phe162Ser mutation (Touret et al., 2001). From the structure, those are indeed far from the external binding site, thereby confirming the difference between binding and kinetic effects.

The Cooperative Regulation of Transport by Intracellular H^+

Positive cooperativity demarks from classical Michaelis-Menten saturation as the hyperbolic shape of the dose-response curve is

bent to yield a S shape curve, termed sigmoid. Being steeper than a classical hyperbolic, the cooperative response often constitutes a molecular switch, the setpoint of which can be modified by the interaction with different allosteric modulators. Hence, most enzymes or transporters possessing a cooperative behavior have been selected by evolution at strategic positions to activate or block critical biochemical pathways. As protons are one of the most, if not the most relevant ions in physiology, evolution has firmly incorporated cooperativity in NHEs kinetics. Technically, it must be noted that using pH as a variable can be misleading at first glance, because it is the cologarithm of the actual free H^+ ion concentration that is the relevant parameter, with sub millimolar concentrations between 10^{-7} and 10^{-8} mol/L in the cytosol in physiological conditions. This is particularly important for graphical representations as the Log scale that is embedded in pH representations can be confusing when analyzing possible cooperativity.

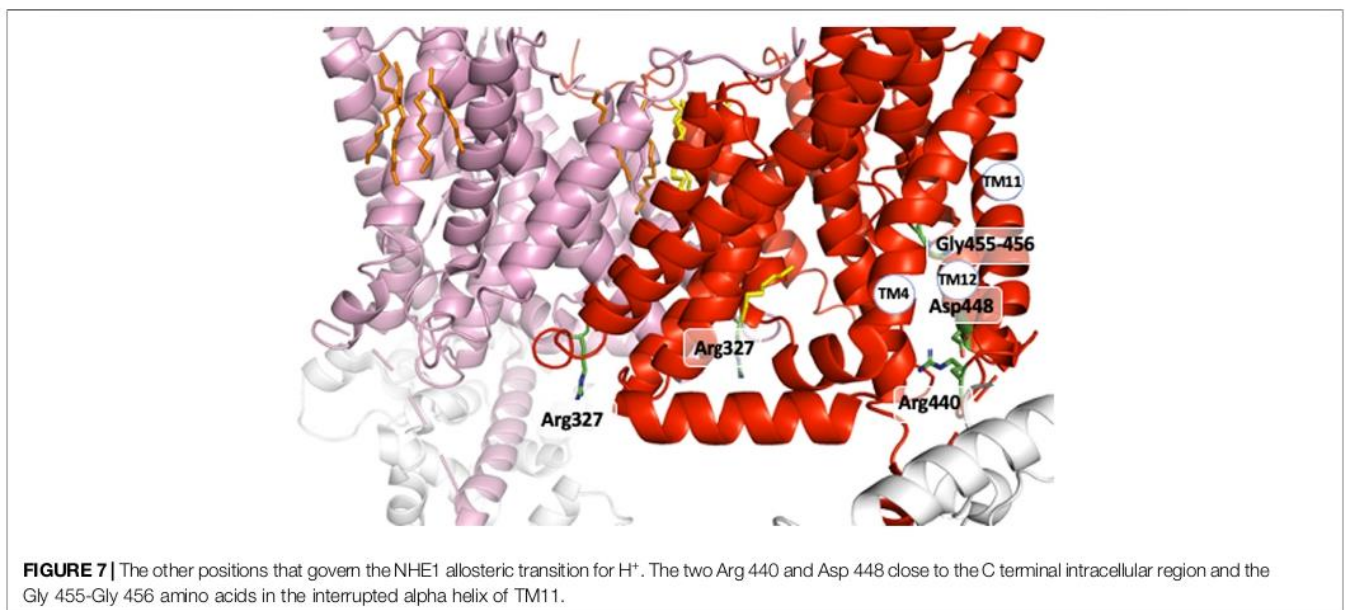
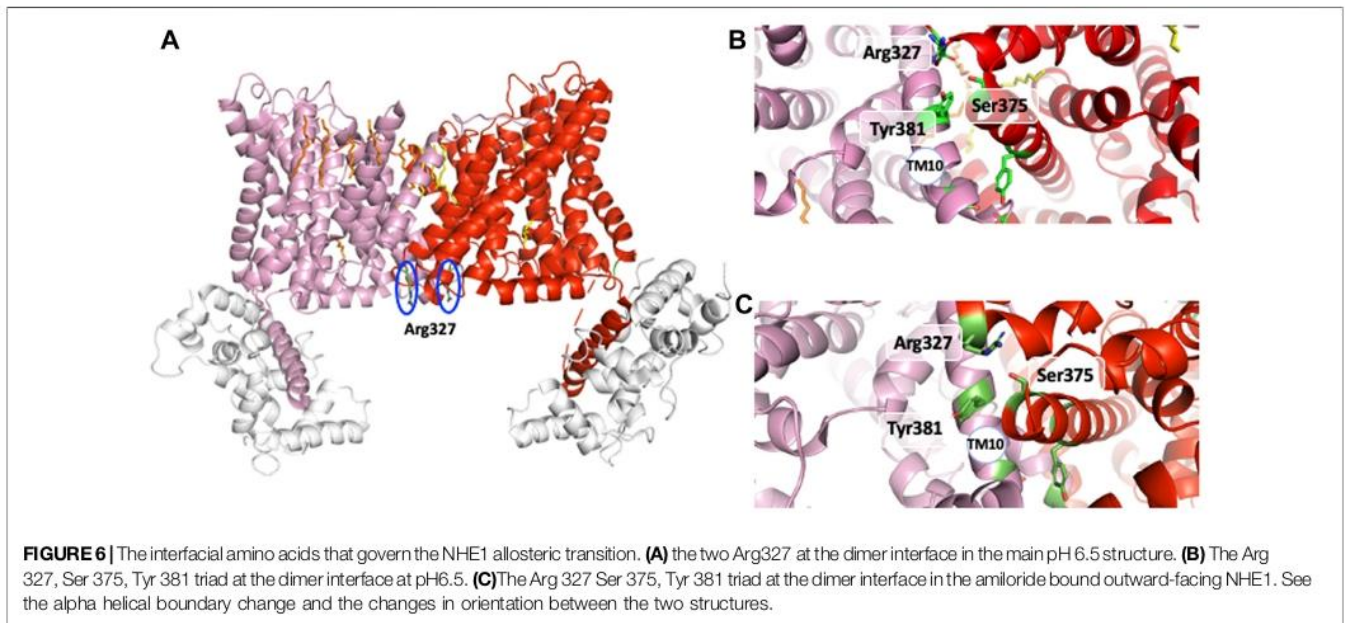
Mathematically, sigmoidal equations rates for enzymes or transporters are different from the logistic equation often used to fit sigmoids and whatever the mechanism, can be written as a fraction of two polynomials for the substrate. This stems from the fact that proteins displaying cooperativity possess more than one binding site for their substrate, leading to multiple equilibria. This means that the reaction order is superior to one for the substrate, and this translates in exponents superior to one for its concentration in the kinetic equations. Another important feature is that those binding sites are neither identical nor independent, meaning that cooperative proteins exist in different conformational states bearing differences in substrate binding or transport. Beyond these general features it is challenging to precisely decipher the underlying mechanisms for any cooperative behavior, because a near infinity of polynomial fractions can fit the same sigmoid. As each equation corresponds to a distinct possible process, it means that it is in principle conceivable to hypothesize an infinite number of mechanisms that would all fit, provided that the constants (that can be fairly complex as explained previously) and exponents are well adjusted. Hence to discriminate between the potential models, extensive information about mutagenesis and/or structure is needed in addition to kinetics and dose responses. Because the required formalism may go beyond the purpose of this review, the interested reader is encouraged to consult advanced enzyme kinetics textbooks such as Bisswanger (2008).

The above-mentioned findings have led to interesting questions concerning the allosteric regulation of NHEs by intracellular H^+ . The first main mechanism proposed after the discovery of the NHEs cooperativity, was that of a monomer with a “proton sensing site” that would allosterically regulate the affinity of the transport site. This led many colleagues to try to identify such a sensor by mutating candidate amino acids, mostly histidines, the pKa of which allows them in principle to bind/unbind H^+ around pH7. However, without entering in mathematical details, a cooperativity model resulting from a mechanism involving a simple binding of an alternative H^+ in a non-transport site would unsatisfactorily fit the data due to the reciprocal dependency of the transport and sensor sites (Lacroix

et al., 2004). Considering the NHEs dimeric structure and a combination of mutagenesis and kinetic analyses we proposed a mechanism in which the two protomers, strongly interlocked within a symmetrical dimer, would oscillate between a low and a high affinity state for H^+ in a concerted manner (Monod et al., 1965). Any change that would affect the balance between these two forms, from covalent modification of the protein to its interaction with different molecules or ions, would change the sigmoidal shape and therefore provide H^+ sensing, without the need for an additional binding site. This is largely mediated through the C-terminal region of NHE1 that contains multiple regulatory sites for signaling pathways. Depending on its interactions with lipids, ATP, proteins and on the balance between its multiple phosphorylations and dephosphorylations (Hendus-Altenburger et al., 2016; Hendus-Altenburger et al., 2019), this region can modify NHE1 cooperativity for protons. In particular, the structure shows that the Pro571-Ser591 short helical antiparallel dimer could be instrumental in this allosteric coupling.

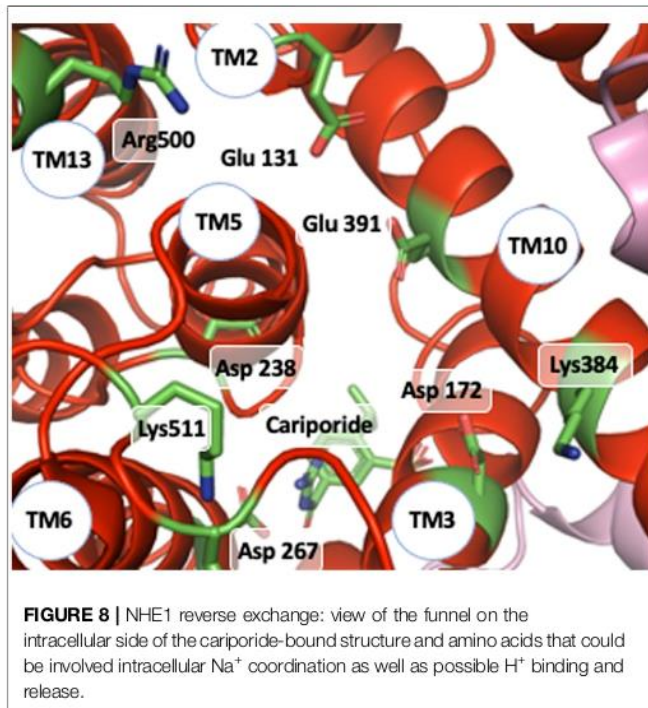
Such regulatory mechanism provides the selective advantage to operate as a sensitive coincidence detector for infinite combinations of stimuli, an action that would be impossible to achieve by direct modification of a proton regulator site.

A strong support for this mechanism came from the identification of distinct mutations that locked NHE1 in non-cooperative conformation and/or the existence of NHEs with lost cooperativity for protons. A similar low affinity non cooperative NHE1 could be obtained respectively through the mutation of conserved Arginines 327 (Lacroix et al., 2004) and 440 (Wakabayashi et al., 2003a; Wakabayashi et al., 2003b), Serine 375 and Tyrosine 381 (Hisamitsu et al., 2006). Interestingly, total (Lacroix et al., 2004) or partial NHE1 C-terminal truncation, such as the above-mentioned Met 561-Ala575 sequence, yielded the same low affinity non-cooperative NHE1 (visible when plotted as a function of H^+ instead of pH in Hisamitsu et al., 2004). Interestingly, Arg 327 is not conserved in the non-cooperative NHE7 that displays a high affinity for intracellular H^+ (Milosavljevic et al., 2014). As arginine's pKa is 12.5, those amino acids are not good candidates for direct H^+ binding and release at physiological pH values. In contrast, bearing a positive charged group at the end of a flexible arm could be extremely useful either to couple to other amino acids or act as a short probes for the electrostatics of their environment. Similarly, the Ser 375 and Tyr 381 are not deprotonable at physiological values but may form hydrogen bond and exert a conformational role. Considering the effects of all these mutations, we can predict that these residues must be placed at strategic positions within the dimer. Indeed, the analysis of the NHE1 structure in different conditions reveals a critical position for the two Arg327 that are situated right at the interface between the two protomers (Figure 6A). In the pH6.5 structure (Figure 6A), these two arginines point the positive extremity of their side chains towards the cytosol, and could work exactly as the previously discussed electrostatic probes. Even more strikingly, Arg 327 is in very close vicinity of Ser 375 and Tyr 381, the two critical residues previously



mapped in the dimer interface (see above) by the Wakabayashi group. In the 6.5 structure, the main backbone carbonyl of Arg 327, and the hydrogens of Ser 375 and Tyr 381 side chain hydroxyl groups are at optimal distances (~ 3 Å) to hydrogen bond. Ser 375 substitution into a cysteine led to a low affinity of NHE1 for protons and this had been interpreted as a possible effect of disulfide bond crosslinking that would block the structure. However, **Figure 4B** shows that these two side chains are pointing in an opposite direction making disulfide bond formation unlikely. Interestingly, the cariporide-bound structure shows a totally different configuration in which Arg 327 is not in a flexible loop.

Indeed, its main chain carbonyl is engaged in an alpha helix, with no possibility to interact with the previous amino acids, its side chain being 6–8 Å apart from the Ser 375 hydroxyl. Moreover, in this conformation, the Tyr 381 side chain is now totally opposite to the dimer interface. Taken together, the input from the structural information highlights the importance of the previously discovered amino acids in a symmetrical dimer. In addition, the conformational changes resulting in the exquisite sensitivity of NHE1 for protons (Lacroix et al., 2004) are uncovered. Arg 440 mutations were also identified for giving a very similar phenotype as those of Arg 327 while Asp 448, Gly 455, and 456 mutations



resulted in an enhanced sensitivity to protons. These positions in the structure are far away from the dimer interface. Gly 455 and 456 are in the TM11 non-helical region (Figure 7). Arg 440 and Asp 448 are present in a perfect pocket constituted by helices TM4, 11, 12, and the CHP binding region (Figure 7). Interestingly, mutations that affect NHE1 activity or its response to intracellular pH have been identified between Leu 432 and Lys 443 by the Fliegel's group (Wong et al., 2019).

It is important to stress that all the mutations that decrease the H⁺ sensing for intracellular H⁺ involve amino acids that cannot be protonated/deprotonated around the NHE1 setpoint for intracellular H⁺, nearby physiological pH. In contrast, they are all at interfacial positions, either at the dimer interface, or at the boundary with the regulatory C-terminal loop or at hinge sequences of NHE1. Another important point is that all the Cryo-EM structures correspond to symmetrical dimers, and not to different conformations within the same dimer. Taken in aggregate, the above summarized studies provide a strong accumulation of results in favor of a concerted cooperative mechanism for proton sensing.

PENDING QUESTIONS: REVERSIBILITY AND STOICHIOMETRY

As mentioned in a previous section of this manuscript, NHE1 is a reversible transporter. This implies some symmetry in the distribution of protonable amino acids that could bind Na⁺ and/or H⁺ within its structure. Indeed, opposite to the cariporide binding site there is a large funnel opening to the intracellular side. Very good candidates such as Glu 131, Asp 172, or Asp 238 (Figure 8) are present in this region and could very

well coordinate Na⁺ as proposed by (Dong et al., 2021), taking into account the structure homology with the Thallium bound PaNhaP structure. Other amino acids such as Glu 391, Lys 511 or Arg 500 could also participate in shaping the electrostatics of this funnel (Figure 8). The critical Asp 267 is situated at a pivotal position between the outward facing funnel that bears the cariporide binding site (see Figure 8) and this inward facing funnel.

Taken together what emerges from this model is that a change of electrostatics due to Na⁺ ion binding in one of these funnels could trigger a reversible conformational change that then would cause Na⁺ translocation towards the other funnel.

In such a mechanism, Na⁺ and H⁺ binding on the previously mentioned carboxylic groups could be mutually exclusive. Such a feature would therefore constitute a molecular basis for the antiport function of NHE1. One important question that remains unanswered yet is the molecular basis for the 1:1 exchange stoichiometry. This is a non-trivial question for at least two reasons: firstly, the proton is the smallest possible cation, and therefore it could bind and unbind different side chains, hydrogen bond, or cross energy barriers to travel through rigid sections of the protein by other mechanisms such as quantum tunnelling effect, like in ice (Atkins and de Paula, 2013) or enzymes (Bothma et al., 2010). Secondly, one must not forget that this 1:1 stoichiometry is a macroscopic feature of the transport, that is measured on a large quantity of molecules and transport cycles. Therefore, it cannot be excluded that different microscopic transport mechanisms averaging to 1:1 could coexist. Solving this fascinating problem will likely require a combination of mutagenesis, coupled to sophisticated kinetics and molecular simulations.

Take Home Messages

As stated in the introduction, the structural determination of NHE1 and NHE9 have provided a long-awaited and decisive breakthrough in the understanding of the Na⁺/H⁺ exchange world. The aim of our short review in the context of this dedicated issue was to put in a historical perspective some of the main findings that shaped the NHE1 knowledge for many years, namely the topology, dimeric structure, biochemical analysis and key mutations. Learning from the past and considering the advances already made in the field, it is obvious that further progress is contingent on combining structural information with data from functional measurements with the adequate methods that will have to use more sophisticated mathematics and modeling. Future progress will also come from setting up more resolute measurement methods such as extremely fast presteady state kinetics.

Finally, while the unraveling of the tridimensional structure of the Na⁺/H⁺ exchanger is clearly a spectacular leap forward in the field, it is gratifying for the pioneers in this research area that most of their vision on their favored molecule has stood the test of time. In the meantime, it is fascinating to see how results that could appear rather abstract are now highlighted in a very visual and even aesthetic perspective in those structures.

Times are changing -so are models but for both the former and the current Na⁺/H⁺ exchanger scientists “beauty is in the eyes of the beholder” (Aronson et al., 1982; Wakabayashi et al., 2003b).

AUTHOR CONTRIBUTIONS

All authors listed have made a substantial, direct, and intellectual contribution to the work and approved it for publication.

REFERENCES

- Ammar, Y. B., Takeda, S., Hisamitsu, T., Mori, H., and Wakabayashi, S. (2006). Crystal Structure of CHP2 Complexed with NHE1-Cytosolic Region and an Implication for pH Regulation. *EMBO J.* 25, 2315–2325. doi:10.1038/sj.emboj.7601145
- Aronson, P. S., Nee, J., and Suhm, M. A. (1982). Modifier Role of Internal H⁺ in Activating the Na⁺-H⁺ Exchanger in Renal Microvillus Membrane Vesicles. *Nature* 299, 161–163. doi:10.1038/299161a0
- Atkins, P., and de Paula, J. (2013). *Elements of Physical Chemistry*. 6th edition. Oxford University Press. ISBN 978-0-19-960811-9.
- Attaphitaya, S., Park, K., and Melvin, J. E. (1999). Molecular Cloning and Functional Expression of a Rat Na⁺/H⁺ Exchanger (NHE5) Highly Expressed in Brain. *J. Biol. Chem.* 274, 4383–4388. doi:10.1074/jbc.274.7.4383
- Bisswanger, H. (2008). *Enzyme Kinetics: Principles and Methods*. Second Edition. Wiley-VCH Verlag GmbH & Co. KGaA.
- Bothma, J. P., Gilmore, J. B., and McKenzie, R. H. (2010). The Role of Quantum Effects in Proton Transfer Reactions in Enzymes: Quantum Tunneling in a Noisy Environment? *New J. Phys.* 12 (27pp), 055002. doi:10.1088/1367-2630/12/5/055002
- Counillon, L., Franchi, A., and Pouyssegur, J. (1993). A Point Mutation of the Na⁺/H⁺ Exchanger Gene (NHE1) and Amplification of the Mutated Allele Confer Amiloride Resistance upon Chronic Acidosis. *Proc. Natl. Acad. Sci. U.S.A.* 90, 4508–4512. doi:10.1073/pnas.90.10.4508
- Counillon, L., Pouyssegur, J., and Reithmeier, R. A. F. (1994). The Na⁺/H⁺ Exchanger NHE-1 Possesses N- and O-Linked Glycosylation Restricted to the First N-Terminal Extracellular Domain. *Biochemistry* 33, 10463–10469. doi:10.1021/bi00200a030
- Counillon, L., Noël, J., Reithmeier, R. A. F., and Pouyssegur, J. (1997). Random Mutagenesis Reveals a Novel Site Involved in Inhibitor Interaction within the Fourth Transmembrane Segment of the Na⁺/H⁺ Exchanger-1. *Biochemistry* 36, 2951–2959. doi:10.1021/bi9615405
- Dong, Y., Gao, Y., Ilie, A., Kim, D., Boucher, A., Li, B., et al. (2021). Structure and Mechanism of the Human NHE1-CHP1 Complex. *Nat. Commun.* 12 (1), 3474. doi:10.1038/s41467-021-23496-z
- Doyen, D., Poët, M., Jarretou, G., Pisani, D. F., Tauc, M., Cougnon, M., et al. (2022). Intracellular pH Control by Membrane Transport in Mammalian Cells. Insights into the Selective Advantages of Functional Redundancy. *Front. Mol. Biosci.* 9, 825028. doi:10.3389/fmolb.2022.825028
- Fafournoux, P., Noël, J., and Pouyssegur, J. (1994). Evidence that Na⁺/H⁺ Exchanger Isoforms NHE1 and NHE3 Exist as Stable Dimers in Membranes with a High Degree of Specificity for Homodimers. *J. Biol. Chem.* 269, 2589–2596. doi:10.1016/s0021-9258(17)41985-5
- Gillfillan, G. D., Selmer, K. K., Roxrud, I., Smith, R., Kyllerman, M., Eiklid, K., et al. (2008). SLIC9A6 Mutations Cause X-Linked Mental Retardation, Microcephaly, Epilepsy, and Ataxia, a Phenotype Mimicking Angelman Syndrome. *Am. J. Hum. Genet.* 82, 1003–1010. doi:10.1016/j.ajhg.2008.01.013
- Hendus-Altenburger, R., Pedraz-Cuesta, E., Olesen, C. W., Papaleo, E., Schnell, J. A., Hopper, J. T. S., et al. (2016). The Human Na⁺/H⁺ Exchanger 1 Is a Membrane Scaffold Protein for Extracellular Signal-Regulated Kinase 2. *BMC Biol.* 14, 31. doi:10.1186/s12915-016-0252-7
- Hendus-Altenburger, R., Lambrugh, M., Terkelsen, T., Pedersen, S. F., Papaleo, E., Lindorff-Larsen, K., et al. (2017). A Phosphorylation-Motif for Tuneable Helix Stabilisation in Intrinsically Disordered Proteins - Lessons from the Sodium Proton Exchanger 1 (NHE1). *Cell. Signal.* 37, 40–51. doi:10.1016/j.cellsig.2017.05.015
- Hendus-Altenburger, R., Wang, X., Sjøgaard-Frich, L. M., Pedraz-Cuesta, E., Sheftic, S. R., Bendsoe, A. H., et al. (2019). Molecular Basis for the Binding and Selective Dephosphorylation of Na⁺/H⁺ Exchanger 1 by Calcineurin. *Nat. Commun.* 10 (1), 3489. doi:10.1038/s41467-019-11391-7
- Hisamitsu, T., Pang, T., Shigekawa, M., and Wakabayashi, S. (2004). Dimeric Interaction between the Cytoplasmic Domains of the Na⁺/H⁺ Exchanger NHE1 Revealed by Symmetrical Intermolecular Cross-Linking and Selective Co-immunoprecipitation. *Biochemistry* 43, 11135–11143. doi:10.1021/bi049367x
- Hisamitsu, T., Ammar, Y. B., Nakamura, T. Y., and Wakabayashi, S. (2006). Dimerization Is Crucial for the Function of the Na⁺/H⁺ Exchanger NHE1. *Biochemistry* 45, 13346–13355. doi:10.1021/bi0608616
- Jinadasa, T., Josephson, C. B., Boucher, A., and Orlowski, J. (2015). Determinants of Cation Permeation and Drug Sensitivity in Predicted Transmembrane Helix 9 and Adjoining Exofacial Re-entrant Loop 5 of Na⁺/H⁺ Exchanger NHE1. *J. Biol. Chem.* 290, 18173–18186. doi:10.1074/jbc.M115.642199
- Karlin, A., and Akabas, M. H. (1998). [8] Substituted-Cysteine Accessibility Method. *Methods Enzymol.* 293, 123–145. doi:10.1016/s0076-6879(98)93011-7
- Khadilkar, A., Iannuzzi, P., and Orlowski, J. (2001). Identification of Sites in the Second Exomembrane Loop and Ninth Transmembrane Helix of the Mammalian Na⁺/H⁺ Exchanger Important for Drug Recognition and Cation Translocation. *J. Biol. Chem.* 276 (47), 43792–43800. doi:10.1074/jbc.M106659200
- Lacroix, J., Poët, M., Maehrel, C., and Counillon, L. (2004). A Mechanism for the Activation of the Na/H Exchanger NHE-1 by Cytoplasmic Acidification and Mitogens. *EMBO Rep.* 5 (1), 91–96. doi:10.1038/sj.embor.7400035
- Lacroix, J., Poët, M., Huc, L., Morello, V., Djerbi, N., Ragno, M., et al. (2008). Kinetic Analysis of the Regulation of the Na⁺/H⁺ Exchanger NHE-1 by Osmotic Shocks. *Biochemistry* 47 (51), 13674–13685. doi:10.1021/bi801368n
- Lazdunski, M., Frelin, C., and Vigne, P. (1985). The Sodium/hydrogen Exchange System in Cardiac Cells: its Biochemical and Pharmacological Properties and its Role in Regulating Internal Concentrations of Sodium and Internal pH. *J. Mol. Cell. Cardiol.* 17, 1029–1042. doi:10.1016/S0022-2828(85)80119-X
- Lemmon, M. A., Flanagan, J. M., Hunt, J. F., Adair, B. D., Bormann, B. J., Dempsey, C. E., et al. (1992). Glycophorin A Dimerization Is Driven by Specific Interactions between Transmembrane Alpha-Helices. *J. Biol. Chem.* 267 (11), 7683–7689. doi:10.1016/s0021-9258(18)42569-0
- Li, X., Kim, J., Yang, J., Dutta, D., and Fliegel, L. (2021). Characterization of Modeled Inhibitory Binding Sites on Isoform One of the Na⁺/H⁺ Exchanger. *Biochimica Biophysica Acta (BBA) - Biomembr.* 1863 (9), 183648. doi:10.1016/j.bbmem.2021.183648
- Milosavljevic, N., Monet, M., Léna, I., Brau, F., Lacas-Gervais, S., Feliciangeli, S., et al. (2014). The Intracellular Na⁺/H⁺ Exchanger NHE7 Effects a Na⁺-Coupled, but Not K⁺-Coupled Proton-Loading Mechanism in Endocytosis. *Cell. Rep.* 7 (3), 689–696. doi:10.1016/j.celrep.2014.03.054
- Mishima, M., Wakabayashi, S., and Kojima, C. (2007). Solution Structure of the Cytoplasmic Region of Na⁺/H⁺ Exchanger 1 Complexed with Essential Cofactor Calcineurin B Homologous Protein 1. *J. Biol. Chem.* 282, 2741–2751. doi:10.1074/jbc.M604092200

FUNDING

This work was supported by CNRS, the Université Côte d’Azur.

ACKNOWLEDGMENTS

We thank all of our collaborators and colleagues for sharing numerous and stimulating findings and discussions on these fascinating transporters.

C. Expression de l'échangeur NHE1

NHE1 est l'isoforme de la famille SLC9 la plus exprimée dans les tissus, et dans la plus grande variété de tissus (Figures 4 et 5).¹⁷ A l'opposé, par exemple NHE4 et NHE6 sont moins exprimés et préférentiellement dans le système digestif et le système nerveux central respectivement.¹⁷

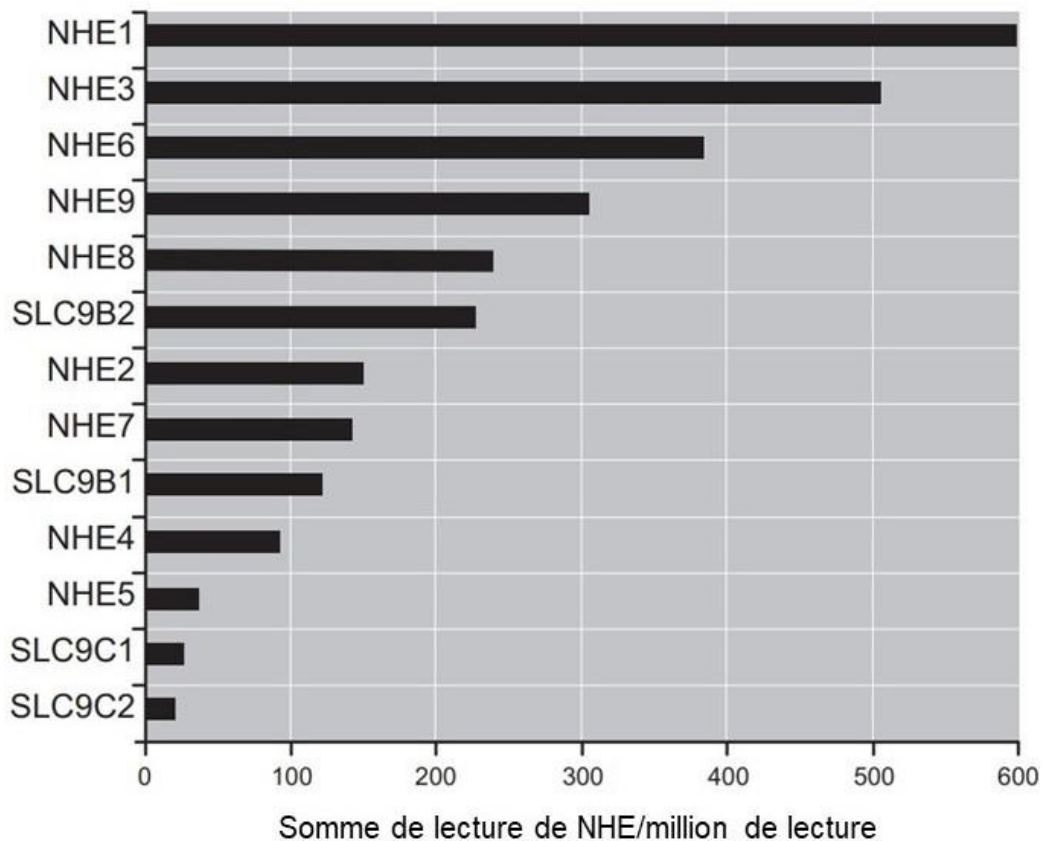


Figure 4. Somme totale des niveaux d'expression d'ARNm pour chaque NHE. NHE1 a l'expression d'ARNm la plus importante parmi l'ensemble des NHE (Pedersen et Counillon)¹

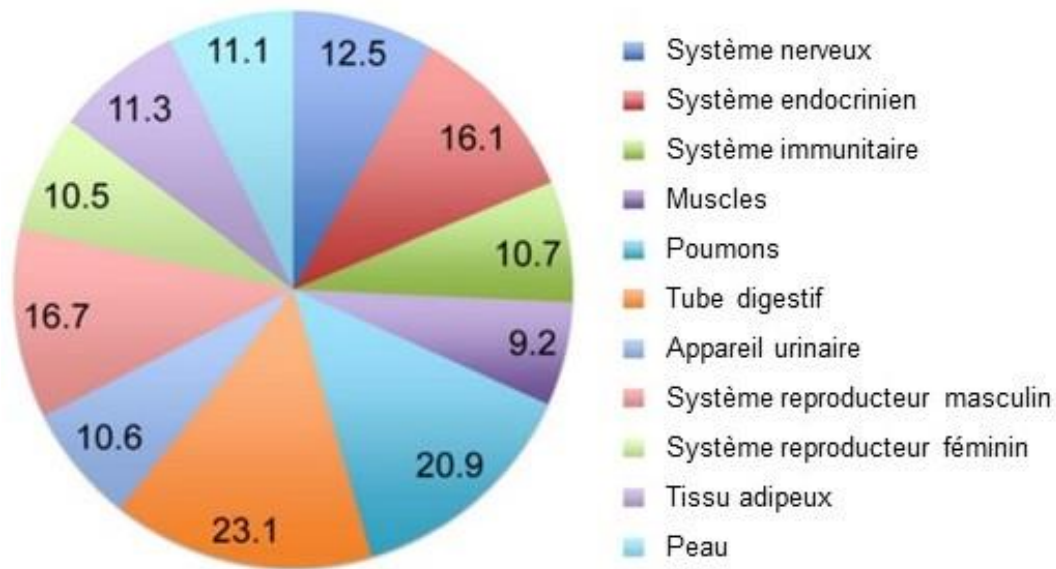


Figure 5. Distribution tissulaire de l'échangeur NHE1. Chaque secteur représente la proportion moyenne de lecture pour chaque grand système physiologique (Pedersen and Counillon)¹

NHE1 est localisé à la membrane, et essentiellement à la membrane basolatérale des cellules épithéliales (Figure 6) excepté dans le syncytio-trophoblaste du placenta où NHE1 pourrait être important pour les transferts électrolytiques entre la mère et le fœtus et impliqué dans les pathologies obstétricales en cas de modification de NHE1.

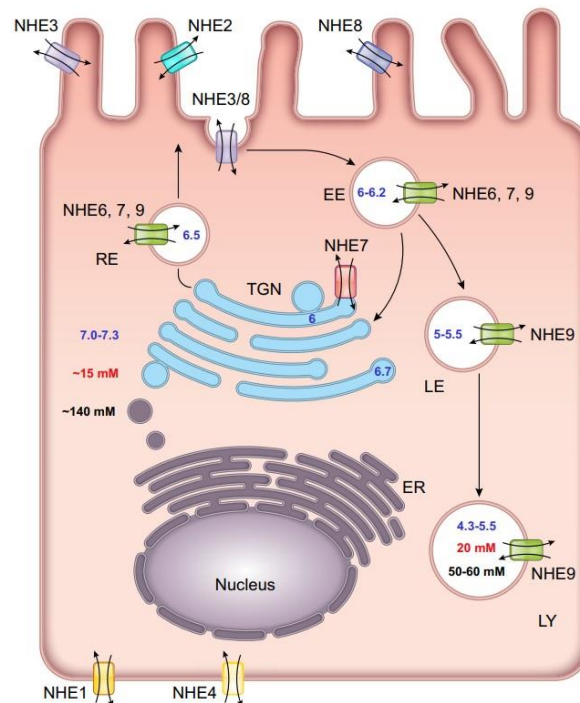


Figure 6. Schéma de la localisation cellulaire de chaque membre de la famille SLC9A dans une cellule épithéliale. NHE1 est essentiellement localisé à la partie basolatérale de la cellule. EE = Early endosome, LE = Late endosome, RE = Recycling endosome, TGN = Trans-Golgi network,

LY = Lysosome, ER = Endoplasmic reticulum, N = Nucleus. Les valeurs de pH, $[Na^+]$, $[H^+]$ sont respectivement représentées en bleu, rouge et noir (Pedersen and Counillon)¹

D. Fonctionnement des transporteurs NHE

L'étude de la fonction des NHE provient essentiellement de travaux de mutagenèse couplée à des mesures fonctionnelles sur NHE1. L'ensemble des NHE ayant une conservation de leur séquence génétique, les conclusions sur le fonctionnement de NHE1 ont globalement été extrapolées à tous les autres NHE.

Comme précédemment décrit, les NHE sont organisés en dimères. Concernant le transport de Na^+ , le fonctionnement des NHE suit un fonctionnement de type Michaelis Menten (allure hyperbolique de la courbe exprimant la vitesse d'activité en fonction de la concentration du substrat), alors que pour le transport des ions H^+ le fonctionnement des NHE suit un fonctionnement allostérique coopératif (allure sigmoïdienne de la courbe exprimant la vitesse d'activité en fonction de la concentration du substrat **Figure 1**).^{18,19}

Le transport effectué par les NHE est très rapide mais ne consomme malgré tout pas beaucoup d'énergie par rapport à d'autres mécanismes (e.g. V-ATPases) car le gradient de sodium est créé par la Na^+/K^+ ATPase qui transporte 3 ions Na^+ par molécule d'ATP. Le coefficient de Hill, qui représente le degré de coopérativité, est >1 pour les protons ce qui signifie que les NHE ont une très faible activité pour des valeurs de pH physiologiques, mais s'activeront fortement dès l'apparition d'une faible acidification cytoplasmique (**Figure 1**). Cette modulation confère aux NHE la capacité de s'activer très rapidement pour de petites acidifications, mais aussi d'intégrer différents signaux cellulaires pour les transformer en changements de pH comme nous le verrons par la suite.

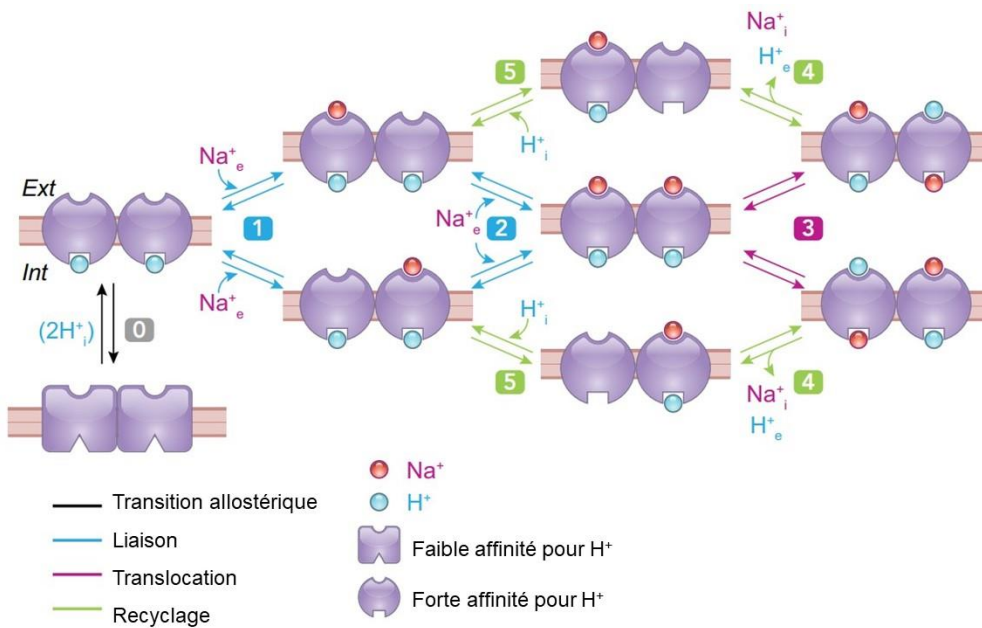
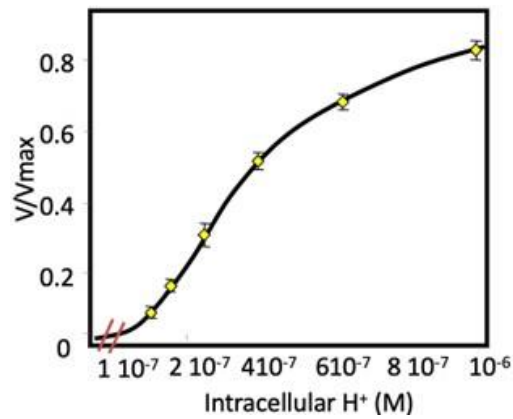


Figure 1. Haut : Courbe sigmoïdale d'activation de NHE1 pour différentes valeurs de concentrations en H⁺ Intracellulaire (d'après Lacroix *et al.*)¹⁸. Bas : Modèle pour les différentes étapes de l'échange réalisé par NHE1. L'étape 0 représente la transition allostérique permettant de passer d'une forme à faible affinité à une forte affinité pour H⁺ après avoir été complètement protoné. Durant les étapes 1 et 2, les 2 sites du dimère fixent séquentiellement Na⁺. Durant l'étape 3 la translocation des ions a lieu, et durant les étapes 4 et 5, les ions Na⁺ et H⁺ transloqués sont ensuite libérés et le recyclage de l'échangeur a lieu pour permettre un nouvel échange (Pedersen and Counillon)¹

Chaque protomère de NHE présente des sites régulateurs et de transport qui vont influencer l'un sur l'autre.

L'affinité des NHE pour le Na⁺ extracellulaire est faible, ce qui permet de faciliter le transport sur le plan cinétique. Les valeurs de Km mesurées pour le Na⁺ extracellulaire sont aux alentours de 10 mM. En même temps, les concentrations extracellulaires de Na⁺

de 140 mM permettent de saturer le transporteur ce qui fait que le fonctionnement des NHE se fait à vitesse maximale par rapport au Na⁺.

Etant donné que les NHE échangent de façon électroneutre un Na⁺ contre un H⁺, la mesure de leur activité est basée sur la mesure de ces concentrations ioniques car elle ne génère pas de courants. Ainsi, l'activité des NHE peut-être mesurée en dosant les flux de H⁺ par l'évaluation en temps réel du pH intracellulaire, ou du transport de Na⁺. Le transport de cations proches du Na⁺ dans la classification périodique de Mendeleiev (Li⁺, K⁺, Rb⁺, Cs⁺) peuvent être plus pratiques à doser. Mg²⁺, Ca²⁺, NH₄⁺, le tétraéthylammonium ou la choline ont été testés pour leur capacité à être transportées par les NHE²⁰, mais pour l'instant seuls les transports de H⁺, Li⁺ et Na⁺ ont été décrits dans la littérature.²⁰⁻²² Les valeurs de Km pour Li⁺ sont proches de celles de Na⁺ entre 5 et 20 mM. NHE3 pourrait transporter NH₄⁺ notamment au niveau rénal mais pas NHE1.^{23,24} Seuls les NHE intracellulaires pourraient transporter le K⁺ cytoplasmique.^{25,26} Cela dit pour NHE6 et 7 notre équipe a pu confirmer le transport de Na⁺ et de Li⁺ mais pas de K⁺.²⁷ En revanche, il a été décrit que NHE9 dans les cellules ciliées de l'oreille interne permet un échange électroneutre K⁺/H⁺.²⁸

Pour mesurer le transport des NHE, il est possible de faire varier et mesurer en temps réel le pH intracellulaire permettant ainsi d'analyser le fonctionnement des transporteurs NHE. Ces méthodes de mesures du pH intracellulaire sont décrites dans l'article Doyen et al. *Frontiers in Molecular Biosciences* 2022 (voir plus loin).²⁹

Plusieurs méthodes (quantitatives^{30,31}, et thermodynamiques²¹) ont permis d'établir que la stoechiométrie des transports effectués par les NHE correspondent à un échange d'1 ion Na⁺ contre 1 ion H⁺. Une fois les dimères de NHE complètement chargés par 2 Na⁺ et 2 H⁺, un transport par mécanisme flip-flop est initialisé.³² Cependant, une stoechiométrie 2:2 ne peut pas être éliminée. Un échange 2:2 pourrait être réalisé au niveau du dimère à l'état stationnaire.³³

Dans les conditions physiologiques, la réalisation du transport par les NHE possède un delta d'énergie libre négatif. Au cours du temps, le transport NHE1 de Na^+ est rendu possible par le maintien du gradient de Na^+ grâce à la présence de Na^+/K^+ ATPase. La réversibilité du transport est rendue possible si l'on inverse les gradients transmembranaires. Cela peut se faire en bloquant suffisamment longtemps la Na^+/K^+ ATPase ou en chargeant les cellules en lithium, puis en les plaçant à pH extracellulaire acide. Cela a été particulièrement démontré concernant NHE1³⁴ et a notamment permis de sélectionner des cellules déficientes en échangeurs de Na^+/H^+ par des techniques de suicide au H^+ .³⁴

Dans la revue ci-dessous récemment publiée par notre équipe « ***Intracellular pH Control by Membrane Transport in Mammalian Cells. Insights Into the Selective Advantages of Functional Redundancy*** », nous présentons les principaux mécanismes de régulation du pH intracellulaire. Nous y rappelons les principales méthodes de mesures de pH intracellulaire dont certaines ont été utilisées pour le sujet de cette thèse : sonde soluble, mais aussi phluorines, nanocapteurs, microélectrodes intracellulaires. Nous y rappelons également la mécanique cellulaire régissant l'équilibre acido-basique : tampons intracellulaires, bicarbonates, molécule d'eau, ainsi que les principaux transporteurs impliqués dans la régulation du pH. Une des interrogations qu'a suscité cet article est le fait que plus d'une soixantaine de gènes codent des transporteurs (ou sous unités) permettant de réguler le pH. Ce nombre très élevé reflète une redondance importante qui ne paraît pas s'expliquer facilement car il a pu être montré qu'avec un transporteur alcalinisant (type NHE), un transporteur acidifiant (type échangeur $\text{Cl}^-/\text{HCO}_3^-$) et des tampons intracellulaires, le pH peut être régulé autour de 7. Grâce à la collaboration de l'Institut Physique de Nice (INPHYNI, Valbonne, France), nous avons utilisé une approche de modélisation mathématique qui aboutit à la conclusion que cette redondance servirait plutôt à amortir les oscillations qui se produisent lors de la régulation du pH.²⁹



Intracellular pH Control by Membrane Transport in Mammalian Cells. Insights Into the Selective Advantages of Functional Redundancy

Denis Doyen^{1,2,3}, Mallorie Poët^{1,2}, Gisèle Jarretou^{1,2}, Didier F. Pisani^{1,2}, Michel Tauc^{1,2}, Marc Cougnon^{1,2}, Mederic Argentina⁴, Yann Bouret³ and Laurent Counillon^{1,2*}

¹Université Côte d'Azur, CNRS, Laboratoire de Physiomédecine Moléculaire, Nice, France, ²Laboratories of Excellence Ion Channel Science and Therapeutics, Nice, France, ³Centre Hospitalier Universitaire de Nice, Service de Médecine Intensive Réanimation, Hôpital Archet 1, Nice, France, ⁴Université Côte d'Azur, CNRS, Institut de Physique de Nice, INPHYNI, Nice, France

OPEN ACCESS

Edited by:

Patricia Marie Kane,
Upstate Medical University,
United States

Reviewed by:

Christian Martin Stock,
Hannover Medical School, Germany
Ira Kurtz,
University of California, Los Angeles,
United States

*Correspondence:

Laurent Counillon,
Laurent.Counillon@univ-cotedazur.fr

Specialty section:

This article was submitted to
Biophysics,
a section of the journal
Frontiers in Molecular Biosciences

Received: 29 November 2021

Accepted: 06 January 2022

Published: 18 February 2022

Citation:

Doyen D, Poët M, Jarretou G,
Pisani DF, Tauc M, Cougnon M,
Argentina M, Bouret Y and Counillon L
(2022) Intracellular pH Control by
Membrane Transport in Mammalian
Cells. Insights Into the Selective
Advantages of
Functional Redundancy.
Front. Mol. Biosci. 9:825028.
doi: 10.3389/fmolb.2022.825028

Intracellular pH is a vital parameter that is maintained close to neutrality in all mammalian cells and tissues and acidic in most intracellular compartments. After presenting the main techniques used for intracellular an vesicular pH measurements we will briefly recall the main molecular mechanisms that affect and regulate intracellular pH. Following this we will discuss the large functional redundancy found in the transporters of H⁺ or acid-base equivalents. For this purpose, we will use mathematical modeling to simulate cellular response to persistent and/or transient acidification, in the presence of different transporters, single or in combination. We will also test the presence or absence of intracellular buffering. This latter section will highlight how modeling can yield fundamental insight into deep biological questions such as the utility of functional redundancy in natural selection.

Keywords: pH regulation, pH measurements, transmembrane transport, mathematical modelling, functional redundancy, natural selection

1 INTRODUCTION

Temperature, pH and mechanical forces are fundamental physical parameters that affect living cells in all phyla. While cell mechanics have recently received a regain of attention, pH and temperature are often regarded as more trivial by non-specialists, possibly because they are easy to set and measure in everyday life, which in contrast is not the case at the cellular and subcellular scales. Also of note both pH and temperature have a vast biological impact from the tiniest molecular mechanisms to the planetary ecosystem. While recent publications show that temperature of biochemical mechanisms is far from being simple to measure and should receive more attention (Chretien et al., 2018; Lane, 2018); this review will deal with several aspects pertaining to pH regulation. As the cologarithm of free H⁺ concentration, pH quantifies the abundance of the smallest cation in the Universe, namely a proton, which is a hydrogen atom stripped of its electron. In the cytosol or in intracellular compartments pH is both one of the most controlled and one of the most challenging to control parameter. The reasons for this situation are at least threefold: 1) many reactions involve the fast release or consumption of protons an/or acid base equivalents, 2) cells are not simply chemical bags and use charge gradients across membranes to generate and store free energy. Those can directly be proton gradients such as in mitochondria, or indirectly provide and electro-osmotic driving force for protons, such as plasma membranes or in those of intracellular compartments, 3) the surface

charge of macromolecules is dictated by their protonation state, which in turn depends on the availability of free H^+ ions, namely on pH. The later reason is of utmost importance because interactions between molecules are built through electrostatics that are dictated by surface charge. In fine, pH, its gradients and dynamics dictate the space and time of macromolecular interactions.

In this context, evolution has selected an array of molecular mechanisms that address the challenge of regulating their pH by transporting acid-base equivalents across membranes. Those comprise pumps, leaks, and secondary transporters that can either translocate H^+ , bicarbonate or other buffers such as monocarboxylates.

In the last decades several colleagues have written excellent and comprehensive reviews on the various aspects of pH regulation in normal and pathological conditions [see for example (Casey et al., 2010; Damaghi et al., 2013; Parker and Boron, 2013; Rolver and Pedersen, 2021)]. In addition, this special issue, the present article is part of, also contains a set of articles covering several aspects of the field. Hence the aim of the present article is instead to provide in a first part a short focus on the methods of intracellular pH measurements and on the physical and chemical principles that govern intracellular pH regulation. In a second part, we will then link those two sections by illustrating how mathematical modeling can address the questions raised by the astonishing multiplicity of pH regulatory membrane transporters.

2 MEASURING CYTOSOLIC PH AND THE PH OF INTRACELLULAR COMPARTMENTS

Accurate determination of intracellular pH is of utmost importance for understanding the mechanisms that regulate this parameter. This requires not only to measure the steady state pH but also the dynamics of pH changes in various conditions. Because of these constraints pH measurements are challenging as they must be as least invasive as possible for cells while having the best spatiotemporal resolution as possible. This detracts from classical biochemical dosage techniques that usually lead to cell disruption or from whole cell patch clamp technique in which the intracellular contents are very rapidly dialyzed into the pipettes. Here also great reviews, that we cannot all cite, have been written on the different methods used to measure steady-state and pH variations both in cytosol and in organelles [see for example (Loiselle and Casey, 2010)].

Different systems have been used, from microelectrodes to the measurement of the diffusion of radiolabeled weak acids (Sardet et al., 1990) or electron microscopical quantification of immunoreactive weak bases in intracellular compartments (Anderson et al., 1984), but the most versatile technique, both for cytosolic and organelle pH measurements, is the use of pH sensitive fluorescent probes, whose absorption and/or emission spectra depend on their protonation state. In this case pH measurements just turn to be fluorescence spectroscopy measurements. Different setups can be used, from videomicroscopes equipped with camera and illumination systems (Milosavljevic et al., 2015) to fluorimeters or microplate readers

equipped with fluorescence. Using fluorescence, pH values can be in principle deduced from a modified Henderson-Hasselbalch equation adapted to fluorescence, or fluorescence ratio when ratiometric probes are used. The advantage of the latter is that they offer internal correction for possible photobleaching or probe leakage. pH calibration is in general mandatory because the optical setup and cellular context can slightly modify the probes spectral properties or their pK_a values. For cytosolic pH this is achieved using Nigericin, a K^+/H^+ ionophore that enables to set precisely intracellular pH, using the fact that extracellular pH equals intracellular pH when extracellular and intracellular potassium concentrations are set at equilibrium. The pH of intracellular compartments requires more sophisticated calibration procedures because organellar lumen must be equilibrated with the cytosol that must be equilibrated with the extracellular medium. Those can use weak acid diffusion such as the null method (Eisner et al., 1989), or use combination of K^+-H^+ and Na^+-H^+ ionophores such as Nigericin and Monensin respectively (Milosavljevic et al., 2014).

2.1 Soluble Probe

Based on the previous considerations, a wide variety of fluorescent dyes whose fluorescence depends on their protonation, and therefore pH, exists and the reader can refer to comprehensive reviews such as (Han and Burgess, 2010). Of course, for optimal sensitivity they must be able to penetrate cells easily and then be retained in their cytosol or compartments. For this, many pH indicators are built as cleavable esters. Furthermore, their pK_{as} must be in the range of the pH values to be measured. Hence, archetypal probes with a pK_a nearby seven have been widely used for cytosolic pH. Those are fluorescein acetoxymethyl esters (e.g. BCECF); benzoxanthene dyes (e.g. SNARF), or cyanine-derived dyes.

To measure the pH of endocytic compartments soluble pH-dependent fluorophores can be coupled to molecules that can be endocytosed such as Dextran or transferrin. Because fluorescein has a pK_a of 6.3, such a strategy will work for early endosomes (Teter et al., 1998), but its use is limited in more acidic compartments such as late endosomes and lysosomes. This can be slightly improved by thiosulfonate derivatives that will slightly reduce fluorescein pK_a (Ohkuma and Poole, 1978) or more strongly by substituting several hydrogen atoms by fluor atoms and carboxylic groups, leading to Oregon Green that has a pK_a around 4.7 (Saric et al., 2017). Non-fluorescein molecules with low pK_{as} are also in use, such as LysoSensor, (Lin et al., 2001), or Boron dipyrromethene (BODIPY) derivatives (Xia et al., 2019). Acridine orange derivatives, that accumulate in acidic organelles when protonated and fluorescent have been also used (Moriyama et al., 1982). Here also ratiometric approaches that can be used by coupling the probe to a pH stable GFP derivative (mCherry) are a great advantage (Saric et al., 2017). Pertaining to technical drawback to pay attention to is that, as the volume of these compartments is very tiny compared to cytosol, the introduced probes that have themselves acid-base properties can modify the compartments' pH.

2.2 Phluorins

The Green Fluorescent Protein (GFP) from *Aequorea Victoria* displays an elegant autocatalytic mechanism of intrinsic

fluorophore formation that involves the sequential cyclization and oxidation of a triad of Tyrosine-Serine-Glycine residues (Barondeau et al., 2003). Rothman and collaborators have generated pH sensitive GFPs by an ingenious combination of site-directed and random mutagenesis close to this aminoacid triad in the protein structure (Miesenbock et al., 1998). Following this work that gave birth to the first ratiometric and supercliptic pH sensitive GFPs termed pHluorins, many versions have been developed, to both increase their fluorescence or shift their pH response to be able to measure pH in more oxidative (mitochondrial matrix) or acidic compartments, such as TGN for example (Llopis et al., 1998; Mahon, 2011). Another important advantage is that cDNAs encoding these pHluorins can be adequately fused in frame with those encoding various proteins, to target them into a particular cellular compartment or location. In this respect, a recent work describes the construction of a Lamp-1 fused pHluorin that targets mostly lysosomal compartments and enables to measure luminal lysosomal pH in good accordance with data from the previous literature (Ponsford et al., 2021). In different cell lines, this pHluorin does neither affect lysosomal structure nor function, and has the advantage of being endogenously expressed, making a large set of functional measurements possible without any further treatment.

2.3 Nanosensors

A novel category of pH probes is emerging from biosensor nanotechnologies, and we will give a few examples among many. As a first example, carbon nanodots are much smaller than classical nanosensors and are therefore small enough (5–10 nm) to directly cross membranes instead of being endocytosed and accumulate in intracellular compartments. These nanodots do not exhibit detectable cellular toxicity and can be bound to various molecules, such as fluorescein or rhodamine derivatives or both. This can lead to interesting probes with ratiometric properties over a wide range of pH values (5.2–8.5), making them quite versatile tools to measure cytosolic pH (Shi et al., 2012).

Concerning lysosomal pH, Yue and collaborators (Yue et al., 2021) developed an interesting FRET-based approach, in which they used a split motif design with tetrahedral DNA that changes conformation with pH to build a nanosensor that has a very good signal to noise ratio around pH 6, well in the range of endo-lysosomal pH values. The large advantage is that such nanoparticulate probes can be endocytosed and arrive in lysosomes and endosomes where they will be able to change their emission properties as a function of the pH. Taken together, those novel approaches, which take advantage of the fast development of nanotechnologies represent a future area worth developing in the field of intracellular and organellar pH measurements.

2.4 Intracellular Microelectrodes/ Nanotubes

pH selective microelectrodes have been used for intracellular pH measurements, but as they can cause membrane damage and cytosolic leakage that will impair proper intracellular pH measurements, their use has been rather limited to large cellular

systems like *Xenopus* oocytes. Much smaller electrochemical intracellular pH sensors such as viral-coat proteins-DNA nanotubes modified gold electrodes have been designed. These electrodes take the advantage of the viral coat protein from Cowpea Chlorotic Mottle Virus (CCMV) self-assembly into nanotubes when incubated with double stranded DNA. The resulting nano electrodes are then adsorbed with methylene blue, a compound whose oxidation and reduction peaks shift with pH. This change can be detected electrically resulting in nanoelectrodes that have a large sensitivity from pH 4 to 9 (Ning et al., 2014). In the experimental device, those Nanotubes are grown on DNA coated on a gold sensor plate. The viral protein-based electrodes can then spontaneously insert into cell seeded on the plate without causing damage and be used to record pH changes.

2.5 Limitations and Constraints

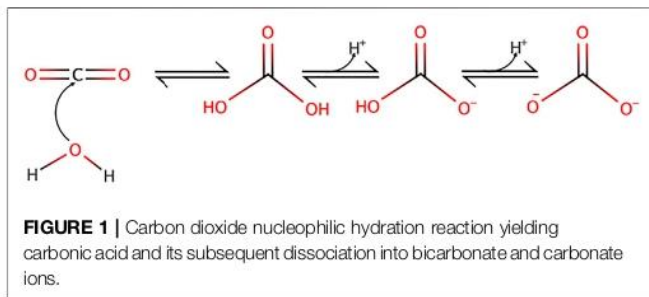
pH measurements can also be limited by the systems that lay before and after the chemical and physical properties of the probes or nanodevices used for the measurement itself. These different drawbacks can be related to the spatiotemporal features of the acquisition systems. In particular, for all measurements using fluorescence, working at very high rates and magnification automatically decreases the number of photons that can be gathered. As probe photobleaching and cell damage limit the possibilities to increase the illumination intensities, extremely sensitive cameras are then needed to overcome this problem. Similarly measuring fast kinetics of pH responses triggered by transient perturbations requires fast perfusion systems in order not to miss precious information such as the occurrence of overshoots. In our group, we could observe that such interesting signals, which were very difficult to observe using classical commercial perfusion systems, were revealed under fast laminar flow using microfluidic perfusion systems (Tran, Noblin, Bouret and Counillon, in preparation).

3 SUMMARY OF CELLULAR ACID-BASE CHEMISTRY

3.1 Intracellular Buffers

Solution chemistry defines the rates and equilibriums of reactions as functions of the free concentrations of reactants and products. In complex chemical systems such as cells, the situation is far from this simplified view because many species are not in their free form and are also intermediates in large reactions networks, making their kinetics dictated by multiple steps. H^+ ions whose small size and reactivity make them capable to combine with nearly all biological molecules are archetypal of this situation.

Indeed, most H^+ ions are combined to a bulk of biological molecules such as proteins, nucleic acids, lipids or smaller molecules, that simply carry protonable groups such as carboxylic acids, amines or phosphates (possibly free as inorganic phosphate and/or pyrophosphate; or associated with larger molecules by phosphodiester bonds). All those can operate as intracellular buffers with pK_{as} that extend over a range of 4–10, far from actual cytosolic pH values that are slightly above 7. However, as cells are extremely crowded with macromolecules,



those are quantitatively important in the net free H^+ balance. Furthermore, as protons constantly bind and unbind from different macromolecular complexes, this strongly reduces their diffusion rates, potentially leading to compartmentalization (Swietach et al., 2005).

3.2 Bicarbonate

The importance of the carbonic acid-bicarbonate equilibrium in setting up free proton concentration has been very nicely explained by several colleagues in excellent articles (see for example (Occhipinti and Boron, 2015)) and thus the aim here is not to go over this topic as much in too much detail but to recall the main features of this buffer. Briefly CO_2 nucleophilic attack by water yields carbonic acid as depicted in **Figure 1**.

Noticeably, the two protonation equilibria pK_{as} are 6.35 and 10.33 respectively, but those are displaced by the CO_2 hydration reaction ($K_{eq} = 2.5 \cdot 10^{-3}$ at $25^\circ C$) (England et al., 2011), making it an excellent biological buffer, which also couples cellular respiration to pH regulation. Bicarbonate has also been selected by evolution as one of the most important biological buffers, in a large part because it solves two main problems at the same time. Firstly, bicarbonate can bridge the gap between the too low and too high pK_a values of acid-base groups of the previously cited biological macromolecules. Secondly, as a gas CO_2 can diffuse very fast in the cytosol, as well as through membranes, this diffusion being facilitated through the structures of several transmembrane proteins (Michenkova et al., 2021). Hence, CO_2 can be viewed a convenient alternative for fast H^+ transport in cells but also across membranes. When hydrated, CO_2 becomes in contrast a classical acid base system that can release or capture protons, diffuse fast in the cytosol but not diffuse freely anymore across membranes. Kinetically and spatially, CO_2 hydration is controlled by multiple isoforms of carbonic anhydrases that are exceptionally efficient enzymes and are specifically expressed extra or intracellularly. Based on their location and the existing gradients, these enzymes are thus instrumental to control CO_2 traffic across membranes and consequently H^+ fluxes (**Figure 2**).

3.3 Water Molecules

The equilibrium of water dissociation into H^+ and OH^- ions is extremely in favor of the H_2O molecule. In pure water at pH 7, the ratio of H_2O over its dissociated forms is superior to 550 millions. As previously stated, cells are also crowded with acid base functions. In these conditions, it would be tempting to

consider that water dissociation/association is marginal in cell physiology. This has to be however taken with caution when considering cytosolic pH for at least two reasons: 1) as water is the biological solvent, H_2O concentration is $> 55 \text{ moles l}^{-1}$ which is orders of magnitude above the other biological molecules and 2) cytosolic pH is close to 7, which is the value at which water dissociation/association is the most labile.

4 MEMBRANE TRANSPORT

As mentioned in the introduction, several reviews provide a high level of detail on membrane transporters involved in pH regulation [see for example (Casey et al., 2010; Parker and Boron, 2013; Pedersen and Counillon, 2019)]. Hence, the aim of the present section is 1) to give a short summary on these transporters in order 2) to select relevant questions pertaining to cellular acid-base physiology and 3) to illustrate how mathematical modeling can provide here interesting clues.

4.1 Cells are not Chemical Reactors and Require Membrane Transport

Metabolism enables cells to extract free energy from the oxidation of a large set of macromolecules. This free energy that is carried mostly by ATP is transferred 1) to coupled chemical reactions, 2) to the creation and maintenance of membrane gradients and 3) to energize molecular motors. A significant fraction of the entropy that accompanies this free energy harvest and utilization is materialized by the generation of H^+ ions which have much more degrees of freedom than hydrogen atoms bound to large molecules. Furthermore, in all eukaryotic cells, the negative intracellular membrane potential also creates an inward proton gradient that would produce an acidic cytoplasm if not counterbalanced by opposite H^+ membrane transport. Conversely, if not maintained also by active pumping by V-ATPases, the acidic pH of intracellular compartment should also dissipate and acidify the cytosol.

Taken together, to maintain a steady-state pH, eukaryotic cells need to divert a significant fraction of their energy to maintain a high level of H^+ transport across their plasma membrane. This is achieved either directly through proton transport or indirectly through the transport of acidobasic molecules that can carry H^+ or buffer capacity. Strikingly, we can observe that membrane transport roughly involves the same chemical moieties as those previously discussed, namely H^+ , carboxylates, ammonium, or bicarbonate. Furthermore, as most of these transporters carry ionized species, their activity is directly or indirectly linked to ion fluxes and membrane potential and therefore to the cellular overall electrical activity.

4.2 More Than 63 Genes Encode pH Regulatory Plasma Membrane Proteins

A comprehensive list of transporter families in humans can be found on several sites for example <https://www.guidetopharmacology.org> (channels and transporters

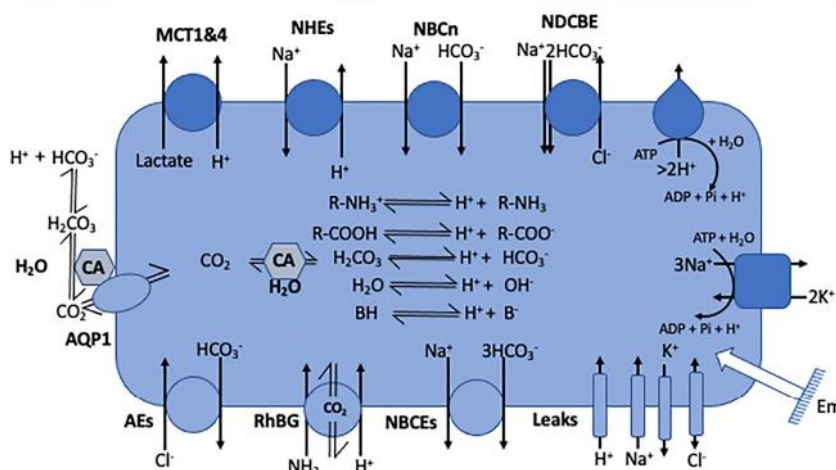


FIGURE 2 | Cell model representing the main families of pH regulating transport mechanisms as listed in **Table 1**. The model also encompasses the electrogenic pumps and the passive channels that set the membrane potential (E_m) and also use the same substrates as the coupling anions and cations that energize some of the pH regulatory transporters. It also represents the inner acid base chemistry that consumes or generates the transported acid-base equivalents.

TABLE 1 | Compilation of the proteins whose main physiological function is to transport H^+ or acid base equivalents across the plasma membrane to regulate pH. Source: <https://www.guidetopharmacology.org>.

Type of Protection	Function in PH regulation	Nomenclature	Number of genes
H^+ -V-ATPase	H^+ translocation subunits	V-ATPase V0 Subunit, V-ATPase V1 Subunit	10, 13
ATP6V0&1	ATP turnover subunits	V-ATPase V1 Subunit	4, 2, 2, 1
Bicarbonate Transporters SLC4 and SLC26	Electroneutral Cl^-/HCO_3^- -Exchange, Electroneutral Cl^-/HCO_3^- -Exchange, Electroneutral Na^+/HCO_3^- -Cotransport, Na^+ -Driven Cl^-/HCO_3^- -Exchange	AE1-4, NBCn1 and 2, NBCe1 and 2, NDCBE	9, 4
Na^+/H^+ Exchangers SLC9a,b and c	Electroneutral NHEs Atypical NHA (possibly electrogenic)	NHE1 to NHE9, SLC9b and C	4
Monocarboxylate Transporters SLC16	Lactate coupled proton transport	MCT1 TO 4	1, 1
NH_3/H^+ Cotransporters SLC42	Ammonium transport	RhBG SLC9b and C	12
Carbonic Anhydrases CA1-CA12	CO_2 hydration->indirect proton transport	Also termed car	63

subfamilies) (IUPHAR/BPS). These transporters whose functions are instrumental for pH regulation are summarized in **Figure 2** and the corresponding gene nomenclature and gene numbers are given in **Table 1**.

This table shows that evolution has invested in about 63 genes in humans to encode proteins or their subunits that are instrumental for H^+ or acid base equivalent transport across the plasma membrane in mammalian cells. This number could be revised upward if one considers all the genes encoding transmembrane transporters and channels that transport other vital substrates but are directly or indirectly coupled to proton transport. Those are phosphate transporters or cotransporters, (SLC20, SLC34) H^+ -coupled metal cotransporters (SLC11), H^+ coupled aminoacid cotransporters (SLC36) or H^+/Ca^{2+} ATPases (PMCA). Furthermore, there is now clear evidence that in their gas form, CO_2 or NH_3 can also cross membranes through the structures of Aquaporins (AQP1) or Rhesus proteins (Rh) that could therefore be considered as involved in pH regulation (Michenkova et al., 2021). There is also a set of transporters

and pumps that establish an acidic pH in the lumen of intracellular compartments and to this end take up protons from the cytosol. However, their steady-state contribution is challenging to quantify because of the multiplicity of different compartments, which all maintain a specific pH, and because of their different turnover rates in vesicular trafficking. For the sake of simplicity, we will from now only consider the plasma membrane proteins that take part in pH regulation.

While several structures had been solved by X ray crystallography, thanks to cryo-Electron Microscopy, many structures that remained unknown for many decades since the cloning of their cDNAs, are now available. Moreover, resolutions are generally sufficient to identify important functional sites for substrate and inhibitor interaction and to locate the functionally important residues previously identified by mutagenesis.

The interested readers can find the cryoEM structures of the Sodium-driven Chloride/Bicarbonate Exchanger NDCBE (SLC4A8) in (Wang et al., 2021), of the electrogenic sodium-bicarbonate cotransporter structure in (Huynh et al., 2018), and

of NHE1 and nine structures in (Winklemann et al., 2020; Dong et al., 2021). Other important structures have been obtained by X-ray diffraction, for AE1 in (Arakawa et al., 2015), and for monocarboxylate transporters (Bosshart et al., 2019; Zhang et al., 2020). Interestingly the 3D structures show a similar folding for the coupled transporters with a dimeric organization that opens possibilities for cooperativity and multiple allosteric regulations. Composite images have also been obtained for V-ATPases (Abbas et al., 2020).

5 ADDRESSING THE REDUNDANCY OF PH REGULATION

Taken together, this rather large number of genes encoding pH membrane regulators questions the significance of such a redundancy as established through natural selection. In part, this can of course be explained by the fact that different cell types need different equipment for transport. In this context, gene duplication during evolution could have selected specialized isoforms whose expression would boost a particular function in a given tissue. For example, the kidney tubule uses a combination of apical H^+ -ATPase and Na^+/H^+ exchangers NHE2 and NHE3 to secrete H^+ ions in order to reabsorb bicarbonate from the tubule lumen, while they express the housekeeping Na^+/H^+ exchanger NHE1 basolaterally for pH regulation (Wang et al., 2001). Similarly, in the small intestine, NHE2 and NHE3 are expressed apically where they mediate Na^+ and water intestinal absorption as well as luminal acidification. In parallel those exchangers have supplementary functions in establishing a pH gradient for divalent metal transport as well as in regulating the intestinal microbiome composition and properties through their action on luminal pH. In parallel, the basolateral NHE1 ensures housekeeping pH regulation (Pedersen and Counillon 2019).

However, this does not fully account for more subtle redundancies. In particular, different molecular machineries having the same overall function for pH regulation, such as NHEs, NBCs, monocarboxylate transporters and in some cases V-ATPases can be expressed in the same cells. Understanding why evolution has selected the expression of such different genes instead of relying on a single robust transporter is nontrivial because redundancy has a cost, which implies that the advantage must be immediate to be selected. This is contrast to human engineering where redundancy can be introduced to prevent future failures that may or may not happen. Beside the evolutionary aspect of this question, documented answers may provide clues to better understand in which pathological situations, e.g. ischemia-reperfusion or cancer, such a redundancy could be functionally beneficial or detrimental.

5.1 Modeling Addresses the Minimal Set of Membrane Transporters for Acid-Base Regulation

To answer the present question, a possible approach would be to identify the minimal set of transmembrane transporters that

would be required to maintain both the steady-state pH of a very simple cellular system close to neutrality and to restore it when subjected to transient and/or persistent perturbations. We and others (Swietach et al., 2005; Occhipinti and Boron, 2015; Counillon et al., 2016) resorted to mathematical modeling to establish cellular systems in which pH regulation by membrane transporters could be simulated adequately. As previously mentioned, it is mandatory to plug in minimal cytosolic chemistry in the form of buffers, bicarbonate and water as well as all membrane potentials and Na^+ , K^+ and Cl^- fluxes through channels that are indirectly coupled to H^+ transport because they will affect the gradients of cotransporters' counterions.

Based on this rationale and on equations built from experimental data for ion transporters and channels, we built a fully tractable model with only two antagonistic housekeeping transporters possessing the kinetic features of NHE1 and AE2. **Figure 3** shows the correspondence between the set of transporters, channels and equilibria present in this minimal system (A) the resulting differential terms (B) and fast-relaxing equilibria (C). Note that the same ion (e.g., Na^+ or HCO_3^-) can appear at multiple places in (B) and/or (C), reflecting the fact that multiple transporters, channels and/or equilibria share the same substrates. We account for NHE and its molar rate ρ_{NHE} exchanging one outer Na^+ with one inner H^+ . Likewise, the Anionic Exchanger AE transports a bicarbonate anion outside of the cell whilst bringing a chloride anion inside at a molar rate ρ_{AE} . Those two exchangers are electroneutral. In parallel, a membrane potential E_m is mainly developed by the electrogenic NaK-ATPase that intakes two K^+ and expels three Na^+ , (with a molar rate ρ_{NaK}), hence maintaining a negative inner voltage. Furthermore, any species X may flow through membrane channels or their equivalents according to its passive electroosmotic gradient and producing a leak λ_X that depends on the permeability of the concerned species. Finally, the membrane potential shall vary to balance the net charge transport with the help of the membrane capacitance. As this approach encompasses all protic reactions, as well as matter and charge conservation, it significantly departs from earlier pH regulation models that only partly take these different variables into account and have for this reason been questioned elsewhere (Kurtz et al., 2008; Nguyen et al., 2011).

The interested reader can find the detailed kinetic terms included in the ρ molar rates present in each individual differential equation in (Bouret et al., 2014). Consequently, we model the cellular system as a set of coupled chemical reactions that put together both the transport mechanisms as well as the cellular chemistry that includes water, bicarbonate, and buffers (**Figure 3C**). Consequently, the whole model for the cellular inner chemistry can be considered as a set of N chemical reactions (involving at least N species). Each reaction may evolve with its chemical extent to reach its equilibria. Accordingly, starting from a given set of concentrations, we reach N simultaneous equilibria depending on N independent extents. To compute them we use a non-linear, zero finding Newton's algorithm, modified to ensure the positivity of the resulting concentrations (that we call the Newton⁺ algorithm).

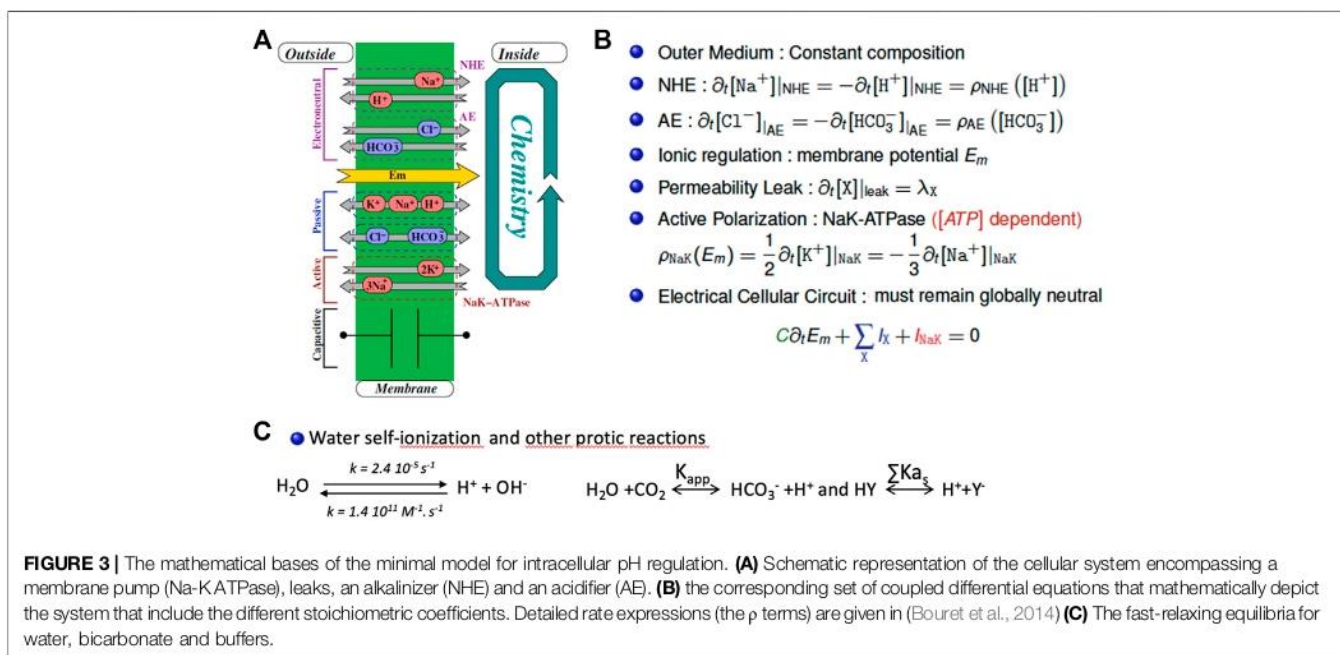


FIGURE 3 | The mathematical bases of the minimal model for intracellular pH regulation. **(A)** Schematic representation of the cellular system encompassing a membrane pump (Na-KATPase), leaks, an alkalinizer (NHE) and an acidifier (AE). **(B)** the corresponding set of coupled differential equations that mathematically depict the system that include the different stoichiometric coefficients. Detailed rate expressions (the ρ terms) are given in (Bouret et al., 2014) **(C)** The fast-relaxing equilibria for water, bicarbonate and buffers.

Let us now impose a perturbation, namely an intake of some species, to these equilibria: under the assumption that the relaxation times of each reaction is fast compared to the transport rates. The system will produce a set of extents that will bring each reaction back to the next allowed equilibrium. From a theoretical point of view, this method is the way to find the evolution of coupled concentrations subject to “slow” perturbations under N algebraic, chemical, and “fast” constraints, and requires a fair amount of algebra as described in our previous work. From an experimental point of view, the water self-ionization constants yield a relaxation time in the microsecond domain for the physiological pH ranges, and, according to literature, we expect the protic reactions to relax with a characteristic time around or below a few milliseconds for the same conditions. Therefore, our approximation is quite correct since any of the used transports requires at least a few seconds to carry out a significant change in cytosolic concentrations. In order to numerically integrate the differential system that we derived, we designed a home-made C++ software, based on an adaptive Runge-Kutta solver which we modified with 1) the effect of the chemical, algebraic constraints and 2) our Newton⁺ algorithm, to ensure that every trial set of concentrations respects the set of equilibria.

Such a simplified model is able to fully recapitulate intracellular pH regulation (Bouret et al., 2014; Counillon et al., 2016). This model predicts a large and robust area of intracellular pH in the range of biological values and a powerful ability to compensate for transient or sustained perturbations. The corresponding simulations are very similar to curves obtained both in our experiments and in the literature, using different techniques to measure intracellular pH, as described in the first section of this manuscript.

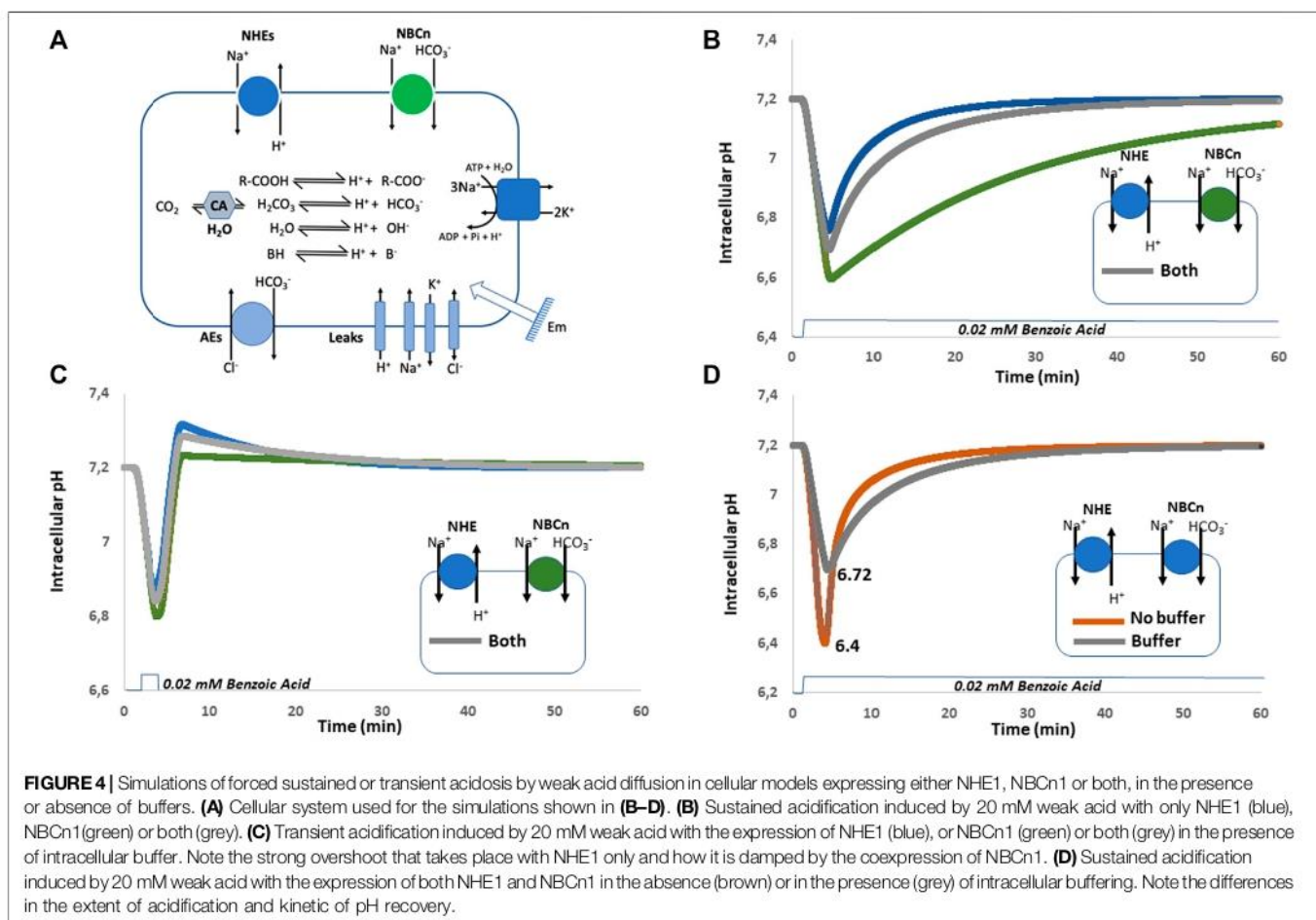
Taken together we can conclude from this model that only one acid loader and one acid extruder working antagonistically are

sufficient for an accurate pH regulation at physiological values. Such a result is striking as it comes in apparent contradiction with our previous analysis from genomes that natural selection has built a large set of redundant transporters. Although one could always argue that a mathematical model cannot encompass all the aspects of a real-life cell, the efficiency of pH regulation found for such a minimal set of effectors seems nevertheless too robust to be an artifact of calculation. It is also supported by the following experimental evidence. In pioneer experiments performed several decades ago, it has been possible to select or build NHE deficient fibroblasts, that can survive and grow perfectly well in cell culture conditions (Pouyssegur et al., 1984), and recover from acute acid challenges in the presence of Na⁺ and bicarbonate as they express NBCn1. Conversely, the same cells re-expressing NHE1 can fully resist an intracellular acidification in the absence of bicarbonate, where NBCn1 is inactive, provided that Na⁺ is present to energize NHE1 (Franchi et al., 1986). Taken together, we can conclude that coupling one strong acid loader with one strong extruder is sufficient to fully compensate for acute intracellular pH variations. Ergo, the reasons nature has chosen to co-express multiple transporters have to be found from a deeper analysis. This will be performed in the next chapters in which we will add functional redundancy to our model.

5.2 Modeling Functional Redundancy

5.2.1 Sustained Acidosis

We constructed a cellular model (Figure 4A) containing the previous minimal ion transport and pH regulating equipment in which we simulated the expression of NHE1, NBCn1, which work both at alkalinizing cells, separately or together. In this later condition we were careful that the sum of their activities triggers the same Na⁺ flux as the NHE1 or NBCn1 only simulations. This is mandatory to make all simulations comparable because if we simply add NHE1 and NBCn1 at the same levels as alone, this will



double the Na^+ loaders' quantity and automatically change the Na^+ fluxes and ionic steady state values of the simulated cells. This will affect all ion and pH regulation in a pleiotropic manner and has to be avoided to make tractable comparisons. Another obvious advantage of the modeling approach is that we can also simulate the absence of cellular buffers, which is biologically impossible as those are in a large part constituted by cellular macromolecules. **Figure 4B** shows a simulation of pH recovery following a sustained acidosis triggered by the addition of 20 mM of a permeant weak acid possessing a pK_a of 4.2 such as benzoic acid, either in cells expressing only NHE1, (blue curve), only NBCn1 (green curve), or both (grey curve). When alone, both NHE1 and NBCn1 can compensate for the acidification, but with a much lower rate for NBCn1, whose effect on H^+ is indirect and slowed down by the coupling with bicarbonate chemistry. When the two transporters are coexpressed, NHE1 seems to dominate the pH recovery as the slower NBCn1 minimally affects the rate of pH recovery. This result is consistent with the previous finding that NHE1 alone is fully able to restore a physiological pH, but again this questions the advantage of redundant NBCn1 expression, which does not seem noticeable when simulating such a sustainable acidification. As the two transporters are coexpressed in many cell types, this indicates again that we

need to further explore a wider range of cellular responses to pH changes to find the clues to this apparent paradox.

5.2.2 Transient pH Changes and Overshoots

As displayed in **Figure 4C**, we now perform a simulation of pH recovery, using the same system with NHE1 only, (Blue curve), NBCn1 only (Green Curve), or both (Grey Curve). The important difference is that the simulated acidosis triggered by the addition of 20 mM of benzoic acid is transient instead of continuous. As previously, the pH recovery is the swiftest in NHE1 only expressing cells but it can be observed that the rapid release of the acidosis triggers here a strong overshoot towards alkaline pH values. In the presence of NBCn1 only, pH drops slightly lower, recovers more slowly but with a negligible overshoot, here also due to coupling to bicarbonate chemistry. Interestingly when both transporters are present, NHE1 overshoot is significantly reduced by NBCn1.

Taken together, these simulations show that the selective advantages of functional redundancy are consistent but rather subtle. Combining a fast H^+ -transporting exchanger with a slower bicarbonate cotransporter preserves the ability to both compensate sustained and transient acidifications and, in the meantime, allows to damp strong overshoots that produce

potentially damaging alkalinization and intracellular Na⁺ overload. This emerging picture constitutes, in our opinion, an area worth of experimental investigation to pursue a deep understanding of this strong redundancy of transporters and channels that regulate physical parameters.

5.2.3 The Interesting Role of Buffers

The simulations in **Figure 4D** illustrate that intracellular buffers couple intracellular chemistry with ion transport in a subtle way. Without buffers, pH drops to a minimal value of 6.4 and then very swiftly recovers due to the conjugated activities of NHE1 and NBCn1. In contrast with intracellular buffers, the lowest pH reached in the same conditions is 6.72, but the recovery itself is slower as it is also damped by the presence of buffers. This longer recovery prolongs the activity period of the above-mentioned transporters and even though pH does not drop as low, this nevertheless increases the transporters' activity resulting in a larger Na⁺ load (by about 20%) and counterions' perturbation. Taken together, this simulation clearly shows that, as buffers protect cells against falling in a lethally low pH area, an interesting consequence is that this occurs at the expense of the recovery rate and engenders greater ionic perturbations that only can be resolved at a metabolic cost.

6 CONCLUDING REMARKS

Taken together studying intracellular pH regulation is both essential and complex. Its measurements that have been pioneered more than 4 decades ago have led to robust and numerous results that paved the way to cloning the genes encoding pH regulatory transporters. The field is experiencing a second birth with the advent of measurement techniques that should enable both greater space resolution and dynamic range. This is particularly important for the study of pH regulation in intracellular compartments, that have always been more challenging because of their small size, rapid movements, multiplicity and by their difficult accessibility inside cells. As previously mentioned, while improving pH quantitation itself is mandatory, it has to be accompanied by parallel development of the experimental setups, namely acquisition and perfusion, and a calibration whose resolution must be in line with the probes' performances.

Another important point is that pH dynamics cannot be simply described as a combination of the transporters' rates

because their activity is coupled to the bulk of all cellular ion channels, active and passive transporters, even if those do not directly act on pH. Furthermore, as protic reactions are massive within a cell, it is also mandatory to take cellular chemistry fully into account as it affects the availability of the transporters' substrates as well as the protonation and deprotonation of groups that act as buffers.

With respect to such a complex biochemistry, building mathematical and computational models can yield valuable insights. For this, they must be based as much as possible on experimentally determined equations of transport and it is mandatory that they fully respect physics and chemistry, notably charge and matter conservation. As shown in this article, this enables to build a minimal intracellular pH regulation and provide subtle insights into fundamental biological questions pertaining to functional redundancy. The resulting simulations indicate that redundancy ensures a tradeoff between safety, kinetics and transient overshoots. Whether the respective gene expression patterns have been shaped by evolution to fully optimize this tradeoff is a fundamental biological question worth investigating. The ease by which it is now possible to perform gene editing in combination with the previously described improvements in measurement techniques opens an area worth investigating to experimentally challenge this output of mathematical modeling.

AUTHOR CONTRIBUTIONS

LC and YB codesigned the manuscript. YB, MA, and LC built the model. YB carried out the mathematical calculations. DD, MP, DP, GJ, MT, MC, and LC Co-wrote the manuscript.

FUNDING

This work was supported by the IDEX UCA JEDI Academie IV financial support (IDEX UCA Jedi Academy II, ANR-15-IDEX-0001, Nice, France).

ACKNOWLEDGMENTS

Payment for publication fees was provided by the Centre Hospitalier Universitaire de Nice (Nice, France).

REFERENCES

- Abbas, Y. M., Wu, D., Bueler, S. A., Robinson, C. V., and Rubinstein, J. L. (2020). Structure of V-ATPase from the Mammalian Brain. *Science* 367 (6483), 1240–1246. doi:10.1126/science.aaz2924
- Anderson, R. G., Falck, J. R., Goldstein, J. L., and Brown, M. S. (1984). Visualization of Acidic Organelles in Intact Cells by Electron Microscopy. *Proc. Natl. Acad. Sci.* 81 (15), 4838–4842. doi:10.1073/pnas.81.15.4838
- Arakawa, T., Kobayashi-Yurugi, T., Alguel, Y., Iwanari, H., Hatae, H., Iwata, M., et al. (2015). Crystal Structure of the Anion Exchanger Domain of

Human Erythrocyte Band 3. *Science* 350 (6261), 680–684. doi:10.1126/science.aaa4335

Barondeau, D. P., Putnam, C. D., Kassmann, C. J., Tainer, J. A., and Getzoff, E. D. (2003). Mechanism and Energetics of green Fluorescent Protein Chromophore Synthesis Revealed by Trapped Intermediate Structures. *Proc. Natl. Acad. Sci.* 100 (21), 12111–12116. doi:10.1073/pnas.2133463100

Bosshart, P. D., Kalbermatter, D., Bonetti, S., and Fotiadis, D. (2019). Mechanistic Basis of L-Lactate Transport in the SLC16 Solute Carrier Family. *Nat. Commun.* 10 (1), 2649. doi:10.1038/s41467-019-10566-6

Bouret, Y., Argentina, M., and Counillon, L. (2014). Capturing Intracellular pH Dynamics by Coupling its Molecular Mechanisms within a Fully Tractable

- Mathematical Model. *PLoS One* 9 (1), e85449. doi:10.1371/journal.pone.0085449
- Casey, J. R., Grinstein, S., and Orlowski, J. (2010). Sensors and Regulators of Intracellular pH. *Nat. Rev. Mol. Cell Biol* 11 (1), 50–61. doi:10.1038/nrm2820
- Chrétien, D., Bénéit, P., Ha, H.-H., Keipert, S., El-Khoury, R., Chang, Y.-T., et al. (2018). Mitochondria Are Physiologically Maintained at Close to 50 °C. *PLoS Biol.* 16 (1), e2003992. doi:10.1371/journal.pbio.2003992
- Counillon, L., Bouret, Y., Marchiq, I., and Pouyssegur, J. (2016). Na⁺/H⁺ + Antiporter (NHE1) and Lactate/H⁺ + Symporters (MCTs) in pH Homeostasis and Cancer Metabolism. *Biochim. Biophys. Acta (Bba) - Mol. Cell Res.* 1863 (10), 2465–2480. doi:10.1016/j.bbamer.2016.02.018
- Damaghi, M., Wojtkowiak, J. W., and Gillies, R. J. (2013). pH Sensing and Regulation in Cancer. *Front. Physiol.* 4, 370. doi:10.3389/fphys.2013.00370
- Dong, Y., Gao, Y., Ilie, A., Kim, D., Boucher, A., Li, B., et al. (2021). Structure and Mechanism of the Human NHE1-CHP1 Complex. *Nat. Commun.* 12 (1), 3474. doi:10.1038/s41467-021-23496-z
- Eisner, D. A., Kenning, N. A., O'Neill, S. C., Pocock, G., Richards, C. D., and Valdeolmillos, M. (1989). A Novel Method for Absolute Calibration of Intracellular pH Indicators. *Pflügers Arch.* 413 (5), 553–558. doi:10.1007/BF00594188
- England, A. H. A., Duffin, A. M., Schwartz, C. P., Uejio, J. S., Prendergast, D., and Saykally, R. J. (2011). On the Hydration and Hydrolysis of Carbon Dioxide. *Chem. Phys. Lett.* 514, 187–195. doi:10.1016/j.cplett.2011.08.063
- Franchi, A., Perucca-Lostanlen, D., and Pouyssegur, J. (1986). Functional Expression of a Human Na⁺/H⁺ Antiporter Gene Transfected into Antiporter-Deficient Mouse L Cells. *Proc. Natl. Acad. Sci.* 83 (24), 9388–9392. doi:10.1073/pnas.83.24.9388
- Han, J., and Burgess, K. (2010). Fluorescent Indicators for Intracellular pH. *Chem. Rev.* 110 (5), 2709–2728. doi:10.1021/cr900249z
- Huynh, K. W., Jiang, J., Abuladze, N., Tsurulnikov, K., Kao, L., Shao, X., et al. (2018). CryoEM Structure of the Human SLC4A4 Sodium-Coupled Acid-Base Transporter NBCe1. *Nat. Commun.* 9 (1), 900. doi:10.1038/s41467-018-03271-3
- International Union of Basic and Clinical Pharmacology/British Pharmacological Society (IUPHAR/BPS). AvailableAt: <https://www.guidetopharmacology.org>.
- Kurtz, I., Kraut, J., Ormekian, V., and Nguyen, M. K. (2008). Acid-base Analysis: a Critique of the Stewart and Bicarbonate-Centered Approaches. *Am. J. Physiology-Renal Physiol.* 294 (5), F1009–F1031. doi:10.1152/ajprenal.00475.2007
- Lane, N. (2018). Hot Mitochondria. *PLoS Biol.* 16 (1), e2005113. doi:10.1371/journal.pbio.2005113
- Lin, H.-J., Herman, P., Kang, J. S., and Lakowicz, J. R. (2001). Fluorescence Lifetime Characterization of Novel Low-pH Probes. *Anal. Biochem.* 294 (2), 118–125. doi:10.1006/abio.2001.5155
- Llopis, J., McCaffery, J. M., Miyawaki, A., Farquhar, M. G., and Tsien, R. Y. (1998). Measurement of Cytosolic, Mitochondrial, and Golgi pH in Single Living Cells with green Fluorescent Proteins. *Proc. Natl. Acad. Sci.* 95 (12), 6803–6808. doi:10.1073/pnas.95.12.6803
- Loiselle, F. B., and Casey, J. R. (2010). Measurement of Intracellular pH. *Methods Mol. Biol.* 637, 311–331. doi:10.1007/978-1-60761-700-6_10.1007/978-1-60761-700-6_17
- Mahon, M. J. (2011). pHluorin2: an Enhanced, Ratiometric, pH-Sensitive green Fluorescent Protein. *Adv. Biosci. Biotechnol.* 2 (3), 132–137. doi:10.4236/abb.2011.23021
- Michenkova, M., Taki, S., Blosser, M. C., Hwang, H. J., Kowatz, T., Moss, F. J., et al. (2021). Carbon Dioxide Transport across Membranes. *Interf. Focus.* 11 (2), 20200090. doi:10.1098/rsfs.2020.0090
- Miesenböck, G., De Angelis, D. A., and Rothman, J. E. (1998). Visualizing Secretion and Synaptic Transmission with pH-Sensitive green Fluorescent Proteins. *Nature* 394 (6689), 192–195. doi:10.1038/28190
- Milosavljevic, N., Monet, M., Léna, I., Brau, F., Lacas-Gervais, S., Feliciangeli, S., et al. (2014). The Intracellular Na⁺/H⁺ Exchanger NHE7 Effects a Na⁺-Coupled, but Not K⁺-Coupled Proton-Loading Mechanism in Endocytosis. *Cel Rep.* 7 (3), 689–696. doi:10.1016/j.celrep.2014.03.054
- Milosavljevic, N., Poet, M., Monet, M., Birgy-Barelli, E., Léna, I., and Counillon, L. (2015). Functional Characterization of Na⁺/H⁺ Exchangers of Intracellular Compartments Using Proton-Killing Selection to Express Them at the Plasma Membrane. *J. Vis. Exp.* 97 52453. doi:10.3791/52453
- Moriyama, Y., Takano, T., and Ohkuma, S. (1982). Acridine Orange as a Fluorescent Probe for Lysosomal Proton Pump1. *J. Biochem.* 92 (4), 1333–1336. doi:10.1093/oxfordjournals.jbchem.a134053
- Nguyen, M. K., Kao, L., and Kurtz, I. (2011). Defining the Buffering Process by a Triprotic Acid without Relying on Stewart-electroneutrality Considerations. *Theor. Biol. Med. Model.* 8, 29. doi:10.1186/1742-4682-8-29
- Ning, L., Li, X., Yang, D., Miao, P., Ye, Z., and Li, G. (2014). Measurement of Intracellular pH Changes Based on DNA-Templated Capsid Protein Nanotubes. *Anal. Chem.* 86 (16), 8042–8047. doi:10.1021/ac500141p
- Occhipinti, R., and Boron, W. F. (2015). Mathematical Modeling of Acid-Base Physiology. *Prog. Biophys. Mol. Biol.* 117 (1), 43–58. doi:10.1016/j.pbiomolbio.2015.01.003
- Ohkuma, S., and Poole, B. (1978). Fluorescence Probe Measurement of the Intralysosomal pH in Living Cells and the Perturbation of pH by Various Agents. *Proc. Natl. Acad. Sci.* 75 (7), 3327–3331. doi:10.1073/pnas.75.7.3327
- Parker, M. D., and Boron, W. F. (2013). The Divergence, Actions, Roles, and Relatives of Sodium-Coupled Bicarbonate Transporters. *Physiol. Rev.* 93 (2), 803–959. doi:10.1152/physrev.00023.2012
- Pedersen, S. F., and Counillon, L. (2019). The SLC9A-C Mammalian Na⁺/H⁺-Exchanger Family: Molecules, Mechanisms, and Physiology. *Physiol. Rev.* 99 (4), 2015–2113. doi:10.1152/physrev.00028.2018
- Ponsford, A. H., Ryan, T. A., Raimondi, A., Cocucci, E., Wycislo, S. A., Fröhlich, F., et al. (2021). Live Imaging of Intra-lysosome pH in Cell Lines and Primary Neuronal Culture Using a Novel Genetically Encoded Biosensor. *Autophagy* 17 (6), 1500–1518. doi:10.1080/15548627.2020.1771858
- Pouyssegur, J., Sardet, C., Franchi, A., L'Allemain, G., and Paris, S. (1984). A Specific Mutation Abolishing Na⁺/H⁺ Antiport Activity in Hamster Fibroblasts Precludes Growth at Neutral and Acidic pH. *Proc. Natl. Acad. Sci.* 81 (15), 4833–4837. doi:10.1073/pnas.81.15.4833
- Rolver, M. G., and Pedersen, S. F. (2021). Putting Warburg to Work: How Imaging of Tumour Acidosis Could Help Predict Metastatic Potential in Breast Cancer. *Br. J. Cancer* 124 (1), 1–2. doi:10.1038/s41416-020-01171-2
- Sardet, C., Counillon, L., Franchi, A., and Pouyssegur, J. (1990). Growth Factors Induce Phosphorylation of the Na⁺/H⁺ + Antiporter, a Glycoprotein of 110 kD. *Science* 247 (4943), 723–726. doi:10.1126/science.2154036
- Saric, A., Grinstein, S., and Freeman, S. A. (2017). Measurement of Autolysosomal pH by Dual-Wavelength Ratio Imaging. *Methods Enzymol.* 588, 15–29. doi:10.1016/bs.mie.2016.09.073
- Shi, W., Li, X., and Ma, H. (2012). A Tunable Ratiometric pH Sensor Based on Carbon Nanodots for the Quantitative Measurement of the Intracellular pH of Whole Cells. *Angew. Chem. Int. Ed.* 51 (26), 6432–6435. doi:10.1002/anie.201202533
- Swietach, P., Leem, C.-H., Spitzer, K. W., and Vaughan-Jones, R. D. (2005). Experimental Generation and Computational Modeling of Intracellular pH Gradients in Cardiac Myocytes. *Biophysical J.* 88 (4), 3018–3037. doi:10.1529/biophysj.104.051391
- Teter, K., Chandy, G., Quiñones, B., Pereyra, K., Machen, T., and Moore, H.-P. H. (1998). Cellubrevin-targeted Fluorescence Uncovers Heterogeneity in the Recycling Endosomes. *J. Biol. Chem.* 273 (31), 19625–19633. doi:10.1074/jbc.273.31.19625
- Wang, T., Hropot, M., Aronson, P. S., and Giebisch, G. (2001). Role of NHE Isoforms in Mediating Bicarbonate Reabsorption along the Nephron. *Am. J. Physiology-Renal Physiol.* 281 (6), F1117–F1122. doi:10.1152/ajprenal.2001.281.6.F1117
- Wang, W., Tsurulnikov, K., Zhekova, H. R., Kayik, G., Khan, H. M., Azimov, R., et al. (2021). Cryo-EM Structure of the Sodium-Driven Chloride/bicarbonate Exchanger NDCBE. *Nat. Commun.* 12 (1), 5690. doi:10.1038/s41467-021-25998-2
- Winkelmann, I., Matsuoka, R., Meier, P. F., Shutin, D., Zhang, C., Orellana, L., et al. (2020). Structure and Elevator Mechanism of the Mammalian Sodium/proton Exchanger NHE9. *EMBO J.* 39 (24), e105908. doi:10.15252/embj.2020105908
- Xia, S., Fang, M., Wang, J., Bi, J., Mazi, W., Zhang, Y., et al. (2019). Near-infrared Fluorescent Probes with BODIPY Donors and Rhodamine and Merocyanine

- Acceptors for Ratiometric Determination of Lysosomal pH Variance. *Sensors Actuators B: Chem.* 294, 1–13. doi:10.1016/j.snb.2019.05.005
- Yue, X., Qiao, Y., Gu, D., Qi, R., Zhao, H., Yin, Y., et al. (2021). DNA-based pH Nanosensor with Adjustable FRET Responses to Track Lysosomes and pH Fluctuations. *Anal. Chem.* 93 (19), 7250–7257. doi:10.1021/acs.analchem.1c00436
- Zhang, B., Jin, Q., Xu, L., Li, N., Meng, Y., Chang, S., et al. (2020). Cooperative Transport Mechanism of Human Monocarboxylate Transporter 2. *Nat. Commun.* 11 (1), 2429. doi:10.1038/s41467-020-16334-1

Conflict of Interest: The authors declare that the research was conducted in the absence of any commercial or financial relationships that could be construed as a potential conflict of interest.

Publisher's Note: All claims expressed in this article are solely those of the authors and do not necessarily represent those of their affiliated organizations, or those of the publisher, the editors and the reviewers. Any product that may be evaluated in this article, or claim that may be made by its manufacturer, is not guaranteed or endorsed by the publisher.

Copyright © 2022 Doyen, Poët, Jarretou, Pisani, Tauc, Cougnon, Argentina, Bouret and Counillon. This is an open-access article distributed under the terms of the Creative Commons Attribution License (CC BY). The use, distribution or reproduction in other forums is permitted, provided the original author(s) and the copyright owner(s) are credited and that the original publication in this journal is cited, in accordance with accepted academic practice. No use, distribution or reproduction is permitted which does not comply with these terms.

E. Rôles de l'échangeur NHE1

NHE1 est essentiellement responsable de la régulation du volume cellulaire et du pH intracellulaire.

L'activité métabolique d'une cellule génère continuellement des protons à l'origine d'une acidose qui est immédiatement corrigée par NHE1 et d'autres transporteurs. Le fonctionnement allostérique coopératif de NHE1 permet une action rapide et très efficace pour corriger des variations minimales de pH.

NHE1 régule le volume cellulaire en réponse à une diminution du volume de la cellule.³⁵ Certains auteurs ont proposé que les senseurs de variation de volume se situeraient soit au niveau de la partie C-terminale soit au niveau de EL1 (extracellular loop 1). En parallèle, notre équipe avait montré que cette réponse aux chocs osmotiques se faisait par un changement de la sensibilité de NHE1 aux ions H⁺ intracellulaires.¹⁸ Ainsi, en cas de choc hypertonique, le dimère NHE1 oscille vers une forme à haute affinité pour les protons et voit son activité majorée, et inversement (Figure 2).

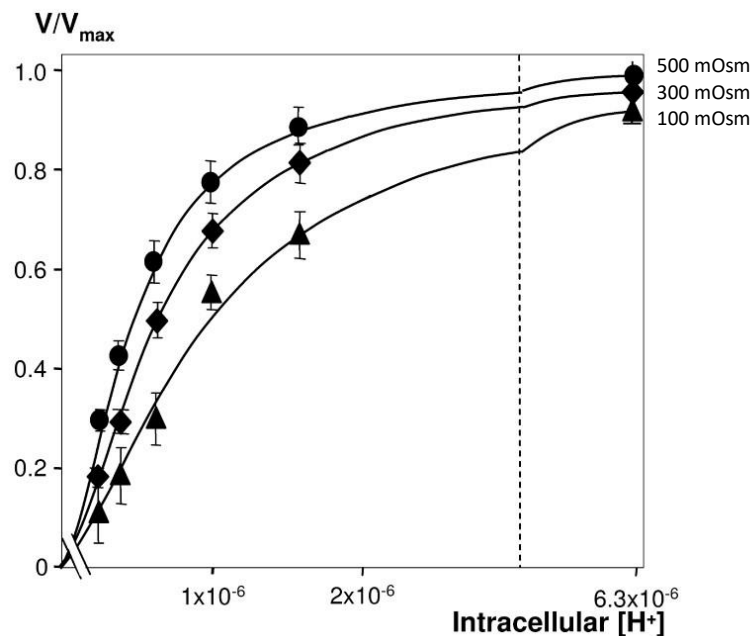


Figure 2. Modulation de l'activité de NHE1 par les chocs osmotiques. L'activité de NHE1 est évaluée par le dosage de l'absorption de ²²Na⁺ à différentes osmolarités extracellulaires déterminées par des concentrations de mannitol variables (100 mOsm, 300 mOsm, 500 mOsm). Chaque point représente V/V_{max} de NHE1 en fonction de la concentration en H⁺. Ces données sont représentatives d'au moins 7

expérimentations indépendantes. A noter l'augmentation de la coopérativité de NHE1 lorsque l'osmolarité augmente (d'après Lacroix *et al.*, Biochemistry, 2008)¹⁸

Par ailleurs, d'autres facteurs comme l'ajout d'agents modifiant la courbure membranaire, les chocs osmotiques, le pH intracellulaire, et les voies de signalisation intracellulaire font varier cette affinité (Figure 3).

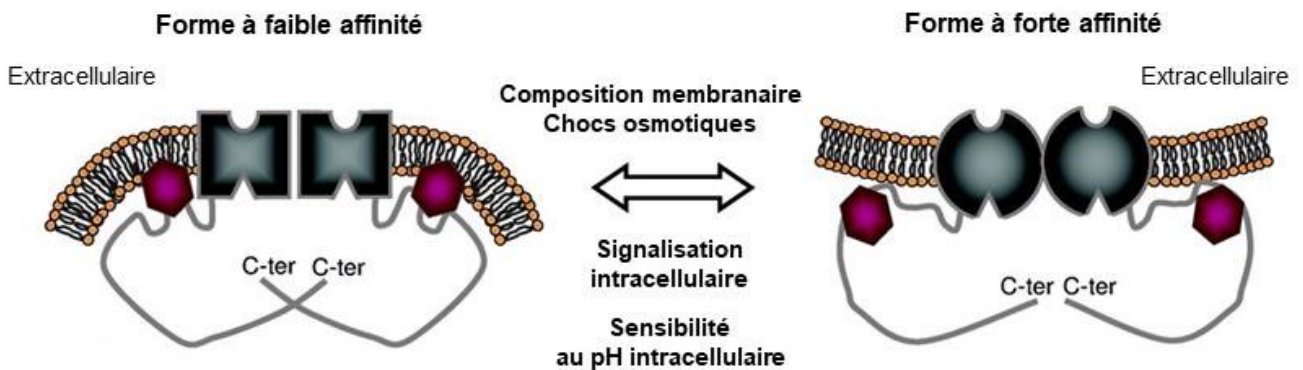


Figure 3. Facteurs régulant le passage de la forme de faible à haute affinité de NHE1 pour les H⁺: composition membranaire, chocs osmotiques, signalisation intracellulaire et sensibilité au pH intracellulaire (d'après Lacroix *et al.*, Biochemistry, 2008)¹⁸

En dehors de ces fonctions de régulation de pH intracellulaire et du volume intracellulaire, NHE1 joue un rôle directement ou indirectement dans d'autres fonctions.

NHE1 est notamment important pour réguler la motilité de plusieurs types cellulaires³⁶ comme les fibroblastes,³⁷ la mobilité des polynucléaires neutrophiles en réponse à un stimulus chimique,³⁸ ou l'excroissance des neurites.³⁹ NHE1 se retrouve à la tête des cellules migratrices et l'inhibition de NHE1 entraîne une altération de cette migration cellulaire.

NHE1 peut retentir sur la migration cellulaire de plusieurs façons. D'abord, la migration s'accompagne de la création d'un gradient de pH intracellulaire parallèle à l'axe de la cellule qui dépend de NHE1.⁴⁰ Ensuite, NHE1 se situe souvent au niveau des sites d'adhésion focale près des intégrines qui pourraient activer NHE1 via la voie RhoA-ROCK (ROCK = Rho-associated protein kinase), activation qui permettrait indirectement la

phosphorylation des focal adhesion kinases qui initie la migration cellulaire.⁴¹ Par ailleurs, la migration cellulaire est favorisée en cas d'adhésion intermédiaire, adhésion qui est d'autant plus importante que l'environnement est acide et donc dépendante de NHE1.⁴² De plus, dans le cycle cellulaire, NHE1 retient indirectement sur le cil primaire important pour la motilité.⁴³ L'activité de NHE1 permettrait aussi de réguler l'expression des gènes impliqués dans la migration cellulaire comme les gènes impliqués dans l'organisation du cytosquelette, l'adhésion cellulaire et l'assemblage de la matrice extracellulaire.⁴⁴ Enfin, au niveau des lamellipodes des fibroblastes, NHE1 lie par sa partie C-terminale le complexe ERM (ezrine, radixine, moesine) qui peut stimuler NHE1 par sa liaison avec ROCK1 et NIK.^{45,46} Une altération du fonctionnement de NHE1 aboutit à un défaut de direction migratoire et de cicatrisation.⁴⁷ En pathologie, NHE1 est aussi impliqué dans la migration des cellules cancéreuses en favorisant un environnement acide qui permet l'activité des protéases et la dégradation de la matrice extracellulaire.⁴⁸ Au-delà de cet environnement acide, NHE1 interagit dans des phénomènes de corégulation avec des canaux ioniques, notamment sodiques lors de ces phénomènes de migration.⁴⁹

En dehors de la migration cellulaire, NHE1 pourrait réguler d'autres fonctions cellulaires comme le trafficking vésiculaire des lysosomes, la macropinocytose et la phagocytose.⁵⁰⁻⁵² NHE1 a de nombreuses interactions via sa partie C-terminale avec d'autres protéines pour réguler fonction, localisation et turnover comme la calmoduline (CAM)⁵³, la calcineurine β -homologous protein 1 (CHP1)⁵⁴, ou la β -arrestine.⁵⁵ Ezrine régule les interactions du cytosquelette avec NHE1 et recrute Akt.⁵⁶ La régulation de NHE1 par ces molécules est plus détaillée chapitre I. F.

F. Régulation de l'échangeur NHE1

Comme précédemment décrit (I. E.), NHE1 est d'abord régulé par les concentrations de protons et les variations de volume de la cellule pour réguler concentrations de H⁺ et de Na⁺. Grâce à son fonctionnement coopératif, de très faibles variations de pH pourront engendrer une activation importante de NHE1 à partir d'un certain niveau de pH. Pour moduler les concentrations de Na⁺, NHE1 s'activera en réponse à une diminution de volume de la cellule plus que par des variations de concentrations ioniques. Comme précédemment décrit également (I. E.), les modifications de conformation membranaire modifient également l'état d'affinité de NHE1 pour les protons.¹⁸

Un autre mode de régulation est l'environnement membranaire notamment le cholestérol et les micro-domaines enrichis en cavéoline qui en contraignant NHE1 exercent une régulation négative sur l'activité de NHE1.⁵⁷ Ceci peut particulièrement être important en situation pathologique comme l'athérosclérose ou au cours du vieillissement.⁵⁷

Les données sur la régulation transcriptionnelle de NHE1 sont limitées. L'expression de NHE1 chez la souris diminue lorsque la concentration intracellulaire de Na⁺ augmente via des voies impliquant des protéines G et l'ubiquitination. L'implication de Nedd4 dans cette régulation transcriptionnelle est discutée.^{55,58}

L'interaction de NHE1 avec CHP1 est importante pour réguler l'expression de NHE1. CHP1 permet de retarder l'internalisation et la dégradation de NHE1.⁵⁹ Une mutation sur CHP1 chez l'homme entraîne une ataxie, comme le knock-out de NHE1 chez la souris.⁶⁰

La partie C-terminale est la principale structure impliquée dans la régulation de NHE1. En effet, les modifications post-traductionnelles régulant NHE1 sont essentiellement représentées par des modifications de la partie C-terminale notamment par des phosphorylations⁶¹, et à un moindre degré par des déphosphorylations. De nombreuses kinases/phosphatases différentes interagissent avec NHE1. Plusieurs clusters d'acides aminés Ser/Thr sont la cible de cette phosphorylation.

Les conséquences d'une phosphorylation de NHE1 aboutissent globalement à une activation de NHE1 par une augmentation de sa sensibilité aux H⁺ intracellulaires. Parmi les principales phosphorylations, les mitogen-activated protein kinases (MAPK) sont fréquemment impliquées soit directement,^{62,63} soit indirectement via ERK (Extracellular signal-regulated kinase) et la RSK (p90 ribosomal S kinase) qui cible la Serine 703.⁶⁴ Il a été décrit que ERK peut phosphoryler au moins 6 sites distincts sur NHE1.⁶²

Toutes les phosphorylations n'entraînent pas forcément une activation du transporteur, par exemple la phosphorylation de Ser 648 médiée par Akt entraîne une inhibition de NHE1.

Si les phosphorylations sont fréquemment rapportées, les déphosphorylations sont moins étudiées mais aussi décrites concernant plusieurs enzymes : la Ser/Thr protéine phosphatase 2A,⁶⁵ la protéine phosphatase 2A,⁶⁶ la calcineurine,⁶⁷ la Tyr phosphatase et la SHP-2 (Src homology-2 domain-containing protein tyrosine phosphatase-2).⁶⁸ Là également la déphosphorylation peut soit inhiber^{69,70} soit activer NHE1.⁷¹

La partie C-terminale de NHE1 est aussi importante dans l'interface du dimère et la régulation de son activité allostérique. Plusieurs modifications post-traductionnelles ou liaison avec des ligands spécifiques peuvent modifier le comportement allostérique de NHE1 lui conférant ainsi une possibilité de moduler son activité. La partie C-terminale permet également de réguler l'ancrage de NHE1 à certaines structures, et de réguler les partenaires de NHE1.

Excepté les kinases ou phosphatases, d'autres ligands potentiels de NHE1 ont été décrits comme des lipides membranaires notamment les phosphoinositides et PI(4,5)P2. PI(4,5)P2 retient sur la fonction en renforçant le lien partie C-terminale-membrane, et en comportant aussi des sites de liaison aux protons. PI(4,5)P2 comporte aussi des sites de liaison à cheval entre le complexe ezrine, radixine, moesine (ERM) rattaché au cytosquelette et 4.1R.⁷² 4.1R est responsable d'une inhibition de NHE1. En cas

d'élévation du Ca^{2+} intracellulaire, la Ca^{2+} -calmoduline (CAM) est activée et se lie à 4.1R, ce qui libère NHE1 pour se lier à $\text{PI}(4,5)\text{P}_2$ aboutissant à une activation de NHE1.

CAM active NHE1 de manière proportionnelle à l'élévation de Ca^{2+} , activation qui dépend de la liaison de CAM à une région auto-inhibitrice de NHE1. La liaison de CAM à cette région dépend d'une phosphorylation d'une tyrosine de CAM et d'une phosphorylation de NHE1 sur Ser 648.⁷³⁻⁷⁵ CAM active aussi NHE1 par d'autres voies comme le rétrécissement cellulaire, les mitogènes et les hormones.^{73,76}

Plusieurs kinases Ser/Thr régulent NHE1 en agissant sur la partie C-terminale dont NIK (NF-kappa- β -inducing kinase) et ERK2.^{62,77} A l'opposé, NHE1 est aussi régulé par des Ser/Thr phosphatases calcineurines qui dépendent aussi de CAM. La plupart des ligands de la partie C-terminale de NHE1 qui participent à sa régulation sont représentés

Figure 7.

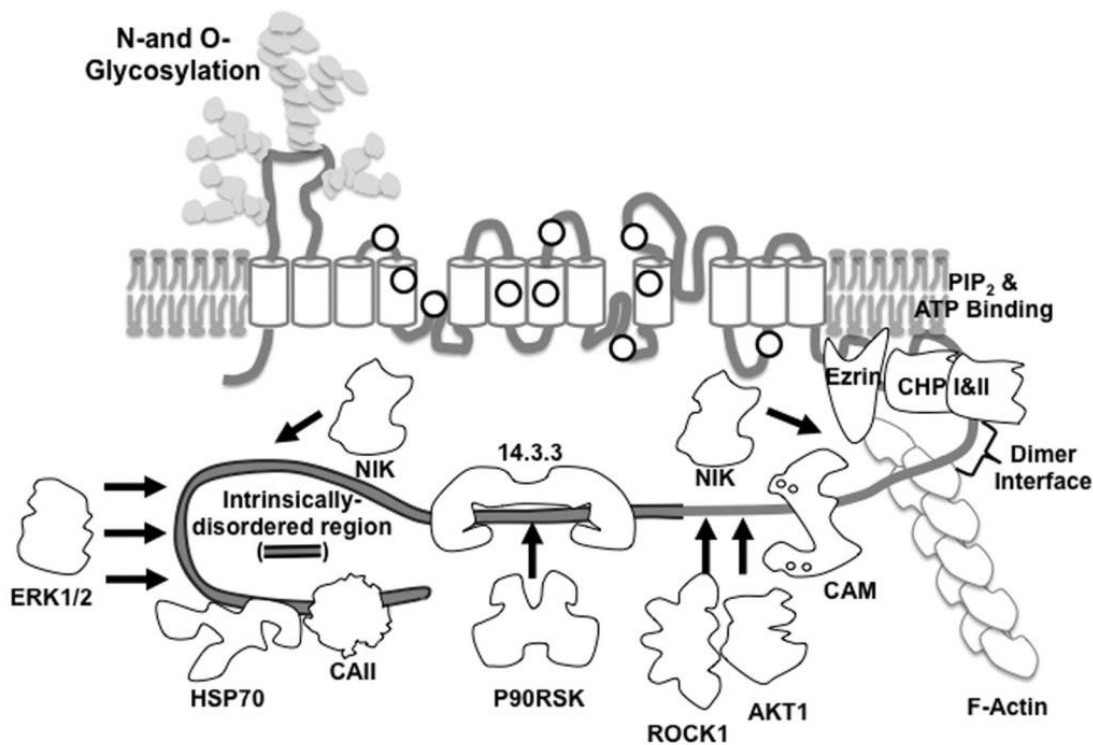


Figure 7. Schéma représentant les principaux domaines de NHE1: les cercles représentent les régions importantes pour le transport. Les flèches montrent les principaux sites de phosphorylation de la partie C-terminale de NHE1. ATP = Adenosine triphosphate, CAII = Carbonic anhydrase II, CAM = Ca^{2+} -Calmoduline, CHP = Calcineurine β -homologous protein, ERK1/2 = Extracellular signal-regulated kinase 1/2, HSP70 = Heat shock protein 70, NIK = NF-

kappa-β-inducing kinase, ROCK1 = Rho kinase 1, P90RSK = p90 ribosomal S kinase, PIP2 = phosphatidylinositol-4,5-bisphosphate (Counillon *et al.*)⁷⁸

Enfin, NHE1 est aussi régulé par des intégrines qui lient NHE1 à d'autres transporteurs comme Na⁺/Ca²⁺.⁷⁹

La régulation de NHE1, son expression et les voies de signalisation – hormones impliquées durant les phénomènes d'ischémie reperfusion sont détaillées chapitre I. H. ci-dessous dans la revue rédigée par notre équipe « ***Role of the Na⁺/H⁺ Exchanger 1 in the Ischemia/Reperfusion Injury*** » (sous chapitres “*Mechanisms and pathways involving NHE1 during ischemia reperfusion, b. et c.*”)

G. Interaction de NHE1 avec les espèces réactives de l'oxygène

Les espèces réactives de l'oxygène (ROS) sont le résultat d'un défaut de la réduction d'O₂ (dioxygène) en H₂O, réaction nécessitant deux ions H⁺ et 2 électrons ce qui aboutit à la formation de dérivés radicalaires libres -l'anion superoxyde O₂⁻ et le radical hydroxyl ·OH (2^{ème} oxydant le plus puissant après le fluor)-, et à des dérivés non-radicaux le peroxyde d'hydrogène H₂O₂. La présence d'un électron libre rend les ROS très instables et très réactifs avec d'autres molécules.⁸⁰ Ils existent à l'état physiologique de manière équilibrée dans la cellule entre leur production et leur élimination via des systèmes anti-oxydants, et sont essentiels au fonctionnement des voies de signalisation intracellulaire. En situation pathologique, les ROS peuvent être produits de manière excessive (âge, athérosclérose) ou alors être moins éliminés (obésité) ce qui est à l'origine d'un stress oxydatif et de dommages tissulaires. C'est le cas dans les phénomènes d'ischémie-reperfusion: infarctus du myocarde, accident vasculaire ischémique, arrêt cardio-respiratoire, ischémie aigue de jambes, ischémie mésentérique, chirurgie ou transplantation d'organes.^{81,82} Les espèces réactives de l'azote (RNS) sont produites en

même temps mais ne font pas l'objet de ce travail. La production de l'ensemble des espèces réactives de l'oxygène et de l'azote est représentée **Figure 8**.

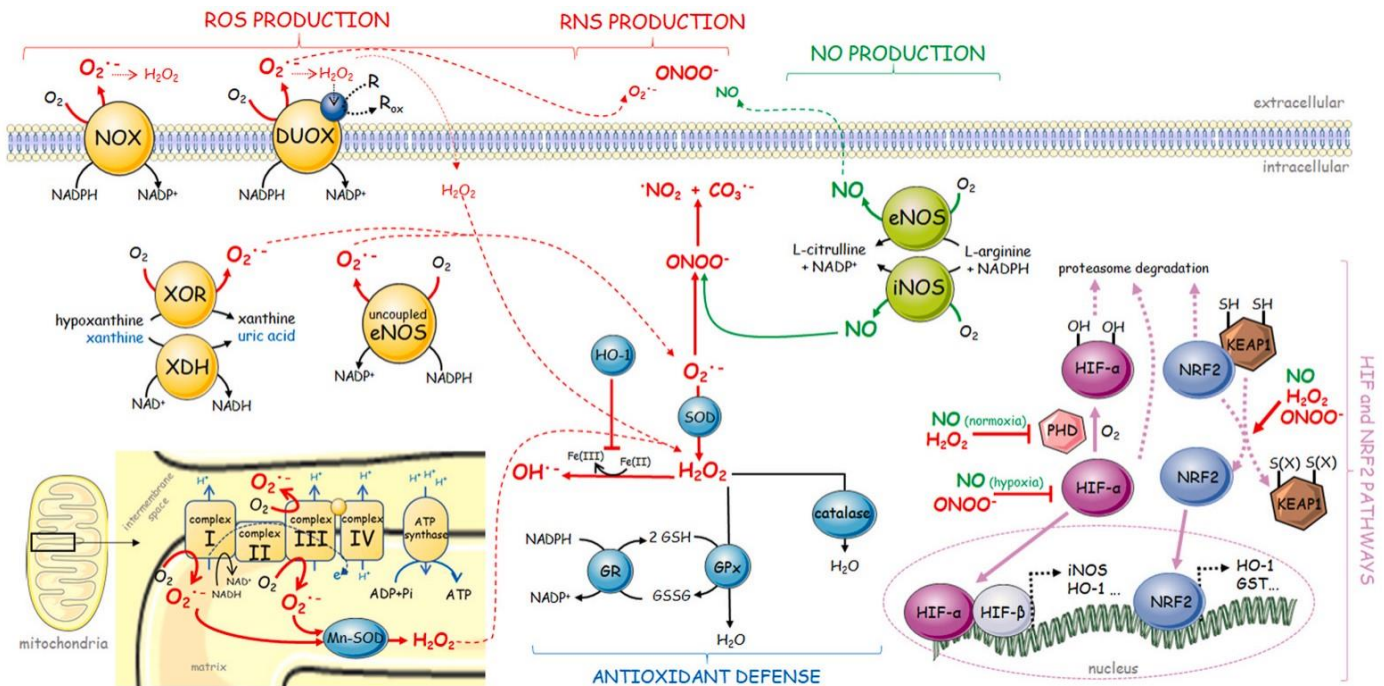


Figure 8. Schéma des principales molécules impliquées dans le stress oxydatif aboutissant à la formation d'espèces réactives de l'oxygène (ROS), d'espèces réactives de l'azote (RNS), du monoxyde d'azote, des défenses antioxydantes (en bleu) et de HIF-1 (en violet). DUOX = dual oxydase, GPx = glutathione peroxydase, GR = glutathione réductase, GST = glutathione S-transferase, HIF = hypoxia inducible factor, HO = hème oxygénase, KEAP1 = Kelchlike ECH-associated protein 1, NOS = nitric oxide synthase, NOX = NADPH oxydase, NRF2 = nuclear factor erythroid-2-related factor 2, PHD = prolyl-hydroxylase, SOD = superoxyde dismutase, XDH = xanthine déshydrogénase, XOR = xanthine oxydo-réductase (Carcy *et al.*)⁸²

Plusieurs systèmes régulent la concentration des ROS. Il existe des systèmes non enzymatiques par les métaux de transition comme le Fer qui avec le H_2O_2 produit le $\cdot OH$. Et il existe des systèmes enzymatiques : les superoxydes dismutases qui transforment $O_2^{\cdot-}$ en H_2O_2 , les catalases et les glutathione peroxydases qui produisent H_2O à partir d' H_2O_2 .⁸³

Les ROS sont produits pour la plupart par la mitochondrie mais aussi au niveau membranaire ou intra-cytoplasmique (NADPH oxydase (nicotinamide adenine

dinucleotide phosphate hydrogen oxydase)). En situation d'ischémie, les complexes I et III mitochondriaux sont altérés et libèrent un excédent d'électrons qui majorent la production de ROS qui en excès accélèrent l'oxydation des cellules, de l'ADN et la mort cellulaire.⁸⁴

NHE1 comme les ROS est un acteur majeur dans l'ischémie-reperfusion (IR). La production de ROS est associée à une augmentation de la concentration intracellulaire de Ca^{2+} responsable d'une ouverture du pore de transition mitochondrial, d'augmentation du cytochrome C et de l'apoptose.⁸⁵ Il a été démontré que NHE1 durant l'IR est directement responsable d'une majoration de la concentration intracellulaire de Ca^{2+} .^{86,87} Il est donc légitime de relier NHE1 et l'élévation des ROS durant l'IR. La régulation de NHE1 par les ROS n'est pourtant que peu décrite. Rothstein *et al.* ainsi que Snabaitis *et al.* ont montré qu' H_2O_2 via la voie ERK peut activer NHE1.^{88,89} Haworth *et al.* avaient déjà plus tôt évoqué l'implication d'ERK dans l'activation de NHE1 durant l'IR.⁹⁰ Gan *et al.* ont également montré que l'exposition de NHE1 à H_2O_2 augmentait son expression.⁹¹ L'effet des autres ROS (O_2^- , $\cdot\text{OH}$) sur NHE1 n'est pas décrit.

L'objectif principal de mon travail expérimental de thèse a donc été de déterminer si l'anion superoxyde O_2^- était capable de réguler NHE1. Comme cela a été le cas nous avons ensuite travaillé à l'identification du mécanisme moléculaire impliqué ce qui nous a permis d'identifier des cystéines clefs de NHE1 dans ce mécanisme mais aussi dans sa régulation par le NO monoxyde d'azote (NO) et son interaction avec le cytosquelette. L'ensemble est décrit dans le manuscrit ci-après chapitre II.

H. Implication de NHE1 durant l'ischémie-reperfusion

Dans le manuscrit ci-dessous, nous avons réalisé une revue invitée exhaustive de la littérature (en cours de finalisation pour soumission) concernant l'implication de NHE1 dans les dommages liés à l'ischémie reperfusion. L'ischémie-reperfusion est une condition pathologique rencontrée dans de nombreuses situations et pouvant concerner

un ou plusieurs organes: infarctus du myocarde, accident vasculaire cérébral ischémique, chirurgie, transplantation... L'ischémie-reperfusion correspond à la succession d'une hypoxie tissulaire suivie d'une réoxygénation. L'ischémie peut être secondaire soit à l'occlusion d'un vaisseau (syndrome coronarien aigu par exemple), soit la diminution de l'apport sanguin comme dans un état de choc. Et la reperfusion correspondra à la revascularisation du vaisseau occlus ou le rétablissement d'un flux sanguin après correction de la cause d'un état de choc. Dans ces situations, l'ischémie initiale est à l'origine de lésions tissulaires qui demandent une reperfusion, mais cette même reperfusion aggrave transitoirement de façon paradoxale les lésions tissulaires. De nombreuses thérapeutiques ont été essayées dans ce contexte comme la cyclosporine, les inhibiteurs de la prolylhydroxylase, le chloramphénicol, le préconditionnement, le postconditionnement,^{81,92-94} mais aussi les inhibiteurs de NHE1. En effet, si NHE1 est capital pour réguler le pH et le volume intracellulaire, il peut être aussi délétère en situation d'ischémie reperfusion où cet échangeur est suractivé et est à l'origine d'aggravation des lésions tissulaires.^{86,95} La suractivation de NHE1 dans ce contexte entraîne notamment une surcharge en sodium puis en calcium qui est responsable d'une activation du pore de transition mitochondrial,⁹⁶ du cytochrome C et diminue le rapport Bcl/Bax.⁹⁷ L'inhibition de NHE1 dans l'IR est une stratégie thérapeutique qui a été testée dans de multiples modèles. NHE1 est l'isoforme de la famille SLC9-A-C la plus étudiée dans le contexte de l'ischémie reperfusion. L'infarctus du myocarde est le modèle d'IR le plus analysé où son expression prédomine par rapport aux autres tissus, mais l'implication de NHE1 dans les lésions d'IR a été décrite dans d'autres tissus comme au niveau du cerveau, du rein et les éléments figurés du sang.¹ De nombreux modèles et espèces ont été étudiés amenant à la conclusion que le rôle de NHE1 dans les lésions d'IR n'est pas spécifique d'une espèce de mammifère.⁹⁸ De nombreux types d'inhibiteurs de NHE1 ont été testés afin de diminuer les effets délétères de la suractivation de NHE1. La plupart de ces inhibiteurs de NHE1 ont une action directe sur l'échangeur représentés

essentiellement par des dérivés acylguanidiniques^{95,99-101} et guanidiniques^{102,103}. Mais de nombreuses voies de signalisation intra-cellulaires différentes ou molécules impliquant NHE1 peuvent être concernées et ciblées pour inhiber de manière indirecte NHE1 notamment les voies impliquant la P90 ribosomal S6 kinase¹⁰⁴, PI3K/Akt/PKG¹⁰⁵, ERK1/2¹⁰⁶, la RAS-GTPase¹⁰⁷, l'angiotensine II¹⁰⁸, la NOS¹⁰⁹ ou l'Apolipoprotéine-E.¹¹⁰ Les protocoles d'administration de ces inhibiteurs sont très variés notamment concernant le temps d'administration. Idéalement, les inhibiteurs de NHE1 devraient être administrés avant l'épisode ischémique ce qui est reproduit par la majorité des protocoles.^{87,111} Mais étant donné que l'événement ischémique n'est le plus souvent pas prévisible la plupart des protocoles décrits utilisent ces inhibiteurs après le début de l'ischémie.^{112,113} Les effets décrits sont en général bénéfiques dans les modèles pré-cliniques essentiellement chez le rat et la souris qu'il s'agisse du coeur, du cerveau et du rein avec notamment une diminution des zones nécrosées suite à l'ischémie et une amélioration fonctionnelle des tissus étudiés. Cependant, les seuls tests cliniques chez l'homme dans le cadre de l'IR myocardique n'ont pas pu confirmer ces bénéfices en terme de mortalité. Cibler NHE1 pour établir de nouvelles thérapeutiques semble pourtant encore être d'intérêt comme en témoigne les résultats spectaculaires chez l'homme des inhibiteurs SGLT2 en terme de mortalité dans l'insuffisance cardiaque^{114,115} quelque soit la cause et l'insuffisance rénale¹¹⁶. Ces inhibiteurs ont de nombreux effets incluant une inhibition de NHE1. Notre revue qui détaille cette implication de NHE1 dans le cadre de l'ischémie reperfusion et dans tous ces modèles différents est présentée ci-dessous.

Role of the Na⁺/H⁺ Exchanger 1 in the Ischemia/Reperfusion Injury

Denis Doyen^{1,2,3}, Didier F. Pisani^{1,2}, Gisèle Jarretou^{1,2}, Marc Cougnon^{1,2}, Michel Tauc^{1,2}, Mallorie Poët^{1,2}, Laurent Counillon^{1,2}

1 Laboratoire de Physiomédecine Moléculaire (LP2M), CNRS, Université Côte d'Azur, Nice, France

2 Laboratories of Excellence Ion Channel Science and Therapeutics, Nice, France

3 Médecine Intensive Réanimation, Centre Hospitalier Universitaire de Nice, Hôpital Pasteur 2, Nice, France

Abstract

The Na⁺/H⁺ exchanger 1 (NHE1) is one of the 9 isoforms of the SLC9A-C mammalian Na⁺/H⁺ exchanger family (1). It is a membrane protein composed of a 500 amino acid N-terminal membrane domain mediating transport and a 315-amino acid hydrophilic cytoplasmic carboxy-terminal domain containing regulatory sites (2, 3). It is ubiquitously expressed, responsible for an electroneutral exchange of Na⁺ and H⁺ and is also crucial for the regulation of intracellular pH and ion homeostasis (1). However, in the setting of ischemia reperfusion NHE1 has been shown to be overactivated and worsen injuries (4, 5). NHE1 is the most NHE isoform studied in ischemia – reperfusion. Its expression predominates in the myocardium but it is also involved in ischemia-reperfusion injuries of other tissues like brain, and kidneys ... (1). This phenomenon has been described in different experimental models and animal species, suggesting that the role of NHE1 in mediating injury is not species specific (6). A lot of inhibitors have been tested with different administration timings in these models to reduce the deleterious effects of NHE1 overactivation in this setting. Here we give an overview of the different tissue models, species, mechanisms and NHE1 inhibitors used where NHE1 has been shown to be involved in the ischemia – reperfusion injuries.

Introduction

Ischemia-Reperfusion (IR) is a pathological condition found in a lot of situations and involving potentially one or multiple organs: cardiac arrest, myocardial infarction, stroke, critical limb ischemia, mesenteric ischemia, surgery, and transplantation (7, 8). Although early reperfusion is needed after ischemia, this reperfusion can paradoxically lead to severe tissues injuries and even death (7).

A lot of therapeutics have been studied to limit IR injuries like cyclosporine, prolylhydroxylase inhibitors, chloramphenicol, ischemic preconditioning or postconditioning, nitric oxide, T cell-based approaches (7, 9-11)... Among these, NHE1 inhibition has been shown to be another potential interesting therapeutic strategy (1).

Mitchell *et al.* were the first to propose the existence of an electroneutral exchange of cations and protons across the mitochondrial membrane in 1966 (12). In 1976, Murer *et al.* further identified a Na⁺/H⁺ exchange in intestinal and renal brush-border membranes (13). Lazdunski *et al.* confirmed later these findings in rat and chicken hearts with amiloride and derivatives (dimethylamiloride, ethylisopropylamiloride) and showed for the first time the involvement of NHE in the IR injuries in the myocardium (4, 5).

The NHE exchanger belongs to the SLC9A family which includes 9 members (NHE1 to 9) (1). NHE1 is a membrane protein composed of a 500 amino acid N-terminal membrane domain mediating transport connected by intracellular and extracellular loops and a 315-amino acid hydrophilic cytoplasmic carboxy-terminal domain containing regulatory sites. NHE1 is organized as asymmetrical homodimer with each subunit undergoing an elevator-like conformational change during exchange (14). The structure of the specific isoform 1 of NHE was first detailed in 1991 (15). Recently Dong *et al.* resolved the NHE1 structure by cryo-EM (14), which provided spectacular insights into the previous structure-function studies on NHE1 further understanding interaction between NHE1 and its inhibitors (16).

During IR, NHE1 stimulation may participate in injuries. In myocardial ischemia, NHE1 overexpression leads to Ca²⁺ overload and contracture (17), an increase in caspase-3-like activity, apoptosis and damage (18). NHE1-null mutant (NHE1^{-/-}) mice or heterozygous mice exhibited respectively less myocardial and neuronal IR injuries than WT mice suggesting that NHE1 increased IR injuries (19, 20). At the opposite in transgenic mouse with overexpression of NHE1, endoplasmic reticulum stress response increased and improved cardioprotection against IR (21, 22), but also increased cardiac remodeling and failure with aging (21). Similarly, Mraiche *et al.* demonstrated that elevated NHE1 levels in transgenic mice induced cardioprotection. However, they also noticed cardiac metabolism alterations (23). The discrepancies in these studies complexified the role of NHE1 in IR outcomes, nevertheless, the most accepted hypothesis is that NHE1 inhibition could confer tissue protection.

IR is associated with pH decrease, Na⁺ accumulation mediated by NHE1 and by Na⁺/K⁺ adenosine triphosphatase (ATP)ase inhibition (24). This is followed by Ca²⁺ overload via the Na⁺/Ca²⁺ exchange which may be responsible for cardiac injuries in myocardial ischemia (5, 25-33). Intracellular Ca²⁺ overload is particularly responsible for structural (apoptosis, hypertrophy) and functional (arrhythmias, hypercontraction) myocardial damages (32). Other transporters are involved in the cellular acidosis such as glutamate-gated N-methyl-D-aspartate (NMDA) receptors, transient receptor potential (TRP) family of ion channels, and acid-sensing ion channels (ASIC), each is thought to contribute to calcium overload and metabolic dysfunction (34-37). During IR, calcium antagonists limit the entry of Ca²⁺ ions via the calcium channel and increased stunning recovery (38). In the same way, a lot of NHE1 inhibitors have been shown to decrease IR injuries with some different outcomes according to the inhibitor, and these effects were not species specific (27, 28, 39).

NHE1 is one of the most studied transporters in the setting of IR. A lot of animal models, protocols, timing of inhibition have been tried. In this work, after a general description of the IR phenomenon, we described the mechanisms and pathways associated with NHE1 during IR, and finally give a systematic overview of all the different models of experiments and panel of NHE1 inhibitors used in the different setting of IR.

Current therapeutic strategies against ischemia reperfusion injury

IR is described in a lot of different clinical and pathological situations (7, 40-43):

- Simple-organ IR: heart (acute coronary syndrome), kidney (acute kidney injury), intestine (mesenteric ischemia), brain (stroke)
- Multiple-organ IR: traumatism (multiple organ failure), sepsis shock (multiple organ failure) circulatory arrest (multiple organ failure, hypoxic brain injury, acute kidney injury)
- IR after major surgery: thoracic surgery (acute lung injury), cardiac surgery (stroke, acute heart failure after cardiopulmonary bypass), peripheral vascular surgery (compartment syndrome), major vascular surgery (acute kidney injury), solid organ transplantation (acute graft failure).

Although early reperfusion is required to avoid organ necrosis or death, reperfusion is also associated with injuries that have to be limited (11). These conditions represent major causes of death worldwide and thus a comprehensive understanding of IR is required in order to optimize its management (44). Several clinical and pharmacological therapeutic strategies have been developed to decrease IR injuries (7, 45).

Local or remote ischemic pre- and post- conditioning are the most clinical used approaches. They correspond to exposure to short episodes of ischemia which highly decrease IR tissue injuries. These approaches are long and invasive and demonstrated positive results mainly in animal models (46).

A lot of pharmacological approaches have been developed but with mitigated results in clinic. The probable reason is that IR is complex, multifactorial, and dynamic and thus timing and duration of drug treatment as well as drugs association are difficult to optimize.

Among these drugs, Prolylhydroxylase (PHD) inhibitors prevent degradation of Hypoxia Induced Factor (HIF) which is a crucial factor in hypoxia adaptation (47). As a result, PHD inhibitors increase switch from oxidative phosphorylation to more glycolysis and thus reduce oxygen consumption. These molecules have shown some protection in heart and kidneys (7, 11, 48).

Pharmacological activation of mitochondrial aldehyde dehydrogenase 2 (ALDH2) and AMPK are another metabolic interventions which have proven some benefit in cardiac ischemia (49, 50), as well as hypusination inhibition of eIF5A by N1-guanyl-1,7-diamineoheptane (GC7) which deserved consideration in multiple ischemic situations as kidney transplantation (51-53) and stroke (54).

Interestingly, therapeutic gases provided also some benefits in IR injuries: Hydrogen which can combine with hydroxyl radicals to produce water and limit the formation of the mitochondrial permeability transition pore (55), and other gases that are endogenous like nitric oxide, hydrogen sulfide and carbon monoxide (7).

Lastly, epigenetic interventions have emerged. In this way, several microRNAs have been developed in the setting of IR : inhibition of the miR-17-92 cluster improved vessel growth and recovery (56), miR-24 expression decreased myocardial infarction (57), or miR-122 silencing provided hepatic protection (58).

Other strategies have been studied including adenosine receptor agonists (59-61), cyclosporine (10), chloramphenicol (9) and T cell-based approaches (62, 63)...

In addition to all these targeted pathways and therapeutic strategies, involvement of NHE1 in IR injuries is well known particularly through its role in regulating intracellular concentration of Na^+ ($[\text{Na}^+]_i$), and subsequent intracellular Ca^{2+} ($[\text{Ca}^{2+}]_i$) overload (5, 25) suggesting that NHE1 inhibition could represent an interesting therapeutic strategy.

Mechanisms and pathways involving NHE1 during ischemia reperfusion

During IR, NHE1 is involved in a lot of pathways, mechanisms and interact with several hormones or other molecules.

a. NHE1 impact on intracellular homeostasis during ischemia-reperfusion

NHE1 impact on intracellular homeostasis during IR is presented **Figure 1**.

[Na⁺]_i overload is one of the main consequences of NHE1 activation during IR. Thus limiting [Na⁺]_i is the first key mechanism which may explain cardioprotection after NHE1 inhibition (64, 65). During ischemia (Figure 1B), the decrease in mitochondrial ATP production leads to a decrease in Na⁺/K⁺ ATPase activity and to increased glycolysis. Consequently, [Na⁺]_i accumulates and protons production increases activating in turn NHE1 (66).

Because NHE1 modulates the driving force of the Na⁺/Ca²⁺ exchanger, [Na⁺]_i increase leads also to [Ca²⁺]_i increase (28, 32). A small increase in [Na⁺]_i leads to a significant rise in [Ca²⁺]_i due to the 3:1 Na⁺/Ca²⁺ stoichiometry of the Na⁺/Ca²⁺ exchanger (28, 67). The consecutive cytoplasmic Ca²⁺ accumulation leads to mitochondrial Ca²⁺ increase which can activate the mitochondrial permeability transition pore responsible for cell death (68).

NHE1 inhibitors reduce [Na⁺]_i rise during ischemia by blockade of Na⁺ current (I_{Na,P}) (69), and limiting [Na⁺]_i rise reduced [Ca²⁺]_i overload and myocardial injury (70). NHE1 inhibitors may exert indirect inhibition on [Ca²⁺]_i overload (65). Bepridil, a calcium channel blocker, or magnesium infusion reduce [Ca²⁺]_i and mimic the same effects as NHE1 inhibitor or preconditioning (26, 27). It has been shown in several studies that [Na⁺]_i overload precedes [Ca²⁺]_i overload (71).

The pH recovery during reperfusion is mainly driven by lactate and CO₂ washout essentially through H⁺/lactate⁻ transport (Figure 1C). On the other hand, Na⁺ coupled acid extrusion participates also in pH recovery through NHE1 exchanger and Na⁺/HCO₃⁻ cotransporter (28, 66, 72). EIPA (5-(N-Ethyl-N-isopropyl)amiloride) targets NHE1 but also Na⁺/HCO₃⁻ cotransporter and demonstrated better outcomes than HOE-694 (3-methylsulphonyl-4-piperidino-benzoyl) guanidine methanesulphonate) showing that additional action than highly NHE1 specific inhibition may provide better results (73).

On another hand, Russ *et al.* found contradictories results and showed that Cariporide (HOE-642 = N-(Aminoiminomethyl)-4-(1-methylethyl)-3-(methylsulfonyl)benzamide) did not attenuate anoxia-induced [Ca²⁺]_i overload nor [Na⁺]_i overload but prevented the recovery of pHi from anoxic acidification which may be cardioprotective (31). However, to our knowledge it is the only study showing these discrepancies.

Other molecules like lysophosphatidylcholine, hydrogen peroxide and lactate which accumulates in the ischemic myocardium are potent NHE1 activator and NHE1 inhibition helps also to decrease cardiac damages from these molecules (24, 28, 74-77). NHE1 activation during IR lowers Bcl-2 to Bax ratio leading to cell apoptosis. NHE1 inhibition with Cariporide increases this Bcl-2 to Bax ratio (78).

b. NHE1 expression and activation during ischemia

NHE1 activation has been widely described during reperfusion (71, 79, 80), and whether it is activated or inhibited during the phase of ischemia is a matter of debate and findings are contradictory (38).

Several studies reported an increase in NHE1 mRNA expression during myocardial ischemia (81) which can be reduced by Cariporide taken orally (78, 82). Differently, in the non-infarcted area of the myocardium after acute cardiac ischemia, mRNA and NHE1 protein expression decreased, which may be related to the decreased spread of cardiac cell injury in rats (83).

Scholz *et al.* and Xiao *et al.* demonstrated that NHE1 is activated at the early phase of ischemia (29, 84). Scholz *et al.* showed also that intracellular $[Na^+]_i$ and $[Ca^{2+}]_i$ increase is followed by extracellular pH decrease and NHE1 inhibition. In case of reperfusion, NHE1 is reactivated and is responsible for a second $[Na^+]_i$ and $[Ca^{2+}]_i$ overload (29).

NHE1 mRNA expression depends on the intensity of ischemia. Low flow ischemia induced an increase in NHE1 mRNA levels whereas lower flow eliminated this increase suggesting that severely damaged tissue may not be able to trigger the ischemic response (85).

At the opposite Pantos *et al.* showed that NHE1 expression decreased after myocardial IR in rats (86). Similarly, Simsek *et al.* showed that NHE1 is internalized during ischemia in cardiac-derived HL-1 cells which may be cardioprotective, as rapid postischemic restoration of the NHE1 activity is known to trigger reperfusion injury (87). Goss *et al.* demonstrated also that NHE1 activity decreases in case of ischemia through an internalization of NHE1 but which is not responsible for a NHE1 activity decrease suggesting that NHE1 remained at least partially at the membrane surface (88). In another work, they also showed that NHE1 is bound to the cytoskeleton but without modification of NHE1 activity in the presence of cytochalasin (88) that is known to impair actin polymerization. Jung *et al.* showed that during ischemic stress DAXX (a molecular chaperone) translocates from the nucleus, binds to the ezrin/radixin/moesin-interacting domain which stimulates NHE1 activity (89).

The variables that may explain these discrepancies are the magnitude of the $[Na^+]_i$ rise during ischemia (38) or the duration of ischemia (90). NHE1 may be activated by initial intracellular acidosis, but further extracellular acidosis curtails NHE1 activity. This may explain why NHE1 inhibitors are less effective if given late during ischemia in some studies (73, 91, 92). However, the major regulator of NHE1 remains $[H^+]_i$ and if it stays at low levels NHE1 keeps its activation. Furthermore, other factors like lipid metabolites and reactive oxygen species increased during ischemia and upregulate NHE1 activity (90).

c. Extracellular factors and cellular pathways regulating NHE1

Physiological and pharmacological factors regulating NHE1 activity are presented in [Figure 2](#).

Endothelin activates NHE1 and may exert deleterious effects on myocardium during IR. Khandoudi *et al.* demonstrated that attenuation in contractile recovery and alterations in metabolite content associated with endothelin were prevented by the use of NHE1 inhibitors (93). NHE1 activation by endothelin may occur through the ERK pathway (94). Angiotensin II, α_1 and α_2 -adrenoceptor agonists, hydrogen peroxide,

thrombin or lysophosphatidylcholine also stimulate NHE1 activity especially through ERK pathway activation during IR (6, 90, 95, 96).

P90 ribosomal s6 kinase (RSK) activates also NHE1 by phosphorylating serine 703 of NHE1. Inhibiting NHE1 by blocking RSK could represent an optimal therapeutic strategy as it would block only agonist activated NHE1 function without blocking basal mandatory homeostatic NHE1 activity. RSK blocking in transgenic mice resulted in reduced myocardial infarction (97).

Moor *et al.* confirmed the involvement of RSK but also of ERK1/2 in regulating NHE1 activity. They showed that these 2 MAP kinases dramatically increase during IR (98). Rothstein *et al.* demonstrated that ERK1/2 phosphorylate the carboxy-tail activates NHE1 and mediate the H₂O₂ induced Ca²⁺ overload (99). Acidosis and phenylephrine activate NHE1 through ERK-dependent pathways by direct phosphorylation on Ser(770) and Ser(771) located in the cytosolic tail of NHE1 (100). ERK-pathway activation of NHE1 depends also on bRAF which induces phosphorylation of Thr653 of the carboxy-tail of NHE1 (94). The platelet activating factor (PAF) stimulates cardiac NHE1 which requires the PAF receptor and the involvement of MAP kinase (101).

Taken together ERK and RSK play therefore an important role in the regulation of NHE1.

Tyrosine kinases (TKs) and Ca²⁺/calmodulin-dependent protein kinase II (CaMKII) are involved in cardiac ischemia recovery and Ras-GTPase in the development of cardiac dysfunction (102). CAMK-II regulates NHE1 by phosphorylating its C-terminal part that leads to its activation (103). Ras-GTPase inhibition with FPT III is associated with a decrease in NHE1 expression suggesting that Ras-GTPase regulates NHE1 activity (102).

During myocardial ischemia NHE1 hyperactivation leads to accumulation of axoplasmic Na⁺ in sympathetic nerve endings which favors the outward transport of norepinephrine via the neuronal norepinephrine transporter. The increased levels of norepinephrine stimulate the myocardial alpha and beta adrenoceptors which in turn aggravate the increase in NHE1 activity and the associated deleterious effects. If myocardial ischemia is prolonged, decrease of beta-adrenoreceptors leads to further release of norepinephrine and deleterious consequences (32). Other environmental factors regulate NHE1 including 17beta-estradiol and Apolipoprotein E. 17beta-estradiol activates the release of NO which inhibits NHE1. 17beta-estradiol during ischemia reduced [Na⁺]_i and [Ca²⁺]_i confirming that NHE1 is associated with [Na⁺]_i and [Ca²⁺]_i overload (104). Differently, Apolipoprotein E may stimulate NHE1 during IR and worsen IR injury. Apolipoprotein E-deficient mice tolerated better IR than wild type mice probably because of NHE1 downregulation (105).

d. NHE1 and ventricular hypertrophy

NHE-1 plays a role in cell growth and may contribute to the remodeling which leads to heart failure particularly associated with ventricular hypertrophy (106). Expression of activated NHE1 results in cardiac hypertrophy in isolated rat neonatal ventricular cardiomyocytes (107). Aldosterone may play an important role in the development of ventricular hypertrophy through NHE1 activity (108). In vitro and in vivo studies suggest that NHE1 inhibitors reduce cardiac hypertrophy (106).

Involvement of NHE1 during ischemia reperfusion according to the organ and tissue

Table 1 shows all NHE1 inhibitors, their models and effects according to the organ or tissue studied. Table 2 represents chemical structure of NHE1 inhibitors with their affinity constant.

a. Studies of NHE1 in the Heart

NHE1 is the most expressed NHE isoform in the myocardium (109) and myocardial ischemia represents the most studied model of IR involving NHE1. Myocardial ischemia is one of the leading cause of death worldwide concerning approximately 15% of all deaths and thus represents a major pathology of interest (44). NHE1 is involved in other cardiomyopathies than myocardial infarction, such as postinfarction remodeling, cardiac hypertrophy, and heart failure (1, 110).

Concerning the heart, the situation of IR is also slightly different as compared to other tissues especially considering its contractile properties. It has become clear that the pathophysiological issue of the reperfusion step in heart is highly harmful to contractile cells due to a huge modification in ionic fluxes involving mainly Na^+ , Ca^{2+} , HCO_3^- and H^+ . Roughly, during the ischemic phase, anaerobic glycolysis highly increases leading to an intracellular metabolic acidosis. The subsequent step of reperfusion leads to an over-activation of both alkalizing actors, Na^+/H^+ antiporter (NHE1) and $\text{Na}^+/\text{HCO}_3^-$ transporters. The immediate consequence of intracellular pH (pH_i) recovery is the massive invasion of the cells by Na^+ that activates the reverse mode of the $\text{Na}^+/\text{Ca}^{2+}$ exchanger dragging extracellular calcium into the cell and thus triggering in fine arrhythmias, cardiac contractures and cell death. Thus, lowering the activity of NHE1, which is at the basis of the reperfusion deleterious process, is of the greatest interest (110, 111).

A lot of different models and species have been used to study the involvement of NHE1 in myocardial infarction and to analyze the efficiency of inhibitors of NHE1 on infarct outcomes. Most of experiments concerned rats, including in vivo (78, 83, 112-127) and ex vivo models (isolated perfused heart of rats (25-

27, 69, 70, 73-76, 84-86, 93, 98, 102, 112, 116, 117, 124, 128-163), isolated non perfused hearts of rats (127), and cell analysis using primary cells (rat cardiomyocytes (4, 18, 31, 33, 94, 96, 98-100, 107, 108, 148, 162, 164-169), rat neonatal myocytes (170), and cell line (rat heart-derived H9c2 myoblastic cells (151))). Mice and rabbit models have been extensively used to. Indeed, numerous works have been developed in mice in vivo (96, 97, 105, 171, 172), ex vivo (isolated perfused mice heart (19, 21-23, 173), isolated non perfused mice heart (174, 175)), in cell models (single ventricular myocytes (17), papillary muscles (21, 105), HL-1 cardiomyocytes (87, 157, 176), mouse cardiomyocytes (22, 173, 177)), and in rabbit in vivo (117, 178-180), ex vivo (isolated perfused rabbit hearts (81, 103, 179, 181-183)), and in cell models (cardiac cells of rabbit (184, 185), ventricular trabeculae of rabbits (185)).

Several studies used less current species as chicken (cardiac cells (4)), guinea pig (isolated guinea pig papillary muscles (186), isolated perfused guinea pig hearts (27, 64, 65, 95, 134, 187), ventricular myocytes of guinea pig (188, 189), isolated perfused ferret heart (28), anesthetized gerbils (190, 191), cat ventricular slices or isolated cat ventricular myocytes (96, 192, 193). In addition to several studies using human materials or derived cells as specimens of human right atrium (194, 195) or ventricular trabeculae (185), and human induced pluripotent stem cell-derived cardiomyocytes (34), some works have been developed in more robust preclinical models as pigs (anesthetized pigs (71, 91, 163, 196-201), pig ventricular myocytes (101), open-chest swine model (163, 202)), dogs (anesthetized dogs (123, 203-212), isolated perfused dog heart (30)).

Finally, NHE1 inhibitors have been studied in three clinical trials (ESCAMI, EXPEDITION, GUARDIAN, see below) in the context of myocardial infarction (213-215).

b. NHE1 inhibitors used in myocardial ischemia reperfusion

Several different classes of direct NHE1 inhibitors have been tested in the setting of myocardial IR. We have also detailed here indirect inhibitors of NHE1 during IR that do not specifically inhibit NHE1 but initially interact with another target and inhibit the NHE1 exchanger only secondarily.

❖ Direct NHE1 inhibitors

Pyrazine and acylguanidine derivatives

Amiloride and derivatives (methyloisobutylamiloride, dimethylamiloride, ethylisopropylamiloride, hexamethylenamiloride) were the first inhibitors of NHE1 described (4, 134, 216). In a lot of different species, amiloride or its derivatives enhanced postischemic ventricular recovery, the rate of force development (+dF/dt), contractility, resting tension, relaxation (26, 76, 93, 128, 129, 133-138), improved aortic flow recovery (73, 131, 135), decreased the Na⁺ overload (25, 136, 137, 197), decreased the incidence of ventricular arrhythmias (95, 130, 132, 135, 139), decreased the formation of contracture (133), the size of the infarcted area (202), prevented cell death (170) and increased ATP (64, 129, 130, 136, 137) glycogen and creatine phosphate content (93, 129, 130). However, these inhibitors have the

disadvantage of not being specific and also affect Na⁺/Ca²⁺ antiporter and L-type Ca²⁺-channels (64, 217), and Na⁺ channels (218). It is not clear whether the effects observed with these inhibitors is related to NHE1 inhibition or other transporters inhibition (64, 219, 220).

Benzene and acylguanidine derivatives

HOE-694 (3-methylsulphonyl-4-piperidinobenzoyl guanidine methanesulphonate) is a highly selective NHE1 inhibitor not affecting the other carriers, and involved in pHi regulation in cardiomyocytes (188). In myocardial ischemia, it demonstrated also beneficial effects in a lot of species. He prevented cell death in myocardial ischemia (170), improved aortic flow and contractility recovery (73, 135). It also improved contractility, left ventricular developed pressure, coronary flow on reperfusion, decreased ventricular arrhythmias (139, 141, 196), reduced end-diastolic pressure rise (181). It showed better results than Amiloride (135). However, EIPA, a derivative of Amiloride, which targets NHE1 but also Na⁺/HCO₃⁻ cotransporter demonstrated better outcomes than HOE-694 showing that additional action than very NHE1 specific inhibition may provide better results (73). Na⁽⁺⁾-HCO₃⁽⁻⁾ cotransporter is also activated by intracellular acidification during IR (221).

Cariporide (HOE-642) is another NHE1 inhibitor which has the advantage to be specific of NHE1 (64, 112) and a lot of studies used this inhibitor to explore its effects on NHE1 and ischemic reperfusion injuries (64, 74, 112). In myocardial ischemia in animals, cariporide administration was associated with improvement of left ventricular developed pressure, end-diastolic pressure (64, 74, 84, 140, 145, 147, 178, 182, 183, 198), decreased Nai and Cai overload, limited progression in left ventricular free-wall thickness (198), improved shortening of the action potential duration (71, 198), mitochondrial and myofibrillar disruption (74), endothelial dysfunction (115, 180), attenuated apoptosis (142), dose-dependent infarct size reduction (91, 178, 180), diminution of ventricular arrhythmias (71, 78, 112, 116, 145, 146), decreased contracture during ventricular fibrillation and the accompanying increases in coronary vascular resistance (116), the calcium overload, the release of cardiac enzymes, myocardial water content (183), and mortality (78, 116). Cariporide provides also beneficial effects when given orally for 1 week (178). Paradoxically, Ayoub *et al.* showed that Cariporide did not reduce ischemic-induced Nai and Cai overload and provides cardioprotective effects by maintaining low pHi after reoxygenation (31).

Eniporide mesylate (EMD 85131 = (2-methyl-5-methylsulfonyl-1-(1-pyrrolyl)-benzoyl-guanidine) or Eniporide hydrochloride (EMD 96785) also specifically inhibit NHE1. These inhibitors demonstrated a dose-related decrease of the size of infarct size in dogs, rabbits and guinea pigs (187, 204, 206), improvement of left ventricular pressure developed (187) endothelial cell function (208). Eniporide showed also in mice improvement of left ventricular developed pressure, end-diastolic pressure, and coronary flow (19).

Cariporide and Eniporide were the only inhibitors prospectively tested in humans. In the GUARDIAN trial, Cariporide has shown benefits only in patients undergoing bypass surgery with a reduction in non-Q wave myocardial infarctions (222). In the ESCAMI trial, eniporide reduced the incidence of heart failure in patients reperfused late (213). But in both GUARDIAN and ESCAMI trials, the primary endpoint studied was not achieved. In the EXPEDITION trial, Cariporide given before coronary artery bypass graft surgery decreased the incidence of myocardial infarction but increased the incidence of cerebrovascular events and finally the mortality (215).

In isolated human atrial heart, improvement was seen with cariporide in adults after ischemia but not in old or very old patients. Myocardial expression of NHE1 protein level did not change according to the age (195).

Rimeporide (EMD 87580 = (2-Methyl-4,5-(methylsulfonyl) benzoyl)guanidine) is another specific NHE1 inhibitor which has also shown cardioprotective effects (100, 159, 223). In dogs, rimeporide improved infarct size, myocardial oedema, and neutrophil accumulation (209). However, Kingma did not confirmed cardioprotection in dogs regardless the timing of rimeporide administration (212).

Sabiporide is considered as a good NHE1 inhibitors thanks to its ability to inhibit initial rates of 22Na^+ uptake (K_i of $5 \pm 1.2 \cdot 10^{-8}$ M). It discriminated efficiently between NHE1, 2, and 3 isoforms (K_i for NHE2: $3 \pm 0.9 \cdot 10^{-6}$ M and $K_i > 1$ mM for NHE3), and its inhibition is more persistent than amiloride and cariporide. In piglets, sabiporide improved cardiac function, enhanced blood flow and attenuated systemic proinflammatory response. NHE1 inhibition by sabiporide may be linked in part with ERK phosphorylation inhibition (126), and inhibition of the expression of inducible nitric oxide synthase (iNOS) (126).

BIIB 513 (benzamide-N-(aminoiminomethyl)-4-[4-(2-furanylcabonyl)-1-piperazinyl]-3-(methylsulfonyl)methanesulfonate) improved infarct size in dog (203, 205, 207), rat (114), guinea pig (65), reduced ventricular arrhythmias (65, 114), improved hypotension, myocardial performance, metabolic acidosis and tissue oxygen delivery (199). One of the mechanisms involved in this cardioprotection with BIIB 513 is the reduction of neutrophil activity (207). Preconditioning was less effective than BIIB 513, but association of both BIIB 513 and preconditioning resulted in a greater-than-additive reduction infarct size/anatomic area at risk (203).

BIIB-723 has mitochondrial effects: this NHE1 inhibitor reduced the permeability transition pore and the production of reactive oxygen species (192). It was compared with Cariporide and Rimeporide which gave the same results. Probably because of the inhibition of reactive oxygen species production, NHE1 inhibitors reduced ERK1/2 and p90 ribosomal S6 kinase phosphorylation (192). Maekawa *et al.* demonstrated that p90 ribosomal S6 kinase (RSK) regulates NHE1 activity by phosphorylating NHE1 serine 703 (97).

FR168888 prevents the deterioration of ventricular function and improved reperfusion-induced elevation in resting tension (161).

Furane and acylguanidine derivatives

KR-32568 (5-(2-methyl-5-fluorophenyl)furan-2-ylcarbonyl]guanidine) reduced infarct size and ventricular arrhythmias in rat (121).

KR-32560 ([5-(2-methoxy-5-fluorophenyl)furan-2-ylcarbonyl]guanidine) dose-dependently reduced infarct size, ventricular arrhythmia in rabbits (122) and increased left ventricular end diastolic pressure (154). KR-32560 also decreased the malondialdehyde content and increased activities of glutathione peroxidase and catalase, involving the Akt-GSK-3beta cell survival pathway (154).

KR-32570 [5-(2-methoxy-5-chloro-5-phenyl)furan-2-ylcarbonyl]guanidine] improved cardiac contractile function and contracture in rat thanks to NHE1 inhibition but also to high-energy phosphates preservation and inhibition of lipid peroxidation (149).

Acylguanidine derivatives

KR-32568 (5-arylfuran-2-ylcarbonyl)guanidine) (119), 4-substituted (benzo[b]thiophene-2-carbonyl)guanidines (120), 4-cyano (benzo[b]thiophene-2-carbonyl)guanidine (KR-33028) (123, 151)) exhibited beneficial effects in rats and dogs with reduction of myocardial infarction and improvement of cardiac function.

Zoniporide (CP-597,396 = N-(Aminoiminomethyl)-5-cyclopropyl-1-(5-quinolinyl)-1H-pyrazole-4-carboxamide) reduced infarct size in rabbit in a dose-dependent manner with higher efficiency than eniporide (179, 224). In rats, zoniporide improved left ventricular end-diastolic developed pressures and coronary perfusion pressures and reduced neutrophil accumulation during myocardial ischemia (148). It also reduced postischemic cardiac contractile dysfunction in primate and ventricular fibrillation in rat (224).

Guanidine derivatives

T-162559 ((5E,7S)-[7-(5-fluoro-2-methylphenyl)-4-methyl-7,8-dihydro-5(6H)-quinolinylideneamino]guanidine dimethanesulphonate) improves cardiac contractility and coronary flow in rat and rabbits, decreases lactate dehydrogenase release and infarct size (117, 118).

TY-51924 (sodium 3-guanidinocarbonyl-2-methyl-6,7,8,9-tetrahydro-5H-cyclohepta[b]pyridine-9-ylmethyl sulfate monoethanolate) reduced infarct size in dog (211).

Other direct NHE1 inhibitors

SL 59.1227 (imidazolypiperidine) decreased in rat and rabbit ventricular arrhythmias, the size of infarct and the mortality (113). SL 59.1227 is more specific for NHE1 than for NHE2 (113).

AICAR (5-Aminoimidazole-4-carboxamide-1-beta-d-ribofuranoside) improved the recovery of developed pressure in myocardial ischemia in rats. It prevented rapid rise of Na^+ on reperfusion through an unidentified pathway which does not involve AMP-activated protein kinase (164, 165).

5-(2,5-dichloro)phenyl and 5-(2-methoxy-5-chloro)phenyl derivatives exhibited high NHE-1 inhibitory activities in rats (152).

AVE4454B used in rat myocardial ischemia improved left ventricular compliance, mean aortic pressure, cardiac work index, and reduced cardiac troponin (70).

AVE-4890 is another specific NHE1 inhibitor that improved mitochondrial dysfunction, left ventricular developed pressure, and reduced LDH release in rats through reduction of mitochondrial permeability transition pore opening (153).

❖ Indirect NHE1 inhibitors

Imetit is a H3-receptor agonist. Through α_2 -adrenoceptor inhibition, imetit leads to NHE1 inhibition and reduces incidence of ventricular fibrillation in guinea pig (95).

Ischemic preconditioning (IPC) i.e. alternating short durations of ischemia and reperfusion inhibit NHE1 and improve recovery of contractile function, lead to more ATP and less creatine kinase release in isolated rats and guinea pig hearts (27). IR is associated with increased expression of NHE1 which is decreased by IPC (75). Goldberg *et al.* showed also that IPC could decrease intracellular sodium overload (197) and Xiao *et al.* demonstrated that IPC reduced Na^+ overload through the abolition of the NHE1 activation induced by angiotensin-2 (147). Yeves *et al.* also demonstrated that angiotensin II stimulates NHE1 through both ROS/NHE1 dependent and independent pathways (96). Keul *et al.* showed that cardioprotection through NHE1 inhibition induced by IPC depends on intact sphingosine-1-phosphate receptor 1 signaling (177).

However, IPC may be less effective than NHE1 inhibitor such as Cariporide which is completely unaffected by preconditioning blockade with 5-hydroxydecanoate (146). Eniporide, Amiloride derivatives and BIIB 513 provide also better benefits than IPC (111, 203, 208). Chronic uptake of sulfonylureas or adenosine-receptor antagonists decrease preconditioning benefits by K(ATP) channel inhibition. In dog, NHE1 inhibitor represents a good alternative: eniporide (EMD 85131) still reduces infarct size although sulfonylureas or adenosine-receptor antagonists administration (206). This shows that preconditioning and NHE-1 inhibition do not overlap pharmacologically (203, 206). Association of cariporide and IPC did not improve beneficial effects of IPC (84). Duration of reperfusion in IPC process must not exceed a long time: Gumina *et al.* showed in dog that after 2 hours of reperfusion further ischemic preconditioning have no longer beneficial effect (210).

U-0126 is a ERK kinase (MEK) inhibitor. It inhibits NHE1 through ERK1/2 MAP kinase pathway inhibition (99). However, it has not yet proven cardioprotection in the setting of IR.

FPT III may reduce NHE1 expression. Ras-GTPase is involved in the development of cardiac dysfunction. FPT III is a Ras-GTPase inhibitor and improved left ventricular contractility and coronary vascular hemodynamics in rats (102, 150).

BIX02565 a specific inhibitor of RSK decreased ischemic pS703-NHE1 activation and improved LVDP (175). However, Karki *et al.* showed in rats that RSK and Ser (703) are not required for NHE1 activation by sustained intracellular acidosis (167).

17beta-estradiol stimulates release of NO which inhibits NHE1 in rats developing blood hypertension. 17beta-estradiol enhanced during IR left ventricular developed pressures and decreased lactate dehydrogenase release (104).

Sildenafil (phosphodiesterase 5A inhibitor) decreased NHE1 activity during reperfusion through NHE1 dephosphorylation (protein phosphatase 1-dependent reduction) and bypassing reactive oxygen species generation. Sildenafil could represent an optimal therapeutic approach as this drug could reduce NHE1 hyperactive state without affecting NHE1 basal activity which may be necessary for housekeeping function. Sildenafil decreases NHE1 phosphorylation and then reduces its hyperactivity (225).

Small interference RNA (siRNA) produced in vitro to specifically silence NHE1 were injected into the apex of left ventricular wall of mouse myocardium and decreased NHE1 expression and activity. The beneficial effects on IR injury have not yet been studied (171).

Hydrogen sulfide via PI3K/Akt/PKG-dependent pathway interaction suppressed NHE1 activity and improved cardiac function during IR (168).

Dietary Omega-3 polyunsaturated fatty acids (ω 3-PUFAs) decreased NHE-1 upregulation in rabbit ventricular myocytes with induced heart failure and decreased the incidence of delayed afterdepolarizations (185). However, the degree of hypertrophy was not decreased with ω 3-PUFAs (185). It is unclear whether ω 3-PUFAs exert a direct or indirect effect on NHE1.

Sodium glucose cotransporter 2 inhibitors (SGLT2i) (Empagliflozin, Dapagliflozin, Canagliflozin, Ertugliflozin) have demonstrated cardioprotective effects in several studies EMPA-REG OUTCOME, VERTIS-CV, CANVAS DECLARE-TIMI 58, and in the SCORED trials (226-230). Number of underlying mechanisms are supposed to explain these effects, including NHE1 activity inhibition as well as Na⁺ and Ca²⁺ overload reduction (231). Particularly, Empagliflozin delayed contracture development and increased mitochondrial respiration post-ischemia (173, 232).

Sevoflurane is an anesthetic gas widely used in surgery and has shown beneficial post-conditioning effects. Sevoflurane given during myocardial reperfusion in rat increased the NO and NOS levels and decreased NHE1 expression. This resulted in a decrease in the size of the infarct size (160). Sevoflurane

may also inhibit the mitochondrial permeability transition pore opening and attenuated cardiomyocyte apoptosis and excessive autophagy (160).

c. Timing of NHE1 inhibitor administration during heart IR

Timing of NHE1 inhibition for the improvement of ischemic reperfusion lesions is variable according to the literature.

Several timing of NHE1 inhibitor administration have been studied and provided cardioprotection in animal models:

- administration **before ischemia** was the most used protocol (25, 27, 65, 71, 74, 78, 93, 95, 102, 104, 113-115, 117-119, 121-123, 129, 130, 132, 135, 137, 138, 140-142, 148, 151, 153, 178, 180, 182, 183, 197, 198, 202, 203, 205-209, 215, 222, 223),
- administration **during ischemia** was often performed (91, 113, 116, 136, 140, 145, 178, 199, 213, 222, 223) as well as **during reperfusion** (25, 65, 76, 84, 129, 131-135, 182, 205)
- several studies have tried perfusion **during all times of IR**, i.e. before and during ischemia and during reperfusion (28, 73, 134, 139, 140, 170)
- few studies have tried perfusion during ischemia and during reperfusion (84, 91, 128) and only one study before and during ischemia (64)

Most of the studies used only one time of inhibitor administration. Nevertheless, several studies have compared different timing which allow to propose the best window of treatment. Generally better cardioprotection was demonstrated if NHE1 inhibitor was given before ischemia than during reperfusion (28, 134, 135, 141, 178, 181, 186), and even no efficiency can be found if inhibitor is given late during ischemia and reperfusion (91), or during reperfusion only (128, 138). Interestingly, multiple times of treatment seem demonstrate a better cardioprotection effect. Toyoda *et al.* concluded that better cardioprotection was obtained if given both before ischemia and during reperfusion than before ischemia alone (182) and Harper *et al.* showed better results if given at all times than if withdrawn during reperfusion (170).

In the studies involving only humans, administration during ischemia reduced incidence of heart failure but did not reduce infarct size or mortality (ESCAMI) (213). In the GUARDIAN trial, the cardioprotective effect was obtained if NHE1 inhibitor was given before ischemia in patients undergoing coronary bypass (GUARDIAN) (222). Avkiran *et al.* confirmed that NHE1 inhibitors probably decrease progression of myocardial ischemia if given prior the most earlier to ischemia (233). Piper *et al.* concluded that NHE1 inhibition before or during ischemia provide better cardioprotective effects than given during reperfusion. They hypothesized that the protection provided by pre-ischemic administration is due to a reduction in Na⁺ and secondary Ca²⁺ influx. However, NHE1 inhibition also has some beneficial effects if performed during reperfusion since it can prolong intracellular acidosis which can prevent hypercontracture (220).

Ideally administration of treatments before the ischemic event represents the best way to prevent ischemic reperfusion lesions (233). However ischemic event is not predictable that means that only chronic treatments in patients at risk could be considered which is not yet available. Otherwise only treatments given after the beginning the ischemia, i.e. during and/or after reperfusion can be considered.

Involvement of NHE1 in IR of other organs

NHE1 during IR has been studied in several other organs than the heart, in particular in the brain whose ischemia is also responsible for a considerable proportion of deaths worldwide (44).

a. NHE1 and the Brain

Different models of experimentation in brain IR were used in the literature : rat brain (234, 235), rat glioma cells (236), isolated mice brain (20, 237-242) and cultured neuron cells of mice (238, 243, 244), isolated brains of gerbils (190, 191).

A lot of NHE1 inhibitors used in heart were also studied in brain IR except SM-20220 (N-(aminoiminomethyl)-1-methyl-1-H-indole-2-carboxamide methanesulfonate) and normobaric oxygen. The NHE1 inhibitor SM-20220 or 60% normobaric oxygen decreased the infarct size and water content in the brain of rats (234, 235). Normobaric oxygen also improved neurological impairment score, and reduced expression of HIF-1 α , aquaporin 4 and NHE1 (235). SM-20220 prevented the progress of cerebral infarct volume in rat thanks to a limiting neutrophils accumulation (234). SM-20220 reduces also neuronal death and cellular swelling through inhibition of both persistent $[Ca^{2+}]_i$ increase and acidification in excitotoxicity (245). SM-20220 provided neuroprotective effects by reducing the ischemia-evoked efflux of free fatty acids (246).

Amiloride reduced cell swelling and $[Na^+]_i$ in rat C6 glioma cells (236). In gerbil, amiloride improved locomotor activity, reduced the activation of astrocytes and microglia in the ischemic hippocampal CA1 region (190). Amiloride reduced energy failure in brain slice model (247). N-methyl-isobutyl-amiloride reduced post-ischemic seizures, microglial activation, and infarct size (248-250).

Cariporide or isoform 1-null mice exhibited reduced infarct size (20, 240). Cariporide in ischemic neurons of mice decreased rise of Ca^{2+} and the second phase of $[Na^+]_i$ rise, and reduced infarct size (20, 237, 241). Cariporide reduced also microglial proinflammatory activation following ischemia (241). NHE1 gene inactivation in mice leads to the same effects as cariporide administration (20, 237). N-methyl-d-aspartate (NMDA) -type glutamate receptors during IR are activated and lead to superoxide production by NADPH oxidase and cell death. NHE1 inhibition with Cariporide reduced NMDA and NADPH activation (243). Cariporide abolished production of superoxide anion, cytokines and inducible nitric oxide synthase (244).

In NHE1 heterozygous (NHE1+/-) mice or homozygous (NHE1-/-), brain infarct and mitochondrial damage were reduced (237, 240).

KR-33028 and Zoniporide attenuated neuronal glutamate-induced LDH release with 18-fold greater potency in vitro, and reduced brain infarct size in vivo with similar potency than Zoniporide (238). Like in myocardium, ERK/p90(RSK) pathway is also stimulated during brain IR and leads to NHE1 activation (239). Selective inhibition of P90(RSK) with fluoromethyl ketone reduced p-NHE1 expression and ischemic infarct volume. Astrocytic and microglial NHE1 in mice may also play an important role during brain IR (241, 242). Finally, ischemic preconditioning inhibits NHE1 expression and induced hippocampal CA1 in gerbils (191).

b. NHE1 and the Kidneys

During renal IR several isoforms of NHE are involved. The cortical NHE1 ARNm expression increased mildly after reperfusion in response to the cell acidosis whereas NHE3 activity is suppressed, and NHE2 and NHE4 expression decreased (251). NHE3 expression decreased during ischemia and leads to an increase in delivery of HCO_3^- . NHE2 and NHE4 are more involved in cell volume regulation and their decrease during IR may reflect cell swelling.

Vitamine D is known to have renoprotective effects. After renal ischemia-reperfusion, 22-oxacalcitriol (a synthetic vitamin D analogue) have shown reduction of renal function deterioration and histological damage associated with downregulation of NHE1 expression in kidneys of rats (252). In the same way, FPTIII decreases NHE1 expression via NO elevation in rats with blood hypertension which is correlated to an improved urine volume and a reduce proteinuria (150).

c. NHE1 and the Lungs

Cariporide in isolated rat lung ischemia decreased bronchoalveolar lavage fluid protein, lung water content, malondialdehyde and mean pulmonary artery pressure and increased superoxide dismutase activity (253). In this model, Ca^{2+} overload was prevented thereby reducing the activation of xanthine oxidase pathway and ROS production (253). In another study, Cariporide in rabbit lungs increased oxygenation, superoxide dismutase activity and reduced proinflammatory cytokines and lung water content (254).

d. NHE1 and other Tissues

Involvement of NHE1 has been described in numerous other tissues including circulating cells. Indeed, Cariporide, Eniporide or T-162559 reduced IR induced platelet swelling in human (112, 117, 118). The same results were described for 2-(5-methoxybenzimidazol-2-ylthio)-5-chloro-2,3-dihydroinden-1-ylidene aminoguanidine hydrobromide (5m) and Zoniporide (125, 148) in rat and for Zoniporide and KR-32568 in rabbit (179, 224). In rabbit erythrocytes, Amiloride, EIPA and Cariporide inhibited successfully NHE1 during IR (112, 130). FR168888 reduced cell swelling in rat thymic lymphocytes (161).

Finally, in pig skeletal muscle, cariporide given before or after 4 hours after ischemia reduced infarction, myeloperoxidase activity and mitochondrial-free Ca(2+) content and increased ATP (255).

Perspectives

In conclusion, involvement of NHE1 in ischemic reperfusion/injury is well described in a lot of organ and tissues, especially in heart and brain. Indeed, heart and brain ischemia represent the leading cause of ischemic death worldwide.

These results have been showed in many species including human confirming that the role of NHE1 in mediating injury is not species specific. A lot of different NHE1 inhibitors have proven efficiency in animals and some benefits in humans. However, since the negative results of GUARDIAN, ESCAMI and EXPEDITION trials, no further NHE1 inhibition study in human have been conducted, although many types of NHE1 inhibitor have not been yet tried. For example, the sodium glucose cotransporter 2 inhibitors decrease NHE1 activity in a very different way than Cariporide and Eniporide used in the trials and showed spectacular benefit very recently in the setting of heart failure but have not yet been used in IR.

Adequate NHE1 inhibitor or combination with others clinical and pharmacological approaches should probably deserve further consideration for the treatment of IR injury. Timing, dosage, and the population are other factors than the inhibitor itself which can influence the effectiveness of the treatment.

Involvement of NHE1 has also not yet been studied in many other ischemic reperfusion conditions (like mesenteric ischemia, sepsis, traumatism, circulatory arrest, surgery, solid organ transplantation ...). Further studies are needed in these settings.

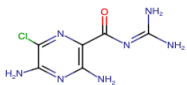
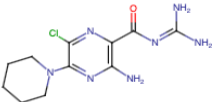
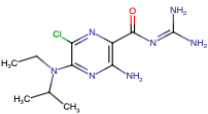
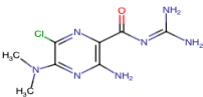
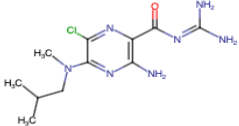
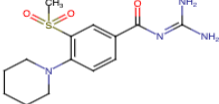
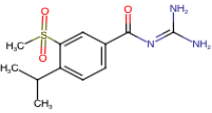
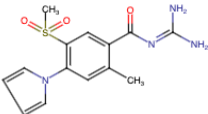
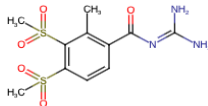
Table 1. Different NHE1 inhibitors, organ models, and effects according to the organ or tissue studied

NHE1 inhibitors	Organ	Timing inhibition	Ischemia duration	Reduce infarct size	∨ Left ventricular end-diastolic pressure	∧ Left ventricular developed pressure	Reduce arrhythmia	Specific effect	Reference
17 beta-estradiol	Heart	R & before I	40 min			+		∨ [Na] ⁺ , [Ca ²⁺] ⁺ , LDH	(104)
AICAR	Heart	Before I	30 min			+		∨ [Na] ⁺	(165)
Amiloride	Heart	During I and R	60 min			+		∧ + dF/dt, -dF/dt	(128)
Amiloride	Heart	Before or during I	15 min				+		(132)
Amiloride, HMA	Heart	During R	15 min					∧ force recovery, ventricular rate	(76)
Amiloride, HMA	Heart		15 min					∧ contractility, resting tension	(26)
Amiloride, DMA, HMA, EIPA	Heart	During R	60 min					∧ tension, relaxation, ∨ contracture	(133)
Amiloride, HOE 694	Heart	Before & after I	20 min				+	∧ cardiac output	(135)
Amiloride, MIA	Heart	Before I	60 min			+		∧ + dF/dt, -dF/dt	(138)
Amiloride, MIA	Heart	During R	60 min					no effect	(138)
Amiloride, EIPA	Heart	Before I	15 min				+		(130)
Amiloride, EIPA	Erythrocytes							∨ [Na] ⁺	(130)
AVE4454B	Brain	Before I						∨ [Na] ⁺ , ∨ swelling	(236)
AVE4454B	Heart	During R	15 min					∧ tension, relaxation, Cl ⁻ , ∨ troponin	(70)
AVE-4890	Heart	During R	40 min			+		∨ LDH	(153)
Methylisobutylamiloride	Heart	Before & after I	45 min					∧ tension, relaxation	(134)
Methylisobutylamiloride	Heart	Before I	30 min			+		∧ + dF/dt, -dF/dt	(93)
DMA	Heart	During R	55 min					∨ CPK release	(129)
DMA	Heart	Before I		+			-		(202)
EIPA	Heart		21 to 30 min			+		∨ ATP depletion	(136)
EIPA	Heart	Before I	20 min					∧ cardiac output, coronary flow	(137)
HOE 694	Heart	Before I	40 min		+	+			(103)
HOE 694	Heart	Before I	7 min				+		(141)
HOE 694	Heart	Before I	20 min				+	∧ contractility	(196)
HOE 694	Heart	Before or after I	45 min		+	+		Before I > After I	(181)
EIPA, HOE 694	Heart	Before or during or after I	30 to 60 min					∧ cardiac output, EIPA>HOE 694	(73)
EIPA, HOE 694	Heart	Before or after I	15 min				+		(139)
DMA, HOE694	Heart	Before I	30 to 60 min					∨ cell death	(170)
Cariporide, Preconditioning	Heart	Before I	45 and 90 min			+			(146)
Cariporide	Heart,						+	∨ platelet swelling	(112)
Cariporide, MIA	Platelets								
Cariporide	Heart	Before I (LPC)			+	+			(74)
Cariporide	Heart	Before I	15 to 36 min		+	+		∨ contracture	(64)
Cariporide, Isof, Sevof	Heart	Before I	60 min		+	+			(140)
Cariporide	Heart	during or after I	30 min		+	+		during I > after I	(84)
Cariporide	Heart	During I	35 min		+	+	+	∨ time to ROSC	(145)
Cariporide, Losartan, IPC	Heart	During I & R	30 min			+			(147)
Cariporide	Heart	During I	7 min 45 s				+	∧ cardiac index	(198)
Cariporide	Heart	Before I or R	30 min	+	+			before I > before R	(178)
Cariporide	Heart	Bef. I – R – IR	30 min	+		+		Before IR > before I	(182)
K/Mg cardioplegia	Heart	Bef. I – R – IR	30 min			-			(182)
Cariporide	Heart	Before I	45 min			+		∧ coronary flow	(183)
Cariporide	Heart	Before I	2 X 10 min					∧ endothelial function	(115)
Cariporide	Heart	Chronic diet or just before I	30 min	+				∧ endothelial function	(180)
Cariporide	Heart	During I, IR	60 min	+				Chronic diet > before I	
Cariporide	Heart	During I					+	Not working late in I	(91)
Cariporide	Heart	During I					+	∧ diastolic and systolic function, mortality	(116)
Cariporide	Heart	Chronic diet	45 min				+	∨ mortality	(78)
Cariporide	Heart	Before I	10 min				+	∨ MAP reduction	(71)
Cariporide	Heart	Before I and R	30 min	+	+	+			(178)
Cariporide	Heart	Before I						∨ MI before surgery	(222)
Cariporide	Heart	Before R						∨ MI before ∧ mortality	(215)
Cariporide	Heart	During I	30 min			+		Only in adult myocard	(195)
Cariporide	Brain	Before I	60 min					∨ microglial inflammation	(241)
Cariporide	Brain	Before I	2 hours					∨ O ₂ ⁻ , Cytokines, NOS	(244)
Cariporide	Brain		2 hours	+					(20)
Cariporide	Brain	During I or R	30-60 min	+					(240)
Cariporide	Brain	Before I	55 min					∧ neurological function	(256)
Cariporide	Brain	During I or R	60 min					∨ microglial inflammation	(241)
Cariporide	Brain	Before I	30 min	+					(237)
Cariporide	Brain	During I	20 min					∨ superoxide prod.	(243)
Cariporide	Lungs							∨ H ₂ O, PAPm	(253)
Cariporide	Erythrocytes							∨ [Na] ⁺	(112)
Cariporide	Platelets							∨ Platelet swelling	(112)
Eniporide mesylate	Heart	Before I	35 min	+	+	+		∨ LDH	(112)
Eniporide mesylate	Heart	Before I or R	60 min	+					(187)
Eniporide mesylate	Heart	Before I	60 min	+					(204)
Eniporide hydrochloride	Heart	Before I	90 min	+				∨ CPK	(206)
Eniporide	Heart	Before R						∧ diastolic function	(208)
FPT III	Heart	Before I	40 min		+	+		No modification	(213)
FPT III	Heart	Before I	40 min			+		∧ Blood pressure	(102)
FPT III	Heart	Before I	40 min			+		∧ relaxation, pressure	(150)
FPT III	Kidneys							∨ urine volume,	(150)

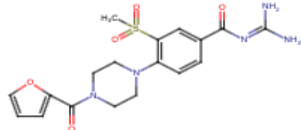
IPC	Heart	Before I	90 min	-				proteinuria	(208)
IPC	Heart	Before I	30 min			+		∖ CPK, [Na ⁺] _i , [Ca ²⁺] _i	(27)
IPC	Heart	Before I	30 min					∧ NHE1 expression	(75)
IPC	Heart	Before I	60 & 90 min	+				IPC < BIIB 513	(203)
IPC, BIIB 513	Heart	Before I	90 min	+				∖ diastolic dysfunction	(208)
IPC, Cariporide	Heart	During I (C.)	60 min			+		IPC < Eniporide	(84)
IPC, Eniporide, Bimakalin	Heart	Before I	60 min	+			+	IPC < Eniporide & Bimakalin	(210)
IPC	Brain	Before I	2 to 5 min					∖ neuronal death	(191)
Eniporide	Heart	Before I	40 min			+	+	∧ coronary flow	(19)
Imetit	Heart	Before I	20 min					∖ noradrenaline	(95)
Zoniporide	Heart	Before I	30 min	+			+		(179)
Zoniporide	Heart	Before I	30 min	+			+		(224)
5m	Heart	Before R	60 min	+					(125)
KR-32560	Heart	Before I	25 min			+	+		(154)
KR-32560	Heart	Before I	30 min	+					(122)
KR-32568	Heart	Before I	30 min	+					(121)
KR-32568	Platelet	Before I	30 min					∖ platelet swelling	(121)
KR-32570	Heart	Before I	30 min				+	∖ LDH, lactate, ∧ ATP	(149)
KR-33028	Heart	Before I	30 min					∖ LDH, ∧ ATP	(151)
KR-33028	Heart	Before I	45 min	+			+		(123)
KR-33028	Brain	During I	12 hours	+				∖ LDH release	(238)
Sildenafil	Heart	Reperfusion	40 min					∧ antioxidant enzyme	(193)
Hydrogen sulfide	Heart	Before I	30 min			+	+	∖ proton efflux	(168)
Acidic reperfusion	Heart	Reperfusion	35 min			+	+		(157)
IPC	Brain	Before I	2 and 5 min	+					(257)
Postconditioning	Heart	Reperfusion	35 min			+	+		(157)
Ethylisopropylamiloride	Heart	Reperfusion	35 min			-	-		(157)
Post conditioning	Heart	Reperfusion	90 min	+		+	+		(212)
N3G	Heart					+	+		(158)
BIIB513	Heart, Brain, Kidneys	During I	30 min					∖ multiorgan injury, mortality	(200)
BIIB513	Heart	Before I	30 min	+				∖ CPK	(114)
BIIB513	Heart	Before I or R	60 min	+				Before I = Before R	(205)
BIIB513	Heart	Before I	60 min	+				∖ Neutrophil activity	(207)
Sabiporide	General	Reperfusion	3 min					∧ LVEF, ∖ TNF α, MPO, TnI	(201)
Sabiporide	Heart	Before I, R	30 min	+					(126)
T-162559, Cariporide, Eniporide	Heart	Before I	25 min	+		+	+	∖ LDH	(117)
T-162559	Platelets	Before I	60 min	+				∖ platelet activity	(118)
T-162559	Heart	Before I	60 min	+					(118)
T-162559, Cariporide, Eniporide	Platelets							∖ NHE1 activity	(117)
TY-51924	Heart	Before R	90 min	+			+		(211)
Rimeporide	Heart	Reperfusion	40 min	+		-	+		(159)
Rimeporide	Heart	Before I, R	90 min	-					(212)
Rimeporide	Heart	During I or R	60 min	+				∖ MPO, infarct if I & R	(209)
22-oxalacitriol	Kidney	Before I	30 min					∖ Renal apoptosis, creatinin	(252)
Normobaric oxygen	Brain	During R	120 min	+				Improve NIS, ∖ H ₂ O	(235)
Empagliflozin	Heart	During I	25 min	+			+	Delayed contracture	(173)
ω3-PUFAs	Heart								(185)
DMA	Brain							∖ LDH release	(258)
Harmaline	Brain							∖ LDH release	(258)
SL 59.1227	Heart	Before I or R	7 & 30 min	+			+	∖ Mortality	(113)
SM-20220	Brain	During I	72 hours	+				∖ H ₂ O	(234)
SM-20220	Brain	Before I						∖ neuronal swelling and death	(245)
Amiloride	Brain							Delayed energy failure	(247)
SM-20220	Brain	Bef. & During I	20 min	+				∖ free fatty acid	(246)
Ethylisopropylamiloride	Brain	Before I	20 min					∖ free fatty acid efflux	(259)
N-methyl-isobutyl-amiloride	Brain	Before I	30 to 60 min	+				∖ TUNEL + cells	(249)
N-methyl-isobutyl-amiloride	Brain	Before I	60 min					∖ seizures	(248)
N-methyl-isobutyl-amiloride	Brain	During & after I		+				∖ microglial activation, lactate	(250)
EIPA	Brain	After I						∖ activation of astrocytes and microglia	(190)
BIX02565	Heart	Before I	20-40 min			-			(175)
Sevoflurane	Heart	During R	30 min	+				∖ NO, NOS, Bcl2	(160)
FR168888	Heart	Before I	32 min				+		(161)
FR168888	Lymphocytes	Before I	32 min					∖ cellular swelling	(161)
Zoniporide	Platelets							∖ platelets swelling	(148)
Zoniporide	Heart	Before I				+	+	∖ MPO activity	(148)

AICAR = 5-amino-1-beta-D: -ribofuranosyl-imidazole-4-carboxamide, Bef. = Before, CI = Cardiac index, CK = Creatine phosphokinase, DMA = Dimethylamiloride, EIPA = Ethylisopropylamiloride, IPC = Ischemic preconditioning, FPTIII = Farnesyl protein transferase inhibitor III, H₂O = water, HMA = Hexamethyleneamiloride, I = ischemia, LDH = Lactate dehydrogenase, LVEF = Left ventricular ejection fraction, MAP = Monophasic action potential, MI = Myocardial infarction, MIA = 5-N-Methy-N-isobutyl amiloride, NIS = Neurological impairment score, NOS = NO synthetase, MPO = Myeloperoxidase, PApM = Mean arterial pulmonary pressures, R = Reperfusion, ROSC = Reestablishment of spontaneous circulation, TNF = Tumor Necrosis Factor, TUNEL = d-UTP nick end-labelling, ω3-PUFAs = Omega-3 polyunsaturated fatty acids

Table 2. Chemical structure of NHE1 inhibitors with their affinity constant

NHE1 Inhibitor	Chemical structure	Ki μ M	IC50 μ M	Reference
Amiloride		1 – 7 3 1 – 1.6 Rat 5 Rat	3.7 – 60 160 +/- 3.4 WT NHE1 >1000 Receptor NHE1	(260) (203) (203) (261) (262) (263)
5-(N,N-Hexamethylene)amiloride		0.013		(260)
Ethylisopropylamiloride		0.01	0.016 – 0.8 1.43 +/- 0.33 WT NHE1 25 +/- 8	(260) (203) (203)
Dimethylamiloride		0.023 – 0.5 0.1	0.19	(260) (261)
Methylisobutylamiloride			0.001	(264)
HOE-694 3-methylsulphonyl-4-piperidinobenzoyl guanidine methanesulphonate		0.16		(261)
HOE 642 (Cariporide (HOE-642))		0.008 – 0.04 0.05	0.03 – 3.4 0.08 > 1000 Receptor NHE1	(260) (243) (203) (112)
Eniporide mesylate EMD 85131 (2-methyl-5-methylsulfonyl-1-(1-pyrrolyl)-benzoyl-guanidine			0.0045 – 0.38	(260)
Rimeporide (EMD 87580 = (2-Methyl-4,5-(methylsulfonyl)benzoyl)guanidine)			0.113 +/- 0.006	(265)

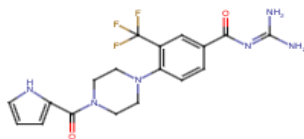
BLIB 513 benzamide-N-(aminoiminomethyl)-4-[4-(2-furanylcarbonyl)-1-piperazinyl]-3-



0.25 +/- 0.06
>1000 Receptor NHE1

(65, 114, 203)
(203)

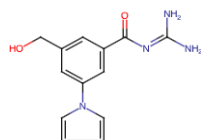
Sabiporide



0.05 +/- 0.0012

(126, 201)

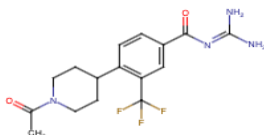
FR168888



3.23 - 6

(161)

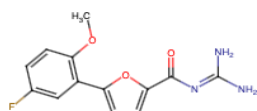
N-[4-(1-acetyl-piperidin-4-yl)-3-trifluoromethyl-benzoyl]-guanidine



>30

(158)

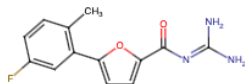
KR-32560 5-(2-methoxy-5-fluorophenyl)furan-2-ylcarbonyl]guanidine



0.05 +/- 0.01

(122, 154)

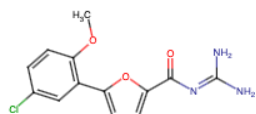
KR-32568 5-(2-methyl-5-fluorophenyl)furan-2-ylcarbonyl]guanidine



0.23

(119)

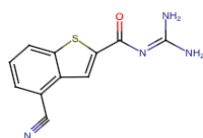
KR-32570 5-(2-methoxy-5-chloro-5-phenyl)furan-2-ylcarbonyl]guanidine



0.05 +/- 0.01

(149, 266)

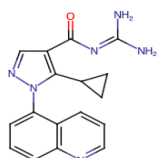
KR-33028 4-cyano (benzo[b]thiophene-2-carbonyl]guanidine



0.0022

(123, 151,
238)

Zoniporide [1-(quinolin-5-yl)-5-cyclopropyl-1H-pyrazole-4-carbonyl] guanidine

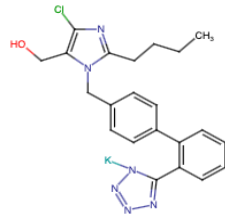
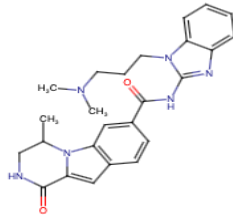


0.059

(267)

50

2-(5-methoxybenzimidazol-2-ylthio)-5-chloro-2,3-dihydroinden-1-ylidene aminoguanidine hydrochloride (5m)		0.00094	(125)
SL 59.1227 3-[(cyclopropylcarbonyl)amino]-N-[2-(dimethylamino)ethyl]-4-[4-(5-methyl-1H-imidazol-4-yl)piperidin-1-yl]benzamide		0.0033 +/- 0.0013	(113)
AICAR 5-Aminoimidazole-4-carboxamide-1-beta-d-ribofuranoside		(165)	
Harmaline		(267)	
T-162559 (5E,7S) [7-(5-fluoro-2-methylphenyl)-4-methyl-7,8-dihydro-5(6H)-quinolinylideneamino] guanidine dimethanesulphonate		0.00096	(117, 118)
Empagliflozin		(173, 226, 232)	
Bimakalim		(210)	
Imetit		(95)	



References

1. Pedersen SF, Counillon L. The SLC9A-C Mammalian Na⁺/H⁺ Exchanger Family: Molecules, Mechanisms, and Physiology. *Physiol Rev* 2019; 99: 2015-2113.
2. Wong KY, McKay R, Liu Y, Towle K, Elloumi Y, Li X, Quan S, Dutta D, Sykes BD, Fliegel L. Diverse residues of intracellular loop 5 of the Na⁺/H⁺ exchanger modulate proton sensing, expression, activity and targeting. *Biochim Biophys Acta Biomembr* 2019; 1861: 191-200.
3. Karmazyn M. NHE-1: still a viable therapeutic target. *J Mol Cell Cardiol* 2013; 61: 77-82.
4. Frelin C, Vigne P, Lazdunski M. The role of the Na⁺/H⁺ exchange system in cardiac cells in relation to the control of the internal Na⁺ concentration. A molecular basis for the antagonistic effect of ouabain and amiloride on the heart. *J Biol Chem* 1984; 259: 8880-8885.
5. Lazdunski M, Frelin C, Vigne P. The sodium/hydrogen exchange system in cardiac cells: its biochemical and pharmacological properties and its role in regulating internal concentrations of sodium and internal pH. *J Mol Cell Cardiol* 1985; 17: 1029-1042.
6. Karmazyn M. Mechanisms of protection of the ischemic and reperfused myocardium by sodium-hydrogen exchange inhibition. *J Thromb Thrombolysis* 1999; 8: 33-38.
7. Eltzschig HK, Eckle T. Ischemia and reperfusion--from mechanism to translation. *Nat Med* 2011; 17: 1391-1401.
8. Melis N, Carcy R, Rubera I, Coughon M, Duranton C, Tauc M, Pisani DF. Akt Inhibition as Preconditioning Treatment to Protect Kidney Cells against Anoxia. *Int J Mol Sci* 2021; 23.
9. Sala-Mercado JA, Wider J, Undyala VV, Jahania S, Yoo W, Mentzer RM, Jr., Gottlieb RA, Przyklenk K. Profound cardioprotection with chloramphenicol succinate in the swine model of myocardial ischemia-reperfusion injury. *Circulation* 2010; 122: S179-184.
10. Piot C, Croisille P, Staat P, Thibault H, Rioufol G, Mewton N, Elbelghiti R, Cung TT, Bonnefoy E, Angoulvant D, Macia C, Raczka F, Sportouch C, Gahide G, Finet G, Andre-Fouet X, Revel D, Kirkorian G, Monassier JP, Derumeaux G, Ovize M. Effect of cyclosporine on reperfusion injury in acute myocardial infarction. *N Engl J Med* 2008; 359: 473-481.
11. Eckle T, Kohler D, Lehmann R, El Kasmi K, Eltzschig HK. Hypoxia-inducible factor-1 is central to cardioprotection: a new paradigm for ischemic preconditioning. *Circulation* 2008; 118: 166-175.
12. Mitchell P. Chemiosmotic coupling in oxidative and photosynthetic phosphorylation. *Biol Rev Camb Philos Soc* 1966; 41: 445-502.
13. Murer H, Hopfer U, Kinne R. Sodium/proton antiport in brush-border-membrane vesicles isolated from rat small intestine and kidney. *Biochem J* 1976; 154: 597-604.
14. Dong Y, Gao Y, Ilie A, Kim D, Boucher A, Li B, Zhang XC, Orłowski J, Zhao Y. Structure and mechanism of the human NHE1-CHP1 complex. *Nat Commun* 2021; 12: 3474.
15. Miller RT, Counillon L, Pages G, Lifton RP, Sardet C, Pouyssegur J. Structure of the 5'-flanking regulatory region and gene for the human growth factor-activatable Na/H exchanger NHE-1. *J Biol Chem* 1991; 266: 10813-10819.
16. Poet M, Doyen D, Van Obberghen E, Jarretou G, Bouret Y, Counillon L. How Does Our Knowledge on the Na⁺/H⁺ Exchanger NHE1 Obtained by Biochemical and Molecular Analyses Keep up With Its Recent Structure Determination? *Front Physiol* 2022; 13: 907587.
17. Baczko I, Mraiche F, Light PE, Fliegel L. Diastolic calcium is elevated in metabolic recovery of cardiomyocytes expressing elevated levels of the Na⁺/H⁺ exchanger. *Can J Physiol Pharmacol* 2008; 86: 850-859.
18. Karki P, Fliegel L. Overexpression of the NHE1 isoform of the Na⁺/H⁺ exchanger causes elevated apoptosis in isolated cardiomyocytes after hypoxia/reoxygenation challenge. *Mol Cell Biochem* 2010; 338: 47-57.
19. Wang Y, Meyer JW, Ashraf M, Shull GE. Mice with a null mutation in the NHE1 Na⁺-H⁺ exchanger are resistant to cardiac ischemia-reperfusion injury. *Circ Res* 2003; 93: 776-782.
20. Luo J, Chen H, Kintner DB, Shull GE, Sun D. Decreased neuronal death in Na⁺/H⁺ exchanger isoform 1-null mice after in vitro and in vivo ischemia. *J Neurosci* 2005; 25: 11256-11268.
21. Cook AR, Bardswell SC, Pretheshan S, Dighe K, Kanaganayagam GS, Jabr RI, Merkle S, Marber MS, Engelhardt S, Avkiran M. Paradoxical resistance to myocardial ischemia and age-related cardiomyopathy in NHE1 transgenic mice: a role for ER stress? *J Mol Cell Cardiol* 2009; 46: 225-233.
22. Imahashi K, Mraiche F, Steenbergen C, Murphy E, Fliegel L. Overexpression of the Na⁺/H⁺ exchanger and ischemia-reperfusion injury in the myocardium. *Am J Physiol Heart Circ Physiol* 2007; 292: H2237-2247.
23. Mraiche F, Wagg CS, Lopaschuk GD, Fliegel L. Elevated levels of activated NHE1 protect the myocardium and improve metabolism following ischemia/reperfusion injury. *J Mol Cell Cardiol* 2011; 50: 157-164.
24. Karmazyn M. The myocardial sodium-hydrogen exchanger (NHE) and its role in mediating ischemic and reperfusion injury. *Keio J Med* 1998; 47: 65-72.
25. Tani M, Neely JR. Role of intracellular Na⁺ in Ca²⁺ overload and depressed recovery of ventricular function of reperfused ischemic rat hearts. Possible involvement of H⁺-Na⁺ and Na⁺-Ca²⁺ exchange. *Circ Res* 1989; 65: 1045-1056.

26. Karmazyn M, Ray M, Haist JV. Comparative effects of Na⁺/H⁺ exchange inhibitors against cardiac injury produced by ischemia/reperfusion, hypoxia/reoxygenation, and the calcium paradox. *J Cardiovasc Pharmacol* 1993; 21: 172-178.
27. Steenbergen C, Perlman ME, London RE, Murphy E. Mechanism of preconditioning. Ionic alterations. *Circ Res* 1993; 72: 112-125.
28. Vandenberg JI, Metcalfe JC, Grace AA. Mechanisms of pHi recovery after global ischemia in the perfused heart. *Circ Res* 1993; 72: 993-1003.
29. Scholz W, Albus U. Na⁺/H⁺ exchange and its inhibition in cardiac ischemia and reperfusion. *Basic Res Cardiol* 1993; 88: 443-455.
30. Harada K, Franklin A, Johnson RG, Grossman W, Morgan JP. Acidemia and hypernatremia enhance postischemic recovery of excitation-contraction coupling. *Circ Res* 1994; 74: 1197-1209.
31. Russ U, Balsler C, Scholz W, Albus U, Lang HJ, Weichert A, Scholkens BA, Gogelein H. Effects of the Na⁺/H⁺-exchange inhibitor Hoe 642 on intracellular pH, calcium and sodium in isolated rat ventricular myocytes. *Pflugers Arch* 1996; 433: 26-34.
32. Leineweber K, Heusch G, Schulz R. Regulation and role of the presynaptic and myocardial Na⁺/H⁺ exchanger NHE1: effects on the sympathetic nervous system in heart failure. *Cardiovasc Drug Rev* 2007; 25: 123-131.
33. Ford KL, Moorhouse EL, Bortolozzi M, Richards MA, Swietach P, Vaughan-Jones RD. Regional acidosis locally inhibits but remotely stimulates Ca²⁺ waves in ventricular myocytes. *Cardiovasc Res* 2017; 113: 984-995.
34. Redd MA, Scheuer SE, Saez NJ, Yoshikawa Y, Chiu HS, Gao L, Hicks M, Villanueva JE, Joshi Y, Chow CY, Cuellar-Partida G, Peart JN, See Hoe LE, Chen X, Sun Y, Suen JY, Hatch RJ, Rollo B, Xia D, Alzubaidi MAH, Maljevic S, Quaife-Ryan GA, Hudson JE, Porrello ER, White MY, Cordwell SJ, Fraser JF, Petrou S, Reichelt ME, Thomas WG, King GF, Macdonald PS, Palpant NJ. Therapeutic Inhibition of Acid-Sensing Ion Channel 1a Recovers Heart Function After Ischemia-Reperfusion Injury. *Circulation* 2021; 144: 947-960.
35. Bhowmick S, Moore JT, Kirschner DL, Curry MC, Westbrook EG, Rasley BT, Drew KL. Acidotoxicity via ASIC1a Mediates Cell Death during Oxygen Glucose Deprivation and Abolishes Excitotoxicity. *ACS Chem Neurosci* 2017; 8: 1204-1212.
36. Conklin DJ, Guo Y, Nystoriak MA, Jagatheesan G, Obal D, Kilfoil PJ, Hoetker JD, Guo L, Bolli R, Bhatnagar A. TRPA1 channel contributes to myocardial ischemia-reperfusion injury. *Am J Physiol Heart Circ Physiol* 2019; 316: H889-H899.
37. El Banani H, Bernard M, Baetz D, Cabanes E, Cozzone P, Lucien A, Feuvray D. Changes in intracellular sodium and pH during ischaemia-reperfusion are attenuated by trimetazidine. Comparison between low- and zero-flow ischaemia. *Cardiovasc Res* 2000; 47: 688-696.
38. Opie LH. Myocardial stunning--are calcium antagonists useful? *Cardiovasc Drugs Ther* 1994; 8 Suppl 3: 533-541.
39. Moffat MP, Ward CA, Bend JR, Mock T, Farhangkhoei P, Karmazyn M. Effects of epoxyeicosatrienoic acids on isolated hearts and ventricular myocytes. *Am J Physiol* 1993; 264: H1154-1160.
40. Grech ED, Jackson MJ, Ramsdale DR. Reperfusion injury after acute myocardial infarction. *BMJ* 1995; 310: 477-478.
41. Granger DN, Korthuis RJ. Physiologic mechanisms of postischemic tissue injury. *Annu Rev Physiol* 1995; 57: 311-332.
42. Odeh M. The role of reperfusion-induced injury in the pathogenesis of the crush syndrome. *N Engl J Med* 1991; 324: 1417-1422.
43. Adembri CDG, A.R.; Novelli G.P. Ischaemia-Reperfusion in Sepsis Springerlink Book 2000: 49-56.
44. Collaborators GBDCoD. Global, regional, and national age-sex-specific mortality for 282 causes of death in 195 countries and territories, 1980-2017: a systematic analysis for the Global Burden of Disease Study 2017. *Lancet* 2018; 392: 1736-1788.
45. Carcy R, Cougnon M, Poet M, Durandy M, Sicard A, Counillon L, Blondeau N, Hauet T, Tauc M, D FP. Targeting oxidative stress, a crucial challenge in renal transplantation outcome. *Free Radic Biol Med* 2021; 169: 258-270.
46. Heusch G. Molecular basis of cardioprotection: signal transduction in ischemic pre-, post-, and remote conditioning. *Circ Res* 2015; 116: 674-699.
47. Semenza GL. Hydroxylation of HIF-1: oxygen sensing at the molecular level. *Physiology (Bethesda)* 2004; 19: 176-182.
48. Hill P, Shukla D, Tran MG, Aragonés J, Cook HT, Carmeliet P, Maxwell PH. Inhibition of hypoxia inducible factor hydroxylases protects against renal ischemia-reperfusion injury. *J Am Soc Nephrol* 2008; 19: 39-46.
49. Chen CH, Budas GR, Churchill EN, Disatnik MH, Hurley TD, Mochly-Rosen D. Activation of aldehyde dehydrogenase-2 reduces ischemic damage to the heart. *Science* 2008; 321: 1493-1495.
50. Miller EJ, Li J, Leng L, McDonald C, Atsumi T, Bucala R, Young LH. Macrophage migration inhibitory factor stimulates AMP-activated protein kinase in the ischaemic heart. *Nature* 2008; 451: 578-582.
51. Melis N, Rubera I, Cougnon M, Giraud S, Mograbi B, Belaid A, Pisani DF, Huber SM, Lacas-Gervais S, Fragaki K, Blondeau N, Vigne P, Frelin C, Hauet T, Durantion C, Tauc M. Targeting eIF5A Hypusination Prevents Anoxic Cell Death through Mitochondrial Silencing and Improves Kidney Transplant Outcome. *J Am Soc Nephrol* 2017; 28: 811-822.

52. Giraud S, Favreau F, Chatauret N, Thuillier R, Maiga S, Hauet T. Contribution of large pig for renal ischemia-reperfusion and transplantation studies: the preclinical model. *J Biomed Biotechnol* 2011; 2011: 532127.
53. Cougnon M, Carcy R, Melis N, Rubera I, Duranton C, Dumas K, Tanti JF, Pons C, Soubeiran N, Shkreli M, Hauet T, Pellerin L, Giraud S, Blondeau N, Tauc M, Pisani DF. Inhibition of eIF5A hypusination reprogrammes metabolism and glucose handling in mouse kidney. *Cell Death Dis* 2021; 12: 283.
54. Bourourou M, Goux E, Melis N, Friard J, Heurteaux C, Tauc M, Blondeau N. Inhibition of eIF5A hypusination pathway as a new pharmacological target for stroke therapy. *J Cereb Blood Flow Metab* 2021; 41: 1080-1090.
55. Ohsawa I, Ishikawa M, Takahashi K, Watanabe M, Nishimaki K, Yamagata K, Katsura K, Katayama Y, Asoh S, Ohta S. Hydrogen acts as a therapeutic antioxidant by selectively reducing cytotoxic oxygen radicals. *Nat Med* 2007; 13: 688-694.
56. Bonauer A, Carmona G, Iwasaki M, Mione M, Koyanagi M, Fischer A, Burchfield J, Fox H, Doebele C, Ohtani K, Chavakis E, Potente M, Tjwa M, Urbich C, Zeiher AM, Dimmeler S. MicroRNA-92a controls angiogenesis and functional recovery of ischemic tissues in mice. *Science* 2009; 324: 1710-1713.
57. Qian L, Van Laake LW, Huang Y, Liu S, Wendland MF, Srivastava D. miR-24 inhibits apoptosis and represses Bim in mouse cardiomyocytes. *J Exp Med* 2011; 208: 549-560.
58. Lanford RE, Hildebrandt-Eriksen ES, Petri A, Persson R, Lindow M, Munk ME, Kauppinen S, Orum H. Therapeutic silencing of microRNA-122 in primates with chronic hepatitis C virus infection. *Science* 2010; 327: 198-201.
59. Eckle T, Krahn T, Grenz A, Kohler D, Mittelbronn M, Ledent C, Jacobson MA, Osswald H, Thompson LF, Unertl K, Eltzschig HK. Cardioprotection by ecto-5'-nucleotidase (CD73) and A2B adenosine receptors. *Circulation* 2007; 115: 1581-1590.
60. Grenz A, Osswald H, Eckle T, Yang D, Zhang H, Tran ZV, Klingel K, Ravid K, Eltzschig HK. The reno-vascular A2B adenosine receptor protects the kidney from ischemia. *PLoS Med* 2008; 5: e137.
61. Hart ML, Jacobi B, Schittenhelm J, Henn M, Eltzschig HK. Cutting Edge: A2B Adenosine receptor signaling provides potent protection during intestinal ischemia/reperfusion injury. *J Immunol* 2009; 182: 3965-3968.
62. Shichita T, Sugiyama Y, Ooboshi H, Sugimori H, Nakagawa R, Takada I, Iwaki T, Okada Y, Iida M, Cua DJ, Iwakura Y, Yoshimura A. Pivotal role of cerebral interleukin-17-producing gammadelta T cells in the delayed phase of ischemic brain injury. *Nat Med* 2009; 15: 946-950.
63. Liesz A, Suri-Payer E, Veltkamp C, Doerr H, Sommer C, Rivest S, Giese T, Veltkamp R. Regulatory T cells are key cerebroprotective immunomodulators in acute experimental stroke. *Nat Med* 2009; 15: 192-199.
64. Hartmann M, Decking UK. Blocking Na(+)-H+ exchange by cariporide reduces Na(+)-overload in ischemia and is cardioprotective. *J Mol Cell Cardiol* 1999; 31: 1985-1995.
65. An J, Varadarajan SG, Camara A, Chen Q, Novalija E, Gross GJ, Stowe DF. Blocking Na(+)/H(+) exchange reduces [Na(+)](i) and [Ca(2+)](i) load after ischemia and improves function in intact hearts. *Am J Physiol Heart Circ Physiol* 2001; 281: H2398-2409.
66. Clanachan AS. Contribution of protons to post-ischemic Na(+) and Ca(2+) overload and left ventricular mechanical dysfunction. *J Cardiovasc Electrophysiol* 2006; 17 Suppl 1: S141-S148.
67. Noble D, Noble SJ, Bett GC, Earm YE, Ho WK, So IK. The role of sodium-calcium exchange during the cardiac action potential. *Ann N Y Acad Sci* 1991; 639: 334-353.
68. Murphy E, Steenbergen C. Mechanisms underlying acute protection from cardiac ischemia-reperfusion injury. *Physiol Rev* 2008; 88: 581-609.
69. Williams IA, Xiao XH, Ju YK, Allen DG. The rise of [Na(+)] (i) during ischemia and reperfusion in the rat heart—underlying mechanisms. *Pflugers Arch* 2007; 454: 903-912.
70. Wang S, Radhakrishnan J, Ayoub IM, Kolarova JD, Taglieri DM, Gazmuri RJ. Limiting sarcolemmal Na+ entry during resuscitation from ventricular fibrillation prevents excess mitochondrial Ca2+ accumulation and attenuates myocardial injury. *J Appl Physiol* (1985) 2007; 103: 55-65.
71. Wirth KJ, Maier T, Busch AE. NHE1-inhibitor cariporide prevents the transient reperfusion-induced shortening of the monophasic action potential after coronary ischemia in pigs. *Basic Res Cardiol* 2001; 96: 192-197.
72. Vaughan-Jones RD, Spitzer KW. Role of bicarbonate in the regulation of intracellular pH in the mammalian ventricular myocyte. *Biochem Cell Biol* 2002; 80: 579-596.
73. Khandoudi N, Laville MP, Bril A. Protective effect of the sodium/hydrogen exchange inhibitors during global low-flow ischemia. *J Cardiovasc Pharmacol* 1996; 28: 540-546.
74. Hoque AN, Haist JV, Karmazyn M. Na(+)-H+ exchange inhibition protects against mechanical, ultrastructural, and biochemical impairment induced by low concentrations of lysophosphatidylcholine in isolated rat hearts. *Circ Res* 1997; 80: 95-102.
75. Gan XT, Chakrabarti S, Karmazyn M. Modulation of Na+/H+ exchange isoform 1 mRNA expression in isolated rat hearts. *Am J Physiol* 1999; 277: H993-998.
76. Karmazyn M. Na+/H+ exchange inhibitors reverse lactate-induced depression in postischemic ventricular recovery. *Br J Pharmacol* 1993; 108: 50-56.
77. Duff HJ. Clinical and in vivo antiarrhythmic potential of sodium-hydrogen exchange inhibitors. *Cardiovasc Res* 1995; 29: 189-193.

78. Humphreys RA, Haist JV, Chakrabarti S, Feng Q, Arnold JM, Karmazyn M. Orally administered NHE1 inhibitor cariporide reduces acute responses to coronary occlusion and reperfusion. *Am J Physiol* 1999; 276: H749-757.
79. Van Emous JG, Schreur JH, Ruigrok TJ, Van Echteld CJ. Both Na⁺-K⁺ ATPase and Na⁺-H⁺ exchanger are immediately active upon post-ischemic reperfusion in isolated rat hearts. *J Mol Cell Cardiol* 1998; 30: 337-348.
80. Xiao XH, Allen DG. Role of Na⁽⁺⁾/H⁽⁺⁾ exchanger during ischemia and preconditioning in the isolated rat heart. *Circ Res* 1999; 85: 723-730.
81. Dyck JR, Lopaschuk GD, Fliegel L. Identification of a small Na⁺/H⁺ exchanger-like message in the rabbit myocardium. *FEBS Lett* 1992; 310: 255-259.
82. Fliegel L. Molecular biology of the myocardial Na⁺/H⁺ exchanger. *J Mol Cell Cardiol* 2008; 44: 228-237.
83. Shimohama T, Suzuki Y, Noda C, Niwano H, Sato K, Masuda T, Kawahara K, Izumi T. Decreased expression of Na⁺/H⁺ exchanger isoform 1 (NHE1) in non-infarcted myocardium after acute myocardial infarction. *Jpn Heart J* 2002; 43: 273-282.
84. Xiao XH, Allen DG. Activity of the Na⁽⁺⁾/H⁽⁺⁾ exchanger is critical to reperfusion damage and preconditioning in the isolated rat heart. *Cardiovasc Res* 2000; 48: 244-253.
85. Dyck JR, Maddaford TG, Pierce GN, Fliegel L. Induction of expression of the sodium-hydrogen exchanger in rat myocardium. *Cardiovasc Res* 1995; 29: 203-208.
86. Pantos C, Mourouzis I, Saranteas T, Paizis I, Xinaris C, Malliopoulou V, Cokkinos DV. Thyroid hormone receptors alpha1 and beta1 are downregulated in the post-infarcted rat heart: consequences on the response to ischaemia-reperfusion. *Basic Res Cardiol* 2005; 100: 422-432.
87. Simsek G, Vaughan-Jones RD, Swietach P, Kandilci HB. Recovery from hypoxia-induced internalization of cardiac Na⁽⁺⁾/H⁽⁺⁾ exchanger 1 requires an adequate intracellular store of antioxidants. *J Cell Physiol* 2019; 234: 4681-4694.
88. Goss GG, Woodside M, Wakabayashi S, Pouyssegur J, Waddell T, Downey GP, Grinstein S. ATP dependence of NHE-1, the ubiquitous isoform of the Na⁺/H⁺ antiporter. Analysis of phosphorylation and subcellular localization. *J Biol Chem* 1994; 269: 8741-8748.
89. Jung YS, Kim HY, Kim J, Lee MG, Pouyssegur J, Kim E. Physical interactions and functional coupling between Daxx and sodium hydrogen exchanger 1 in ischemic cell death. *J Biol Chem* 2008; 283: 1018-1025.
90. Avkiran M. Rational basis for use of sodium-hydrogen exchange inhibitors in myocardial ischemia. *Am J Cardiol* 1999; 83: 10G-17G; discussion 17G-18G.
91. Klein HH, Pich S, Bohle RM, Lindert-Heimberg S, Nebendahl K. Na⁽⁺⁾/H⁽⁺⁾ exchange inhibitor cariporide attenuates cell injury predominantly during ischemia and not at onset of reperfusion in porcine hearts with low residual blood flow. *Circulation* 2000; 102: 1977-1982.
92. Klein HH, Bohle RM, Pich S, Lindert-Heimberg S, Wollenweber J, Schade-Brittinger C, Nebendahl K. Time-dependent protection by Na⁺/H⁺ exchange inhibition in a regionally ischemic, reperfused porcine heart preparation with low residual blood flow. *J Mol Cell Cardiol* 1998; 30: 795-801.
93. Khandoudi N, Ho J, Karmazyn M. Role of Na⁽⁺⁾-H⁺ exchange in mediating effects of endothelin-1 on normal and ischemic/reperfused hearts. *Circ Res* 1994; 75: 369-378.
94. Li X, Augustine A, Sun D, Li L, Fliegel L. Activation of the Na⁽⁺⁾/H⁽⁺⁾ exchanger in isolated cardiomyocytes through beta-Raf dependent pathways. Role of Thr(653) of the cytosolic tail. *J Mol Cell Cardiol* 2016; 99: 65-75.
95. Imamura M, Lander HM, Levi R. Activation of histamine H₃-receptors inhibits carrier-mediated norepinephrine release during protracted myocardial ischemia. Comparison with adenosine A₁-receptors and alpha₂-adrenoceptors. *Circ Res* 1996; 78: 475-481.
96. Yeves AM, Caldiz CI, Aiello EA, Villa-Abrille MC, Ennis IL. Reactive oxygen species partially mediate high dose angiotensin II-induced positive inotropic effect in cat ventricular myocytes. *Cardiovasc Pathol* 2015; 24: 236-240.
97. Maekawa N, Abe J, Shishido T, Itoh S, Ding B, Sharma VK, Sheu SS, Blaxall BC, Berk BC. Inhibiting p90 ribosomal S6 kinase prevents (Na⁺)-H⁺ exchanger-mediated cardiac ischemia-reperfusion injury. *Circulation* 2006; 113: 2516-2523.
98. Moor AN, Gan XT, Karmazyn M, Fliegel L. Activation of Na⁺/H⁺ exchanger-directed protein kinases in the ischemic and ischemic-reperfused rat myocardium. *J Biol Chem* 2001; 276: 16113-16122.
99. Rothstein EC, Byron KL, Reed RE, Fliegel L, Lucchesi PA. H₂O₂-induced Ca²⁺ overload in NRVM involves ERK1/2 MAP kinases: role for an NHE-1-dependent pathway. *Am J Physiol Heart Circ Physiol* 2002; 283: H598-605.
100. Cocco E, Karki P, Cojocar C, Fliegel L. Phenylephrine and sustained acidosis activate the neonatal rat cardiomyocyte Na⁺/H⁺ exchanger through phosphorylation of amino acids Ser770 and Ser771. *Am J Physiol Heart Circ Physiol* 2009; 297: H846-858.
101. Ajiro Y, Saegusa N, Giles WR, Stafforini DM, Spitzer KW. Platelet-activating factor stimulates sodium-hydrogen exchange in ventricular myocytes. *Am J Physiol Heart Circ Physiol* 2011; 301: H2395-2401.
102. Benter IF, Juggi JS, Khan I, Akhtar S. Inhibition of Ras-GTPase, but not tyrosine kinases or Ca²⁺/calmodulin-dependent protein kinase II, improves recovery of cardiac function in the globally ischemic heart. *Mol Cell Biochem* 2004; 259: 35-42.

103. Liu H, Cala PM, Anderson SE. Na/H exchange inhibition protects newborn heart from ischemia/reperfusion injury by limiting Na⁺-dependent Ca²⁺ overload. *J Cardiovasc Pharmacol* 2010; 55: 227-233.
104. Anderson SE, Kirkland DM, Beyschau A, Cala PM. Acute effects of 17beta-estradiol on myocardial pH, Na⁺, and Ca²⁺ and ischemia-reperfusion injury. *Am J Physiol Cell Physiol* 2005; 288: C57-64.
105. Dworschak M, d'Uscio LV, Breukelmann D, Hannon JD. Increased tolerance to hypoxic metabolic inhibition and reoxygenation of cardiomyocytes from apolipoprotein E-deficient mice. *Am J Physiol Heart Circ Physiol* 2005; 289: H160-167.
106. Karmazyn M. Therapeutic potential of Na-H exchange inhibitors for the treatment of heart failure. *Expert Opin Investig Drugs* 2001; 10: 835-843.
107. Mraiche F, Fliegel L. Elevated expression of activated Na⁽⁺⁾/H⁽⁺⁾ exchanger protein induces hypertrophy in isolated rat neonatal ventricular cardiomyocytes. *Mol Cell Biochem* 2011; 358: 179-187.
108. Karmazyn M, Liu Q, Gan XT, Brix BJ, Fliegel L. Aldosterone increases NHE-1 expression and induces NHE-1-dependent hypertrophy in neonatal rat ventricular myocytes. *Hypertension* 2003; 42: 1171-1176.
109. Fliegel L, Dyck JR, Wang H, Fong C, Haworth RS. Cloning and analysis of the human myocardial Na⁺/H⁺ exchanger. *Mol Cell Biochem* 1993; 125: 137-143.
110. Karmazyn M, Gan XT, Humphreys RA, Yoshida H, Kusumoto K. The myocardial Na⁽⁺⁾-H⁽⁺⁾ exchange: structure, regulation, and its role in heart disease. *Circ Res* 1999; 85: 777-786.
111. Karmazyn M, Sostaric JV, Gan XT. The myocardial Na⁺/H⁺ exchanger: a potential therapeutic target for the prevention of myocardial ischaemic and reperfusion injury and attenuation of postinfarction heart failure. *Drugs* 2001; 61: 375-389.
112. Scholz W, Albus U, Counillon L, Gogelein H, Lang HJ, Linz W, Weichert A, Scholkens BA. Protective effects of HOE642, a selective sodium-hydrogen exchange subtype 1 inhibitor, on cardiac ischaemia and reperfusion. *Cardiovasc Res* 1995; 29: 260-268.
113. Lorrain J, Briand V, Favennec E, Duval N, Grosset A, Janiak P, Hoornaert C, Cremer G, Latham C, O'Connor SE. Pharmacological profile of SL 59.1227, a novel inhibitor of the sodium/hydrogen exchanger. *Br J Pharmacol* 2000; 131: 1188-1194.
114. Wu D, Stassen JM, Seidler R, Doods H. Effects of BIIB513 on ischemia-induced arrhythmias and myocardial infarction in anesthetized rats. *Basic Res Cardiol* 2000; 95: 449-456.
115. Symons JD, Schaefer S. Na⁽⁺⁾/H⁽⁺⁾ exchange subtype 1 inhibition reduces endothelial dysfunction in vessels from stunned myocardium. *Am J Physiol Heart Circ Physiol* 2001; 281: H1575-1582.
116. Gazmuri RJ, Ayoub IM, Kolarova JD, Karmazyn M. Myocardial protection during ventricular fibrillation by inhibition of the sodium-hydrogen exchanger isoform-1. *Crit Care Med* 2002; 30: S166-171.
117. Kusumoto K, Igata H, Abe A, Ikeda S, Tsuboi A, Imamiya E, Fukumoto S, Shiraishi M, Watanabe T. In vitro and in vivo pharmacology of a structurally novel Na⁺-H⁺ exchange inhibitor, T-162559. *Br J Pharmacol* 2002; 135: 1995-2003.
118. Fukumoto S, Imamiya E, Kusumoto K, Fujiwara S, Watanabe T, Shiraishi M. Novel, non-acylguanidine-type Na⁽⁺⁾/H⁽⁺⁾ exchanger inhibitors: synthesis and pharmacology of 5-tetrahydroquinolinylidene aminoguanidine derivatives. *J Med Chem* 2002; 45: 3009-3021.
119. Lee S, Yi KY, Hwang SK, Lee BH, Yoo SE, Lee K. (5-Arylfuran-2-ylcarbonyl)guanidines as cardioprotectives through the inhibition of Na⁺/H⁺ exchanger isoform-1. *J Med Chem* 2005; 48: 2882-2891.
120. Lee S, Lee H, Yi KY, Lee BH, Yoo SE, Lee K, Cho NS. 4-Substituted (benzo[b]thiophene-2-carbonyl)guanidines as novel Na⁺/H⁺ exchanger isoform-1 (NHE-1) inhibitors. *Bioorg Med Chem Lett* 2005; 15: 2998-3001.
121. Roh HY, Jung IS, Park JW, Yun YP, Yi KY, Yoo SE, Kwon SH, Chung HJ, Shin HS. Cardioprotective effects of [5-(2-methyl-5-fluorophenyl)furan-2-ylcarbonyl]guanidine (KR-32568) in an anesthetized rat model of ischemia and reperfusion heart injury. *Pharmacology* 2005; 75: 37-44.
122. Park JW, Roh HY, Jung IS, Yun YP, Yi KY, Yoo SE, Kwon SH, Chung HJ, Shin HS. Effects of [5-(2-methoxy-5-fluorophenyl)furan-2-ylcarbonyl]guanidine (KR-32560), a novel sodium/hydrogen exchanger-1 inhibitor, on myocardial infarct size and ventricular arrhythmias in a rat model of ischemia/reperfusion heart injury. *J Pharmacol Sci* 2005; 98: 439-449.
123. Oh KS, Seo HW, Yi KY, Lee S, Yoo SE, Lee BH. Effects of KR-33028, a novel Na⁺/H⁺ exchanger-1 inhibitor, on ischemia and reperfusion-induced myocardial infarction in rats and dogs. *Fundam Clin Pharmacol* 2007; 21: 255-263.
124. Xu WT, Jin N, Xu J, Xu YG, Wang QJ, You QD. Design, synthesis and biological evaluation of novel substituted benzoylguanidine derivatives as potent Na⁺/H⁺ exchanger inhibitors. *Bioorg Med Chem Lett* 2009; 19: 3283-3287.
125. Zhang R, Dong J, Xu YG, Hua WY, Wen N, You QD. Synthesis and bioactivity of substituted indan-1-ylideneaminoguanidine derivatives. *Eur J Med Chem* 2009; 44: 3771-3776.
126. Doods H, Wu D. Sabiporide reduces ischemia-induced arrhythmias and myocardial infarction and attenuates ERK phosphorylation and iNOS induction in rats. *Biomed Res Int* 2013; 2013: 504320.
127. Pai P, Lai CJ, Lin CY, Liou YF, Huang CY, Lee SD. Effect of superoxide anion scavenger on rat hearts with chronic intermittent hypoxia. *J Appl Physiol* (1985) 2016; 120: 982-990.

128. Karmazyn M. Amiloride enhances postischemic ventricular recovery: possible role of Na⁺-H⁺ exchange. *Am J Physiol* 1988; 255: H608-615.
129. Meng HP, Lonsberry BB, Pierce GN. Influence of perfusate pH on the postischemic recovery of cardiac contractile function: involvement of sodium-hydrogen exchange. *J Pharmacol Exp Ther* 1991; 258: 772-777.
130. Scholz W, Albus U, Linz W, Martorana P, Lang HJ, Scholkens BA. Effects of Na⁺/H⁺ exchange inhibitors in cardiac ischemia. *J Mol Cell Cardiol* 1992; 24: 731-739.
131. Matsuda N, Kuroda H, Ashida Y, Okada M, Mori T. Possible involvement of Na⁽⁺⁾-H⁺ exchange in the early phase of reperfusion in myocardial stunning. *J Surg Res* 1992; 53: 529-534.
132. Mochizuki S, Seki S, Ejima M, Onodera T, Taniguchi M, Ishikawa S. Na⁺/H⁺ exchanger and reperfusion-induced ventricular arrhythmias in isolated perfused heart: possible role of amiloride. *Mol Cell Biochem* 1993; 119: 151-157.
133. Meng HP, Maddaford TG, Pierce GN. Effect of amiloride and selected analogues on postischemic recovery of cardiac contractile function. *Am J Physiol* 1993; 264: H1831-1835.
134. Moffat MP, Karmazyn M. Protective effects of the potent Na/H exchange inhibitor methylisobutyl amiloride against post-ischemic contractile dysfunction in rat and guinea-pig hearts. *J Mol Cell Cardiol* 1993; 25: 959-971.
135. du Toit EF, Opie LH. Role for the Na⁺/H⁺ exchanger in reperfusion stunning in isolated perfused rat heart. *J Cardiovasc Pharmacol* 1993; 22: 877-883.
136. Pike MM, Luo CS, Clark MD, Kirk KA, Kitakaze M, Madden MC, Cragoe EJ, Jr., Pohost GM. NMR measurements of Na⁺ and cellular energy in ischemic rat heart: role of Na⁽⁺⁾-H⁺ exchange. *Am J Physiol* 1993; 265: H2017-2026.
137. Navon G, Werrmann JG, Maron R, Cohen SM. ³¹P NMR and triple quantum filtered ²³Na NMR studies of the effects of inhibition of Na⁺/H⁺ exchange on intracellular sodium and pH in working and ischemic hearts. *Magn Reson Med* 1994; 32: 556-564.
138. Myers ML, Mathur S, Li GH, Karmazyn M. Sodium-hydrogen exchange inhibitors improve postischemic recovery of function in the perfused rabbit heart. *Cardiovasc Res* 1995; 29: 209-214.
139. Yasutake M, Ibuki C, Hearse DJ, Avkiran M. Na⁺/H⁺ exchange and reperfusion arrhythmias: protection by intracoronary infusion of a novel inhibitor. *Am J Physiol* 1994; 267: H2430-2440.
140. Mathur S, Karmazyn M. Interaction between anesthetics and the sodium-hydrogen exchange inhibitor HOE 642 (cariporide) in ischemic and reperfused rat hearts. *Anesthesiology* 1997; 87: 1460-1469.
141. Yasutake M, Avkiran M. Exacerbation of reperfusion arrhythmias by alpha 1 adrenergic stimulation: a potential role for receptor mediated activation of sarcolemmal sodium-hydrogen exchange. *Cardiovasc Res* 1995; 29: 222-230.
142. Chakrabarti S, Hoque AN, Karmazyn M. A rapid ischemia-induced apoptosis in isolated rat hearts and its attenuation by the sodium-hydrogen exchange inhibitor HOE 642 (cariporide). *J Mol Cell Cardiol* 1997; 29: 3169-3174.
143. Dyck JR, Lopaschuk GD. Glucose metabolism, H⁺ production and Na⁺/H⁺-exchanger mRNA levels in ischemic hearts from diabetic rats. *Mol Cell Biochem* 1998; 180: 85-93.
144. Mosca SM, Cingolani HE. [The Na⁺/Ca²⁺ exchanger as responsible for myocardial stunning]. *Medicina (B Aires)* 2001; 61: 167-173.
145. Gazmuri RJ, Ayoub IM, Hoffner E, Kolarova JD. Successful ventricular defibrillation by the selective sodium-hydrogen exchanger isoform-1 inhibitor cariporide. *Circulation* 2001; 104: 234-239.
146. Haist JV, Hirst CN, Karmazyn M. Effective protection by NHE-1 inhibition in ischemic and reperfused heart under preconditioning blockade. *Am J Physiol Heart Circ Physiol* 2003; 284: H798-803.
147. Xiao XH, Allen DG. The role of endogenous angiotensin II in ischaemia, reperfusion and preconditioning of the isolated rat heart. *Pflugers Arch* 2003; 445: 643-650.
148. Clements-Jewery H, Sutherland FJ, Allen MC, Tracey WR, Avkiran M. Cardioprotective efficacy of zoniporide, a potent and selective inhibitor of Na⁺/H⁺ exchanger isoform 1, in an experimental model of cardiopulmonary bypass. *Br J Pharmacol* 2004; 142: 57-66.
149. Lee BH, Seo HW, Yi KY, Lee S, Lee S, Yoo SE. Effects of KR-32570, a new Na⁺/H⁺ exchanger inhibitor, on functional and metabolic impairments produced by global ischemia and reperfusion in the perfused rat heart. *Eur J Pharmacol* 2005; 511: 175-182.
150. Benter IF, Francis I, Khan I, Cojocel C, Juggi JS, Yousif MH, Canatan H, Alshawaf EH, Akhtar S. Signal transduction involving Ras-GTPase contributes to development of hypertension and end-organ damage in spontaneously hypertensive rats-treated with L-NAME. *Pharmacol Res* 2005; 52: 401-412.
151. Jung YS, Kim MY, Kim MJ, Oh KS, Yi KY, Lee S, Yoo SE, Lee BH. Pharmacological profile of KR-33028, a highly selective inhibitor of Na⁺/H⁺ exchanger. *Eur J Pharmacol* 2006; 535: 220-227.
152. Lee S, Kim T, Lee BH, Yoo SE, Lee K, Yi KY. 3-Substituted-(5-aryl-furan-2-yl-carbonyl)guanidines as NHE-1 inhibitors. *Bioorg Med Chem Lett* 2007; 17: 1291-1295.
153. Javadov S, Choi A, Rajapurohitam V, Zeidan A, Basnakian AG, Karmazyn M. NHE-1 inhibition-induced cardioprotection against ischaemia/reperfusion is associated with attenuation of the mitochondrial permeability transition. *Cardiovasc Res* 2008; 77: 416-424.

154. Jung IS, Lee SH, Yang MK, Park JW, Yi KY, Yoo SE, Kwon SH, Chung HJ, Choi WS, Shin HS. Cardioprotective effects of the novel Na⁺/H⁺ exchanger-1 inhibitor KR-32560 in a perfused rat heart model of global ischemia and reperfusion: Involvement of the Akt-GSK-3 β cell survival pathway and antioxidant enzyme. *Arch Pharm Res* 2010; 33: 1241-1251.
155. Garciarena CD, Fantinelli JC, Caldiz CI, Chiappe de Cingolani G, Ennis IL, Perez NG, Cingolani HE, Mosca SM. Myocardial reperfusion injury: reactive oxygen species vs. NHE-1 reactivation. *Cell Physiol Biochem* 2011; 27: 13-22.
156. Nunez IP, Fantinelli J, Arbelaez LF, Mosca SM. Mitochondrial KATP channels participate in the limitation of infarct size by cariporide. *Naunyn Schmiedebergs Arch Pharmacol* 2011; 383: 563-571.
157. Andersen AD, Bentzen BH, Salling H, Klingberg H, Kanneworff M, Grunnet M, Pedersen SF. The cardioprotective effect of brief acidic reperfusion after ischemia in perfused rat hearts is not mimicked by inhibition of the Na⁽⁺⁾/H⁽⁺⁾ exchanger NHE1. *Cell Physiol Biochem* 2011; 28: 13-24.
158. Huber JD, Bentzien J, Boyer SJ, Burke J, De Lombaert S, Eickmeier C, Guo X, Haist JV, Hickey ER, Kaplita P, Karmazyn M, Kemper R, Kennedy CA, Kirrane T, Madwed JB, Mainolfi E, Nagaraja N, Soleymanzadeh F, Swinamer A, Eldrup AB. Identification of a potent sodium hydrogen exchanger isoform 1 (NHE1) inhibitor with a suitable profile for chronic dosing and demonstrated cardioprotective effects in a preclinical model of myocardial infarction in the rat. *J Med Chem* 2012; 55: 7114-7140.
159. Fantinelli J, Gonzalez Arbelaez LF, Mosca SM. Cardioprotective efficacy against reperfusion injury of EMD-87580: Comparison to ischemic postconditioning. *Eur J Pharmacol* 2014; 737: 125-132.
160. Cao J, Xie H, Sun Y, Zhu J, Ying M, Qiao S, Shao Q, Wu H, Wang C. Sevoflurane post-conditioning reduces rat myocardial ischemia reperfusion injury through an increase in NOS and a decrease in phosphorylated NHE1 levels. *Int J Mol Med* 2015; 36: 1529-1537.
161. Yamauchi T, Ichikawa H, Sawa Y, Fukushima N, Kagisaki K, Maeda K, Matsuda H, Shirakura R. The contribution of Na⁺/H⁺ exchange to ischemia-reperfusion injury after hypothermic cardioplegic arrest. *Ann Thorac Surg* 1997; 63: 1107-1112.
162. Kandilci HB, Richards MA, Fournier M, Simsek G, Chung YJ, Lakhal-Littleton S, Swietach P. Cardiomyocyte Na⁽⁺⁾/H⁽⁺⁾ Exchanger-1 Activity Is Reduced in Hypoxia. *Front Cardiovasc Med* 2020; 7: 617038.
163. Gazmuri RJ, Radhakrishnan J, Ayoub IM. Sodium-Hydrogen Exchanger Isoform-1 Inhibition: A Promising Pharmacological Intervention for Resuscitation from Cardiac Arrest. *Molecules* 2019; 24.
164. Segalen C, Longnus SL, Baetz D, Counillon L, Van Obberghen E. 5-aminoimidazole-4-carboxamide-1- β -D-ribofuranoside reduces glucose uptake via the inhibition of Na⁺/H⁺ exchanger 1 in isolated rat ventricular cardiomyocytes. *Endocrinology* 2008; 149: 1490-1498.
165. Moopanar TR, Xiao XH, Jiang L, Chen ZP, Kemp BE, Allen DG. AICAR inhibits the Na⁺/H⁺ exchanger in rat hearts-possible contribution to cardioprotection. *Pflugers Arch* 2006; 453: 147-156.
166. Vila-Petroff M, Mundina-Weilenmann C, Lezcano N, Snabaitis AK, Huergo MA, Valverde CA, Avkiran M, Mattiazzi A. Ca⁽²⁺⁾/calmodulin-dependent protein kinase II contributes to intracellular pH recovery from acidosis via Na⁽⁺⁾/H⁽⁺⁾ exchanger activation. *J Mol Cell Cardiol* 2010; 49: 106-112.
167. Karki P, Cocco E, Fliegel L. Sustained intracellular acidosis activates the myocardial Na⁽⁺⁾/H⁽⁺⁾ exchanger independent of amino acid Ser(703) and p90(rsk). *Biochim Biophys Acta* 2010; 1798: 1565-1576.
168. Hu LF, Li Y, Neo KL, Yong QC, Lee SW, Tan BK, Bian JS. Hydrogen sulfide regulates Na⁺/H⁺ exchanger activity via stimulation of phosphoinositide 3-kinase/Akt and protein kinase G pathways. *J Pharmacol Exp Ther* 2011; 339: 726-735.
169. Feger BJ, Starnes JW. Exercise alters the regulation of myocardial Na⁽⁺⁾/H⁽⁺⁾ exchanger-1 activity. *Am J Physiol Regul Integr Comp Physiol* 2013; 305: R1182-1189.
170. Harper IS, Bond JM, Chacon E, Reece JM, Herman B, Lemasters JJ. Inhibition of Na⁺/H⁺ exchange preserves viability, restores mechanical function, and prevents the pH paradox in reperfusion injury to rat neonatal myocytes. *Basic Res Cardiol* 1993; 88: 430-442.
171. Morgan PE, Correa MV, Ennis IL, Diez AA, Perez NG, Cingolani HE. Silencing of sodium/hydrogen exchanger in the heart by direct injection of naked siRNA. *J Appl Physiol* (1985) 2011; 111: 566-572.
172. Prasad V, Lorenz JN, Miller ML, Vairamani K, Nieman ML, Wang Y, Shull GE. Loss of NHE1 activity leads to reduced oxidative stress in heart and mitigates high-fat diet-induced myocardial stress. *J Mol Cell Cardiol* 2013; 65: 33-42.
173. Uthman L, Nederlof R, Eerbeek O, Baartscheer A, Schumacher C, Buchholtz N, Hollmann MW, Coronel R, Weber NC, Zuurbier CJ. Delayed ischaemic contracture onset by empagliflozin associates with NHE1 inhibition and is dependent on insulin in isolated mouse hearts. *Cardiovasc Res* 2019; 115: 1533-1545.
174. Vanier HV, Mraiche F, Li X, Fliegel L. Gender-specific effects of exercise on cardiac pathology in Na⁽⁺⁾/H⁽⁺⁾ exchanger overexpressing mice. *Mol Cell Biochem* 2012; 368: 103-110.
175. Shi X, O'Neill MM, MacDonnell S, Brookes PS, Yan C, Berk BC. The RSK Inhibitor BIX02565 Limits Cardiac Ischemia/Reperfusion Injury. *J Cardiovasc Pharmacol Ther* 2016; 21: 177-186.

176. Andersen AD, Poulsen KA, Lambert IH, Pedersen SF. HL-1 mouse cardiomyocyte injury and death after simulated ischemia and reperfusion: roles of pH, Ca²⁺-independent phospholipase A₂, and Na⁺/H⁺ exchange. *Am J Physiol Cell Physiol* 2009; 296: C1227-1242.
177. Keul P, van Borren MM, Ghanem A, Muller FU, Baartscheer A, Verkerk AO, Stumpel F, Schulte JS, Hamdani N, Linke WA, van Loenen P, Matus M, Schmitz W, Stypmann J, Tiemann K, Ravesloot JH, Alewijnse AE, Hermann S, Spijkers LJ, Hiller KH, Herr D, Heusch G, Schafers M, Peters SL, Chun J, Levkau B. Sphingosine-1-Phosphate Receptor 1 Regulates Cardiac Function by Modulating Ca²⁺ Sensitivity and Na⁺/H⁺ Exchange and Mediates Protection by Ischemic Preconditioning. *J Am Heart Assoc* 2016; 5.
178. Linz W, Albus U, Crause P, Jung W, Weichert A, Scholkens BA, Scholz W. Dose-dependent reduction of myocardial infarct mass in rabbits by the NHE-1 inhibitor cariporide (HOE 642). *Clin Exp Hypertens* 1998; 20: 733-749.
179. Knight DR, Smith AH, Flynn DM, MacAndrew JT, Ellery SS, Kong JX, Marala RB, Wester RT, Guzman-Perez A, Hill RJ, Magee WP, Tracey WR. A novel sodium-hydrogen exchanger isoform-1 inhibitor, zoniporide, reduces ischemic myocardial injury in vitro and in vivo. *J Pharmacol Exp Ther* 2001; 297: 254-259.
180. Jung O, Albus U, Lang HJ, Busch AE, Linz W. Effects of acute and chronic treatment with the sodium hydrogen exchanger 1 (NHE-1) inhibitor cariporide on myocardial infarct mass in rabbits with hypercholesterolaemia. *Basic Clin Pharmacol Toxicol* 2004; 95: 24-30.
181. Hendriks M, Mubagwa K, Verdonck F, Overloop K, Van Hecke P, Vanstapel F, Van Lommel A, Verbeken E, Lauweryns J, Flameng W. New Na⁽⁺⁾-H⁺ exchange inhibitor HOE 694 improves postischemic function and high-energy phosphate resynthesis and reduces Ca²⁺ overload in isolated perfused rabbit heart. *Circulation* 1994; 89: 2787-2798.
182. Toyoda Y, Khan S, Chen W, Parker RA, Levitsky S, McCully JD. Effects of NHE-1 inhibition on cardioprotection and impact on protection by K/Mg cardioplegia. *Ann Thorac Surg* 2001; 72: 836-843; discussion 843-834.
183. Cun L, Ronghua Z, Bin L, Jin L, Shuyi L. Preconditioning with Na⁺/H⁺ exchange inhibitor HOE642 reduces calcium overload and exhibits marked protection on immature rabbit hearts. *ASAIO J* 2007; 53: 762-765.
184. van Borren MM, Baartscheer A, Wilders R, Ravesloot JH. NHE-1 and NBC during pseudo-ischemia/reperfusion in rabbit ventricular myocytes. *J Mol Cell Cardiol* 2004; 37: 567-577.
185. van Borren MM, den Ruijter HM, Baartscheer A, Ravesloot JH, Coronel R, Verkerk AO. Dietary Omega-3 Polyunsaturated Fatty Acids Suppress NHE-1 Upregulation in a Rabbit Model of Volume- and Pressure-Overload. *Front Physiol* 2012; 3: 76.
186. Vanheel B, de Hemptinne A, Leusen I. Acidification and intracellular sodium ion activity during stimulated myocardial ischemia. *Am J Physiol* 1990; 259: C169-179.
187. Aldakkak M, Stowe DF, Heisner JS, Spence M, Camara AK. Enhanced Na⁺/H⁺ exchange during ischemia and reperfusion impairs mitochondrial bioenergetics and myocardial function. *J Cardiovasc Pharmacol* 2008; 52: 236-244.
188. Loh SH, Sun B, Vaughan-Jones RD. Effect of Hoe 694, a novel Na⁽⁺⁾-H⁺ exchange inhibitor, on intracellular pH regulation in the guinea-pig ventricular myocyte. *Br J Pharmacol* 1996; 118: 1905-1912.
189. Satoh H, Sugiyama S, Nomura N, Terada H, Hayashi H. Importance of glycolytically derived ATP for Na⁺ loading via Na⁺/H⁺ exchange during metabolic inhibition in guinea pig ventricular myocytes. *Clin Sci (Lond)* 2001; 101: 243-251.
190. Hwang IK, Yoo KY, An SJ, Li H, Lee CH, Choi JH, Lee JY, Lee BH, Kim YM, Kwon YG, Won MH. Late expression of Na⁺/H⁺ exchanger 1 (NHE1) and neuroprotective effects of NHE inhibitor in the gerbil hippocampal CA1 region induced by transient ischemia. *Exp Neurol* 2008; 212: 314-323.
191. Lee JC, Cho JH, Kim IH, Ahn JH, Park JH, Cho GS, Chen BH, Shin BN, Tae HJ, Park SM, Ahn JY, Kim DW, Cho JH, Bae EJ, Yong JH, Kim YM, Won MH, Lee YL. Ischemic preconditioning inhibits expression of Na⁽⁺⁾/H⁽⁺⁾ exchanger 1 (NHE1) in the gerbil hippocampal CA1 region after transient forebrain ischemia. *J Neurol Sci* 2015; 351: 146-153.
192. Garciarena CD, Caldiz CI, Correa MV, Schinella GR, Mosca SM, Chiappe de Cingolani GE, Cingolani HE, Ennis IL. Na⁺/H⁺ exchanger-1 inhibitors decrease myocardial superoxide production via direct mitochondrial action. *J Appl Physiol (1985)* 2008; 105: 1706-1713.
193. Yeves AM, Garciarena CD, Nolly MB, Chiappe de Cingolani GE, Cingolani HE, Ennis IL. Decreased activity of the Na⁺/H⁺ exchanger by phosphodiesterase 5A inhibition is attributed to an increase in protein phosphatase activity. *Hypertension* 2010; 56: 690-695.
194. Hatta E, Yasuda K, Levi R. Activation of histamine H₃ receptors inhibits carrier-mediated norepinephrine release in a human model of protracted myocardial ischemia. *J Pharmacol Exp Ther* 1997; 283: 494-500.
195. Simm A, Friedrich I, Scheubel RJ, Gursinsky T, Silber RE, Bartling B. Age dependency of the cariporide-mediated cardio-protection after simulated ischemia in isolated human atrial heart muscles. *Exp Gerontol* 2008; 43: 691-699.
196. Sack S, Mohri M, Schwarz ER, Arras M, Schaper J, Ballagi-Pordany G, Scholz W, Lang HJ, Scholkens BA, Schaper W. Effects of a new Na⁺/H⁺ antiporter inhibitor on postischemic reperfusion in pig heart. *J Cardiovasc Pharmacol* 1994; 23: 72-78.

197. Goldberg SP, Digerness SB, Skinner JL, Killingsworth CR, Katholi CR, Holman WL. Ischemic preconditioning and Na⁺/H⁺ exchange inhibition improve reperfusion ion homeostasis. *Ann Thorac Surg* 2002; 73: 569-574.
198. Ayoub IM, Kolarova J, Yi Z, Trevedi A, Deshmukh H, Lubell DL, Franz MR, Maldonado FA, Gazmuri RJ. Sodium-hydrogen exchange inhibition during ventricular fibrillation: Beneficial effects on ischemic contracture, action potential duration, reperfusion arrhythmias, myocardial function, and resuscitability. *Circulation* 2003; 107: 1804-1809.
199. Wu D, Bassuk J, Arias J, Doods H, Adams JA. Cardiovascular effects of Na⁺/H⁺ exchanger inhibition with BIIB513 following hypovolemic circulatory shock. *Shock* 2005; 23: 269-274.
200. Wu D, Russano K, Kouz I, Abraham WM. NHE1 inhibition improves tissue perfusion and resuscitation outcome after severe hemorrhage. *J Surg Res* 2013; 181: e75-81.
201. Lin X, Lee D, Wu D. Protective effects of NHE1 inhibition with sabiporide in an experimental model of asphyxia-induced cardiac arrest in piglets. *Resuscitation* 2013; 84: 520-525.
202. Fukuta M, Wakida Y, Iwa T, Uesugi M, Kobayashi T. Role of Na⁽⁺⁾-H⁺ exchange on reperfusion related myocardial injury and arrhythmias in an open-chest swine model. *Pacing Clin Electrophysiol* 1996; 19: 2027-2033.
203. Gumina RJ, Buerger E, Eickmeier C, Moore J, Daemmgen J, Gross GJ. Inhibition of the Na⁽⁺⁾/H⁽⁺⁾ exchanger confers greater cardioprotection against 90 minutes of myocardial ischemia than ischemic preconditioning in dogs. *Circulation* 1999; 100: 2519-2526; discussion 2469-2572.
204. Gumina RJ, Mizumura T, Beier N, Schelling P, Schultz JJ, Gross GJ. A new sodium/hydrogen exchange inhibitor, EMD 85131, limits infarct size in dogs when administered before or after coronary artery occlusion. *J Pharmacol Exp Ther* 1998; 286: 175-183.
205. Gumina RJ, Daemmgen J, Gross GJ. Inhibition of the Na⁽⁺⁾/H⁽⁺⁾ exchanger attenuates phase 1b ischemic arrhythmias and reperfusion-induced ventricular fibrillation. *Eur J Pharmacol* 2000; 396: 119-124.
206. Gumina RJ, Beier N, Schelling P, Gross GJ. Inhibitors of ischemic preconditioning do not attenuate Na⁺/H⁺ exchange inhibitor mediated cardioprotection. *J Cardiovasc Pharmacol* 2000; 35: 949-953.
207. Gumina RJ, Auchampach J, Wang R, Buerger E, Eickmeier C, Moore J, Daemmgen J, Gross GJ. Na⁽⁺⁾/H⁽⁺⁾ exchange inhibition-induced cardioprotection in dogs: effects on neutrophils versus cardiomyocytes. *Am J Physiol Heart Circ Physiol* 2000; 279: H1563-1570.
208. Gumina RJ, Moore J, Schelling P, Beier N, Gross GJ. Na⁽⁺⁾/H⁽⁺⁾ exchange inhibition prevents endothelial dysfunction after I/R injury. *Am J Physiol Heart Circ Physiol* 2001; 281: H1260-1266.
209. Corvera JS, Zhao ZQ, Schmarkey LS, Katzmark SL, Budde JM, Morris CD, Ehring T, Guyton RA, Vinten-Johansen J. Optimal dose and mode of delivery of Na⁺/H⁺ exchange-1 inhibitor are critical for reducing postsurgical ischemia-reperfusion injury. *Ann Thorac Surg* 2003; 76: 1614-1622.
210. Gumina RJ, El Schultz J, Moore J, Beier N, Schelling P, Gross GJ. Cardioprotective-mimetics reduce myocardial infarct size in animals resistant to ischemic preconditioning. *Cardiovasc Drugs Ther* 2005; 19: 315-322.
211. Sasamori J, Hasegawa T, Takaya A, Watanabe Y, Tanaka M, Ogino Y, Chiba T, Aihara K. The cardioprotective effects of novel Na⁺/H⁺ exchanger inhibitor TY-51924 on ischemia/reperfusion injury. *J Cardiovasc Pharmacol* 2014; 63: 351-359.
212. Kingma JG. Inhibition of Na⁽⁺⁾/H⁽⁺⁾ Exchanger With EMD 87580 does not Confer Greater Cardioprotection Beyond Preconditioning on Ischemia-Reperfusion Injury in Normal Dogs. *J Cardiovasc Pharmacol Ther* 2018; 23: 254-269.
213. Zeymer U, Suryapranata H, Monassier JP, Opolski G, Davies J, Rasmanis G, Linssen G, Tebbe U, Schroder R, Tiemann R, Machnig T, Neuhaus KL, Investigators E. The Na⁽⁺⁾/H⁽⁺⁾ exchange inhibitor eniporide as an adjunct to early reperfusion therapy for acute myocardial infarction. Results of the evaluation of the safety and cardioprotective effects of eniporide in acute myocardial infarction (ESCAMI) trial. *J Am Coll Cardiol* 2001; 38: 1644-1650.
214. Bhattaram VA, Nagaraja NV, Peters T, Machnig T, Kroesser S, Kovar A, Derendorf H. Population pharmacokinetics of eniporide and its metabolite in healthy subjects and patients with acute myocardial infarction. *J Clin Pharmacol* 2005; 45: 631-639.
215. Mentzer RM, Jr., Bartels C, Bolli R, Boyce S, Buckberg GD, Chaitman B, Haverich A, Knight J, Menasche P, Myers ML, Nicolau J, Simoons M, Thulin L, Weisel RD, Investigators ES. Sodium-hydrogen exchange inhibition by cariporide to reduce the risk of ischemic cardiac events in patients undergoing coronary artery bypass grafting: results of the EXPEDITION study. *Ann Thorac Surg* 2008; 85: 1261-1270.
216. Piwnica-Worms D, Lieberman M. Microfluorometric monitoring of pH_i in cultured heart cells: Na⁺-H⁺ exchange. *Am J Physiol* 1983; 244: C422-428.
217. Orłowski J, Kandasamy RA. Delineation of transmembrane domains of the Na⁺/H⁺ exchanger that confer sensitivity to pharmacological antagonists. *J Biol Chem* 1996; 271: 19922-19927.
218. Bhagatwala J, Harris RA, Parikh SJ, Zhu H, Huang Y, Kotak I, Seigler N, Pierce GL, Egan BM, Dong Y. Epithelial sodium channel inhibition by amiloride on blood pressure and cardiovascular disease risk in young prehypertensives. *J Clin Hypertens (Greenwich)* 2014; 16: 47-53.

219. Scholz W, Albus U. Potential of selective sodium-hydrogen exchange inhibitors in cardiovascular therapy. *Cardiovasc Res* 1995; 29: 184-188.
220. Piper HM, Balser C, Ladilov YV, Schafer M, Siegmund B, Ruiz-Meana M, Garcia-Dorado D. The role of Na⁺/H⁺ exchange in ischemia-reperfusion. *Basic Res Cardiol* 1996; 91: 191-202.
221. Doggrel SA, Hancox JC. Is timing everything? Therapeutic potential of modulators of cardiac Na⁽⁺⁾ transporters. *Expert Opin Investig Drugs* 2003; 12: 1123-1142.
222. Theroux P, Chaitman BR, Danchin N, Erhardt L, Meinertz T, Schroeder JS, Tognoni G, White HD, Willerson JT, Jessel A. Inhibition of the sodium-hydrogen exchanger with cariporide to prevent myocardial infarction in high-risk ischemic situations. Main results of the GUARDIAN trial. Guard during ischemia against necrosis (GUARDIAN) Investigators. *Circulation* 2000; 102: 3032-3038.
223. Baumgarth M, Beier N, Gericke R. (2-Methyl-5-(methylsulfonyl)benzoyl)guanidine Na⁺/H⁺ antiporter inhibitors. *J Med Chem* 1997; 40: 2017-2034.
224. Tracey WR, Allen MC, Frazier DE, Fossa AA, Johnson CG, Marala RB, Knight DR, Guzman-Perez A. Zoniporide: a potent and selective inhibitor of the human sodium-hydrogen exchanger isoform 1 (NHE-1). *Cardiovasc Drug Rev* 2003; 21: 17-32.
225. Escudero DS, Perez NG, Diaz RG. Myocardial Impact of NHE1 Regulation by Sildenafil. *Front Cardiovasc Med* 2021; 8: 617519.
226. Zinman B, Wanner C, Lachin JM, Fitchett D, Bluhmki E, Hantel S, Mattheus M, Devins T, Johansen OE, Woerle HJ, Broedl UC, Inzucchi SE, Investigators E-RO. Empagliflozin, Cardiovascular Outcomes, and Mortality in Type 2 Diabetes. *N Engl J Med* 2015; 373: 2117-2128.
227. Neal B, Perkovic V, Matthews DR. Canagliflozin and Cardiovascular and Renal Events in Type 2 Diabetes. *N Engl J Med* 2017; 377: 2099.
228. Wiviott SD, Raz I, Bonaca MP, Mosenzon O, Kato ET, Cahn A, Silverman MG, Zelniker TA, Kuder JF, Murphy SA, Bhatt DL, Leiter LA, McGuire DK, Wilding JPH, Ruff CT, Gause-Nilsson IAM, Fredriksson M, Johansson PA, Langkilde AM, Sabatine MS, Investigators D-T. Dapagliflozin and Cardiovascular Outcomes in Type 2 Diabetes. *N Engl J Med* 2019; 380: 347-357.
229. Bhatt DL, Szarek M, Pitt B, Cannon CP, Leiter LA, McGuire DK, Lewis JB, Riddle MC, Inzucchi SE, Kosiborod MN, Cherney DZI, Dwyer JP, Scirica BM, Bailey CJ, Diaz R, Ray KK, Udell JA, Lopes RD, Lapuerta P, Steg PG, Investigators S. Sotagliflozin in Patients with Diabetes and Chronic Kidney Disease. *N Engl J Med* 2021; 384: 129-139.
230. Cannon CP, Pratley R, Dagogo-Jack S, Mancuso J, Huyck S, Masiukiewicz U, Charbonnel B, Frederich R, Gallo S, Cosentino F, Shih WJ, Gantz I, Terra SG, Cherney DZI, McGuire DK, Investigators VC. Cardiovascular Outcomes with Ertugliflozin in Type 2 Diabetes. *N Engl J Med* 2020; 383: 1425-1435.
231. Verma S. Potential Mechanisms of Sodium-Glucose Co-Transporter 2 Inhibitor-Related Cardiovascular Benefits. *Am J Cardiol* 2019; 124 Suppl 1: S36-S44.
232. Uthman L, Baartscheer A, Schumacher CA, Fiolet JWT, Kuschma MC, Hollmann MW, Coronel R, Weber NC, Zuurbier CJ. Direct Cardiac Actions of Sodium Glucose Cotransporter 2 Inhibitors Target Pathogenic Mechanisms Underlying Heart Failure in Diabetic Patients. *Front Physiol* 2018; 9: 1575.
233. Avkiran M, Marber MS. Na⁽⁺⁾/H⁽⁺⁾ exchange inhibitors for cardioprotective therapy: progress, problems and prospects. *J Am Coll Cardiol* 2002; 39: 747-753.
234. Suzuki Y, Matsumoto Y, Ikeda Y, Kondo K, Ohashi N, Umemura K. SM-20220, a Na⁽⁺⁾/H⁽⁺⁾ exchanger inhibitor: effects on ischemic brain damage through edema and neutrophil accumulation in a rat middle cerebral artery occlusion model. *Brain Res* 2002; 945: 242-248.
235. Yang D, Ma L, Wang P, Yang D, Zhang Y, Zhao X, Lv J, Zhang J, Zhang Z, Gao F. Normobaric oxygen inhibits AQP4 and NHE1 expression in experimental focal ischemic stroke. *Int J Mol Med* 2019; 43: 1193-1202.
236. Jakubovicz DE, Klip A. Lactic acid-induced swelling in C6 glial cells via Na⁺/H⁺ exchange. *Brain Res* 1989; 485: 215-224.
237. Wang Y, Luo J, Chen X, Chen H, Cramer SW, Sun D. Gene inactivation of Na⁺/H⁺ exchanger isoform 1 attenuates apoptosis and mitochondrial damage following transient focal cerebral ischemia. *Eur J Neurosci* 2008; 28: 51-61.
238. Lee BK, Lee DH, Park S, Park SL, Yoon JS, Lee MG, Lee S, Yi KY, Yoo SE, Lee KH, Kim YS, Lee SH, Baik EJ, Moon CH, Jung YS. Effects of KR-33028, a novel Na⁺/H⁺ exchanger-1 inhibitor, on glutamate-induced neuronal cell death and ischemia-induced cerebral infarct. *Brain Res* 2009; 1248: 22-30.
239. Manhas N, Shi Y, Taunton J, Sun D. p90 activation contributes to cerebral ischemic damage via phosphorylation of Na⁺/H⁺ exchanger isoform 1. *J Neurochem* 2010; 114: 1476-1486.
240. Ferrazzano P, Shi Y, Manhas N, Wang Y, Hutchinson B, Chen X, Chanana V, Gerdts J, Meyerand ME, Sun D. Inhibiting the Na⁺/H⁺ exchanger reduces reperfusion injury: a small animal MRI study. *Front Biosci (Elite Ed)* 2011; 3: 81-88.
241. Shi Y, Chanana V, Watters JJ, Ferrazzano P, Sun D. Role of sodium/hydrogen exchanger isoform 1 in microglial activation and proinflammatory responses in ischemic brains. *J Neurochem* 2011; 119: 124-135.
242. Begum G, Song S, Wang S, Zhao H, Bhuiyan MIH, Li E, Nepomuceno R, Ye Q, Sun M, Calderon MJ, Stolz DB, St Croix C, Watkins SC, Chen Y, He P, Shull GE, Sun D. Selective knockout of astrocytic Na⁽⁺⁾/H⁽⁺⁾ exchanger isoform 1

reduces astrogliosis, BBB damage, infarction, and improves neurological function after ischemic stroke. *Glia* 2018; 66: 126-144.

243. Lam TI, Brennan-Minnella AM, Won SJ, Shen Y, Hefner C, Shi Y, Sun D, Swanson RA. Intracellular pH reduction prevents excitotoxic and ischemic neuronal death by inhibiting NADPH oxidase. *Proc Natl Acad Sci U S A* 2013; 110: E4362-4368.

244. Liu Y, Kintner DB, Chanana V, Algharabli J, Chen X, Gao Y, Chen J, Ferrazzano P, Olson JK, Sun D. Activation of microglia depends on Na⁺/H⁺ exchange-mediated H⁺ homeostasis. *J Neurosci* 2010; 30: 15210-15220.

245. Matsumoto Y, Yamamoto S, Suzuki Y, Tsuboi T, Terakawa S, Ohashi N, Umemura K. Na⁺/H⁺ exchanger inhibitor, SM-20220, is protective against excitotoxicity in cultured cortical neurons. *Stroke* 2004; 35: 185-190.

246. Pilitsis JG, Diaz FG, O'Regan MH, Phillis JW. Inhibition of Na⁽⁺⁾/H⁽⁺⁾ exchange by SM-20220 attenuates free fatty acid efflux in rat cerebral cortex during ischemia-reperfusion injury. *Brain Res* 2001; 913: 156-158.

247. Robertson NJ, Bhakoo K, Puri BK, Edwards AD, Cox IJ. Hypothermia and amiloride preserve energetics in a neonatal brain slice model. *Pediatr Res* 2005; 58: 288-296.

248. Helmy MM, Tolner EA, Vanhatalo S, Voipio J, Kaila K. Brain alkalosis causes birth asphyxia seizures, suggesting therapeutic strategy. *Ann Neurol* 2011; 69: 493-500.

249. Kendall GS, Robertson NJ, Iwata O, Peebles D, Raivich G. N-methyl-isobutyl-amiloride ameliorates brain injury when commenced before hypoxia ischemia in neonatal mice. *Pediatr Res* 2006; 59: 227-231.

250. Robertson NJ, Kato T, Bainbridge A, Chandrasekaran M, Iwata O, Kapetanakis A, Faulkner S, Cheong J, Iwata S, Hristova M, Cady E, Raivich G. Methyl-isobutyl amiloride reduces brain Lac/NAA, cell death and microglial activation in a perinatal asphyxia model. *J Neurochem* 2013; 124: 645-657.

251. Wang Z, Rabb H, Craig T, Burnham C, Shull GE, Soleimani M. Ischemic-reperfusion injury in the kidney: overexpression of colonic H⁺-K⁺-ATPase and suppression of NHE-3. *Kidney Int* 1997; 51: 1106-1115.

252. Hamzawy M, Gouda SAA, Rashed L, Morcos MA, Shoukry H, Sharawy N. 22-oxalacitriol prevents acute kidney injury via inhibition of apoptosis and enhancement of autophagy. *Clin Exp Nephrol* 2019; 23: 43-55.

253. Lin X, Li M, Zhou R, Yu H, Zhou L, Li Q, Liu B. [Cariporide pretreatment attenuated warm ischemia/reperfusion injury in an isolated rat lung: a study on antioxidative mechanism]. *Sheng Wu Yi Xue Gong Cheng Xue Za Zhi* 2010; 27: 132-137.

254. Li Y, Zhou JS, Liu B. [Cariporide Pretreatment Attenuates Lung Ischemia-Reperfusion Injury in Rabbits]. *Sichuan Da Xue Xue Bao Yi Xue Ban* 2015; 46: 394-398.

255. McAllister SE, Moses MA, Jindal K, Ashrafpour H, Cahoon NJ, Huang N, Neligan PC, Forrest CR, Lipa JE, Pang CY. Na⁺/H⁺ exchange inhibitor cariporide attenuates skeletal muscle infarction when administered before ischemia or reperfusion. *J Appl Physiol* (1985) 2009; 106: 20-28.

256. Cengiz P, Kleman N, Uluc K, Kendigelen P, Hagemann T, Akture E, Messing A, Ferrazzano P, Sun D. Inhibition of Na⁺/H⁺ exchanger isoform 1 is neuroprotective in neonatal hypoxic ischemic brain injury. *Antioxid Redox Signal* 2011; 14: 1803-1813.

257. Lee JC, Cho GS, Kim IH, Park JH, Cho JH, Ahn JH, Bae EJ, Ahn JY, Park CW, Cho JH, Kim YM, Won MH, Lee HY. p63 Expression in the Gerbil Hippocampus Following Transient Ischemia and Effect of Ischemic Preconditioning on p63 Expression in the Ischemic Hippocampus. *Neurochem Res* 2015; 40: 1013-1022.

258. Vornov JJ, Thomas AG, Jo D. Protective effects of extracellular acidosis and blockade of sodium/hydrogen ion exchange during recovery from metabolic inhibition in neuronal tissue culture. *J Neurochem* 1996; 67: 2379-2389.

259. Phillis JW, Ren J, O'Regan MH. Inhibition of Na⁽⁺⁾/H⁽⁺⁾ exchange by 5-(N-ethyl-N-isopropyl)-amiloride reduces free fatty acid efflux from the ischemic reperfused rat cerebral cortex. *Brain Res* 2000; 884: 155-162.

260. Rolver MG, Elingaard-Larsen LO, Andersen AP, Counillon L, Pedersen SF. Pyrazine ring-based Na⁽⁺⁾/H⁽⁺⁾ exchanger (NHE) inhibitors potently inhibit cancer cell growth in 3D culture, independent of NHE1. *Sci Rep* 2020; 10: 5800.

261. Counillon L, Scholz W, Lang HJ, Pouyssegur J. Pharmacological characterization of stably transfected Na⁺/H⁺ antiporter isoforms using amiloride analogs and a new inhibitor exhibiting anti-ischemic properties. *Mol Pharmacol* 1993; 44: 1041-1045.

262. Numata M, Orłowski J. Molecular cloning and characterization of a novel (Na⁺,K⁺)/H⁺ exchanger localized to the trans-Golgi network. *J Biol Chem* 2001; 276: 17387-17394.

263. Tse CM, Levine SA, Yun CH, Brant SR, Pouyssegur J, Montrose MH, Donowitz M. Functional characteristics of a cloned epithelial Na⁺/H⁺ exchanger (NHE3): resistance to amiloride and inhibition by protein kinase C. *Proc Natl Acad Sci U S A* 1993; 90: 9110-9114.

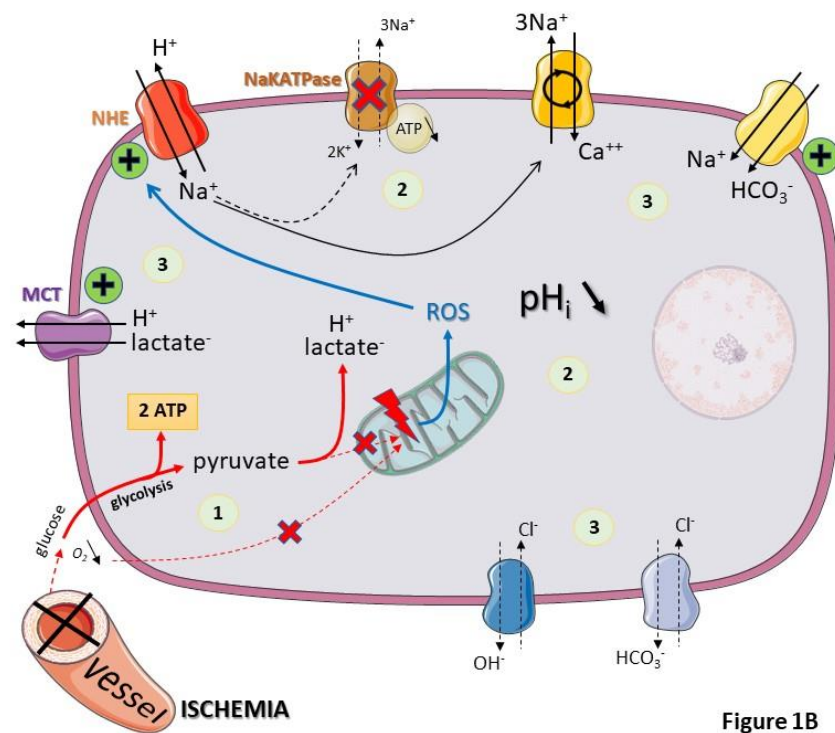
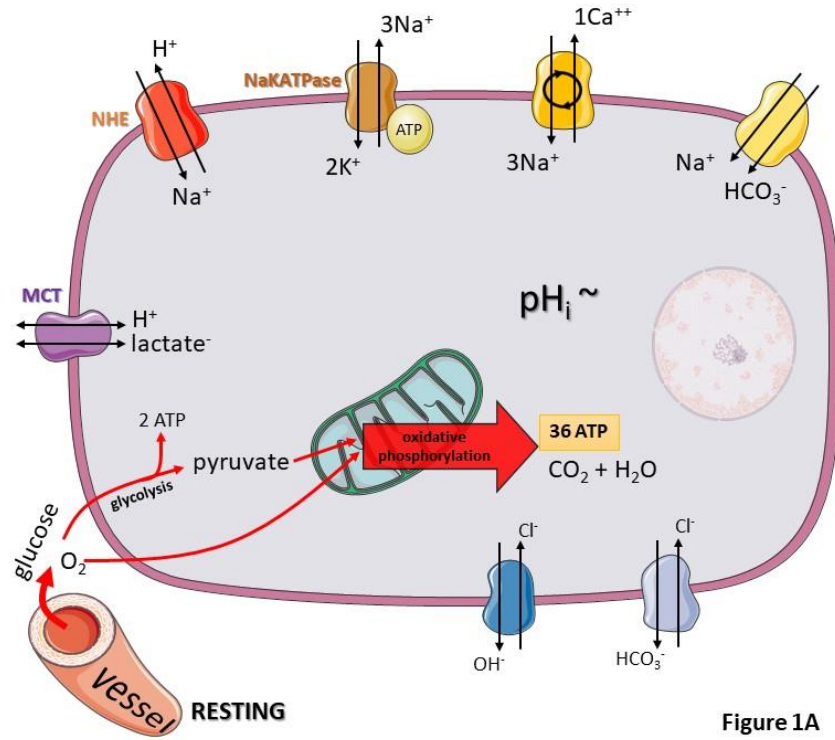
264. Nemeth ZH, Deitch EA, Lu Q, Szabo C, Hasko G. NHE blockade inhibits chemokine production and NF-kappaB activation in immunostimulated endothelial cells. *Am J Physiol Cell Physiol* 2002; 283: C396-403.

265. Chen L, Chen CX, Gan XT, Beier N, Scholz W, Karmazyn M. Inhibition and reversal of myocardial infarction-induced hypertrophy and heart failure by NHE-1 inhibition. *Am J Physiol Heart Circ Physiol* 2004; 286: H381-387.

266. <https://drugs.ncats.io/drug/31SF23L56C>.

267. Masereel B, Pochet L, Laeckmann D. An overview of inhibitors of Na⁽⁺⁾/H⁽⁺⁾ exchanger. *Eur J Med Chem* 2003; 38: 547-554.

Figure 1. Impact of NHE1 on cellular homeostasis before and after ischemia. Panel A: resting. Panel B: ischemia. Panel C: reperfusion



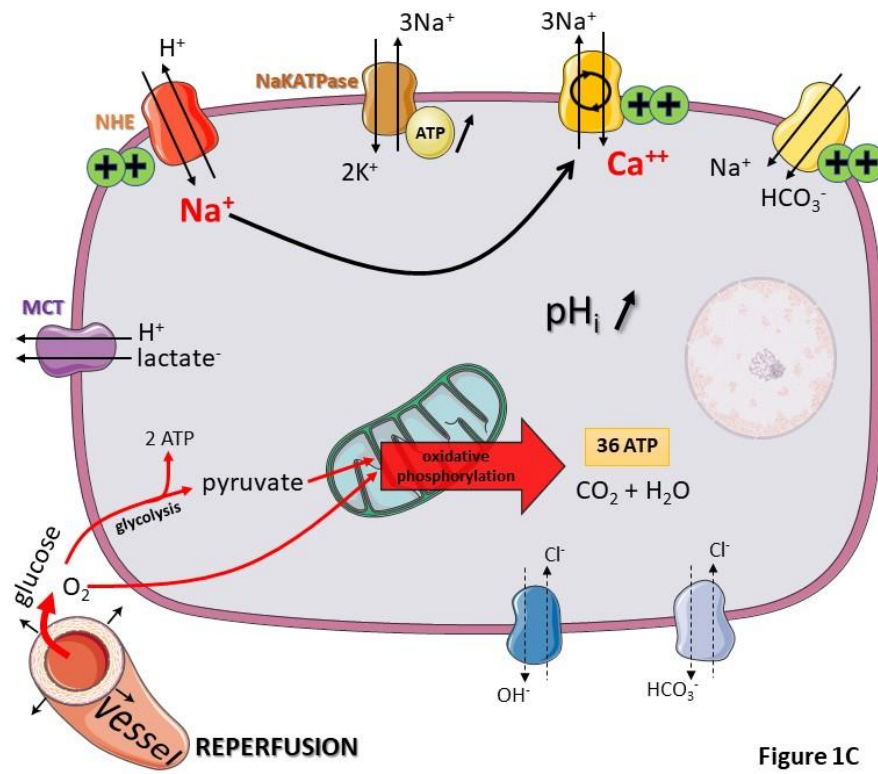
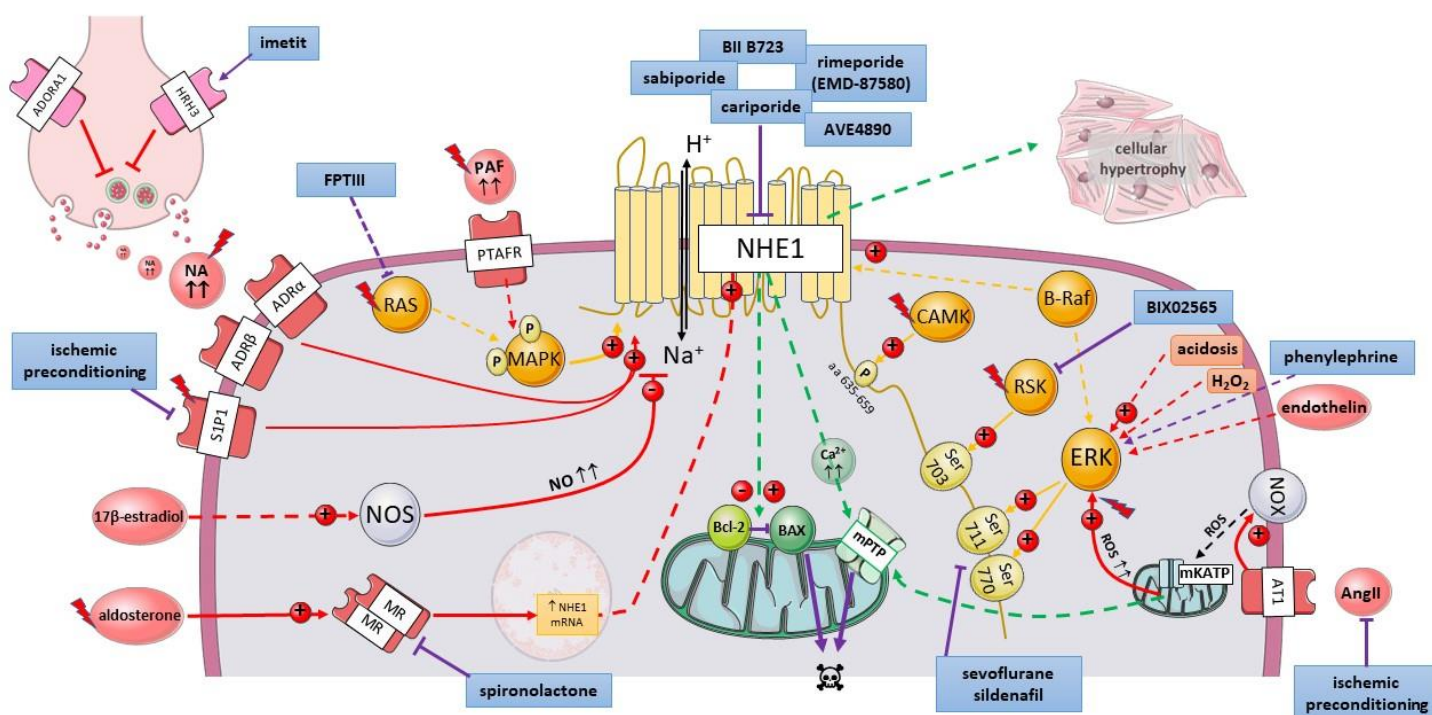


Figure 1C

Figure 2. Physiological and pharmacological factors regulating NHE1 activity. ADORA1 = Adenosine A1 Receptor, $ADR\alpha$ = Adrenergic alpha receptor, $ADR\beta$ = Adrenergic beta receptor, AngII = Angiotensin II, AT1 = Angiotensin II receptor, CAMK = Ca^{2+} /calmodulin-dependent protein kinase, ERK = Extracellular signal regulated kinase, HRH3 = Histamine receptor H3, MAPK = Mitogen-activated protein kinase, mKATP = mitochondrial ATP-dependent K^+ channels, mPTP = mitochondrial permeability transition pore, MR = Mineralocorticoid receptor, NA = Noradrenaline, NOS = NO synthetase, NOX = NADPH oxydase, PAF = Platelet activating factor, PTAFR = Platelet-activating factor receptor, ROS = Reactive oxygen species, RSK = 90 kDa ribosomal S6 kinase, S1P1 = Sphingosine 1-phosphate receptor



II. Régulation de NHE1 par les espèces réactives de l'oxygène

A. Résumé

L'étude de la régulation de NHE1 par les espèces réactives de l'oxygène a fait l'objet des travaux expérimentaux de mon travail de thèse qui sont présentés ci-dessous sous la forme d'un manuscrit en cours de préparation pour soumission.

Les ROS sont produits en excès au cours des phénomènes d'IR et sont à l'origine du stress oxydatif et des lésions tissulaires. Ces lésions tissulaires sont notamment liées à une production de Ca^{2+} qui elle-même entretient la production de ROS.¹¹⁷ La suractivation de NHE1 au cours de l'IR est également à l'origine de lésions tissulaires là aussi en partie à cause de surcharge en Ca^{2+} .⁹⁶ Il est donc légitime de se demander s'il existe un lien entre les ROS et NHE1 au cours de l'IR. Par ailleurs plusieurs enzymes intervenant dans la production de ROS (e.g. NADPH oxydases, Superoxide dismutase) produisent ou consomment des ions H^+ qui sont par ailleurs substrats de NHE1. Peu de données sont disponibles concernant la régulation de NHE1 par les ROS la plupart d'entre eux étant instables et difficilement accessibles à une expérimentation. Les seules données concernant NHE1 et ROS bien documentées concernent les conséquences d' H_2O_2 sur NHE1. H_2O_2 active NHE1 et ceci de manière indirecte par 2 voies de signalisation intra-cellulaire impliquant respectivement PKC et ERK.⁸⁹ H_2O_2 augmente également l'expression de NHE1.⁹¹ En revanche, la régulation par l'anion superoxyde O_2^- est peu décrite.

Mon travail de thèse a permis de montrer que la production d'anion superoxyde active également NHE1 (exposition à la Ménadione à l'origine de production d' O_2^-) et que l'inhibition de flavoenzymes productrices de superoxyde (Diphényliodonium) provoque une baisse de sa sensibilité aux ions H^+ . Parmi les acides aminés constitutifs de NHE1, les cystéines ont un profil particulièrement intéressant du fait de leur groupement thiol qui peut être le siège de nombreuses modifications notamment d'oxydo-réduction ou de protonation/déprotonation.

Nous avons ainsi pu constater que l'activation de NHE1 par O_2^- dépend de la présence des cystéines de NHE1 puisqu'elle est complètement perdue en leur absence. Afin d'identifier exactement quelle cystéine en particulier pouvait être impliquée, des mutants individuels des différentes cystéines ont été créés. Les cystéines 133 et 477 particulièrement sont des cystéines cruciales pour cette activation par O_2^- . Par ailleurs, nous avons confirmé les résultats de la littérature qui montrent qu' H_2O_2 active également NHE1 et démontré que cette activation ne dépend pas de la présence de cystéines.

Pour comprendre le mécanisme moléculaire de l'implication des cystéines dans cette régulation de NHE1 par O_2^- , nous avons analysé plusieurs modifications covalentes possibles potentiellement responsables de cette régulation : nitrosylation, glutathionylation, et formation de ponts disulfures. Nos travaux ont permis de montrer que NHE1 était effectivement nitrosylé et que cette nitrosylation se faisait sur la cystéine 421, qui ne fait pas partie de celles identifiées plus haut, mais que nous avons détecté ni formation de ponts disulfures ni de glutathionylation. Au cours des différentes expérimentations, nous avons pu constater que les mutants en cystéines, en particulier le mutant cysless présentaient des différences de forme et de mobilité cellulaire par rapport aux cellules exprimant le NHE1 sauvage. Après expériences de wound healing, nous avons pu confirmer que, par rapport au NHE1 sauvage, les mutants Cysless présentaient un mouvement plus désordonné, une perte d'inhibition de contact et un arrondissement cellulaire. Ces différences n'étaient pas en rapport avec une différence d'expression de fibronectine ou de vinculine, mais en rapport probablement au moins en partie avec le complexe Ezrine – Radixine – Moesine. En effet, l'interaction de NHE1 avec le complexe Ezrine – Radixine – Moesine est perdue dans le mutant cysless.

L'ensemble de ces expérimentations a donc permis de mettre en évidence une connexion clef entre la production de ROS, la régulation du pH intracellulaire, la mobilité et l'adhésion cellulaires.

B. Matériel et méthodes

Nous présentons ici l'ensemble des méthodologies utilisées tout au long de mon travail de thèse.

Culture cellulaire

La lignée cellulaire PS120 (proton suicide 120 minutes) issue d'un clône de fibroblastes de poumon de hamster chinois déficient du transporteur NHE1 (lignée CCL39 (ATCC)) a été cultivée à 37°C dans une atmosphère à 5% de CO₂ dans un milieu Dulbecco's Modified Eagles supplémenté avec de la streptomycine 50 µg/mL, pénicilline 50 UI/mL et 7.5% de sérum de veau foetal inactivé par la chaleur. Ces cellules ont été transfectées en utilisant de la Lipofectamine 3000 (Thermofisher Scientific) selon les instructions du fabricant, de manière à exprimer soit la forme sauvage de NHE1, soit les différents mutants cystéine de NHE1.

Mutagenèse Dirigée

A l'aide du vecteur pECElres-Neo généré par Lacroix *et al.*,¹⁶ les différents mutants de NHE1 avec les cysteines remplacées une à une par des alanines ont été obtenus par mutagenèse dirigée avec le Kit Quickchange II (Agilent®).

Les primers utilisés sont les suivants (forward sequences) :

NHE1 Cys1>>Ala F: 5'CCTCTGGCCGCCCTCATGAAGATAGG3'

NHE1 Cys2>>Ala F: 5'CCCGGAGAGCGCCCTGCTGATCGTGG3'

NHE1 Cys3>>Ala F: 5'CATGTACGCCGTGGCCCTGGTGGGCGG3'

NHE1 Cys4>>Ala F: 5'CCTGCTCTTCGCCCTCATCGCCCG3'

NHE1 Cys5>>Ala F: 5'GCACTTCCCCATGGCTGACCCGTTCTCAC3'

NHE1 Cys6>>Ala F: 5'GCATCGAAGACATGGCTGGCCACTACGG3'

NHE1 Cys7>>Ala F: 5'GAAATATGTGAAGAAGGCTCTGATAGCTGGC3'

NHE1 Cys8>>Ala F: 5'GGATACAGCGCGCCCTCAGTGACCCAG3'

Sélection des mutants

La sélection des populations cellulaires exprimant de manière stable NHE1 sauvage ou muté a été faite en utilisant 500 µg/mL de G418 pendant 3 semaines.

Composition des différents tampons pour l'acidification intracellulaire

Le tampon de charge est une solution de chlorure d'ammonium: 50 mM de NH₄Cl de chlorure d'ammonium, 70 mM de chlorure de choline, 5 mM de KCl, 2 mM de CaCl₂, 1 mM de MgCl₂, 5 mM de glucose, tamponnée à pH 7,4 avec 15 mM de MOPS.

Le tampon de rinçage est une solution de chlorure de choline: 120 mM de chlorure de choline, 5 mM de KCl, 1 mM de MgCl₂, 2 mM de CaCl₂, 5 mM de glucose, tamponnés à un pH de 7.0 avec 15 mM d'HEPES.

Le tampon de récupération est une solution de chlorure de sodium : 120 mM de chlorure de sodium, 5 mM de KCl, 1 mM de MgCl₂, 2 mM de CaCl₂, 5 mM de glucose, tamponnés à un pH de 7.4 avec 15 mM d'HEPES.

Proton suicide

Tout au long de la culture cellulaire la sélection des populations exprimant de manière stable NHE1 sauvage ou muté est faite par le biais d'une acidification intracellulaire à l'aide des tampons précédemment définis. Cette sélection est également réalisée durant la sélection des mutants précédemment décrite (effectuée au G148). Pour cette sélection, les cellules sont incubées 1h à 37°C dans une atmosphère sans CO₂ dans du tampon de charge au chlorure d'ammonium. Elles sont ensuite rapidement rincées par deux fois avec la solution de chlorure de choline, et finalement les cellules sont incubées de nouveaux 1h à 37°C dans une atmosphère sans CO₂ dans la solution de récupération au chlorure de sodium .

Mesure de l'activité de NHE1 par absorption de Lithium

Pour les expériences de flux de lithium, des plaques 24 puits ont étéensemencées de telle sorte que le tapis cellulaire soit confluant 3 jours après. Les plaques sont alors mises à incuber dans le tampon de charge au chlorure d'ammonium durant différents temps afin d'obtenir différentes valeurs de pH intracellulaire à 37°C dans une atmosphère sans CO₂. Les plaques sont ensuite rapidement rincées par deux fois avec la solution de chlorure de choline, puis incubées pendant 1 minute dans une solution de chlorure de lithium (15 mM de LiCl, 105 mM de chlorure de choline, 5 mM de KCl, 1 mM de MgCl₂, 2 mM de CaCl₂, 5 mM de glucose, tamponnés à pH 7.2 avec 15 mM d'HEPES). L'absorption de lithium est ensuite stoppée par quatre rapides rinçages dans du PBS (Phosphate Buffer Saline) froid. Les cellules sont ensuite solubilisées dans de l'acide nitrique 0.25 N (HNO₃, Sigma[®]) et le lithium intracellulaire est mesuré par spectrométrie d'absorption atomique (Perkin Elmer, Spectromètre PinAAcle 900Z[®]).

Détermination du pH intracellulaire

La détermination du pH intracellulaire est effectuée à l'aide d'une acidification intracellulaire à 37°C dans une atmosphère sans CO₂. Pour ce faire, les cellules ont été incubées durant différents temps pour obtenir différentes valeurs de pH intracellulaire dans le tampon de charge au chlorure d'ammonium, puis elles sont rapidement rincées avec la solution de chlorure de choline. L'étalonnage des valeurs de pH intracellulaire obtenues a été réalisé en mesurant en vidéo-microscopie ou avec un lecteur multiplaques (Safas[®]) la fluorescence du BCECF-AM (ThermoFisher Scientific[®]), un indicateur de pH ratiométrique à double excitation et perméant. Les signaux de fluorescence relatifs au pH intracellulaire ont été calibrés en utilisant l'ionophore échangeur K⁺/H⁺ Nigéricine. Pour cela, les cellules ont été perfusées dans une solution de 140 mM KCl, 20 mM de MES ou d'HEPES et 2.5 μM de nigéricine ajusté à différents pH. Les valeurs de pH intracellulaire

pour chaque temps de chargement d'ammonium ont été déterminées à l'aide de l'étalonnage expérimental.

Immunofluorescence

Les cellules sontensemencées et cultivées sur des lamelles de verre. Une fois prêtes, elles sont fixées pendant 10 minutes à 37°C avec du PBS, 4% de paraformaldehyde, 3% de sucrose et ajusté au pH 7.4. Les cellules sont perméabilisées pendant 10 minutes avec du Triton 0.3X dans du PBS. Les lamelles sont incubées 30 minutes dans une solution de blocage 4% bovine serum albumine sans acide gras (Sigma®) dans du PBS. L'incubation pour les anticorps primaires, secondaires ou la phalloïdine (Sigma®) est pour chacun d'une heure et ce fait à chaque fois avec du PBS à 1% BSA sans acide gras et 0.05% Tween 20. Les noyaux sont marqués pendant 10 minutes avec la coloration Hoescht (Thermo Fisher Scientific®) au 1/2000 dans du PBS. Entre chaque étape, tous les rinçages sont effectués avec du PBS. Les lamelles sont montées sur des lames de verre avec du Prolong Diamond Antifade Mountant (Thermo Fisher Scientific®). Les observations ont été réalisées avec le confocal ZEISS® LSM 800, et la quantification avec Image J® (Rasband, W.S., ImageJ, U. S. National Institutes of Health, Bethesda, Maryland, USA, <http://imagej.nih.gov/ij/>, 1997-2012)

La fluorescence à champ large a été observée à l'aide d'objectifs à huile 100X sur un microscope ZEISS® Axiovert 200 M équipé d'un CCD CoolSnap HQ®. L'acquisition des images a été réalisée à l'aide du système ZEN®. L'analyse d'image a été réalisée à l'aide de FIJI®.

Wound healing

Les différentes lignées cellulaires mutantes et de type sauvage ont été cultivées dans des plaques de 24 cellules dans du DMEM normal avec du glucose et du bicarbonate (Invitrogen®) 7.5% de FCS inactivé par la chaleur.

Les cellules ont été cultivées jusqu'à confluence et des bandes droites (home made guide[®]) ont été faites avec une pointe dans la monocouche. Des images ont été acquises en continu pendant 24 heures en utilisant la microscopie à contraste de phase (objectif Axio Observer D1 10X, ZEISS[®]) avec une image toutes les 10 minutes, les cellules étant maintenues dans une atmosphère de 37°C, 5% CO₂. La cicatrisation a été quantifiée à l'aide d'ImageJ[®]. Nous avons quantifié la vitesse des lignées cellulaires en mesurant la distance du front de migration parcourue en 24H. Les mesures ont été effectuées des deux côtés de l'éraflure et plusieurs endroits de l'éraflure ont été filmés. Au moins 3 plaques 24 puits indépendantes ont été analysées.

Préparation des membranes cellulaires

Une boîte de culture cellulaire confluente de 100 mm de chaque lignée est rincée avec du PBS froid, puis rapidement avec de l'eau froide et laissée pendant 10 minutes sur la glace avec 1 mL de milieu hypotonique Tris EDA[®] (10mM Tris, 1 mM EDTA) avec un inhibiteur de protéase (Sigma) et avec ou sans iodoacétamide (Sigma) à une concentration finale de 10 µM, 50 µM ou 100 µM. La solution d'iodoacétamide est préparée de manière extemporanée à chaque utilisation car elle est très sensible à la lumière.

Les Western Blots sont réalisés pour les échantillons avec et sans iodoacétamide sur un gel SDS-Page[®] dans des conditions non réductrices (LDS Sample buffer Non reducing (4X) Thermo Fisher Scientific[®]).

Protocole de détection de la S-nitrosylation

Pour cela, un test Biotin Switch est utilisé. Il est réalisé selon un protocole adapté du Biotin Switch assay kit de Cayman Chemical.

A l'abri de toute lumière directe, une boîte de culture cellulaire confluente de 100 mm de chaque lignée est lavée avec trois aliquots successifs de tampon de lavage froid en

utilisant une fraction du dernier lavage pour gratter et transférer les cellules dans un tube de 2 mL. Un culot cellulaire est généré par centrifugation à 500G pendant 5 minutes à 4°C. Tous les échantillons sont conservés sur de la glace. Chaque culot cellulaire est remis en suspension avec 0.5 mL de tampon A contenant le réactif de blocage. Les échantillons sont placés sur un agitateur avec une légère agitation pendant 7 heures à 4°C. Des lysats clarifiés sont générés par centrifugation des échantillons pendant 10 minutes à 4°C. Les surnageants sont transférés dans des tubes coniques froids de 15 mL en polypropylène et les protéines sont précipitées avec 4 volumes d'acétone glacée pendant une nuit à -20°C. Un culot protéique compact est obtenu par centrifugation à 3000 G pendant 10 minutes à 4°C. Chaque culot protéique est remis en suspension dans 0.5 mL de tampon B contenant les réactifs de réduction et de marquage. Les échantillons sont incubés pendant une heure à température ambiante sur un agitateur rotatif. Les protéines sont précipitées avec 2 mL d'acétone glacée pendant une nuit à -20°C. A la lumière directe, un culot protéique compact est produit par centrifugation à 3000 G pendant 10 minutes à 4°C. Chaque culot protéique est remis en suspension avec 0.5 mL de tampon de lavage froid et transféré dans des dispositifs de filtration centrifuge Amicon Ultra -0,5 (Merck®) et rincé 5 fois avec du PBS par centrifugation à 14000 G pendant 10 minutes à 4°C et une dernière fois avec du tampon de lavage froid. Pour chaque échantillon, 100 à 200 µL de tampon de lavage sont ajoutés. Un aliquot de chaque échantillon est prélevé pour l'Input. Les tubes sont conservés à -80°C. Dans un tube conique de 15 mL, le volume nécessaire de résine d'agarose streptavidine (Thermo Fisher Scientific®) est administré à raison de 5 µL de résine par échantillon. La résine est rincée 5X par centrifugation à 1000 G pendant 2 minutes à 4°C avec 1 mL de PBS, PBS 0.1% BSA, PBS 0.1% SDS 1% NP40 et à la fin remise en suspension avec PBS 0.1% SDS 1% Igepal (Sigma®) le même volume que le volume initial de résine. Pour chaque échantillon, 10 µL de cette suspension de résine sont déposés dans une colonne Pierce de 2 mL, puis 2 mL de PBS, enfin 500 µg d'extrait protéique. Le tout est élué et rincé 5X

avec 2 mL de PBS, PBS 0.1% BSA et PBS 0.1% SDS 1% Igepal. La résine est reprise avec 100 µL de PBS et placée dans un tube avec 400 µL de solution 2% SDS 0.4M urée (Sigma[®]), chauffée à 95°C pendant 10 minutes et refroidie sur glace pendant 10 minutes. Enfin, chaque 500 µL est transféré dans des filtres Amicon Ultra -0,5 et rincé 5X avec du PBS par centrifugation à 14000 G pendant 10 minutes à 4°C et une dernière fois avec du Wash Buffer froid.

L'analyse des Western blots se fait sur un gel SDS Page dans des conditions réductrices. La quantification des Western Blots est réalisée avec ImageJ.

Détection de la S-Glutathionylation par un test de biotine switch modifié

Les cellules ont été lysées avec un tampon RIPA complété par un cocktail d'inhibiteurs de protéase et de phosphatase (Merck[®]). 1 mg de protéines a été incubé avec 50 mM de N-éthyl maléimide à 4°C pour alkyler de façon stable les thiols libres. Du DL-Dithiothreitol à 60 mM est ajouté pour réduire les thiols non alkylés. Les échantillons ont ensuite été nettoyés à l'aide de filtres centrifuges Amicon Ultra -0,5 (Merck[®]), conformément aux recommandations du fabricant. Le lysat résultant a ensuite été oxydé avec 1 mM de diamide et incubé avec 1 mM de glutathion éthylène ester biotinylé (Thermo Fisher Scientific[®]). Après élimination de l'excès de GSH et des oxydants, 1 mg de l'échantillon a été incubé avec 100 µL de billes de streptavidine-agarose lavées pendant 2 heures sous rotation à 4°C. Après 5 lavages avec un tampon RIPA, les échantillons ont été élués avec un tampon Laemli réducteur classique, bouillis 10 minutes et chargés sur un gel de page SDS et analysés par Western Blot.

Immunoprécipitation de NHE1

Les cellules ont été lysées dans une solution de sodium 140 mM contenant 50 mM de Tris, pH 7.2 et 1% d'Igéal (Merck[®]). Un cocktail d'inhibiteurs de protéase et de phosphatase (Merck[®]) a été ajouté. L'anticorps NHE1 de Merck[®] (MAB3140) a été incubé

à raison de 1 µg d'anticorps pour 2 mg de lysat protéique pendant la nuit à 4°C. Le lendemain, des Dynabeads magnétiques de protéine G (Thermo Fisher Scientific[®]) lavés ont été ajoutés pour une rotation de 1H à 4°C. Après 5X5 min de lavage avec le tampon de lyse, l'éluion des échantillons a été faite avec du Laemli réducteur et bouillie 5 min à 95°C, puis réalisée par Western Blot classique. Pour chaque expérience, deux gels ont été faits en parallèle, un pour l'expression de NHE1 avec un anticorps primaire de chez BD et l'autre pour l'expression du complexe ERM (signalisation cellulaire totale ERM) ou de GSH (protéine liée Merck[®]).

Western Blot

Les échantillons des différentes expériences ont été analysés sur des gels d'acrylamide/bisacrylamide à 7.5% (SDS PAGE, Biorad mini gel system[®]), transférés sur des membranes PVDF (Immobilon P, Millipore[®]). Les immunoblots ont ensuite été traités avec du lait écrémé à 5% et les anticorps primaires commerciaux appropriés contre NHE1 (BD Biosciences[®]), ERM total (Cell Signaling[®]) ou GSH lié aux protéines (Merck[®]) et les anticorps secondaires correspondants (conjugués à la HRP), comme décrit par Counillon *et al.*¹²

Analyse des données et traitement

Les images et les Western Blots ont été quantifiés à l'aide du logiciel ImageJ[®]. Les données ont été compilées à l'aide du logiciel Microsoft Excel[®]. Sauf indication contraire, les points expérimentaux correspondent à la compilation d'au moins cinq expériences indépendantes, chaque point expérimental étant déterminé au moins en double. Tous les points expérimentaux sont accompagnés de l'erreur standard de la moyenne pour les barres d'erreur.

Réactifs :

Diphenyleneiodonium Chloride (DPI) ref D2926, Menadione ref M5625, Iodoacetamide ref I1149, Phalloidin TRIC P1951, Igepal ref I8896, Tris EDTA Buffer ref T9285, Sigma Fast Protease Inhibitor Cocktail tablets ref S8830, Sodium Dodecyl Sulfate (SDS) ref L3771, Urea ref U5378, Bovine Serum Albumin (BSA) fatty free acid Ref A7030 sont de chez Merck®.

H₂O₂ 3% 10 volumes single est un produit de chez Gifrer®.

S-Nitrosylated Protein Detection Kit Biotin Switch ref 10006518 est de chez Cayman Chemical®.

Amicon Ultra -0.5 centrifugal filter devices ref UFC503096 sont de chez Millipore®.

Pierce centrifuge columns 2 mL ref 89897 sont de chez Pierce®.

LDS Sample Buffer Non-Reducing (4x) ref 84788, Streptavidin Agarose Resin ref 20353, ProLong Diamond Antifade Mountant ref P36961, DMEM ref 11965092 sont des produits de chez Thermo Fisher Scientific®.

Quickchange II ref 200523 est d'Agilent®.

Anticorps

Purified mouse anti-NHE1 ref 611774 est de chez BD Biosciences®.

Purified mouse anti- NHE1 ref MAB 3140 est de chez Millipore®.

Monoclonal anti-beta actine antibody produced in mouse, monoclonal anti-fibronectin antibody produced in mouse ref F7387 sont de chez Merck®.

Hoechst ref 33342, goat anti-mouse Alexa Fluor 488 ref A28175 sont des produits de chez Thermo Fisher Scientific®.

C. Présentation de l'article complet

Cysteines in the Na⁺/H⁺ exchanger NHE1 are essential for superoxide ion regulation and cell motility

Denis Doyen, Gisèle Jarretou, Etienne Boulter, Zeinab Rekab, Didier Pisani, Marc Cougnon, Michel Tauc, Emmanuel Van Obberghen, Nina Milosavljevic, Ellen Van Obberghen-Schilling, Marie Véronique Clément, Laurent Counillon and Mallorie Poët

Université Côte d'Azur, CNRS, LP2M, Nice 06107, France.

Abstract (224 words; 250 max)

The objectives of this study were (i) to investigate whether and how the superoxide anion $O_2^{\cdot-}$ regulates the activity of the Na^+/H^+ exchanger NHE1, and (ii) to identify which regions and which amino acids of NHE1 are involved. WT NHE1 is activated by Menadione (33 μ M), a $O_2^{\cdot-}$ donor, and inhibited by Diphenyleneiodonium (DPI, 10 μ M) that decreases $O_2^{\cdot-}$ production. This activation by Menadione and inhibition by DPI are lost in a Cysless mutant of NHE1 in which all cysteines are replaced by alanine. We then tested the inhibition by DPI on mutants of NHE1 on each of its cysteines and identified cysteines 133 and 477 as essential in this mechanism.

We next analyzed the possible covalent modifications involved by searching for disulfide bond formation; S-nitrosylation and protein S-glutathionylation using non reducing SDS PAGE; biotin switch and immunoprecipitation. Doing this we found that cysteine 421 is nitrosylated, but we could detect neither disulphide bridges nor glutathionylation.

Remarkably, we observed a very different adhesion and migration profile of cells expressing the Cysless NHE1 mutant compared to the WT isoform. By coimmunoprecipitation of NHE1 with the ERM complex (Ezrin/Radixin/Moesin) we established that its cysteines are crucial for its binding to the ERM complex and therefore to cortical actin. Taken together our work reveals a key connection between the production of reactive oxygen species, the regulation of intracellular pH and cell motility and adhesion.

Introduction

The Na⁺/H⁺ Exchanger NHE1 is a transmembrane transporter that belongs to the SLC9A gene family of mammalian antiporters. It is expressed at similar levels in all mammalian cells and tissues and shares a high level of sequence homology among vertebrates (Pedersen and Counillon, *Physiological Reviews* 2019). NHE1 performs the electroneutral exchange of one Na⁺ against one H⁺ and is fully reversible (Grinstein et al. 1984). While extracellular Na⁺ is required as an energy coupling cation, intracellular H⁺ ions both work as allosteric activators and transported substrates. Consequently, as NHE1 is both able to accurately sense cytosolic pH and to extrude H⁺ ions, it is one of the major transmembrane transporters for intracellular pH regulation. Because of its ability to transport extracellular Na⁺ into the cytosol, NHE1 also plays an important role in cell volume regulation upon hypertonic shocks and in cell shape determination.

As one of the most widely studied Na⁺/H⁺ exchangers, NHE1 also stands as a paradigm for its regulation by multiple signaling pathways including ATP (Ikeda et al. 1997), lipids (Aharonowitz et al. 2000; Hendus-Haltenburger et al. 2020); protein interaction (for review see Pedersen and Counillon 2019), tunable phosphorylation (Hendus-Haltenburger et al. 2017), or mechanical cues (Lacroix et al. 2008), that all act on the NHE1 cytosolic tail to modify the transporters' cooperative response to cytosolic H⁺ ions. In this respect NHE1 can be viewed as a coincidence detector that integrates multiple signals of different nature, leading to a very fine tuning of cytosolic pH and volume according to the cells physiological state and demands.

NHE1 is also able to transport Lithium that is situated between H⁺ and Na⁺ in the first column of the periodic table and is inhibited by acylguanidines the most used being pyrazinoylguanidine type inhibitors (e.g. Amiloride) or benzoylguanidine-type (e.g. Cariporide) (Rolver et al. 2019).

The NHE1 long-awaited three-dimensional structure has been recently solved thanks to CryoEM (Dong et al. 2020). It reveals a dimeric organization of the membrane region where each protomer, of 13 transmembrane segments each, can bind and transport ions. This topology also enables the C-terminal region of NHE1 to face the cytosol where it will be exposed to the multiple signals mentioned above. Of note the NHE1 cryoEM structures at different pH values and with the Cariporide inhibitor show extremely consistent positions of the residues that had been identified as important for NHE1 function, inhibitory interaction, or regulation by intracellular H⁺ (Poët et al. 2022).

While the covalent modification of serine and threonine has been widely described as a mechanism of regulation of NHE1 by phosphorylation; much less is known on other covalent

modifications that could be instrumental in NHE1 regulation in physiological or pathological situations. In that respect, cysteines are intriguing amino acids as their thiol side chain can (i) deprotonate to yield a thiolate form ($pK_a = 8.3$) and could therefore participate in the fine tuning of NHE1 activity by H^+ ions, (ii) function as a sensor of reactive oxygen/nitrogen species flipping between the reduced and oxidized state and, (iii) make reversible covalent bonds, namely through disulfide bridges or through the formation of S-nitrosylated or S-glutathionylated cysteines. NHE1 possesses 9 cysteines with the first one in a cleavable signal peptide, the next five in the transmembrane region of NHE1 and the three last ones in its cytosolic regulatory tail. Interestingly, Wakabayashi's group generated a cysless mutant (in which all the cysteines have been replaced by alanines) (Wakabayashi et al. 2000) that was expressed at the plasma membrane and being fully functional and cytosolic pH sensitive like the WT NHE1. However, this does not exclude that some or all of these cysteines could be involved in more subtle regulation mechanisms. Therefore, we decided to explore the potential role of cysteines in NHE1 regulation by superoxide ($O_2^{\cdot-}$), H_2O_2 , their possible covalent modifications and impact on cell mechanics.

For this we used fast lithium uptake measurements, biotin switch techniques, coimmunoprecipitations and cell imaging on antiporter-deficient fibroblasts (PS120 cell line, Pouysségur et al. 1984) stably transfected either with a WT, the above-mentioned cysless NHE1 mutant (Wakabayashi et al. 2000) and all cysteine to alanine point mutants of NHE1. In brief, we provide a set of results showing a novel regulation mechanism of NHE1 by $O_2^{\cdot-}$ that requires a triad of critical cysteines in the protein structure, the mapping of Cysteine covalent modifications in native conditions and finally, we reveal an unexpected connection between the NHE1 cysteines and the F-actin cytoskeleton which impacts on cell adhesion and motility.

Results

Activation of WT and Cysless NHE1 by H_2O_2 and Superoxide ion

Fibroblasts stably transfected by a WT or a cysless NHE1 were exposed either directly to H_2O_2 or to Menadione, a $O_2^{\cdot-}$ donor. Figure 1 shows that as previously published (Huc et al., 2007), both WT and the cysless NHE1 are fully activated by H_2O_2 exposure in a timely manner. We then exposed both WT and Cysless mutants for different lengths of time to NH_4^+ (see methods) to reach distinct intracellular values and compared the transporters' allosteric response to intracellular protons. As shown in Figure 1, we observe that H_2O_2 increases the transporters' response to intracellular acidification both in WT and the cysless mutant. This means that NHE1

regulation by H_2O_2 does not require the presence of cysteines in the transporter but involves other signaling pathways such as p38 or protein kinase C as described (Snabaitis et al. 2002). Our findings reveal also that the cysless mutant, that displays the same intracellular proton regulation as the WT NHE1 (Supplementary figure 1), is fully regulable as well.

To test for NHE1 activation by $\text{O}_2^{\cdot-}$, we incubated cells expressing either the WT or the Cysless mutant to menadione for different periods, which resulted in an increase of $\text{O}_2^{\cdot-}$ levels as quantified in (Supplementary figure 2). This produced a biphasic effect on WT NHE1 activity with a rise in lithium transport that reached a peak within 45 minutes and then decreased. Such biphasic or periodic effects of menadione exposure have been documented in (Kizhuveetil et al., 2019). In parallel, we observed that upon menadione exposure, the cells started to swell and lose adhesion after 45 minutes (Supplementary figure 3), explaining NHE1 inhibition as this transporter's activity is decrease by cell swelling and rounding. The antiporter-deficient PS120 cells were also rounding with menadione showing that this effect was not NHE1-dependent. Of note, such a rounding was not observed for H_2O_2 treatment. In contrast, the cysless mutant was very poorly activated by menadione showing that NHE1 cysteines are part of the NHE1 activation mechanism by $\text{O}_2^{\cdot-}$.

We then tested the allosteric response of NHE1 to intracellular protons in the presence of menadione. As seen in Figure 2A, NHE1 activation here again is mediated by an increase in its cooperative response whilst this effect is not present in the cysless mutant.

Taken together our results show that the two reactive oxygen species H_2O_2 and $\text{O}_2^{\cdot-}$ both activate NHE1 but by a completely different mechanism that involves the transporter's cysteines for $\text{O}_2^{\cdot-}$.

Exposure of WT and cysteine mutants to Diphenylene Iodonium

As the quantitative assessing of an activation mechanism, that displays a biphasic response with a potential indirect inhibition of NHE1 is not satisfactory, we used Diphenylene Iodonium (DPI) a wide-spectrum inhibitor of $\text{O}_2^{\cdot-}$ production by NADPH oxidases (and XOR/XDH Bortolotti et al., 2021) that produce both superoxide and H^+ ions (for review, see Brandes et al., 2014).

As shown in Figure 2B DPI very robustly decreased WT NHE1 activation by intracellular protons. This means that in physiological conditions NHE1 already displays an activation by the endogenous production of $\text{O}_2^{\cdot-}$ that is decreased by DPI. To further delve into this mechanism, we then treated the cells with both μM DPI and DDC, which is an inhibitor of the superoxide

dismutase. We reason that if this mechanism is correct, blocking both O_2^- production and degradation would result in a steady state level that would not affect the NHE1 response. As expected, DDC is able to totally reverse the DPI effect (figure 2B). Importantly, figure 2C illustrates that the cysless mutant fails to respond to DPI. Taken together, our experiments demonstrate that the NHE1 sensitivity to intracellular H^+ is modulated by the superoxide ion and that this regulation requires NHE1 cysteines as it is absent in the cysless mutant.

Role of individual mutants of NHE1 cysteines

To identify the cysteines involved in the above-described regulation, we generated all the mutants in which each cysteine of NHE1 was individually mutated into an alanine (Quickchange II Mutagenesis kit, Agilent). We then stably transfected each of these mutants into NHE-deficient PS120 cells using G418 selection (500 μ g/ml). All mutants were expressed (see the loading controls in Figures 5B and 8A) and functional as all G418 selected cells expressing each mutant were fully able to survive an acute intracellular acidification.

We then evaluated the effect of DPI (10 μ M, 3H) on the allosteric response of each of these mutants to H^+ . We preferred to measure this response to the O_2^- production inhibitor as testing for the effect of the menadione O_2^- donor is much less straightforward and quantitative due to the biphasic effect obtained with this compound. Our results are represented in Figure 3. Among all the cysteine mutants, those at positions 133, 477 and 538 do not show any response to DPI. Those cysteines occupy very interesting positions in the NHE1 structure (Figure 4). Indeed, cysteine 477 is facing the extracellular side of the transporter and is found just before the start of the last transmembrane segment of NHE1 (TM13) that directly connects with the regulatory C-terminal tail. Symmetrically cysteine 133 is situated at the very beginning of the second transmembrane segment and is part of the highly hydrophilic PES sequence facing the intracellular side. Finally, cysteine 538 is located at the beginning of the NHE1 C-terminal tail at the extremity of a short helical region facing the CHP1 protein partner. Taken together these locations results in a triad of cysteines situated at critical regions of the protein to detect O_2^- produced on both the intracellular and extracellular sides of NHE1.

NHE1 cysteines covalent modification

Based on our previous results that identified critical cysteines in NHE1 we next explored whether some of its cysteines could undergo covalent modifications that could explain their regulation by O_2^- (for review see Hawkins and Davies 2019) For this purpose, we tested the

presence of possible interprotein disulfide bonds using iodoacetamide alkylation to prevent unspecific disulfide bonds in the SDS-denatured protein. We then checked for S-nitrosylation using biotin switch and for S-glutathionylation using both biotin switch and direct detection of glutathionylated cysteines using western blots.

Figure 5a shows that exposure of WT NHE1 to iodoacetamide does not modify its electrophoretic pattern in native gels. This indicates that NHE1 does not make any particular disulfide bond with another protein that would have been missed from previous studies.

We then performed biotin switch experiments on WT NHE1 and on all the individual mutants, in the absence of any NO donor (See methods) to be sure not to artificially force any unspecific cysteine nitrosylation. As illustrated in the representative Western Blot and its quantification (Figure 5B-C), we observed that the positive signal for nitrosylation was totally abolished when cysteine 421 was replaced by an alanine. This unambiguously identifies this cysteine, that lies in the middle of NHE1 TM11 in a densely packed region of the protein, as the target for nitrosylation in native conditions. This also shows that none of the previously identified cysteines for O₂⁻-regulation are nitrosylated.

Next we investigated whether NHE1 could be cysteine-glutathionylated (Ghezzi 2013). As such a thiol covalent modification involves first an oxidation step, we reasoned that the glutathionylation of cysteines 133, 477 and 538 could be a pertinent mechanism to mediate O₂⁻-regulation. We used two independent protocols, biotin switch and western blot detection of glutathionylated cysteines (see Materials and Methods), using the cysless mutant as a control. Despite much effort we did not detect any positive signal in the WT NHE1 compared to the cysless mutant in the experimental conditions tested (Figure 5D). This strongly suggests that either NHE1 is not glutathionylated or that the quantity of glutathionylated NHE1 is too low to be detectable.

Role of NHE1 cysteines in cell shape and migration

From the start we were intrigued by the fact that the cells expressing the cysless mutant had a shape and behavior different from those transfected with WT NHE1. As this transporter has been found to be instrumental in cell shape, adhesion and migration (for review see Pedersen and Counillon 2019), we decided to investigate whether cysteines could be involved in the contribution of NHE1 in these cellular features.

To quantify the-cell phenotype, we performed wound healing experiments. Figure 6a and the supplementary Movie compare the migration of NHE deficient fibroblasts as a control with cells transfected with NHE1 or with the cysless mutant. While the NHE1 transfected cells migrate

in a coordinated manner and exhibit contact inhibition, the cells expressing the *cysless* mutant have a disordered migration with a rounded shape and a large defect in contact inhibition. This results in a significantly slower migration rate of the *cysless* mutant compared to WT as shown in the quantification of Figure 6b. This phenotype is similar, but more pronounced than the observed migration of the NHE-deficient PS120 cells. As Na^+/H^+ exchange is fully functional in both WT and *cysless* mutant our findings illustrate that NHE1 can impact on cell shape adhesion and motility in a Na^+/H^+ transport independent manner.

To investigate the possible proteins involved, we next quantified the production of fibronectin and vinculin using Immunofluorescence, but we found no significant differences between WT and the *cysless* mutant (Figure 7).

Finally, we tested whether the *cysless* cellular phenotype could reside in the interaction of the transporter with the F-actin cytoskeleton. As previously reported, this occurs through the ERM protein complex that binds NHE1 at a site encompassed in the 552-560 stretch of sequence in the C-terminal tail (Denker et al. 2000, Denker et al. 2002). For this, we immunoprecipitated the WT and *cysless* NHE1 (see Materials and Methods) and used western blotting to test whether the ERM complex coimmunoprecipitated with NHE1. As illustrated in Figure 8A, the ERM complex showed very poor, if any, coimmunoprecipitation with the *cysless* mutant compared to the WT exchanger. These data indicate that the NHE1 cysteines are involved in the formation of the ERM complex with NHE1.

We next performed the same immunoprecipitation experiments with the 8 NHE1 cysteine individual point mutants. The quantification of the western blots displayed in Figure 8B reveals that no single cysteine is significantly involved in this interaction.

Discussion

In proteins, cysteines are probably the most versatile aminoacids in terms of both possible structural and regulatory functions. Their side chain is hydrophobic but at the same time can deprotonate, with a pKa close to 8; indicating that a significant fraction of cysteines can become negatively charged in proteins. Cysteines can also be oxidized and form a covalent bond, either to generate disulfide bridges or to become covalently modified by groups of different nature. Hence, while much attention has been given on Ser, Thr or Tyr phosphorylation, the study of cysteine modifications is signaling appears to have been surprisingly neglected. Among the possible reasons is that cysteines are still often mistakenly classified as polar residues, frequently seen as relatively inert, while they are in fact either hydrophobic or charged but not polar. Another complexity is that redox chemistry deals with very labile species, making the reactive oxygen species that can react with cysteines much more difficult to monitor and quantify experimentally.

The aim of our work was firstly to investigate whether the Na⁺/H⁺ NHE1 cysteines are playing a role in the regulation of this transporter, and secondly to identify those that were involved in such tuning mechanisms.

We found that the superoxide ion (O₂⁻) is able to activate WT NHE1 but not a NHE1 mutant in which all cysteines have been replaced with alanine. In contrast, hydrogen peroxide (H₂O₂) also activates NHE1 but identically for the WT and the cystless mutant. This indicates that the two mechanisms of activation are different. As hydrogen peroxide is generated by the protonation of superoxide by the superoxide dismutase, our results also unambiguously show that O₂⁻ activation is not due to its transformation into H₂O₂ that would in turn activate NHE1. Furthermore, H₂O₂ activation has been found to be mediated by the p38 stress kinase pathway (Snabaitis et al., 2002).

To identify which cysteine could be involved in this superoxide activation we generated eight cysteine to alanine individual mutants in the NHE1 sequence. Alanine substitution is the most obvious choice because it straightforwardly removes the thiol group of the cysteine residue, leaving the methyl group of the side chain intact. To avoid unexpected variations, we selected stable complete populations instead of individual clones. All were functional and could insert at the plasma membrane, with a slightly different ratio of the fully glycosylated plasma membrane form versus the TGN immature form (Counillon et al., 1994) as seen from the loading controls on the western blots (figure 5 and 8). To measure the sensitivity of these mutants to protons we used DPI, instead of menadione because with the latter the NHE1 response was biphasic (Figure

2A) and hence accurate measurements are difficult. We therefore reasoned that using DPI for such a screen was more appropriate for the following reasons (i) DPI inhibition recapitulated the menadione effect (Figure 2) between WT and Cysless mutant, (ii) DPI is a wide-range $O_2^{\cdot-}$ production inhibitor, and (iii) its effect was reversed by the superoxide dismutase inhibitor, DDC (Figure 2).

This screen revealed that the mutations of two cysteines, Cys 133 and Cys 477, abolish the DPI effect, in a dominant manner. Cysteine 133 is located one helix turn to the intracellular N-terminal end of transmembrane segment 2 that faces a large intracellular funnel that is paved by aminoacids involved in ion transport (Poët et al., 2022). The second cysteine at position 477 is situated on the extracellular side of NHE1, at the start of the last transmembrane segment, that possesses two interesting features. Firstly, it contains an interrupted region and secondly it leads to the intracellular regulatory region of NHE1. In sum, we have identified these two cysteines as an extracellular and an intracellular sensor of $O_2^{\cdot-}$. Both are situated in critical regions for NHE1 ion binding and/or transport (Figure 4). Sequence comparison (Supplementary figure 4) shows that Cysteine 133 is conserved among the plasma membrane NHEs, while cysteine 477 is present only in NHE1 and replaced by a positively charged aminoacid in the NHE2-9 isoforms. This suggests that its presence in this extracellular loop has been strongly selected by evolution to confer $O_2^{\cdot-}$ regulation to this isoform.

We next tried to understand how these cysteines could detect superoxide, and for this, we tried to map what could modify these cysteines in response to superoxide. We tested three main covalent modifications that could have been directly or indirectly involved: disulfide bonds; S-nitrosylation and S- glutathionylation. While we did not detect any evidence of disulfide bonds and S-glutathionylation, we found that cysteine 421 is nitrosylated. As also shown in supplementary Figure 4, this cysteine is conserved only in NHE2. Although the identification of this aminoacid is of great interest for understanding the mechanism of regulation of NHE1 by NO, it clearly does not give a clue for the superoxide activation mechanism. Taken together, pinpointing the modification of Cysteines 133 and 477 upon $O_2^{\cdot-}$ exposure remains to be completed in further studies. Interestingly it can be noticed that the cysteines 133, 431 and 477 identified in this work are not conserved in the different NHE isoforms that all have their specificities of expression and localization. This indicates that their regulation by reactive oxygen species are distinct; which makes sense in a physiological context.

A particularly unanticipated observation we made was that cells harbouring the cysless mutant, that does not exhibit any distinct transport features from the WT NHE1, displayed a

much more rounded shape and disordered motility compared to WT NHE1. This unambiguously shows that at least a part of NHE1 contribution in cell mechanical behavior is not directly dictated by the ion exchange that is instrumental in creating an intracellular pH gradient important for cell migration (Martin et al. 2011). Furthermore, to the best of our knowledge this is the first time that such spectacular change at the whole cell level can be attributed to cysteine mutations in a transporter.

Interestingly, we did not detect any significant differences in fibronectin, vinculin, or integrins organization but instead found that the ERM complex, that binds NHE1 between aminoacids 552 and 560 was not anymore coimmunoprecipitated with the cysless mutant. This constitutes an important clue in the cysless mutants' phenotype. Therefore, we performed coimmunoprecipitation on all our mutants to identify the possible cysteines that could be involved. While we initially thought that cysteines 532 and/or 561 that are on each side of the PIP₂/ERM site could be interesting candidates, no individual mutant could reproduce the cysless phenotype, neither concerning cell shape and migration, nor in ERM coimmunoprecipitation. This indicates that a combination of cysteines, which remains to be identified, governs the interaction of NHE1 with the ERM complex and actin cytoskeleton. Of note we were not exhaustive in investigating all possibly affected cytoskeletal and adhesion proteins and we cannot exclude that in addition to ERM, the cysless mutant could also have an impaired direct or indirect interaction with other proteins. This will be the subject of further studies.

Our present work shows that the Na⁺/H⁺ exchanger NHE1 is activated by O₂⁻ and identifies critical cysteines of the transporter involved in this mechanism. It also points to the role of NHE1 cysteines residues in the transporters' interaction with F-actin via the ERM complex, and consequently in cell migration. Our findings therefore establish NHE1 as a pivotal membrane protein at the interface between pH regulation, redox regulation, and cell motility. Hence, we anticipate that dysregulation of these newly discovered functions NHE1 could be involved in disease situations.

Materials and Methods

Cell Culture and Transfection.

Exchanger-deficient fibroblasts (PS120 cell line) were grown in Dulbecco's modified Eagle medium supplemented with 50 µg/mL streptomycin, 50 units/mL penicillin, and 7.5% v/v fetal calf serum at 37 °C in a humidified atmosphere of 5% CO₂ and 95% air. Transfections were performed using Lipofectamin 3000 (Thermofisher Scientific), as described by the manufacturer. Cell populations stably expressing either wild-type or mutant NHEs were selected using 500 µg mL⁻¹ G418 for 3 weeks. For lithium uptake experiments, 24 well-plates were seeded and incubated during 3 days until 100% confluence.

Cell acidification at different intracellular pH values

For all experiments, intracellular acidification was obtained with the application of an ammonium loading solution containing: 50 mM NH₄Cl, 70 mM choline chloride, 5 mM KCl, 2 mM CaCl₂, 1 mM MgCl₂, 5 mM glucose, buffered at pH 7.4 with 15 mM MOPS, for different durations to obtain distinct intracellular pH values. This was followed by rapid rinses in the choline chloride solution (120 mM Choline Chloride, 5 mM KCl, 1 mM MgCl₂, 2 mM CaCl₂, 5 mM Glucose, buffered at pH 7.0 with 15 mM HEPES). Calibration of the obtained intracellular pH values was obtained by measuring BCECF/AM fluorescence (SAFAS multiplate reader). The fluorescence signals relative to pHi were calibrated using the K⁺/H⁺ exchanging ionophore nigericin. For this purpose, the cells were incubated within a solution of 140 mM KCl, 20 mM HEPES, and 2.5 µM nigericin adjusted to pH 7. The pHi values for each individual ammonium loading time were obtained by interpolation of the grey level values and adjusted to the experimental calibration.

NHE-1 activity measurement by lithium uptake

Cells seeded on 24 well plates were acidified at different pH values as above and then incubated in 15 mM LiCl, 105 mM Choline Chloride, 5 mM KCl, 1 mM MgCl₂, 2 mM CaCl₂, 5 mM Glucose, buffered at pH 7.2 with 15 mM HEPES for 1 min. Lithium uptake was then stopped by four rapid rinses in ice-cold phosphate buffered saline (PBS). Cells were solubilized in 0.25 N nitric acid (trace metal grade HNO₃, Sigma), and the intracellular lithium was measured using atomic absorption spectrometry (Perkin Elmer, Spectrometer PinAAcle 900Z[®]).

Site Directed Mutagenesis

The different cysteine to alanine mutants of NHE1 were generated using the Quickchange II site directed mutagenesis kit (Agilent); on the pECE Ires-Neo vector generated by (Lacroix et al. 2004) using the primers listed below (forward sequences).

NHE1 Cys1>>Ala F: 5'CCTCTGGCCGCCCTCATGAAGATAGG3'

NHE1 Cys2>>Ala F: 5'CCCGGAGAGCGCCCTGCTGATCGTGG3'

NHE1 Cys3>>Ala F: 5'CATGTACGCCGTGGCCCTGGTGGGCGG3'

NHE1 Cys4>>Ala F: 5'CCTGCTCTTCGCCCTCATCGCCCG3'

NHE1 Cys5>>Ala F: 5'GCACTTCCCATGGCTGACCCGTTCCCTCAC3'

NHE1 Cys6>>Ala F: 5'GCATCGAAGACATGGCTGGCCACTACGG3'

NHE1 Cys7>>Ala F: 5'GAAATATGTGAAGAAGGCTCTGATAGCTGGC3'

NHE1 Cys8>>Ala F: 5'GGATACAGCGCGCCCTCAGTGACCCAG3'

Immunofluorescence staining

Fibroblasts were fixed in 4% v/v paraformaldehyde with 3% sucrose w/v at 37°C for 10 minutes and permeabilized with 0.2% v/v triton-100. Vinculin primary antibody is made from rabbit and secondary alexa 594 from goat (ThermoFisher scientific). Hoechst 33342 (ThermoFisher scientific) has been added with secondary antibody to stain nuclei. Coverslips were mounted in ProLong Gold antifade (ThermoFisher scientific). Actine filaments staining was performed with phalloidin-TRITC at 50µg/ml (Merck). For fibronectin, extracellular fibronectin was detected with anti-fibronectin antibodies. Pictures were taken from X63 magnification (ZEISS® LSM 800). Vinculin stainings were analyzed with widefield fluorescence Zeiss Axio-observer 7 microscope 63× oil objectives (numerical aperture of 1.4) equipped with a CoolSnap HQ CCD. Image acquisition was performed using ZEN 3.6 software. Image analysis was performed using ImageJ (Rasband, W.S., ImageJ, U.S. National Institutes of Health, Bethesda, Maryland, USA, <http://imagej.nih.gov/ij/>, 1997–2012).

Cell Wound Healing experiments:

Different mutants and wild type cell lines were grown in 24 multiwell plates in normal DMEM with glucose and bicarbonate (Thermo Fisher scientific) supplemented with 7.5% v/v heat inactivated FCS.

Cells were grown until confluency and straight (homemade guide) scratches were made with a tip in the monolayer. Images were acquired continuously for 24 hours using phase contrast

microscopy (10× objective Axio Observer 7, Zeiss) with one image every 10 minutes, cells being maintained in a 37°C, 5% CO₂ atmosphere. Wound healing was quantified using ImageJ. We measured the speed of cell lines by recording the migration front distance covered in 24H. Measures were done from both side of scratch and several locations of scratches were filmed. At least 3 independent 24 well plates were analyzed.

Western Blot

Samples from the different experiments were run on 7.5% acrylamide/bisacrylamide gels (SDS PAGE; Biorad mini gel system); transferred onto PVDF membranes (Immobilon P, Millipore). Immunoblots were then processed with 5% v/v nonfat milk and the appropriate commercial first antibodies against NHE-1 (BD Biosciences); total ERM (Cell Signaling) or Protein-Bound GSH (Merck) and corresponding secondary (HRP-conjugated) antibodies as described by Counillon et al (1994).

S-Nitrosylation detection using biotin switch experiments:

We used a protocol adapted from Cayman Chemical's Biotin Switch assay kit.

Under indirect light, one 100 mm confluent is used. All steps are performed on ice. The cell pellet generated is resuspended with 0.5 ml of Buffer A containing Blocking Reagent, and shaken for 7 hours at 4°C. After clarification, supernatants are transferred into cold 15 ml conical polypropylene tubes and the proteins are precipitated with 4 volumes of ice-cold acetone overnight at -20°C. After centrifugation each protein pellet is resuspended with 0.5ml of buffer B containing reducing and labeling reagents and incubated for 1h at room temperature under rotation. The proteins are again precipitated with of ice-cold acetone overnight at -20°C. Resulting protein pellets are resuspended with cold Wash Buffer and transferred into Amicon Ultra -0,5 centrifugal filter devices (Merck) to be rinsed 5x with PBS as recommended by the manufacturer. Streptavidin agarose resin (Thermo Fisher Scientific) was rinsed 5X at 4°C with PBS, PBS 0.1 % BSA, PBS 0.1% SDS 1% NP40 and at the end resuspended with PBS 0.1% SDS 1% Igepal (Merck). 500 µg of the protein extract and 10 µL of this resin suspension are put into a 2 mL Pierce centrifuge column, then rinsed 5X with PBS, PBS 0.1% BSA and PBS 0.1% SDS 1% Igepal. The resin is removed from the column and bound proteins are eluted with PBS and 2% SDS plus 0.4 M urea (Sigma), heated at 95°C for 10 minutes and cooled on ice for 10 minutes. Finally, the eluted fraction is cleaned by Amicon Ultra -0.5 centrifugal filter devices. Western blots analysis is done on an SDS-Page gel under reducing conditions.

S-Glutathionylation detection using modified biotin switch assay:

Cells were lysed with RIPA buffer complemented with protease and phosphatase inhibitor cocktail (Merck). 1 mg of proteins was incubated with 50 mM N-ethyl maleimide at 4°C to stably alkylate free thiols. DL-Dithiothreitol at 60 mM is added to reduce the not alkylated thiol. Samples were then cleaned with Amicon Ultra -0.5 centrifugal filter devices (Merck) as recommended by the manufacturer. The resulting lysate was then oxidized with 1mM diamide and incubated with 1 mM biotinylated glutathione ethylene ester (Thermo Fisher Scientific). After removal of the excess of GSH and oxidants, 1 mg of the sample was incubated with 100 µL of washed streptavidin-agarose beads for 2 hours under rotation at 4°C. After 5X washing with RIPA buffer samples were eluted with classical reducing Laemli buffer, boiled for 10 min and loaded on SDS-page gel and western blot analysis.

Immunoprecipitation of NHE1:

Cells were lysed in a 140 mM sodium solution containing 50 mM tris, pH 7,2 and 1% igepal (Merck). Protease and phosphatase inhibitor cocktail (Merck) was added. NHE1 antibody from Merck (MAB3140) was incubated with a ratio of 1 µg of antibody for 2 mg of protein lysate overnight at 4°C. The next day, washed magnetic Dynabeads protein G (Thermo fisher scientific) were added for 1H rotation at 4°C. After 5X5 min washes with lysis buffer, samples elution were done with reducing Laemli solution and boiled for 5 min at 95°C. Finally, the samples were run in a classical western blot experiment. Two gels were made for each experiment, with one detected for NHE1 (another primary antibody from BD laboratories) and the other detected for the target meaning ERM (cell signaling total ERM) or GSH (protein bound Merck).

Data Analysis and treatment

Images and western blots were quantified with ImageJ. Data were compiled using Microsoft Excel software. Unless stated otherwise, the experimental points correspond to the compilation of at least five independent experiments, with each experimental point determined at least in duplicate. All experimental points are provided with standard error of the mean for error bars.

References

- Aharonovitz O, Zaun HC, Balla T, York JD, Orlowski J, Grinstein S. Intracellular pH regulation by Na⁺/H⁺ exchange requires phosphatidylinositol 4,5-bisphosphate. *J Cell Biol* 150: 213–224, 2000. doi:10.1083/jcb.150.1.213.
- Bortolotti M, Polito L, Battelli MG, and Bolognesi A. Xanthine oxidoreductase: One enzyme for multiple physiological tasks. *Redox Biol*. 2021 May; 41: 101882. Published online 2021 Jan 27. doi: 10.1016/j.redox.2021.101882 PMID: PMC7879036 PMID: 33578127
- Brandes R, P, NorbertWeissmann N, Schröder K. Noxfamily NADPH oxidases: Molecular mechanisms of activation. *Free Radical Biology and Medicine* 76(2014) 208–226
<https://doi.org/10.1016/j.freeradbiomed.2014.07.046>
- Counillon L, Pouysségur J, Reithmeier RA. The Na⁺/H⁺ exchanger NHE-1 possesses N- and O-linked glycosylation restricted to the first N-terminal extracellular domain. *Biochemistry*. 1994 Aug 30;33(34):10463-9. doi: 10.1021/bi00200a030. PMID: 8068684.
- Direct binding of the Na⁺-H exchanger NHE1 to ERM proteins regulates the cortical cytoskeleton and cell shape independently of H⁺ translocation.
Denker SP, Huang DC, Orlowski J, Furthmayr H, Barber DL. *Mol Cell*. 2000 Dec;6(6):1425-36. doi: 10.1016/s1097-2765(00)00139-8. PMID: 11163215
- Denker SP, Barber DL. Cell migration requires both ion translocation and cytoskeletal anchoring by the Na-H exchanger NHE1. *J Cell Biol*. 2002 Dec 23;159(6):1087-96. doi: 10.1083/jcb.200208050. Epub 2002 Dec 16. PMID: 12486114; PMCID: PMC2173980.
- Dong Y, Gao Y, Ilie A, Kim D, Boucher A, Li B, Zhang XC, Orlowski J, Zhao Y. Structure and mechanism of the human NHE1-CHP1 complex. *Nat Commun*. 2021 Jun 9;12(1):3474. doi: 10.1038/s41467-021-23496-z. PMID: 34108458; PMCID: PMC8190280.
- Ghezzi P. Protein glutathionylation in health and disease. *Biochim Biophys Acta*. 2013 May;1830(5):3165-72. doi: 10.1016/j.bbagen.2013.02.009. Epub 2013 Feb 15. PMID: 23416063.
- Grinstein S, Goetz JD, Rothstein A. 22Na⁺ fluxes in thymic lymphocytes. II. Amiloridesensitive Na⁺/H⁺ exchange pathway; reversibility of transport and asymmetry of the modifier site. *J Gen Physiol* 84: 585–600, 1984. doi:10.1085/jgp.84.4.585.
- Hawkins CL, Davies MJ. Detection, identification, and quantification of oxidative protein modifications. *J Biol Chem*. 2019 Dec 20;294(51):19683-19708. doi: 10.1074/jbc.REV119.006217.
- Hendus-Altenburger R, Lambrugh M, Terkelsen T, Pedersen SF, Papaleo E, Lindorff-Larsen K, Kragelund BB. A phosphorylation-motif for tuneable helix stabilisation in intrinsically disordered proteins. Lessons from the sodium proton exchanger 1 (NHE1). *Cell Signal* 37: 40–51, 2017. doi:10.1016/j.celsig.2017.05.015.
- Hendus-Altenburger R, Vogensen J, Pedersen ES, Luchini A, Araya-Secchi R, Bendsoe AH, Prasad NS, Prestel A, Cardenas M, Pedraz-Cuesta E, Arleth L, Pedersen SF, Kragelund BB. The intracellular lipid-binding domain of human Na⁺/H⁺ exchanger 1 forms a lipid-protein co-structure essential for activity. *Commun Biol*. 2020 Dec 3;3(1):731. doi: 10.1038/s42003-020-01455-6. PMID: 33273619; PMCID: PMC7713384.
- Huc L, Tekpli X, Holme JA, Rissel M, Solhaug A, Gardyn C, Le Moigne G, Gorria M, Dimanche-Boitrel MT, Lagadic-Gossmann D. c-Jun NH2-terminal kinase-related Na⁺/H⁺ exchanger isoform 1 activation controls

hexokinase II expression in benzo(a)pyrene-induced apoptosis. *Cancer Res.* 2007 Feb 15;67(4):1696-705. doi: 10.1158/0008-5472.CAN-06-2327.

Ikeda T, Schmitt B, Pouysségur J, Wakabayashi S, Shigekawa M. Identification of cytoplasmic subdomains that control pH-sensing of the Na⁺/H⁺ exchanger (NHE1): pH-maintenance, ATP-sensitive, and flexible loop domains. *J Biochem* 121: 295–303, 1997. doi:10.1093/oxfordjournals.jbchem.a021586.

Kizhuveetil U, Palukuri MV, Sharma P, Karunagaran D, Rengaswamy R, Suraishkumar G K. Entrainment of superoxide rhythm by menadione in HCT116 colon cancer cells. *Sci Rep.* 2019 Mar 4;9(1):3347. doi: 10.1038/s41598-019-40017-7.

Lacroix J, Poët M, Huc L, Morello V, Djerbi N, Ragno M, Rissel M, Tekpli X, Gounon P, Lagadic-Gossmann D, Counillon L. Kinetic analysis of the regulation of the Na⁺/H⁺ exchanger NHE-1 by osmotic shocks. *Biochemistry.* 2008 Dec 23;47(51):13674-85. doi: 10.1021/bi801368n. PMID: 19035652.

Martin C, Pedersen SF, Schwab A, Stock C. Intracellular pH gradients in migrating cells. *Am J Physiol Cell Physiol.* 2011 Mar;300(3):C490-5. doi: 10.1152/ajpcell.00280.2010.

Rolver MG, Elingaard-Larsen LO, Andersen AP, Counillon L, Pedersen SF. Pyrazine ring-based Na⁺/H⁺ exchanger (NHE) inhibitors potently inhibit cancer cell growth in 3D culture, independent of NHE1. *Sci Rep.* 2020 Apr 2;10(1):5800. doi: 10.1038/s41598-020-62430-z.

Pedersen SF, Counillon L. The SLC9A-C Mammalian Na⁺/H⁺ Exchanger Family: Molecules, Mechanisms, and Physiology. *Physiol Rev.* 2019 Oct 1;99(4):2015-2113. doi: 10.1152/physrev.00028.2018. PMID: 31507243.

Poët M, Doyen D, Van Obberghen E, Jarretou G, Bouret Y, Counillon L. How Does Our Knowledge on the Na⁺/H⁺ Exchanger NHE1 Obtained by Biochemical and Molecular Analyses Keep up With Its Recent Structure Determination? *Front Physiol.* 2022 Jul 15;13:907587. doi: 10.3389/fphys.2022.907587.

Pouysségur J, Sardet C, Franchi A, L'Allemain G, Paris S. A specific mutation abolishing Na⁺/H⁺ antiport activity in hamster fibroblasts precludes growth at neutral and acidic pH. *Proc Natl Acad Sci USA* 81: 4833–4837, 1984. doi:10.1073/pnas.81.15.4833.

(Rasband, W.S., ImageJ, U. S. National Institutes of Health, Bethesda, Maryland, USA, <http://imagej.nih.gov/ij/>, 1997–2012)

Snabaitis AK, Hearse DJ, Avkiran M. Regulation of sarcolemmal Na⁽⁺⁾/H⁽⁺⁾ exchange by hydrogen peroxide in adult rat ventricular myocytes. *Cardiovasc Res.* 2002 Feb 1;53(2):470-80. doi: 10.1016/s0008-6363(01)00464-3. PMID: 11827698.

Wakabayashi S, Pang T, Su X, Shigekawa M. A novel topology model of the human Na⁽⁺⁾/H⁽⁺⁾ exchanger isoform 1. *J Biol Chem* 275: 7942–7949, 2000. doi:10.1074/jbc.275.11.7942.

Acknowledgements

We thank our colleagues Shigeo Wakabayashi (Osaka University Japan) and Stine Pedersen (Copenhagen University Denmark) for providing us with the pECE expression vector for the cysless mutant and the protocol for NHE1 Immunoprecipitation used in this work. This work was funded by the Centre National de la Recherche Scientifique (CNRS) and the University Côte d'Azur.

Legends to the Figures

Figure 1: Modulation of WT NHE-1 and cysless mutant activities by exposure to H₂O₂ (1 mM, 90 minutes). (A) Cells expressing wild type (WT) NHE-1 Rates of NHE-1 activity were determined by measuring cariporide-dependent Li⁺ intracellular concentration conducted with and without H₂O₂. Plots represent the % of the initial values against time. Data are representative of 6 independent experiments. Error bars are standard error of the mean.

(B-C) Cells expressing either WT NHE1 (B) or the cysless mutant (C) were acidified at different intracellular pH and the activity of NHE1 was measured after incubation with H₂O₂ for 30 minutes. Note that for both WT and mutant, H₂O₂ exposure activates NHE1 by increasing its response to intracellular acidification.

Figure 2: Modulation of WT NHE1 and the cysless mutant activities by O₂^{·-}.

(A) Rates of NHE-1 (empty symbols) and the Cysless mutant (dark symbols) were determined by measuring cariporide-dependent Li⁺ intracellular concentration conducted with and without 33 μM Menadione, a O₂^{·-} donor. Plots represent the % of the initial values against time. Data are representative of 6 independent experiments. Error bars are standard error of the mean.

(B-C) Cells expressing either WT NHE1 (B) or the cysless mutant (C) were acidified at different intracellular pH values and the activity of NHE1 was measured by initial rates of Lithium uptake in control conditions (empty symbols) or after incubation with 10 μM DPI (dark symbols) for 3 hours. The curves are the compilation of 10 independent experiments each.

Figure 3: Comparison of Cysteine-Alanine individual mutants

Cells expressing each individual cysteine mutant of NHE1 were acidified at different intracellular pH values and the activity of NHE1 was measured by initial rates of lithium uptake in control conditions (empty symbols) or after incubation with 10 μM DPI (dark symbols) for 3 hours.

Figure 4: Position of the different NHE1 cysteines in the NHE1 three-dimensional structure generated using Pymol (7dsv pdb file). The two protomers of the symmetrical dimer are respectively represented in pink and red and the cysteines are indicated only on one protomer for simplicity. Note that cysteines 464 and 794 are not represented on this figure as this region is not resolved in the present structure. The arrows represent the two cysteines whose mutation in alanine results in a loss of inhibition by DPI.

Figure 5 NHE1 Covalent Modification of cysteines

- (A) Non-reducing SDS Page of WT NHE1 and the Cysless mutant incubated with 0, 10 and 50 μ M of Iodoacetamide.
- (B) Representative Western Blot. Top panel: S-Nitrosylation detection on WT NHE1; the cysless mutant and all individual cysteine mutants. Bottom panel: Loading control. Note the absence of immunodetection on the top panel for the C421A mutant.
- (C) Quantification of the Western Blots (n=4) of the S-Nitrosylation detection.
- (D) Representative western blot for S-Glutathionylation detection, using a Protein-S Glutathionylation antibody. WT NHE1 and the cysless mutant were immunoprecipitated, ran on non-reducing SDS PAGE and transferred to Nylon before western blotting. Note the absence of immunodetection in the Anti-GSS-P lanes despite the positive signals in the Anti-NHE1 loading control.

Figure 6: Comparison of the WT NHE1 and Cysless mutant shape and mobility

- (A) Representative photographs of wound healing experiments performed on fibroblasts expressing either the WT NHE1, no Na^+/H^+ exchanger (PS120 cell line); or the Cysless mutant. The corresponding complete movies are shown in supplementary materials.
- (B) Quantification of the Wound Healing Experiments

Figure 7: Immunofluorescence experiments

- (A) Representative images immunofluorescence staining of fibronectin deposition (green) by WT NHE1 and the Cysless mutant (top panels) and actin labeling (red; bottom panels). Note the absence of significant differences.
- (B) Fibronectin deposition quantification for WT NHE1 and the Cysless mutant. Note the absence of significant differences.
- (C) Representative images of immunofluorescence vinculin staining for WT NHE1; NHE deficient and Cysless mutant expressing fibroblasts. Note the absence of significant differences.

Figure 8: WT NHE1 and Cysless Mutant ERM coimmunoprecipitation

- (A) Representative Western Blot showing that the ERM complex that coimmunoprecipitates with WT NHE1 does not co-immunoprecipitate with the Cysless mutant and to variable extents with the individual cysteine mutants. Top panel: Loading control of NHE1 immunoprecipitation

(Merck Antibody) revealed with an Anti-NHE1 antibody (BD Biosciences). Bottom panel: ERM complex detection (Cell Signaling antibody)

(B) Quantification on four independent coimmunoprecipitation experiments.

Figures

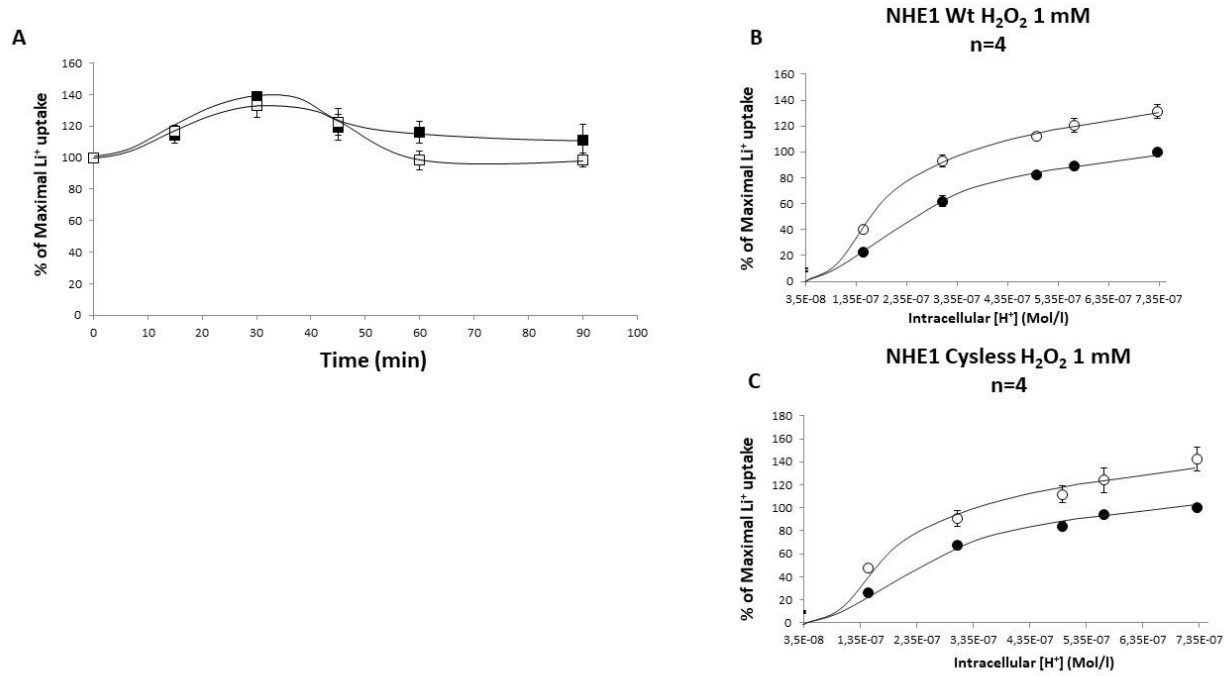


FIGURE1

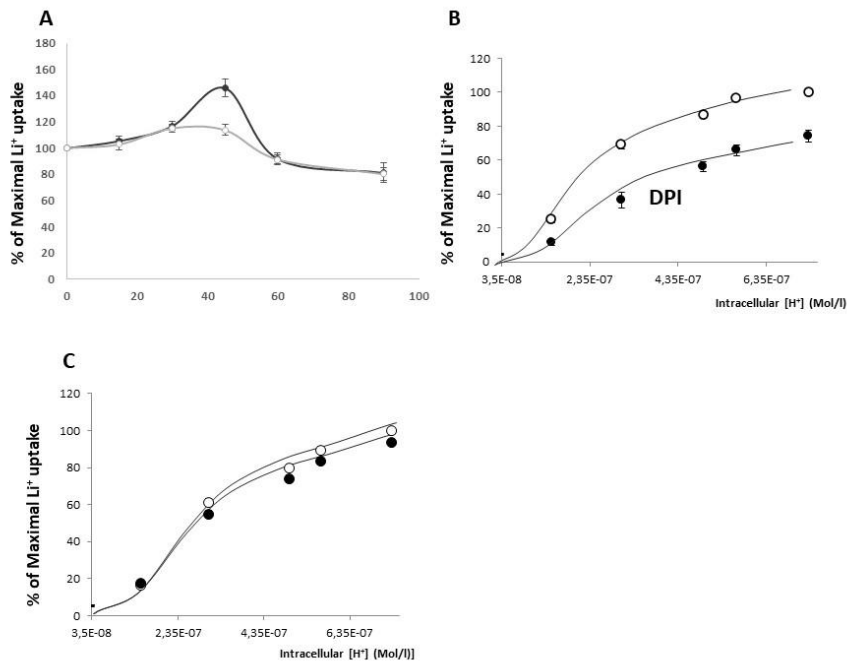


FIGURE2

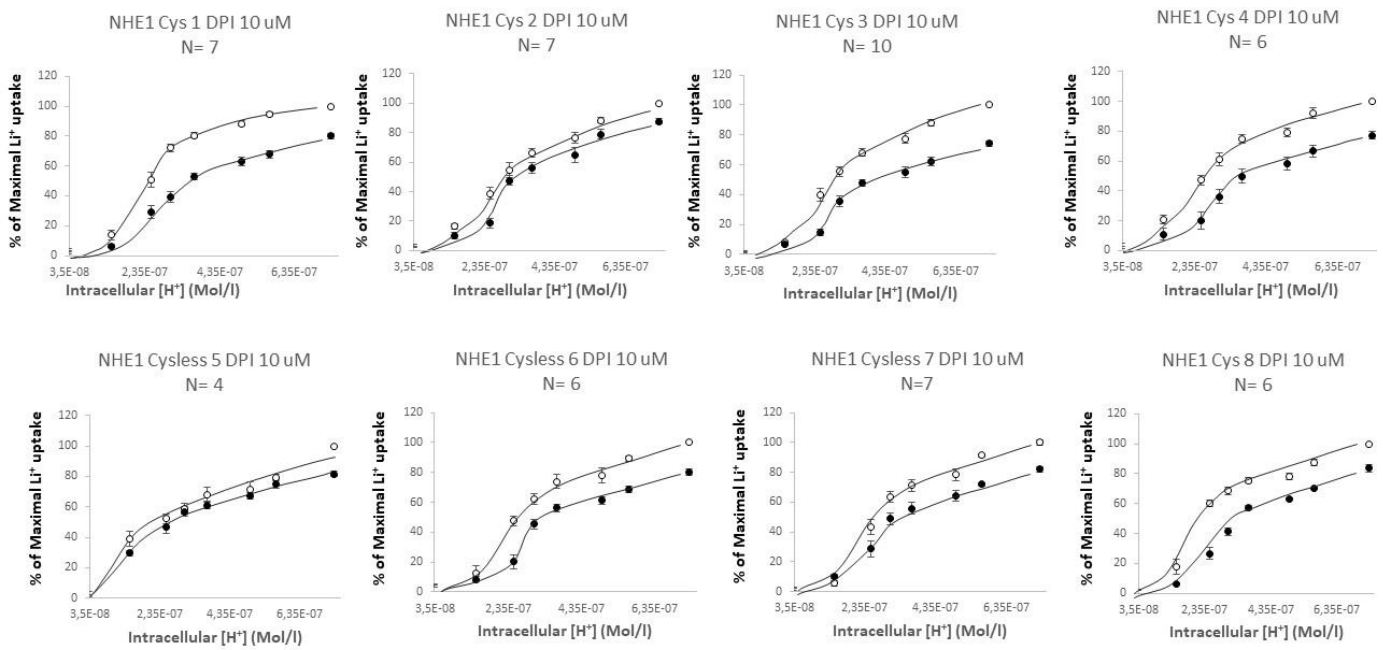


FIGURE 3

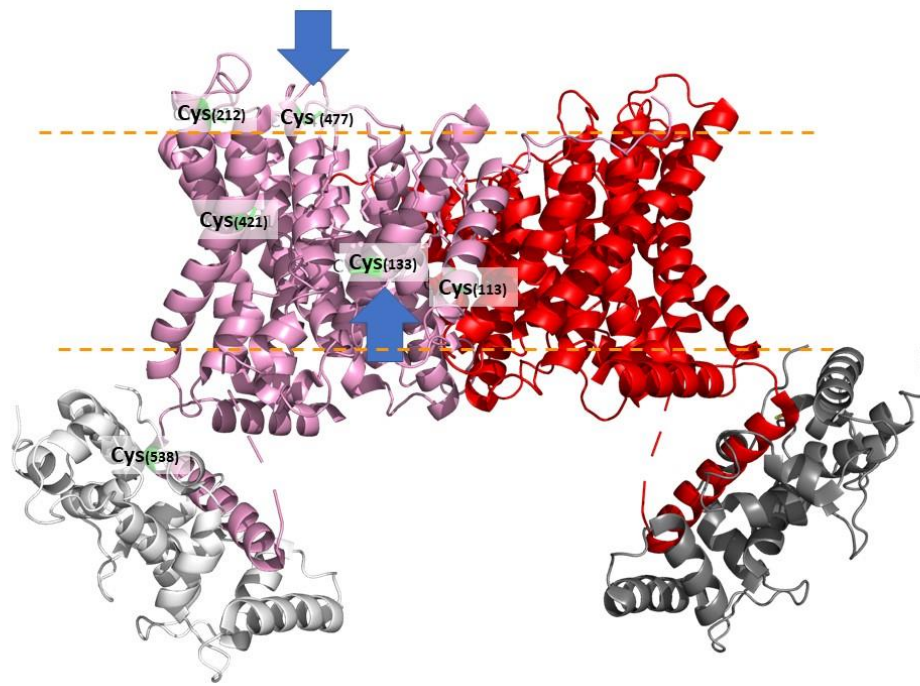


FIGURE 4

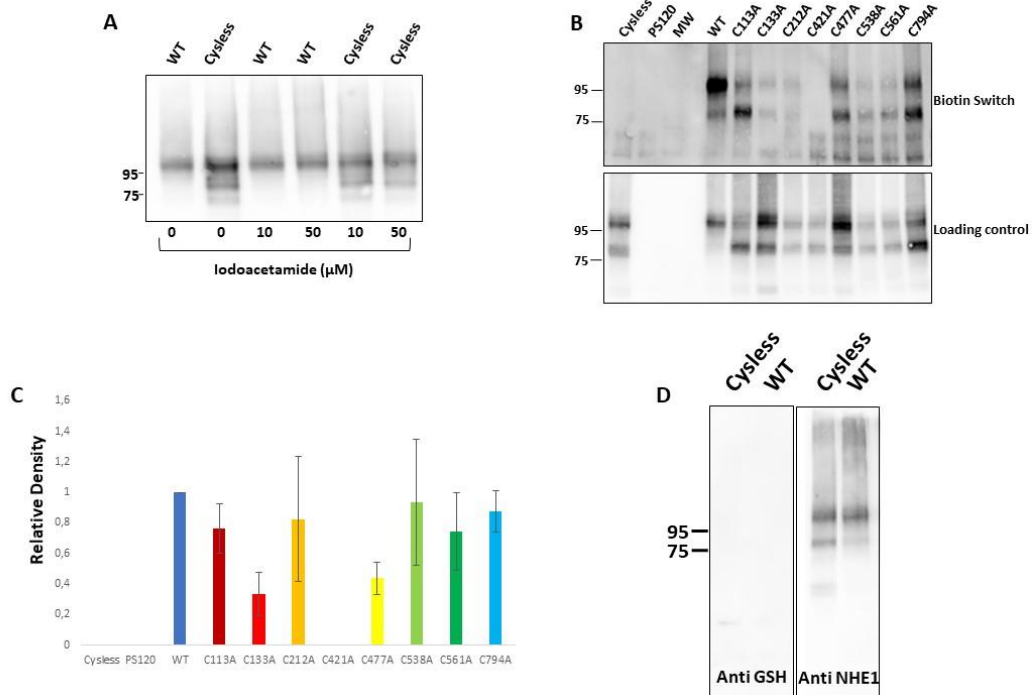


FIGURE 5

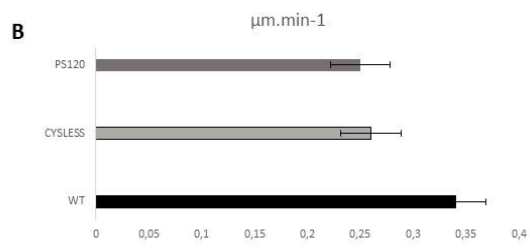
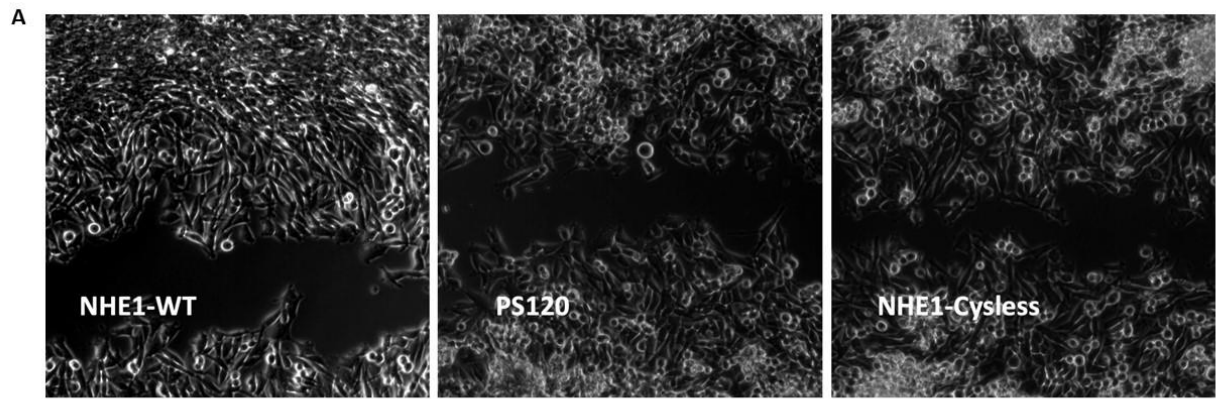


FIGURE 6

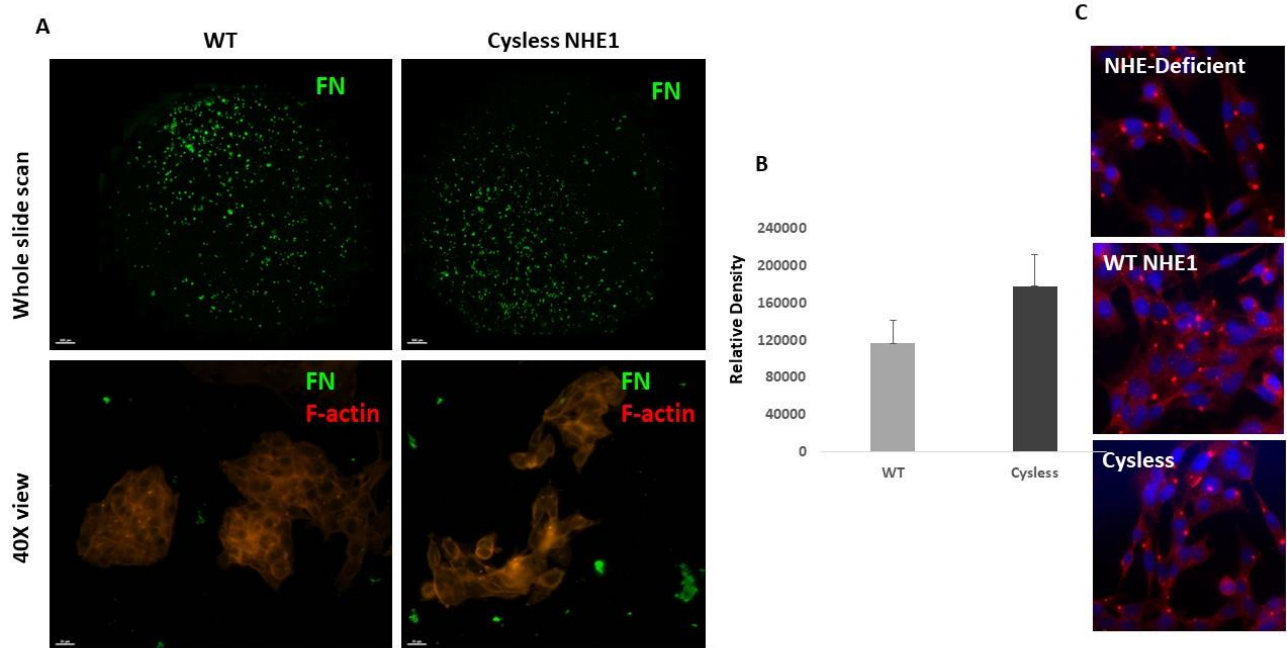


FIGURE 7

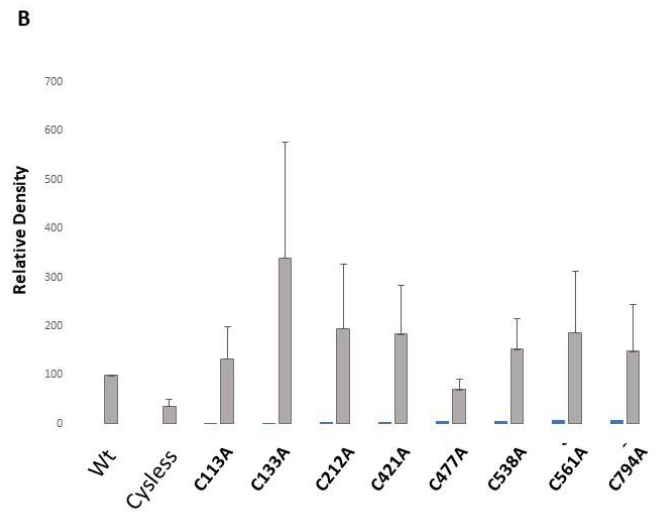
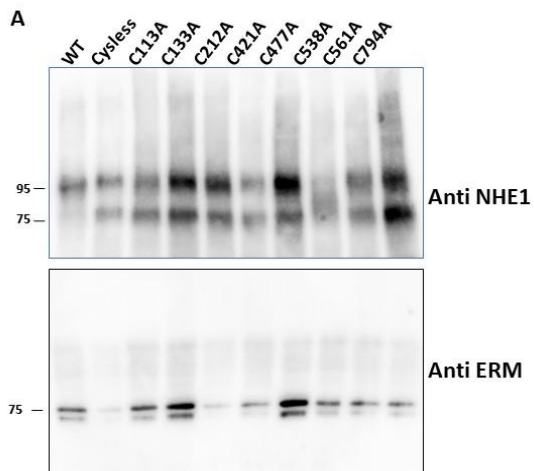
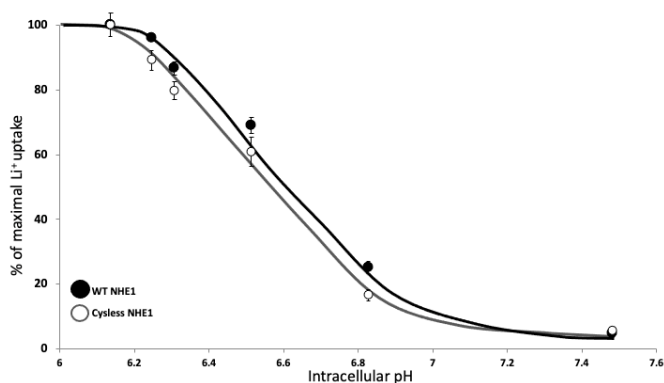


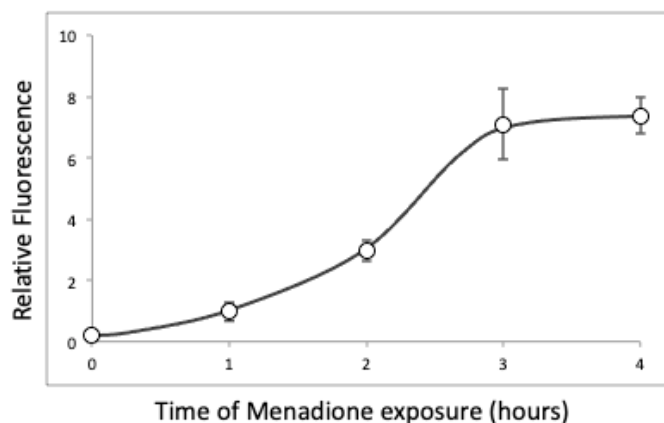
FIGURE 8

Supplementary Information

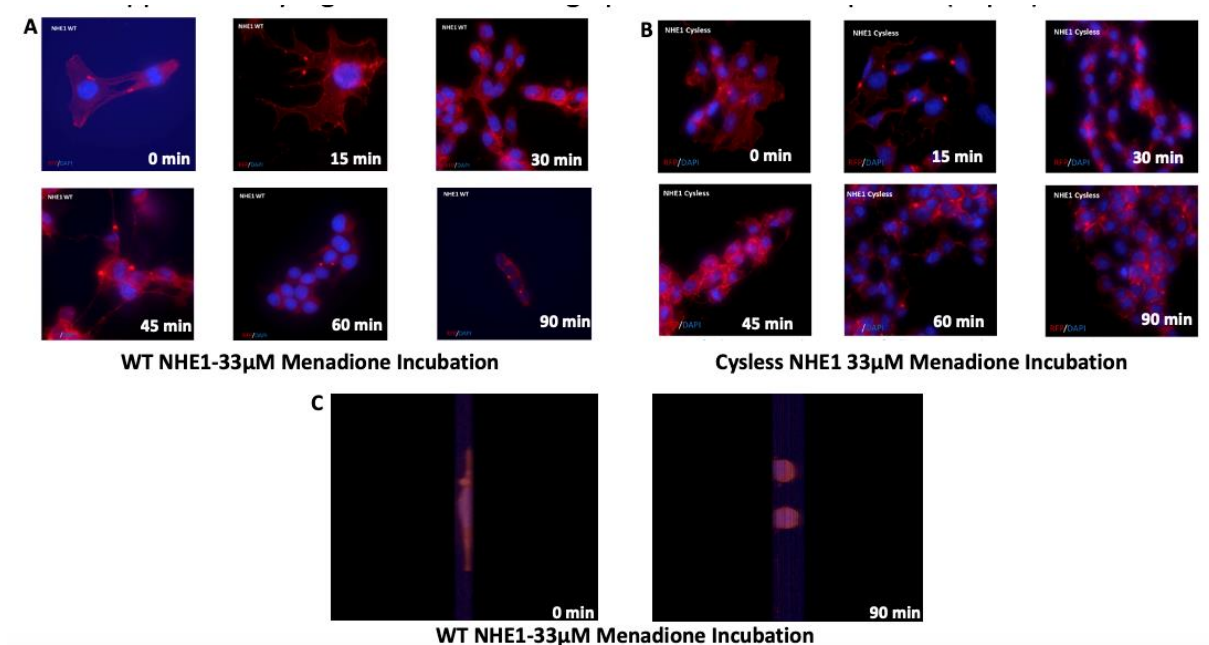
Supplementary Figure 1: Comparison of the WT NHE1 and Cysless mutant cooperative response to intracellular pH by measure by initial rates of Lithium uptake in cells acidified at different pH values (see materials and methods). Note that the two curves are totally identical showing that replacing the cysteines by alanines in the mutant does not affect its allosteric regulation.



Supplementary Figure 2: Quantification of Menadione oxidant effect



Supplementary Figure 3: Effect of menadione exposure on cell morphology: NHE-deficient fibroblast transfected with either the WT NHE1 or the corresponding Cysless mutant were exposed to 33 μ M menadione for different durations. Cells were then fixed at the indicated times and stained for immunofluorescence with RFP-phalloidin and DAPI. **A and B** Images were taken with a Zeiss microscope with a 63x immersion objective. **C** Z-stack reconstitution of cells expressing WT-NHE1 exposed to 33 μ M menadione at 0 and 90 minutes. Images were taken every 0.26 μ M using confocal microscopy.



Supplementary Figure 4: Cysteine conservation in NHEs sequences

The human NHE1 sequence was used to perform multiple alignments with the NHE2 to NHE9 isoforms. NHE1 cysteines are labeled in red as the conserved cysteines in other NHEs. The residues differing from NHE1 cysteines in the aligned other isoforms are labelled in green.

Score:680 bits (1754), Expect:0.0,
Method:Compositional matrix adjust.,
Identities:362/747(48%), Positives:493/747(65%), Gaps:51/747(6%)

```

Query  90  PVLGIDYTHVRTPFEISLWILLACLMKIGFHVIPITISSIVPESCLLIIVVGLLVGGLIKGV 149
Sbjct  69  PVFTLDYDPHVQIPFEITLWILLASLAKIGFHLHYHKLPTIVPESCLLIMVGLLLGGIIFGV 128

Query  150  GE-TPPFLQSDVFFLFLPPPIILDAGYFLPLRQFTENLGTILIFAVVGTLWNAFFLGGML 208
Sbjct  129  DEKSPPMAMKTDVFFLYLLPPIVLDAGYFMPTRPFFENeIGTIFWYAVVGTLWNSIGIGVSL 188

Query  209  YAVCLVGGEQINNIGLLDNLLFGSIIISAVDPVAVLAVFEEIHINELLHILVFGESLLNDA 268
Sbjct  189  FGIcQIEAFGLSDITLLQNLLFGSLISAVDPVAVLAVFENIHVNEQLYLILVFGESLLNDA 248

Query  269  VTVVLYHLFEFANYEHVGIVDIFLGFSLFFVVALGGVVLGVVYGVIAAFTSRFTSHIRV 328
Sbjct  249  VTVVLYNLFKSFCQMKTIETIDVFAGIANFFVVGIGGVLIGIFLGFIAAFTTRFTHNIRV 308

Query  329  IEPLFVFLYSYMAVLSAELFHLSGIMALIASGVVMPYPVEANISHKSHTTIKYFLKMWSS 388
Sbjct  309  IEPLFVFLYSYLSYITAEMFHLSGIMAITACAMTMNKYVEENVSQKSYTTIKYFMKMLSS 368

Query  389  VSETLIFIFLGVSTVAGSHHWNWTFVISTLLFCLIARVLGVGLTWFINKFRIVKLTPKD 448
Sbjct  369  VSETLIFIFMGVSTVGVKNHEWNWAFVCFTLAFcLMWRALGVFVLTQVINRFRTIPLTFKD 428

Query  449  QFIIAYGGLRGAIAFSLGYLLDKKHFPMCDLFLTAIITVIFFTVFVQGMTIRPLVDLLAV 508
Sbjct  429  QFIIAYGGLRGAICFALVFLPAAVFPRKkLFITAAIVVIFFTVFILGITIRPLVEFLDV 488

Query  509  KKKQETKRSINEEIHQFLDHLTGIEDIcGHYGHWWKDKLNRFNKKYVKKCLIAGERS 568
Sbjct  489  KRSNKKQAVSEEIYCRLFDHVKTGIEDVcGHWGHNFWRDKFKKFDKYLKLLIR-ENQ 547

Query  569  KEPQLIAFYHKMEMKQAIELVESGGMGKIPSAVSTVSMQNIHPKSLPSEIRILPALSKDKE 628
Sbjct  548  PKSSIVSLYKLEIKHAIEMAETGMISTVPTFASLNDCR-----EEKIRKVTSSSET 598

Query  629  EEIRKILRNQLKTRQRLRSYNRHTLVADPYEEAWNQMLLRQ-----KAR 674
Sbjct  599  DEIRELLSRNLQIRQRTL SYNRSLSLTADT SERQAKEILIRRRHSLRESIRKDSSSLNREH 658

Query  675  QLEQKINNYLTPAH-KLDSPTMSRARIG-SDPLAYEPKED--LPVITIDPA----- 722
Sbjct  659  RASTSTSRYSLSLPKNTKLEPKLQKRRTISIADGNSSDSDADAGTTVLNLQPRARRFLPEQ 718

Query  723  -SPQSPESVDLVNEELKGV-LGLSRD-----PAKVAEEDDDGGIMMR---SKETSSP 772
Sbjct  719  FSKKSPQSYKM---EWKNEVDVDSGRDMPSTPPTPHSREKGTQTSGLLQQPLLSKDQSGS 775

```

Query 773 GTDDVFTPAPSDSPSSQRIQRCLSDPG 799
Sbjct 776 EREDSLTEGIPPKPPRLVWRA-SEPG 801

>NP_004165.2 sodium/hydrogen exchanger 3 isoform 1 [Homo sapiens]

Sequence ID: Query_60993 Length: 834
Range 1: 41 to 779

Score:489 bits (1258), Expect:3e-164,
Method:Compositional matrix adjust.,
Identities:306/758(40%), Positives:454/758(59%), Gaps:58/758(7%)

Query 88 AFPVLGIDYTHVRTPFPEISLWILLACLMKIGFHVPTISSIVPESCLLIVVGLLVGGLIK 147
Sbjct 41 GFQVVTFEWAHVQDPYVIALWILVASLAKIGFHLSHKVTSVVPESALLIVLGLVLGGIVW 100

Query 148 GVGETPPF-LQSDVFFLFLPPIILDAGYFLPLRQFTENLGTILIFAVVGTLWNAFFLGG 206
Sbjct 101 AADHIASFTLTPTVFFVFLPPIVLDAGYFMPNRLFFGNLGTILLYAVVGTWNAATTGL 160

Query 207 LMYAVCLVGGEQINNIGLLDNLLFGSIISAVDPVAVLAVFEEIHINELLHILVFGESLLN 266
Sbjct 161 SLYGVFLSGLMGDLQIGLLDFLLFGSLMAAVDPVAVLAVFEEVHVNEVLFIIIVFGESLLN 220

Query 267 DAVTVVLYHLFEFANY--EHVGIVDIFLGFSLFFVVALGGVVLGVVYGVIAAFTSRFTS 324
Sbjct 221 DAVTVVLYNVFESFVALGGDNVTGVDCVKGIVSFFVSLGGTLGVVFAFLLSLVTRFTK 280

Query 325 HIRVIEPLFVFLYSYMAVLSAELFHLGIMALIASGVVMRPYVEANISHKSHTTIKYFLK 384
Sbjct 281 HVRIIEPGFVFIISYLSYLTSEMLSLSAILAITFCGICCKYVKANISEQSATTVRYTMK 340

Query 385 MWSSVSETLIFIFLGVSTVAGS-HHWNWTFVISTLLFCCLIARVLGVGLTWFINKFRIVK 443
Sbjct 341 MLASSAETIIFMFLGISAVNPFITWNTAFVLLTLVFIISVYRAIGVVLQTWLLNRYRMVQ 400

Query 444 LTPKDQFIIAYGGLRGAIASFSLGYLLDKKHFFMCDLFLTAITVIFFTVFVQGMTIRPLV 503
Sbjct 401 LEPIDQVVLSYGGLRGAVAFALVLLDGDVKVKEKNLNFVSTIIIVFFTVIFQGLTIKPLV 460

Query 504 DLLAVKKKQETKRSINEEIHQFLDHLTGIEDIQGHYGHHHWKDKLNRFNKKYVKKCLLI 563
Sbjct 461 QWLKVKRSEHREPLRNEKLGRAFHDHLSAIEDISGQIGHNYLRDKWSHFDRKFLSRVLM 520

Query 564 --AGERSKEPQLIAFYHKMEMKQAIELVESG-----GMGKIPSAVSTVSMQNIHPKSLP 615
Sbjct 521 RRSAQKSRD-RILNVFHELNLKDAISYVAEGERRGLAFIRSPSTDNVVNV-DFTPRSST 578

Query 616 SERILPALSCKD-----EEEIRKI-----LRNNLQKTRQRLRS-YNRH 652
Sbjct 579 VEASVSYLLRENVSAVCLDMQSLEQRRRSIRDAEDMVTHHTLQQYLYKPRQEYKHLYSRH 638

Query 653 TLVADPYEEAWNQMLLRQKARQLEQKINNYLTVPAHKLDSPTMSRARIIGSDPLAYEPKE 712
Sbjct 639 ELTPTE-DEKQDREIFHRTMRKRLESFKSTKLGLNQNKKAALKYKRERAQKRRNSIPNG 697

Query 713 DLPVITIDPASPQSPESVDLVNEELKGVGLSRDPAKVAEEDDDGGIMMRSKETSSP 772
Sbjct 698 KLPM-----ESPAQ---NFTIKEKDLELS-DTEEPNYDEEMSGGIEFLASVTKDT 744

Query 773 GTDDVFTPAPSD---SPSSQRIQRCLSDPGPHPEPGE 806
Sbjct 745 ASD---SPAGIDNPFVSPDEALDRSLLARLPPWLSPEGE 779

>EAX01790.1 solute carrier family 9 (sodium/hydrogen exchanger), member 4 [Homo sapiens]

Sequence ID: Query_60994 Length: 722
Range 1: 52 to 648

Score:565 bits(1455), Expect:0.0,
Method:Compositional matrix adjust.,
Identities:290/608(48%), Positives:403/608(66%), Gaps:30/608(4%)

Query 84 KPRKAFPVLGIDYTHVRTPFPEISLWILLACLMKIGFHVPTISSIVPESCLLIVVGLLVG 143
Sbjct 52 EPEEGISVFEVDYDYVQIPYEVTLWILLASLAKIGFHLHRLPGLMPESCLLILVGLV 111

Query 144 GLIKGVG-ETPPFLQSDVFFLFLPPIILDAGYFLPLRQFTENLGTILIFAVVGTLWNAF 202
Sbjct 112 GIIFGTDHKSPPVMDSSIIYFLYLLPPIVLEGGYFMPTRPFFENIGSILWWAVL GALINAL 171

Query 203 FLGGLMYAVCLVGGEQINNIGLLDNLLFGSIISAVDPVAVLAVFEEIHINELLHILVFG 262
Sbjct 172 GIGLSLYLICQVKAFGLGDVNLLQNLLFGSLISAVDPVAVLAVFEEARVNEQLYMMIFGE 231

Query 263 SLLNDAVTVVLYHL---FEFANYEHVGIVDIFLGFSLFFVVALGGVVLGVVYGVIAAFT 319
Sbjct 232 ALLNDGITVLYNMLIAFTKMKHFEDIETVDILAGCARFIVVGLGGVLFVGFISAFI 291

Query 320 SRFTSHIRVIEPLFVFLYSYMAVLSAELFHLGIMALIASGVVMRPYVEANISHKSHTTI 379
Sbjct 292 TRFTQNISAIEPLIVFMFSYLSYLAETLYLSGILAITACAVTMKKYVEENVSQTSYTTI 351

Query 380 KYFLKMWSSVSETLIFIFLGVSTVAGSHHWNWTFVISTLLFCCLIARVLGVGLTWFINKF 439
Sbjct 352 KYFMKMLSSVSETLIFIFMGVSTVGNHEWNWAFICFTLAFQCIWRAISVFALFYISNQF 411

Query 440 RIVKLTpkdqfiiaygglrgaiafslgylldkhhfpmCDLFLTAITVIFFTVFVQGMTI 499
 Sbjct 412 RTFFFSIKDQCIIIFYSGVRGAGSFSLAFLFLSLFPRKkMFVTATLVVIYFTVFIQGITV 471

Query 500 RPLVDLLAVKKKQETKRSINEEIH-----QFLDHLITGIEDICGHYGH 544
 Sbjct 472 GPLVRYLDVKKTKN-KESINEELHIRSSRFSSNHFLVFWVQLMDHLKAGIEDVCGHWSHY 530

Query 545 HWKDKLNRFNKKYVKKCLiAGERSKEPQLIAFYHKMEMKQAIELVESGGMGKIPSAVSTV 604
 Sbjct 531 QVRDKFKKFDHRYLRKILIRKNLPKS-SIVSLYKKLEMKQAIEMVETGILSSTAFSI--- 586

Query 605 SMQNIHPKSLPSERILPALSKDKEEIRKILRNNLQKTRQRLRSYNRHTLVADPYEEAWN 664
 Sbjct 587 -----PHQAQRIQGIKRLSPEDVESIRDILTSNMYQVRQRTLSYNKYNLKPQTSEKQAK 640

Query 665 QMLLRRQK 672
 Sbjct 641 EILIRRN 648

>AAI42672.1 Solute carrier family 9 (sodium/hydrogen exchanger), member 5 [Homo sapiens]
 Sequence ID: Query_60995 Length: 896
 Range 1: 40 to 646

Score:462 bits(1190), Expect:1e-153,
 Method:Compositional matrix adjust.,
 Identities:269/609(44%), Positives:393/609(64%), Gaps:28/609(4%)

Query 95 DYTHVRTPFEISLWILLACLMKIGFHVIPITISSIVPESCLLIVVGLLVGGLIKGVETPP 154
 Sbjct 40 QWHEVEAPYLVALWILVASLAKIVFHLSRKVTSLVPESCLLILLGLVGGIVLAVAKKAE 99

Query 155 F-LQSDVFFLFLLPPIILDAGYFLPLRQFTENLGTILIFAVVGTLWNAFFLGGMLYAVCL 213
 Sbjct 100 YQLEPGTFFLFLLPPIVLDSGYFMP SRLFFDNLGAILTYAVVGTLWNAFTTGAALWGLQQ 159

Query 214 VG--GEQINNIGLLDNLLFGSIIISAVDPVAVLAVFEEIHINELLHILVFGESLLNDAVTV 271
 Sbjct 160 AGLVAPRVQ-AGLLDFLLFGSLISAVDPVAVLAVFEEVHVNETLFIIVFGESLLNDAVTV 218

Query 272 VLYHLFEFANY--EHVGIVDIFLGLSFFVVALGGVVLGVVYGVIAAFTSRFTSHIRVI 329
 Sbjct 219 VLYKVCNSFVEMGSANVQATDYLKGVASLFFVSLGGAAGLVFAFLALTRFTKRVRII 278

Query 330 EPLFVFLYSYMAYLSAELFHLSGIMALIASGVVMPYVEANISHKSHTTIKYFLKMWSSV 389
 Sbjct 279 EPLLVFLLYAAYLTAEMASLSAILAVTMCGLGCKKYVEANISHKSRTTVKYTMKTLASC 338

Query 390 SETLIFIFLGVSTVAGSHHWNWT--FVISTLLFCLiARVLGVLGLTWFINKFRIVKLTpk 447
 Sbjct 339 AETVIFMLLGISAVDSSK-WAWDSGLVLGTLIFILFFRALGVVLQTVWVNLQFRLVPLDKI 397

Query 448 DQFIIAYGGLRGAIAFSLGylldkhhfpmCDLFLTAITVIFFTVFVQGMTIRPLVDLLA 507
 Sbjct 398 DQVMSYGGLRGAVAFALVILLDRTKVPAKdYFVATTIVVVFVTVIVQGLTIKPLVKWLK 457

Query 508 VKKKQETKRSINEEIHITQFLDHLITGIEDICGHYGHHWKDKLNRFNKKYVKKCLiAGER 567
 Sbjct 458 VKRSEHHKPTLNQELHEHTFDHILAAVEDVVGHHGYHYWRDRWEQDKKYSQLLMRrsa 517

Query 568 SK-EPQLIAFYHKMEMKQAIELVESGG-----MGKIPS--AVSTVSMQNIHPKS-- 613
 Sbjct 518 YRIRDQIWDVYIYRLNIRDAISFVDQGGHVLSSSTGLTLPSMPSRNSVAETSVTNLLRESGS 577

Query 614 ---LPSERILPALS-KDKEEIRKILRNNLQKTRQRLRSYNRHTLVADPYEEAWNQMLL 668
 Sbjct 578 GACLDLQVIDTVRSGRDREDAVMHLLCGGLYKPRRRYKASCSRHFISED AQERQDKEVF 637

Query 669 RRQKARQLE 677
 Sbjct 638 QQNMKRRLE 646

>AAH35029.1 (a, 701 aa) Solute carrier family 9 (sodium/hydrogen exchanger), member 6 [Homo sapiens]
 Sequence ID: Query_60996 Length: 701
 Range 1: 181 to 539

Score:187 bits(476), Expect:2e-53,
 Method:Compositional matrix adjust.,
 Identities:122/370(33%), Positives:198/370(53%), Gaps:30/370(8%)

Query 159 DVFFLELLPPIILDAGYFLPLRQFTENLGTILIFAVVGTLWNAFFLGGMLYAVCL---VG 215
 Sbjct 181 EVFVNILLPPIIFYAGYSLKRRHFFRNLSILAYAF LGTAISCFVIGSIMYGVTLMKVT 240

Query 216 GEQINNIGLLDNLLFGSIIISAVDPVAVLAVFEEIHINELLHILVFGESLLNDAVTVVL-- 273
 Sbjct 241 GQLAGDFYFTDCLLFGAIVSATDPVTVLAIFHELQVDVELYALLFGESVLDNAVAIVLSS 300

Query 274 -----YHLFEFANYEHVGIVDIFLGLSFFVVALGGVVLGVVYGVIAAFTSRF 322
 Sbjct 301 SIVAYQPAGDNSHTFDVTAMFKSIG---IFLGI FS-----GSFAMGAATGVV TALVTKF 351

Query 323 TS--HIRVIEPLFVFLYSYMAYLSAELFHLSGIMALIASGVVMPYVEANISHKSHTTIK 380

Sbjct 352 TKLREFQLLETGLFFLMSWSTFLLAEAWGFTGVVAVLFCGITQAHYTYNNLSTESQHRTK 411

Query 381 YFLKMWSSVSETLIFIFLGVSTVAGSHH-WNWTFFVISTLLFCLLIARVLGVLGLTWFINKF 439

Sbjct 412 QLFELLNFLAENFIFSVMGLTLFTFQNHVFNPTFVVGAFVAIFLGRAANIYPLSLLNLG 471

Query 440 RIVKLTTPKDQFIIAYGGLRGAIASFSLGYLLDKKHFFPMDLFLTAIITVIFFTVFVQGMTI 499

Sbjct 472 RRSKIGSNFQHMMFAGLRGAMAFALA-IRDTATYARQMMFSTLL-IVFFTVMVFGGGT 529

Query 500 RPLVDLLAVK 509

Sbjct 530 TAMLSCLHIR 539

>NP_001244220.1 sodium/hydrogen exchanger 7 isoform 1 precursor [Homo sapiens]
Sequence ID: Query_60997 Length: 726
Range 1: 181 to 558

Score:188 bits(477), Expect:2e-53,
Method:Compositional matrix adjust.,
Identities:129/389(33%), Positives:204/389(52%), Gaps:31/389(7%)

Query 159 DVFFFLFLLPPIILDAGYFLPLRQFTENLGTILIFAVVGTLWNAFFLGGMLYAVCL---VG 215

Sbjct 181 EVFFNILLPPIIFHAGYSLKRRHFFRNLSILAYAFVLTAVSCFTIGNLMYGVVKLMKIM 240

Query 216 GEQINNIGLLDNLLFGSII SAVDPVAVLAVFEEIHINELLHILVFGESLLNDAVTVVL-- 273

Sbjct 241 GQLSDKFYTYDCLFFGAIISATDPVTVLAI FNELHADVDLYALLFGESVLNDAVAIVLSS 300

Query 274 -----YHLFEFANYEHVGI VDFLGLSFFVVALGGVLVGVVYGVIAAFTSRF 322

Sbjct 301 SIVAYQPAGLNTHAFDAAAFFKSVG---IFLGIFS-----GSFTMGAVTGVVVALVTKF 351

Query 323 TS--HIRVIEPLFVFLYSYMAYLSAELFHLSGIMALIASGVVMPYVEANISHKSHTTIK 380

Sbjct 352 TKLHCFPLELETALFFLMSWSTFLLAEACGFTGVVAVLFCGITQAHYTYNNLSVESRSRTK 411

Query 381 YFLKMWSSVSETLIFIFLGVSTVAGSHH-WNWTFFVISTLLFCLLIARVLGVLGLTWFINKF 439

Sbjct 412 QLFVFLHLAENFIFSVMGLALFTFQKHVFSPIFIIGAFVAIFLGRAAHYPLSFFLNLG 471

Query 440 RIVKLTTPKDQFIIAYGGLRGAIASFSLGYLLDKKHFFPMDLFLTAIITVIFFTVFVQGMTI 499

Sbjct 472 RRHKIGWNFQHMMFSGLRGAMAFALA-IRDTASYARQMMFTTLL-IVFFTVMVIGGGT 529

Query 500 RPLVDLLAVK-KKQETKRSINEEIHQTQFL 527

Sbjct 530 TPMLSWLNIRVGVVEEPSEEDQNEHHWQYF 558

>NP_001247420.1 sodium/hydrogen exchanger 8 isoform 1 [Homo sapiens]
Sequence ID: Query_60998 Length: 597
Range 1: 65 to 501

Score:218 bits(555), Expect:8e-65,
Method:Compositional matrix adjust.,
Identities:144/441(33%), Positives:245/441(55%), Gaps:33/441(7%)

Query 106 SLWILLAELMKIGFHVPIPTISSIVPESCLLIVVGLLVGGLIKGV-----GETPPFLQS 158

Sbjct 65 SLLVLAICIIILVHL-LIRYRLHFLPESVAVVSLGILMGAVIKIIEFKKLANWKEEMFRP 123

Query 159 DVFFFLFLLPPIILDAGYFLPLRQFTENLGTILIFAVVGTLWNAFFLGGMLY----- 209

Sbjct 124 NMFLLLLPPIIFESGYSLHKGNFQNIQSITLFAVFGTAISAFVVGGGIYFLGQGFVV 183

Query 210 ----AVCLVVGGEQINNIGLLDNLLFGSII SAVDPVAVLAVFEEIHINELLHILVFGESL 264

Sbjct 184 CVCVFVCFILQADVISKLNMTDSFAFGSLISAVDPVATIAIFNALHVDVPLNMLVFGESI 243

Query 265 LNDAVTVVLYHLFEEFA--NYEHVGI VDFLGLSFFV-VALGGVLVGVVYGVIAAFTSR 321

Sbjct 244 LNDAVSIVLTNTAEGLTRKNMSDVSQWTFQLQALDYFLKMFSGAALGTLTGLISALVLK 303

Query 322 FTSHIRV-----IEPLFVFLYSYMAYLSAELFHLSGIMALIASGVVMPYVEANISHKSH 376

Sbjct 304 ---HIDLRKTPSLEBFGMMIIFAYLPYGLAEGISLSGIMALIFSGIVMSHYTHHNLSPVTQ 360

Query 377 TTIKYFLKMWSSVSETLIFIFLGVSTVAGSHHWNWTFFVISTLLFCLLIARVLGVLGLTWF 436

Sbjct 361 ILMQQLTRTVAFVLCETCVFAFLGLSIFSFPHKFEISFVIWCIVLVLFGRAVNIPLSYLL 420

Query 437 NKFRIVKLTTPKDQFIIAYGGLRGAIASFSLGYLLDKKHFFPMDLFLTAIITVIFFTVFVQ 496

Sbjct 421 NFFRDHKITPKMMFIMWFSGLRGAIYPALSLHLDLEPMEKRLQIGTTTTIVIVLFTILLG 480

Query 497 MTIRPLVDLLAVKKKQETKRS 517

Sbjct 481 GSTMPLIRLMDIEDAKAHRRN 501

>BAD69592.1 sodium/proton exchanger NHE9 [Homo sapiens]

Sequence ID: Query_60999 Length: 645

Range 1: 132 to 506

Score:192 bits(487), Expect:3e-55,

Method:Compositional matrix adjust.,

Identities:125/377(33%), Positives:206/377(54%), Gaps:12/377(3%)

```
Query 159 DVFFLELLPPIILDAGYFLPLRQFTENLGTILIFAVVGTLWNAFFLGGLMYAV--C LVGG 216
Sbjct 132 EIFFNVLPPPIIFHAGYSLKRRHFFQNLGSILTYAFLGTAISCIIVIGLIMYGFVKAMIHA 191

Query 217 EQINN--IGLLDNLLFGSIIISAVDPVAVLAVFEEIHINELLHILVFGESLLNDAVTVVLY 274
Sbjct 192 GQLKNGDFHFTDCLFFGSLMSATDPVTVLAIHFHELHVDPDLYTLLFGESVLNDAVAIVLT 251

Query 275 HLFEEFANYEHVGIVDIFLGFLS---FFVVALGGVLVGVVYGVIAAFTSRFT--SHIRVI 329
Sbjct 252 YSISIYSPKENPNFAFAAFFQSVGNFLGIFAGSFAMGSAYAIITALLTKFTKLCEFPML 311

Query 330 EPLFVFLYSYMAYLSAELFHLSGIMALIASGVVMRPYVEANISHKSHTTIKYFLKMWSSV 389
Sbjct 312 ETGLFFLLSWSAFLSAEAAGLTGIVAVLFCGVTQAHYTYNNLSSDSKIRTKQLFEFNMFL 371

Query 390 SETLIFIFLVSTVAGSHH-WNWT FVISTLLFC LIARVLGVLGLTWFINKFRIVKLT PKD 448
Sbjct 372 AENVIFCYMGLALFTFQNHIFNALFILGAFLAIFVARACNIYPLSFLNLGRKQKIPWNF 431

Query 449 QFIIAYGGLRGAIASFSLGYLLDKKHFPMDLFLTAIITVIFFTVVFQGMTIRPLVDLLAV 508
Sbjct 432 QHMMMFSGLRGAIAFALA-IRNTESQPKQMMFTTLL-LVFFTVVWVFGGTPMLTWLQI 489

Query 509 KKKQETKRSINEEIHQT 525
Sbjct 490 RVGVLDLLENLKEDPSSQ 506
```

Supplementary Movies: wound healing experiments were performed for NHE deficient fibroblasts of fibroblasts stably expressing WT NHE1 or Cysless NHE1. Representative movies can be downloaded at:

WT NHE1 wound healing movie

<https://filesender.renater.fr/?s=download&token=f4476f28-bd76-429e-b713-78afc073ab4f>

Cysless NHE1 wound healing movie

<https://filesender.renater.fr/?s=download&token=a40e8c87-cc6e-4aaf-b5a5-5070215b5a06>

NHE-deficient fibroblasts wound healing movie

<https://filesender.renater.fr/?s=download&token=d518c1c0-1e56-4894-9baa-fc03e7561f0c>

III. Conclusions - Perspectives

Apparu très tôt dans l'évolution, retrouvé dans tous les règnes animaux⁴, et d'expression ubiquitaire à la membrane plasmique de la plupart des tissus¹⁷, NHE1 est sans conteste un échangeur capital dans la physiologie des organismes vivants en régulant pH et volémie intra-cellulaire. Son fonctionnement allostérique¹⁸ lui permet de réguler avec grande précision et rapidité les variations de pH intracellulaire capital à la survie cellulaire. Inversement, dans beaucoup de situations pathologiques son hyperactivation a été constatée et associée à des conséquences délétères et parfois fatales comme dans les phénomènes d'ischémie-reperfusion, mais aussi dans les cancers, ou le vieillissement. La complexité de la régulation de NHE1 notamment par son fonctionnement allostérique, la conformation membranaire, la composition de la membrane plasmique à proximité, son implication dans la motilité cellulaire et surtout la multitude de voies de signalisation intracellulaires interagissant avec sa partie C-terminale laisse comprendre que NHE1 est au centre de nombreuses réactions physiologiques comme pathologiques. En situation pathologique, les ROS en excès produits par le stress oxydatif participent à la modification de la régulation de NHE1 qui peut devenir délétère.

Notre travail expérimental a permis de montrer que parmi ces ROS l'anion superoxyde $O_2^{\cdot-}$ majore l'activité de NHE1 comme ce qui était démontré avec le peroxyde d'hydrogène H_2O_2 . Cependant, à l'inverse d' H_2O_2 , nous avons pu constater que les conséquences d' $O_2^{\cdot-}$ sur NHE1 dépendent de la présence de cystéines. Nous avons pu mettre en évidence en outre qu'une nitrosylation d'une cystéine de NHE1 existe à l'état basal. Les nitrosylations interviennent dans de nombreux processus cellulaires essentiels dans la signalisation intracellulaire¹¹⁸ ou l'apoptose^{119,120} et pourraient donc jouer un rôle important dans le stress oxydatif en rapport avec NHE1. Nos travaux ont montré de plus que ces cystéines étaient capitales pour permettre une organisation normale de la motilité cellulaire. Au total, nos travaux ont permis d'établir une connexion entre production

d'espèces réactives de l'oxygène, régulation du pH intracellulaire par NHE1 et la motilité et l'adhésion cellulaire.

Dans les suites de ce travail de thèse, de nombreuses pistes de recherche restent en suspens. Si ce travail a pu montrer que la Ménadione et donc qu' $O_2^{\cdot-}$ active directement NHE1, pour des raisons de faisabilité expérimentale nous n'avons pas fait un criblage des cystéines responsables de l'activation de NHE1 par $O_2^{\cdot-}$ en utilisant la Ménadione mais que avec le DPI. Il pourrait notamment être intéressant de vérifier comme avec le DPI que les cystéines 133 et 477 sont les cystéines clefs. Concernant l'implication des cystéines dans la forme et la migration cellulaire, nous avons trouvé qu'il n'y avait pas une cystéine plus impliquée qu'une autre ; il serait intéressant de tester les combinaisons de mutations de cystéines afin de vérifier si une association de 2 ou plusieurs cystéines ne pourrait pas être clef dans cette implication. Toujours concernant la forme cellulaire, nous avons pu montrer que l'implication des cystéines dans la forme cellulaire était en rapport avec la liaison du complexe ERM avec les filaments d'actine, mais nous n'avons pas étudié un possible lien avec les autres éléments du cytosquelette comme les microtubules et les filaments intermédiaires. Enfin, concernant l'adhésion cellulaire nous n'avons pas pu montrer que la vinculine ou la fibronectine étaient en lien avec NHE1 ; les autres molécules d'adhésion cellulaire, peut-être moins évidentes devront être analysées afin d'identifier si d'autres molécules interviennent dans ce phénotype.

Si l'on s'intéresse maintenant d'un point de vue plus macroscopique à l'implication de NHE1 dans le stress oxydatif, très peu de données sont disponibles dans le domaine de la réanimation. Une perspective intéressante serait d'étudier l'implication de NHE1 dans des modèles de pathologie d'IR comme le sepsis et l'arrêt cardiaque. Le sepsis et l'arrêt cardiaque engendrent une ischémie et donc une hypoxie tissulaire qui imposent une reperfusion pour limiter les lésions ischémiques et sauver le ou les organes concernés. Cependant, cette reperfusion incontournable aggrave paradoxalement à la phase initiale

ces lésions ischémiques.¹²¹ La Figure 9 illustre la cinétique d'évolution des lésions au cours de l'ischémie-reperfusion.

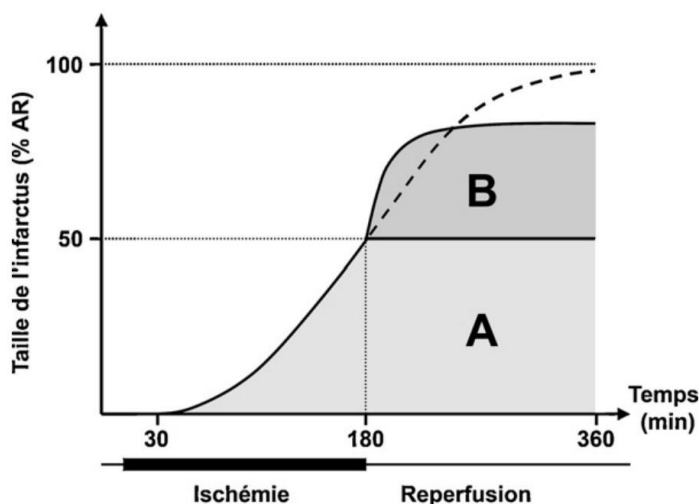


Figure 9. Représentation graphique de l'évolution de la taille de l'infarctus d'un organe après ischémie puis reperfusion. Les lésions évoluent de manière linéaire au cours de l'ischémie (aire A) puis continuent de se majorer après reperfusion de manière exponentielle, et enfin se stabilisent avec la normalisation de la mécanique cellulaire (d'après Cour et Argau)¹²¹

Si les conséquences de l'IR sont assez bien décrits en terme de mécanismes de mort cellulaire et d'altérations de la fonction, les causes qui sous-tendent ces lésions sont moins claires. La mitochondrie joue sans doute un rôle central à la fois dans l'induction des lésions cellulaires notamment par l'activation du pore de transition mitochondrial, mais aussi dans la transmission de signaux cytoprotecteurs. L'ischémie n'est pas seulement la conséquence d'une occlusion complète du vaisseau et de la circulation sanguine, mais peut être aussi la conséquence d'une simple diminution de la circulation sanguine comme dans le sepsis. L'arrêt cardiaque est un modèle d'IR plus facile à comprendre où l'ischémie est représentée par l'arrêt circulatoire du patient quel qu'en soit la cause, et la reperfusion représentée par la reprise d'une circulation sanguine efficace. A notre connaissance, il n'existe pas de données concernant NHE1 et son implication chez l'homme dans ces 2 pathologies là. Le clinicien reste très souvent

impuissant dans ces 2 pathologies où la mortalité dépasse 50% et où aucune avancée thérapeutique franche n'a été apportée au cours des 2 dernières décennies. Confirmer l'implication de NHE1 dans ces pathologies pourrait ouvrir des voies thérapeutiques séduisantes. Une demande d'appel offre interne est en cours d'écriture pour financer un projet étudiant l'implication de NHE1 dans le sepsis¹²² et l'arrêt cardiaque.¹²³ Ce projet incluerait une partie pré-clinique chez la souris chez qui un sepsis peut être reproduit soit par ligature mésentérique soit par injection de LPS (Lipopolysaccharide), et un modèle clinique où NHE1 pourrait être étudié sur les éléments figurés du sang (plaquettes, globules rouges ou lymphocytes) à partir d'un simple prélèvement sanguin.

Au cours des situations de stress oxydatif comme les phénomènes d'ischémie-reperfusion, de nombreux inhibiteurs de NHE1 ont été développés et ont montré des bénéfices presque quelle que soit l'espèce et quel que soit le tissu. Cependant, chez l'homme les seuls inhibiteurs testés en recherche clinique n'ont pas montré de résultats suffisamment importants pour justifier la poursuite de leur développement et leur recommandation dans la prise en charge de ces situations pathologiques.

Ces résultats ont découragé la poursuite de développement de ces inhibiteurs. Pourtant, de nombreux types d'inhibiteurs plus ou moins sélectifs de NHE1 ont probablement encore à faire leurs preuves. La place clef de NHE1 dans ces phénomènes laisse penser qu'il s'agit d'une cible thérapeutique encore séduisante. Le succès récent des inhibiteurs de SGLT2 qui entraînent indirectement une inhibition de NHE1 dans la cardiopathie ischémique^{114,116,124-126} ou l'insuffisance rénale sévère^{127,128} est un bon exemple.

La très récente mise au point de l'analyse en cryo-microscopie de NHE1¹¹ a permis de mieux comprendre les sites et acides aminés impliqués dans la stabilisation du dimère de NHE1, la transition allostérique, la régulation par les voies de signalisation intracellulaire, et les interactions pharmacologiques laissant entrevoir peut-être de nouvelles possibilités de développement thérapeutique.

Parmi les nouvelles molécules pharmacologiques intéressantes, nous retrouvons le GC7 (N1-guanyl-1,7-diaminoheptane) qui a démontré des bénéfices importants sur des modèles pré-cliniques intéressants d'ischémie reperfusion développés par notre équipe en transplantation rénale^{129,130} et dans l'accident vasculaire ischémique¹³¹. GC7 inhibe l'hypusination d'eIF5A (eukaryotic initiation factor 5A) (Figure 10). La Figure 11 représente les bénéfices observés de l'administration de GC7 chez la souris après une ischémie cérébrale.¹³¹

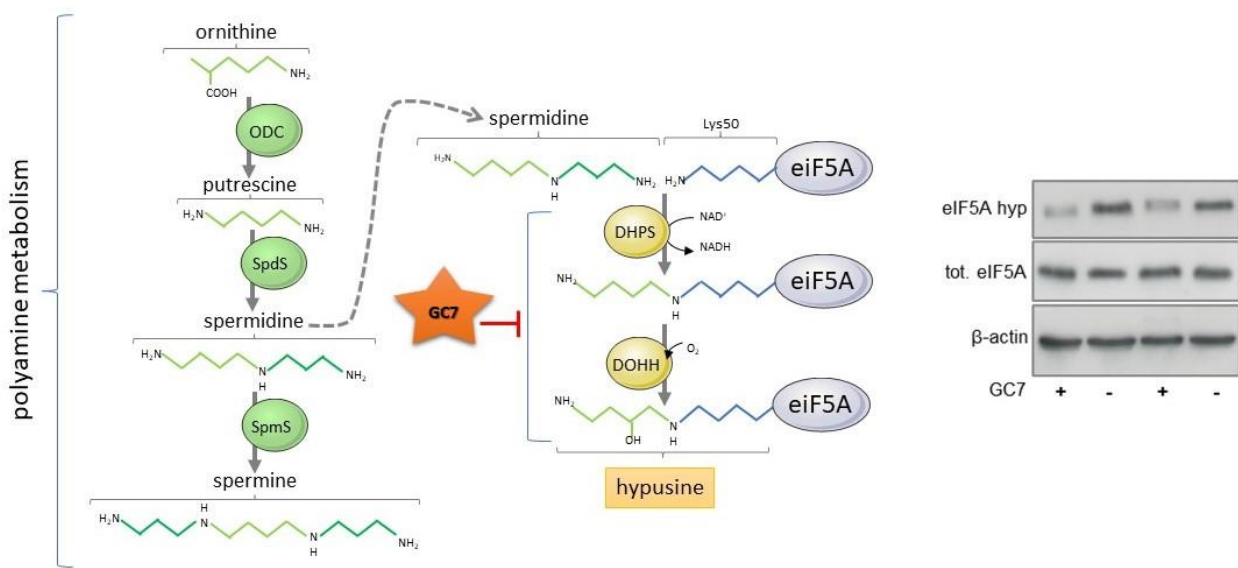


Figure 10. A gauche : Inhibition de l'hypusination du facteur eIF5A par le GC7. A droite : diminution de l'expression du facteur eIF5A en présence du GC7 (Western Blot). DHPS = diminution de l'expression du facteur eIF5A en présence du GC7 (Western Blot). DHPS = Deoxyhypusine synthase, DOHH = Deoxyhypusine hydroxylase, eIF5A = Eukaryotic initiation factor 5A, GC7 = N1-guanyl-1,7-diaminoheptane (d'après Cougnon *et al.*)¹³².

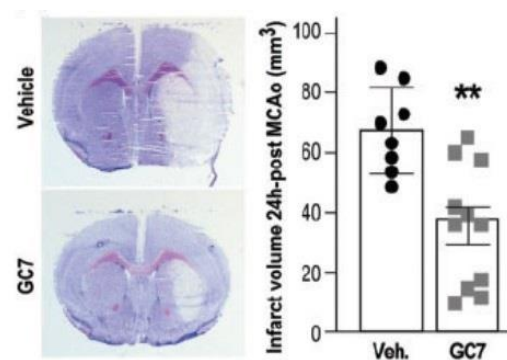


Figure 11. Administration de GC7 chez la souris soumise à une occlusion de l'artère cérébrale sylvienne. A gauche : infarctus cérébral représenté en coupe anatomopathologique sans GC7 (en haut) et avec GC7 (en bas). A droite : représentation graphique du volume cérébral sans et avec GC7. GC7 = N1-guanyl-1,7-diaminoheptane, tMCAo = Transient middle cerebral artery occlusion.¹³¹

L'hypusination d'eIF5A est une modification post-traductionnelle impliquée dans les phénomènes de croissance et les réactions métaboliques qui peuvent être délétères en situation d'ischémie reperfusion. Son inhibition par GC7 modifie le métabolisme et protège les cellules hypoxiques en ischémie-reperfusion. Un des effets très intéressants du GC7 mesuré mais non encore publié par notre équipe est l'inhibition de NHE1 sur des lignées cellulaires cardiaques en IR (**Figure 12**). Comme précédemment décrit chapitre I. H. NHE1 participe aux effets délétères de l'IR, et son inhibition notamment au cours des phénomènes d'IR cardiaques est une stratégie qui a montré des bénéfices dans de nombreux modèles.

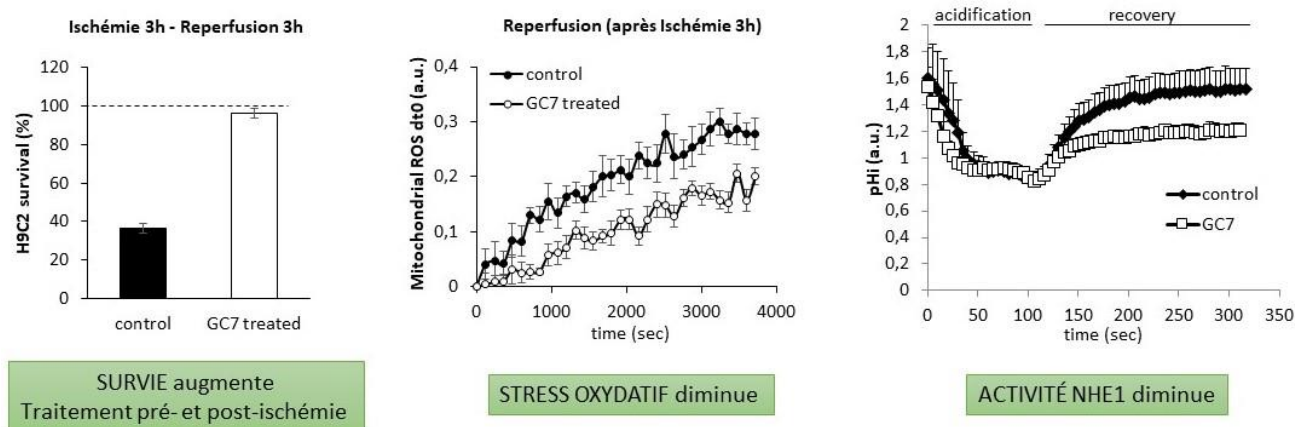


Figure 12. Expérimentations sur des cellules "cardiomyocyte-like" de rat (H9C2). A gauche : augmentation de la survie cellulaire après 3H d'ischémie en cas d'exposition au GC7. Au milieu : diminution de la détection des espèces réactives d'oxygène après 3H d'ischémie en cas d'exposition au GC7. A droite : pH intracellulaire plus diminué après acidification en cas d'exposition au GC7 témoignant d'une inhibition de NHE1 (*data non publiées*)

Une demande d'ANR a été déposée par notre équipe en collaboration avec les équipes du Dr D. Baetz (Laboratoire CarMen, Université Claude Bernard, Lyon), du Dr M. Bernard (Centre de Résonance Magnétique Biologique et Médical, Université d'Aix-Marseille) et du chirurgien cardiaque Dr S. Lopez (Institut Arnault Tzanck, Saint Laurent du Var) pour étudier à partir de cardiomyocytes primaires isolés de déchets opératoires l'efficacité du GC7 sur ces cellules myocardiques en situation d'IR. En effet, jusque là les expérimentations du GC7 sur les cellules cardiaques n'ont pas concerné des cellules cardiaques humaines.

Enfin, le développement d'analyse génomique élargie en collaboration avec l'équipe de notre laboratoire des Dr Stoyan Ivanov et Dr Maxim Artyomov (LP2M) pourrait être un autre moyen de confirmer dans ces situations là l'implication de NHE1 et d'autres partenaires.

Il est prévu que je reste à part entière membre de l'équipe « Transports Ioniques » du LP2M, la localisation du laboratoire et de mon service étant très proches sur le site Pasteur à Nice. Il est prévu également d'intégrer une interne de Médecine Intensive Réanimation dans cette même équipe pour favoriser la poursuite de tous ces projets.

IV. Bibliographie

1. Pedersen SF, Counillon L. The SLC9A-C Mammalian Na(+)/H(+) Exchanger Family: Molecules, Mechanisms, and Physiology. *Physiol Rev* 2019;99:2015-113.
2. Lee HC. The voltage-sensitive Na⁺/H⁺ exchange in sea urchin spermatozoa flagellar membrane vesicles studied with an entrapped pH probe. *J Biol Chem* 1985;260:10794-9.
3. Donowitz M, Ming Tse C, Fuster D. SLC9/NHE gene family, a plasma membrane and organellar family of Na(+)/H(+) exchangers. *Mol Aspects Med* 2013;34:236-51.
4. Lane N, Martin WF. The origin of membrane bioenergetics. *Cell* 2012;151:1406-16.
5. Mitchell P. Chemiosmotic coupling in oxidative and photosynthetic phosphorylation. *Biol Rev Camb Philos Soc* 1966;41:445-502.
6. Harold FM, Papineau D. Cation transport and electrogenesis by *Streptococcus faecalis*. II. Proton and sodium extrusion. *J Membr Biol* 1972;8:45-62.
7. Murer H, Hopfer U, Kinne R. Sodium/proton antiport in brush-border-membrane vesicles isolated from rat small intestine and kidney. *Biochem J* 1976;154:597-604.
8. Mitchell P. Chemiosmotic coupling in oxidative and photosynthetic phosphorylation. 1966. *Biochim Biophys Acta* 2011;1807:1507-38.
9. Saier MH, Jr., Tran CV, Barabote RD. TCDB: the Transporter Classification Database for membrane transport protein analyses and information. *Nucleic Acids Res* 2006;34:D181-6.
10. Brett CL, Donowitz M, Rao R. Evolutionary origins of eukaryotic sodium/proton exchangers. *Am J Physiol Cell Physiol* 2005;288:C223-39.
11. Dong Y, Gao Y, Ilie A, et al. Structure and mechanism of the human NHE1-CHP1 complex. *Nat Commun* 2021;12:3474.
12. Counillon L, Pouyssegur J, Reithmeier RA. The Na⁺/H⁺ exchanger NHE-1 possesses N- and O-linked glycosylation restricted to the first N-terminal extracellular domain. *Biochemistry* 1994;33:10463-9.
13. Noel J, Germain D, Vadnais J. Glutamate 346 of human Na⁺-H⁺ exchanger NHE1 is crucial for modulating both the affinity for Na⁺ and the interaction with amiloride derivatives. *Biochemistry* 2003;42:15361-8.
14. Poet M, Doyen D, Van Obberghen E, Jarretou G, Bouret Y, Counillon L. How Does Our Knowledge on the Na(+)/H(+) Exchanger NHE1 Obtained by Biochemical and Molecular Analyses Keep up With Its Recent Structure Determination? *Front Physiol* 2022;13:907587.

15. Counillon L, Franchi A, Pouyssegur J. A point mutation of the Na⁺/H⁺ exchanger gene (NHE1) and amplification of the mutated allele confer amiloride resistance upon chronic acidosis. *Proc Natl Acad Sci U S A* 1993;90:4508-12.
16. Lacroix J, Poet M, Maehrel C, Counillon L. A mechanism for the activation of the Na/H exchanger NHE-1 by cytoplasmic acidification and mitogens. *EMBO Rep* 2004;5:91-6.
17. Ramskold D, Wang ET, Burge CB, Sandberg R. An abundance of ubiquitously expressed genes revealed by tissue transcriptome sequence data. *PLoS Comput Biol* 2009;5:e1000598.
18. Lacroix J, Poet M, Huc L, et al. Kinetic analysis of the regulation of the Na⁺/H⁺ exchanger NHE-1 by osmotic shocks. *Biochemistry* 2008;47:13674-85.
19. Beliveau R, Demeule M, Potier M. Molecular size of the Na⁺-H⁺ antiport in renal brush border membranes, as estimated by radiation inactivation. *Biochem Biophys Res Commun* 1988;152:484-9.
20. Kinsella JL, Aronson PS. Properties of the Na⁺-H⁺ exchanger in renal microvillus membrane vesicles. *Am J Physiol* 1980;238:F461-9.
21. Grinstein S, Cohen S, Rothstein A. Cytoplasmic pH regulation in thymic lymphocytes by an amiloride-sensitive Na⁺/H⁺ antiport. *J Gen Physiol* 1984;83:341-69.
22. Moolenaar WH, Boonstra J, van der Saag PT, de Laat SW. Sodium/proton exchange in mouse neuroblastoma cells. *J Biol Chem* 1981;256:12883-7.
23. Nagami GT. Luminal secretion of ammonia in the mouse proximal tubule perfused in vitro. *J Clin Invest* 1988;81:159-64.
24. Nakamura N, Tanaka S, Teko Y, Mitsui K, Kanazawa H. Four Na⁺/H⁺ exchanger isoforms are distributed to Golgi and post-Golgi compartments and are involved in organelle pH regulation. *J Biol Chem* 2005;280:1561-72.
25. Nakamura TY, Iwata Y, Arai Y, Komamura K, Wakabayashi S. Activation of Na⁺/H⁺ exchanger 1 is sufficient to generate Ca²⁺ signals that induce cardiac hypertrophy and heart failure. *Circ Res* 2008;103:891-9.
26. Numata M, Orłowski J. Molecular cloning and characterization of a novel (Na⁺,K⁺)/H⁺ exchanger localized to the trans-Golgi network. *J Biol Chem* 2001;276:17387-94.
27. Milosavljevic N, Monet M, Lena I, et al. The intracellular Na⁽⁺⁾/H⁽⁺⁾ exchanger NHE7 effects a Na⁽⁺⁾-coupled, but not K⁽⁺⁾-coupled proton-loading mechanism in endocytosis. *Cell Rep* 2014;7:689-96.
28. Hill JK, Brett CL, Chyou A, et al. Vestibular hair bundles control pH with (Na⁺, K⁺)/H⁺ exchangers NHE6 and NHE9. *J Neurosci* 2006;26:9944-55.
29. Doyen D, Poet M, Jarretou G, et al. Intracellular pH Control by Membrane Transport in Mammalian Cells. Insights Into the Selective Advantages of Functional Redundancy. *Front Mol Biosci* 2022;9:825028.

30. Grinstein S, Goetz JD, Rothstein A. 2Na^+ fluxes in thymic lymphocytes. II. Amiloride-sensitive Na^+/H^+ exchange pathway; reversibility of transport and asymmetry of the modifier site. *J Gen Physiol* 1984;84:585-600.
31. Jean T, Frelin C, Vigne P, Barbry P, Lazdunski M. Biochemical properties of the Na^+/H^+ exchange system in rat brain synaptosomes. Interdependence of internal and external pH control of the exchange activity. *J Biol Chem* 1985;260:9678-84.
32. Lazdunski M, Petitclerc C, Chappelet D, Lazdunski C. Flip-flop mechanisms in enzymology. A model: the alkaline phosphatase of *Escherichia coli*. *Eur J Biochem* 1971;20:124-39.
33. Fuster D, Moe OW, Hilgemann DW. Steady-state function of the ubiquitous mammalian Na^+/H^+ exchanger (NHE1) in relation to dimer coupling models with $2\text{Na}^+/\text{H}^+$ stoichiometry. *J Gen Physiol* 2008;132:465-80.
34. Pouyssegur J, Sardet C, Franchi A, L'Allemain G, Paris S. A specific mutation abolishing Na^+/H^+ antiport activity in hamster fibroblasts precludes growth at neutral and acidic pH. *Proc Natl Acad Sci U S A* 1984;81:4833-7.
35. Krump E, Nikitas K, Grinstein S. Induction of tyrosine phosphorylation and Na^+/H^+ exchanger activation during shrinkage of human neutrophils. *J Biol Chem* 1997;272:17303-11.
36. Schwab A, Fabian A, Hanley PJ, Stock C. Role of ion channels and transporters in cell migration. *Physiol Rev* 2012;92:1865-913.
37. Schneider L, Cammer M, Lehman J, et al. Directional cell migration and chemotaxis in wound healing response to PDGF-AA are coordinated by the primary cilium in fibroblasts. *Cell Physiol Biochem* 2010;25:279-92.
38. Ritter M, Schratzberger P, Rossmann H, et al. Effect of inhibitors of Na^+/H^+ -exchange and gastric H^+/K^+ ATPase on cell volume, intracellular pH and migration of human polymorphonuclear leucocytes. *Br J Pharmacol* 1998;124:627-38.
39. Sin WC, Moniz DM, Ozog MA, Tyler JE, Numata M, Church J. Regulation of early neurite morphogenesis by the Na^+/H^+ exchanger NHE1. *J Neurosci* 2009;29:8946-59.
40. Martin C, Pedersen SF, Schwab A, Stock C. Intracellular pH gradients in migrating cells. *Am J Physiol Cell Physiol* 2011;300:C490-5.
41. Mitra SK, Schlaepfer DD. Integrin-regulated FAK-Src signaling in normal and cancer cells. *Curr Opin Cell Biol* 2006;18:516-23.
42. Paradise RK, Lauffenburger DA, Van Vliet KJ. Acidic extracellular pH promotes activation of integrin $\alpha(v)\beta(3)$. *PLoS One* 2011;6:e15746.
43. Satir P, Christensen ST. Overview of structure and function of mammalian cilia. *Annu Rev Physiol* 2007;69:377-400.
44. Putney LK, Barber DL. Expression profile of genes regulated by activity of the Na^+/H^+ exchanger NHE1. *BMC Genomics* 2004;5:46.

45. Hebert M, Potin S, Sebbagh M, Bertoglio J, Breard J, Hamelin J. Rho-ROCK-dependent ezrin-radixin-moesin phosphorylation regulates Fas-mediated apoptosis in Jurkat cells. *J Immunol* 2008;181:5963-73.
46. Baumgartner M, Sillman AL, Blackwood EM, et al. The Nck-interacting kinase phosphorylates ERM proteins for formation of lamellipodium by growth factors. *Proc Natl Acad Sci U S A* 2006;103:13391-6.
47. Denker SP, Barber DL. Cell migration requires both ion translocation and cytoskeletal anchoring by the Na-H exchanger NHE1. *J Cell Biol* 2002;159:1087-96.
48. Cardone RA, Greco MR, Zeeberg K, et al. A novel NHE1-centered signaling cassette drives epidermal growth factor receptor-dependent pancreatic tumor metastasis and is a target for combination therapy. *Neoplasia* 2015;17:155-66.
49. Brisson L, Driffort V, Benoist L, et al. NaV1.5 Na(+) channels allosterically regulate the NHE-1 exchanger and promote the activity of breast cancer cell invadopodia. *J Cell Sci* 2013;126:4835-42.
50. Commisso C, Davidson SM, Soydaner-Azeloglu RG, et al. Macropinocytosis of protein is an amino acid supply route in Ras-transformed cells. *Nature* 2013;497:633-7.
51. Dykes SS, Steffan JJ, Cardelli JA. Lysosome trafficking is necessary for EGF-driven invasion and is regulated by p38 MAPK and Na⁺/H⁺ exchangers. *BMC Cancer* 2017;17:672.
52. Fukushima T, Waddell TK, Grinstein S, Goss GG, Orlowski J, Downey GP. Na⁺/H⁺ exchange activity during phagocytosis in human neutrophils: role of Fcγ receptors and tyrosine kinases. *J Cell Biol* 1996;132:1037-52.
53. Wakabayashi S, Bertrand B, Ikeda T, Pouyssegur J, Shigekawa M. Mutation of calmodulin-binding site renders the Na⁺/H⁺ exchanger (NHE1) highly H⁺-sensitive and Ca²⁺ regulation-defective. *J Biol Chem* 1994;269:13710-5.
54. Pang T, Su X, Wakabayashi S, Shigekawa M. Calcineurin homologous protein as an essential cofactor for Na⁺/H⁺ exchangers. *J Biol Chem* 2001;276:17367-72.
55. Simonin A, Fuster D. Nedd4-1 and beta-arrestin-1 are key regulators of Na⁺/H⁺ exchanger 1 ubiquitylation, endocytosis, and function. *J Biol Chem* 2010;285:38293-303.
56. Wu KL, Khan S, Lakhe-Reddy S, et al. Renal tubular epithelial cell apoptosis is associated with caspase cleavage of the NHE1 Na⁺/H⁺ exchanger. *Am J Physiol Renal Physiol* 2003;284:F829-39.
57. Tekpli X, Huc L, Lacroix J, et al. Regulation of Na⁺/H⁺ exchanger 1 allosteric balance by its localization in cholesterol- and caveolin-rich membrane microdomains. *J Cell Physiol* 2008;216:207-20.
58. Ishibashi H, Dinudom A, Harvey KF, Kumar S, Young JA, Cook DI. Na⁺-H⁺ exchange in salivary secretory cells is controlled by an intracellular Na⁺ receptor. *Proc Natl Acad Sci U S A* 1999;96:9949-53.

59. Matsushita M, Tanaka H, Mitsui K, Kanazawa H. Dual functional significance of calcineurin homologous protein 1 binding to Na(+)/H(+) exchanger isoform 1. *Am J Physiol Cell Physiol* 2011;301:C280-8.
60. Mendoza-Ferreira N, Coutelier M, Janzen E, et al. Biallelic CHP1 mutation causes human autosomal recessive ataxia by impairing NHE1 function. *Neurol Genet* 2018;4:e209.
61. Sardet C, Counillon L, Franchi A, Pouyssegur J. Growth factors induce phosphorylation of the Na+/H+ antiporter, glycoprotein of 110 kD. *Science* 1990;247:723-6.
62. Hendus-Altenburger R, Pedraz-Cuesta E, Olesen CW, et al. The human Na(+)/H(+) exchanger 1 is a membrane scaffold protein for extracellular signal-regulated kinase 2. *BMC Biol* 2016;14:31.
63. Malo ME, Li L, Fliegel L. Mitogen-activated protein kinase-dependent activation of the Na+/H+ exchanger is mediated through phosphorylation of amino acids Ser770 and Ser771. *J Biol Chem* 2007;282:6292-9.
64. Takahashi E, Abe J, Gallis B, et al. p90(RSK) is a serum-stimulated Na+/H+ exchanger isoform-1 kinase. Regulatory phosphorylation of serine 703 of Na+/H+ exchanger isoform-1. *J Biol Chem* 1999;274:20206-14.
65. Misik AJ, Perreault K, Holmes CF, Fliegel L. Protein phosphatase regulation of Na+/H+ exchanger isoform I. *Biochemistry* 2005;44:5842-52.
66. Snabaitis AK, D'Mello R, Dashnyam S, Avkiran M. A novel role for protein phosphatase 2A in receptor-mediated regulation of the cardiac sarcolemmal Na+/H+ exchanger NHE1. *J Biol Chem* 2006;281:20252-62.
67. Hisamitsu T, Nakamura TY, Wakabayashi S. Na(+)/H(+) exchanger 1 directly binds to calcineurin A and activates downstream NFAT signaling, leading to cardiomyocyte hypertrophy. *Mol Cell Biol* 2012;32:3265-80.
68. Xue J, Zhou D, Yao H, et al. Novel functional interaction between Na+/H+ exchanger 1 and tyrosine phosphatase SHP-2. *Am J Physiol Regul Integr Comp Physiol* 2007;292:R2406-16.
69. Bianchini L, Woodside M, Sardet C, Pouyssegur J, Takai A, Grinstein S. Okadaic acid, a phosphatase inhibitor, induces activation and phosphorylation of the Na+/H+ antiport. *J Biol Chem* 1991;266:15406-13.
70. Pedersen SF, King SA, Rigor RR, Zhuang Z, Warren JM, Cala PM. Molecular cloning of NHE1 from winter flounder RBCs: activation by osmotic shrinkage, cAMP, and calyculin A. *Am J Physiol Cell Physiol* 2003;284:C1561-76.
71. Boedtkjer E, Aalkjaer C. Insulin inhibits Na+/H+ exchange in vascular smooth muscle and endothelial cells in situ: involvement of H2O2 and tyrosine phosphatase SHP-2. *Am J Physiol Heart Circ Physiol* 2009;296:H247-55.

72. Nunomura W, Denker SP, Barber DL, Takakuwa Y, Gascard P. Characterization of cytoskeletal protein 4.1R interaction with NHE1 (Na(+)/H(+) exchanger isoform 1). *Biochem J* 2012;446:427-35.
73. Garnovskaya MN, Mukhin YV, Turner JH, Vlasova TM, Ullian ME, Raymond JR. Mitogen-induced activation of Na⁺/H⁺ exchange in vascular smooth muscle cells involves janus kinase 2 and Ca²⁺/calmodulin. *Biochemistry* 2003;42:7178-87.
74. Snabaitis AK, Cuello F, Avkiran M. Protein kinase B/Akt phosphorylates and inhibits the cardiac Na⁺/H⁺ exchanger NHE1. *Circ Res* 2008;103:881-90.
75. Garnovskaya MN, Mukhin YV, Vlasova TM, Raymond JR. Hypertonicity activates Na⁺/H⁺ exchange through Janus kinase 2 and calmodulin. *J Biol Chem* 2003;278:16908-15.
76. Mukhin YV, Vlasova T, Jaffa AA, et al. Bradykinin B2 receptors activate Na⁺/H⁺ exchange in mIMCD-3 cells via Janus kinase 2 and Ca²⁺/calmodulin. *J Biol Chem* 2001;276:17339-46.
77. Yan W, Nehrke K, Choi J, Barber DL. The Nck-interacting kinase (NIK) phosphorylates the Na⁺-H⁺ exchanger NHE1 and regulates NHE1 activation by platelet-derived growth factor. *J Biol Chem* 2001;276:31349-56.
78. Counillon L, Bouret Y, Marchiq I, Pouyssegur J. Na(+)/H(+) antiporter (NHE1) and lactate/H(+) symporters (MCTs) in pH homeostasis and cancer metabolism. *Biochim Biophys Acta* 2016;1863:2465-80.
79. Yi YH, Ho PY, Chen TW, et al. Membrane targeting and coupling of NHE1-integrin α 5 β 3-NCX1 by lipid rafts following integrin-ligand interactions trigger Ca²⁺ oscillations. *J Biol Chem* 2009;284:3855-64.
80. Schieber M, Chandel NS. ROS function in redox signaling and oxidative stress. *Curr Biol* 2014;24:R453-62.
81. Eltzschig HK, Eckle T. Ischemia and reperfusion--from mechanism to translation. *Nat Med* 2011;17:1391-401.
82. Carcy R, Cougnon M, Poet M, et al. Targeting oxidative stress, a crucial challenge in renal transplantation outcome. *Free Radic Biol Med* 2021;169:258-70.
83. Gutteridge JMC, Halliwell B. Mini-Review: Oxidative stress, redox stress or redox success? *Biochem Biophys Res Commun* 2018;502:183-6.
84. Orrenius S, Gogvadze V, Zhivotovsky B. Mitochondrial oxidative stress: implications for cell death. *Annu Rev Pharmacol Toxicol* 2007;47:143-83.
85. Jassem W, Fuggle SV, Rela M, Koo DD, Heaton ND. The role of mitochondria in ischemia/reperfusion injury. *Transplantation* 2002;73:493-9.
86. Lazdunski M, Frelin C, Vigne P. The sodium/hydrogen exchange system in cardiac cells: its biochemical and pharmacological properties and its role in regulating internal concentrations of sodium and internal pH. *J Mol Cell Cardiol* 1985;17:1029-42.

87. Tani M, Neely JR. Role of intracellular Na⁺ in Ca²⁺ overload and depressed recovery of ventricular function of reperfused ischemic rat hearts. Possible involvement of H⁺-Na⁺ and Na⁺-Ca²⁺ exchange. *Circ Res* 1989;65:1045-56.
88. Rothstein EC, Byron KL, Reed RE, Fliegel L, Lucchesi PA. H₂O₂-induced Ca²⁺ overload in NRVM involves ERK1/2 MAP kinases: role for an NHE-1-dependent pathway. *Am J Physiol Heart Circ Physiol* 2002;283:H598-605.
89. Snabaitis AK, Hearse DJ, Avkiran M. Regulation of sarcolemmal Na⁺/H⁺ exchange by hydrogen peroxide in adult rat ventricular myocytes. *Cardiovasc Res* 2002;53:470-80.
90. Haworth RS, McCann C, Snabaitis AK, Roberts NA, Avkiran M. Stimulation of the plasma membrane Na⁺/H⁺ exchanger NHE1 by sustained intracellular acidosis. Evidence for a novel mechanism mediated by the ERK pathway. *J Biol Chem* 2003;278:31676-84.
91. Gan XT, Chakrabarti S, Karmazyn M. Modulation of Na⁺/H⁺ exchange isoform 1 mRNA expression in isolated rat hearts. *Am J Physiol* 1999;277:H993-8.
92. Sala-Mercado JA, Wider J, Undyala VV, et al. Profound cardioprotection with chloramphenicol succinate in the swine model of myocardial ischemia-reperfusion injury. *Circulation* 2010;122:S179-84.
93. Piot C, Croisille P, Staat P, et al. Effect of cyclosporine on reperfusion injury in acute myocardial infarction. *N Engl J Med* 2008;359:473-81.
94. Eckle T, Kohler D, Lehmann R, El Kasmi K, Eltzschig HK. Hypoxia-inducible factor-1 is central to cardioprotection: a new paradigm for ischemic preconditioning. *Circulation* 2008;118:166-75.
95. Frelin C, Vigne P, Lazdunski M. The role of the Na⁺/H⁺ exchange system in cardiac cells in relation to the control of the internal Na⁺ concentration. A molecular basis for the antagonistic effect of ouabain and amiloride on the heart. *J Biol Chem* 1984;259:8880-5.
96. Murphy E, Steenbergen C. Mechanisms underlying acute protection from cardiac ischemia-reperfusion injury. *Physiol Rev* 2008;88:581-609.
97. Humphreys RA, Haist JV, Chakrabarti S, Feng Q, Arnold JM, Karmazyn M. Orally administered NHE1 inhibitor cariporide reduces acute responses to coronary occlusion and reperfusion. *Am J Physiol* 1999;276:H749-57.
98. Karmazyn M. Mechanisms of protection of the ischemic and reperfused myocardium by sodium-hydrogen exchange inhibition. *J Thromb Thrombolysis* 1999;8:33-8.
99. Moffat MP, Karmazyn M. Protective effects of the potent Na/H exchange inhibitor methylisobutyl amiloride against post-ischemic contractile dysfunction in rat and guinea-pig hearts. *J Mol Cell Cardiol* 1993;25:959-71.
100. Piwnica-Worms D, Lieberman M. Microfluorometric monitoring of pHi in cultured heart cells: Na⁺-H⁺ exchange. *Am J Physiol* 1983;244:C422-8.

101. Loh SH, Sun B, Vaughan-Jones RD. Effect of Hoe 694, a novel Na(+)-H+ exchange inhibitor, on intracellular pH regulation in the guinea-pig ventricular myocyte. *Br J Pharmacol* 1996;118:1905-12.
102. Kusumoto K, Igata H, Abe A, et al. In vitro and in vivo pharmacology of a structurally novel Na+-H+ exchange inhibitor, T-162559. *Br J Pharmacol* 2002;135:1995-2003.
103. Fukumoto S, Imamiya E, Kusumoto K, Fujiwara S, Watanabe T, Shiraishi M. Novel, non-acylguanidine-type Na(+)/H(+) exchanger inhibitors: synthesis and pharmacology of 5-tetrahydroquinolinylidene aminoguanidine derivatives. *J Med Chem* 2002;45:3009-21.
104. Maekawa N, Abe J, Shishido T, et al. Inhibiting p90 ribosomal S6 kinase prevents (Na+)-H+ exchanger-mediated cardiac ischemia-reperfusion injury. *Circulation* 2006;113:2516-23.
105. Hu LF, Li Y, Neo KL, et al. Hydrogen sulfide regulates Na+/H+ exchanger activity via stimulation of phosphoinositide 3-kinase/Akt and protein kinase G pathways. *J Pharmacol Exp Ther* 2011;339:726-35.
106. Moor AN, Gan XT, Karmazyn M, Fliegel L. Activation of Na+/H+ exchanger-directed protein kinases in the ischemic and ischemic-reperfused rat myocardium. *J Biol Chem* 2001;276:16113-22.
107. Benter IF, Juggi JS, Khan I, Akhtar S. Inhibition of Ras-GTPase, but not tyrosine kinases or Ca2+/calmodulin-dependent protein kinase II, improves recovery of cardiac function in the globally ischemic heart. *Mol Cell Biochem* 2004;259:35-42.
108. Xiao XH, Allen DG. The role of endogenous angiotensin II in ischaemia, reperfusion and preconditioning of the isolated rat heart. *Pflugers Arch* 2003;445:643-50.
109. Cao J, Xie H, Sun Y, et al. Sevoflurane post-conditioning reduces rat myocardial ischemia reperfusion injury through an increase in NOS and a decrease in phosphorylated NHE1 levels. *Int J Mol Med* 2015;36:1529-37.
110. Dworschak M, d'Uscio LV, Breukelmann D, Hannon JD. Increased tolerance to hypoxic metabolic inhibition and reoxygenation of cardiomyocytes from apolipoprotein E-deficient mice. *Am J Physiol Heart Circ Physiol* 2005;289:H160-7.
111. Steenbergen C, Perlman ME, London RE, Murphy E. Mechanism of preconditioning. Ionic alterations. *Circ Res* 1993;72:112-25.
112. Klein HH, Pich S, Bohle RM, Lindert-Heimberg S, Nebendahl K. Na(+)/H(+) exchange inhibitor cariporide attenuates cell injury predominantly during ischemia and not at onset of reperfusion in porcine hearts with low residual blood flow. *Circulation* 2000;102:1977-82.
113. Wu D, Bassuk J, Arias J, Doods H, Adams JA. Cardiovascular effects of Na+/H+ exchanger inhibition with BIIB513 following hypovolemic circulatory shock. *Shock* 2005;23:269-74.

114. Zinman B, Wanner C, Lachin JM, et al. Empagliflozin, Cardiovascular Outcomes, and Mortality in Type 2 Diabetes. *N Engl J Med* 2015;373:2117-28.
115. Lee S, Yi KY, Hwang SK, Lee BH, Yoo SE, Lee K. (5-Arylfuran-2-ylcarbonyl)guanidines as cardioprotectives through the inhibition of Na⁺/H⁺ exchanger isoform-1. *J Med Chem* 2005;48:2882-91.
116. Cannon CP, Pratley R, Dagogo-Jack S, et al. Cardiovascular Outcomes with Ertugliflozin in Type 2 Diabetes. *N Engl J Med* 2020;383:1425-35.
117. Gorlach A, Bertram K, Hudecova S, Krizanova O. Calcium and ROS: A mutual interplay. *Redox Biol* 2015;6:260-71.
118. Hess DT, Matsumoto A, Kim SO, Marshall HE, Stamler JS. Protein S-nitrosylation: purview and parameters. *Nat Rev Mol Cell Biol* 2005;6:150-66.
119. Melino G, Bernassola F, Knight RA, Corasaniti MT, Nistico G, Finazzi-Agro A. S-nitrosylation regulates apoptosis. *Nature* 1997;388:432-3.
120. Li J, Billiar TR, Talanian RV, Kim YM. Nitric oxide reversibly inhibits seven members of the caspase family via S-nitrosylation. *Biochem Biophys Res Commun* 1997;240:419-24.
121. Cour MA, L. Ischémie-reperfusion et protection cellulaire. *Réanimation* 2010;19:185-90.
122. Carrico CJ, Meakins JL, Marshall JC, Fry D, Maier RV. Multiple-organ-failure syndrome. *Arch Surg* 1986;121:196-208.
123. Lazzarin T, Tonon CR, Martins D, et al. Post-Cardiac Arrest: Mechanisms, Management, and Future Perspectives. *J Clin Med* 2022;12.
124. Neal B, Perkovic V, Matthews DR. Canagliflozin and Cardiovascular and Renal Events in Type 2 Diabetes. *N Engl J Med* 2017;377:2099.
125. Wiviott SD, Raz I, Bonaca MP, et al. Dapagliflozin and Cardiovascular Outcomes in Type 2 Diabetes. *N Engl J Med* 2019;380:347-57.
126. Bhatt DL, Szarek M, Pitt B, et al. Sotagliflozin in Patients with Diabetes and Chronic Kidney Disease. *N Engl J Med* 2021;384:129-39.
127. Heerspink HJL, Stefansson BV, Correa-Rotter R, et al. Dapagliflozin in Patients with Chronic Kidney Disease. *N Engl J Med* 2020;383:1436-46.
128. The E-KCG, Herrington WG, Staplin N, et al. Empagliflozin in Patients with Chronic Kidney Disease. *N Engl J Med* 2023;388:117-27.
129. Giraud S, Kerforne T, Zely J, et al. The inhibition of eIF5A hypusination by GC7, a preconditioning protocol to prevent brain death-induced renal injuries in a preclinical porcine kidney transplantation model. *Am J Transplant* 2020;20:3326-40.

130. Melis N, Rubera I, Cougnon M, et al. Targeting eIF5A Hypusination Prevents Anoxic Cell Death through Mitochondrial Silencing and Improves Kidney Transplant Outcome. *J Am Soc Nephrol* 2017;28:811-22.

131. Bourourou M, Gouix E, Melis N, et al. Inhibition of eIF5A hypusination pathway as a new pharmacological target for stroke therapy. *J Cereb Blood Flow Metab* 2021;41:1080-90.

132. Cougnon M, Carcy R, Melis N, et al. Inhibition of eIF5A hypusination reprogrammes metabolism and glucose handling in mouse kidney. *Cell Death Dis* 2021;12:283.